`

IMPROVING DELIVERY OF MOLECULARLY TARGETED AGENTS TO GLIOMA

A DISSERTATION
SUBMITTED TO THE FACULTY OF THE GRADUATE SCHOOL
OF THE UNIVERSITY OF MINNESOTA
BY

Sagar Suresh Agarwal

IN PARTIAL FULFILLMENT OF THE REQUIREMENTS
FOR THE DEGREE OF
DOCTOR OF PHILOSOPHY

William F. Elmquist

June 2011

ACKNOWLEDGEMENTS

I would like to thank several people without the support of whom this journey would not have been possible. I would like to thank my committee members, Drs Ronald Sawchuk, Richard Brundage and John Ohlfest for graciously serving on my thesis committee and for their important contributions towards my graduate education. I cannot thank enough, Dr. Richard Brundage, for being more like a friend than a teacher, always willing to answer my questions with a smile that made me forget all problems.

I want to thank the Elmquist lab members, Guoyu Pan, Ying Chen, Li Li, Tianli Wang, Ramola Sane, Rajneet Oberoi, Shruthi Vaidhyanathan and Rajendar Mittapalli, for making graduate life fun and enjoyable. Your friendship, encouragement, and help was invaluable to me.

I do not have enough words to express my gratitude and appreciation towards Nagdeep Giri and Naveed Shaik for their help, support, mentorship and encouragement. I thank them for teaching me the fundamentals of lab work and inspiring me to realize my potential in work and in life. They were my two elder brothers, who nurtured me at every step and guided me when I deviated. I would also like to thank Laura Maertens for being a great friend and always being there whenever I needed her. I have learnt a lot from her and I thank her for that.

If I was able to be successful in this program, it was because of numerous friends who made this journey a memorable experience. Varun Goel, Rima Patel, Kedar Patwardhan, Amruta Patwardhan, Megan Hicks, Martha Giri, Arvind Menon, Vijay Ivaturi, Abhijit Supekar, Ramola Sane, Khushboo Kothari, Amit Gangar and Chaitali Passey were the support structure that helped me keep afloat even in the most difficult times. Special thanks to Ramola, Khushboo and Amit, for some of life's most cherished moments have come because of them. I owe my sanity and smiles to them.

I also would like to extend my sincere appreciation to the faculty and staff at the Department of Pharmaceutics, especially, Candy McDermott and Erica Flynn, for all

their administrative support as well as their friendship. I still remember Candy's broad smile which greeted me when I first came into this department and which still does when I walk into the department office.

I would like to acknowledge the Edward Rippie Fellowship, Ronald Sawchuk Fellowship and the University of Minnesota Doctoral Dissertation Fellowship for providing the funding for my graduate research. I must thank Jim Fisher for his tremendous help at the CPAS lab over the past four years. He has been a great resource and without him I might have been lost.

I want to thank my parents and my family for the continued support, encouragement and love. Thank you mom and dad, because of you, I could dream. I am indebted to Dharmpal Aggarwal, who was the inspiration behind my decision to pursue higher education in the U.S. Thank you mausaji, without you, this dream would not have been realized.

Finally, it was the belief of one man which made it all possible. He inspired me and motivated me to realize my potential. He guided me towards my destination and illuminated my path with his intellect at every step. He became my friend when I needed one and gave me love when I missed home. He laid the foundations of my scientific aptitude but also taught me how to be a good human being. He is the guiding light that has provided direction to my life. Thank you Dr. William F. Elmquist, for what I am today is because of you. I will forever cherish the lessons learnt under your tutelage, in both my professional and personal life.

This thesis is dedicated to my parents, Lata and Suresh Agarwal, for their unconditional love, support and encouragement. For working tirelessly, and sacrificing personal pleasures so that I could get the best education possible. For equipping me with principles, moral integrity and character, and teaching me to brace life with confidence and respect. This thesis is dedicated to my proud parents.

Abstract

Treatment of glioblastoma multiforme is at a crossroads. Promising new molecularly-targeted agents have failed to show any significant clinical benefit. Treatment is particularly challenging since the tumor resides in a tissue that is considered to be a pharmacological and immunological sanctuary due to the presence of the blood-brain barrier. Protective mechanisms at the blood-brain barrier (BBB), such as the endothelial tight junctions and drug efflux transporters, restrict the passage of most large and small molecules into the brain. Limited drug delivery to the tumor is a plausible explanation for the failure of molecularly-targeted therapy in glioma. If therapeutic agents do not reach their target, regardless of their potency, they cannot be effective. The objective of this work was to show that active efflux transporters at BBB restrict delivery of potent molecularly-targeted agents to their targets. More importantly, the aim was to demonstrate that the targets in question are in invasive tumor cells that are left behind after surgery and remain shielded behind an intact blood-brain barrier. The ultimate goal of this endeavor is to improve delivery of molecularly-targeted therapy to the tumor and show that this can translate to enhanced efficacy against this lethal disease.

We show that brain distribution of the tyrosine kinase inhibitors, gefitinib, erlotinib and sorafenib, is restricted due to active efflux mediated by p-glycoprotein (P-gp) and the breast cancer resistance protein (BCRP). We further demonstrate that delivery of these drugs to the brain increases dramatically when the two transporters are genetically absent or pharmacologically inhibited. Using a rat xenograft model and a spontaneous mouse model of glioma, we show that the BBB is heterogeneously disrupted in the brain. The blood-brain barrier is disrupted in the tumor core resulting in high tumoral concentrations

of erlotinib and dasatinib. However, it is intact in areas immediately adjacent to the tumor, and therefore restricts drug delivery to these sites. Thus, clinical assessment of drug delivery when using drug concentrations in tumor core (the resected tissue) as a guide for the adequacy of drug delivery can be misleading. Furthermore, we show that increasing drug delivery to these areas, by genetic deletion or pharmacological inhibition of P-gp and BCRP, results in a remarkable enhancement in efficacy of the tyrosine kinase inhibitor, dasatinib. Finally, we show that efficacy of dasatinib increases dramatically in tumor bearing transgenic mice, that are deficient in P-gp and BCRP, and consequently, these mice survive for a significantly longer time compared to the wild-type mice.

These observations underline that restricted delivery of molecularly-targeted agents to their targets can be a significant determinant of drug efficacy against glioma. In an invasive tumor, such as glioblastoma, it is important to realize that the target resides within the invasive glioma cells, that remain shielded by an intact blood-brain barrier, and evade chemotherapy. Overall, this work highlights the need to develop strategies to improve drug delivery to the invasive tumor in glioma and translate these strategies to the clinic.

TABLE OF CONTENTS

LIST OF TABLES

CHAPTER IV

CHAPTER V

LIST OF FIGURES

CHAPTER IA

DELIVERY OF MOLECULARLY-TARGETED THERAPY TO MALIGNANT GLIOMA, A DISEASE OF THE WHOLE BRAIN

This chapter has been published as a review article in Expert Reviews in Molecular Medicine, Vol. 13, e17, May 2011

Glioblastoma multiforme (GBM), due to its invasive nature, can be considered a disease of the entire brain. Despite recent advances in surgery, radiotherapy, and chemotherapy, current treatment regimens only have a marginal impact on patient survival. A critical challenge faced by cancer researchers is to effectively deliver drugs to invasive glioma cells residing in a sanctuary within the central nervous system. The blood-brain barrier (BBB) restricts delivery of many small and large molecules into the brain. Drug delivery to the brain is further restricted by active efflux transporters present at the BBB, that efflux drugs out of the brain back into the blood. Current clinical assessment of drug delivery and hence efficacy is based on the measured drug levels in the bulk tumor mass, that is usually removed by surgery. Mounting evidence that suggests the inevitable relapse and lethality of GBM is due to a failure to effectively treat invasive glioma cells. These invasive cells hide in areas of the brain that are shielded by an intact blood-brain barrier where they continue to grow and give rise to the recurrent tumor. Effective delivery of chemotherapeutics to the invasive glioma cells is therefore critical, and long-term efficacy will depend upon the ability of a molecularly targeted agent to penetrate an intact and functional BBB throughout the entire brain. This review highlights the various aspects of the blood-brain barrier and the brain-tumor cell barrier that can significantly influence drug response. Finally, we discuss the special challenge of glioma as a disease of the whole brain that lends particular emphasis to the need to effectively deliver drug across the BBB to include the central tumor and the invasive glioma cells.

1A.1 Introduction

The last two decades have witnessed major advances in molecular and cellular biology that have substantially improved our understanding of human malignancies. Unfortunately, these past two decades have also seen a significant rise in the incidence of malignant brain tumors along with only a modest increase in the survival rates associated with them, which are often poor (1). Out of the approximately 22,020 new cases of primary malignant brain tumors that were estimated to be diagnosed in 2010, 80 % were expected to be malignant gliomas (2, 3). Gliomas represent a group of highly malignant and lethal tumors of the brain which, despite all therapeutic advances, have an extremely poor prognosis. The median survival of patients with glioblastoma multiforme (GBM), the most common and most malignant subtype of glioma, is only 12-18 months (4). The current standard of care in GBM is temozolomide combined with radiation, a treatment that has been proven to prolong patient survival by a few months (4). Many new molecularly targeted agents that were developed to inhibit signaling pathways critical for glioma growth and proliferation have failed to elicit any clinical benefit (5). Compared to treatment of other types of tumors, targeting tumors of the CNS is particularly challenging due to the location of the tumor in a pharmacological and immunological sanctuary within the central nervous system (CNS). The blood-brain barrier (BBB) presents a major obstacle to systemic chemotherapy and is capable of significantly limiting drug response (6). Drug efflux transporters at the BBB restrict the passage of drugs into the brain and thus shield the tumor cells from exposure to cytotoxic chemotherapy. In addition to the BBB, the presence of similar drug efflux pumps within

tumor cells further protects them from chemotherapy. Systemically administered drugs thus have to cross these two sequential barriers to reach their intended molecular target. This review focuses on the special challenge that these multiple barriers pose to molecularly targeted and cytotoxic chemotherapeutic drugs. The aim is to provide an overview of the various molecular targets and target-directed chemotherapy for glioma. We review the most important ATP-driven transporters at the BBB and in tumor cells and their role in limiting the delivery and hence efficacy of systemic chemotherapy. Finally, we summarize how treatment of an infiltrative tumor like GBM requires targeting the invasive tumor cells that often reside in areas away from the primary tumor, cells that are not removed by surgery and are shielded by multiple barriers where they continue to grow and give rise to the recurrent tumor (7).

1A.2 Malignant glioma

Malignant glioma represents one the greatest challenges faced by the neuro-oncology community. Gliomas are tumors thought to arise from glial progenitor and glial cells and include astrocytoma, glioblastoma, oligodendroglioma, ependymoma, mixed glioma and a few other rare histologies (2). These tumors account for 32% of all primary brain tumors and 80% of all malignant primary brain tumors diagnosed in the United States (2). The World Health Organization (WHO) classifies gliomas into 4 grades based on their histological features and malignancy. Grade I (pilocytic astrocytoma) and grade II (diffuse astrocytoma) tumors are slow growing and the least malignant forms of glioma, while grade III tumors (anaplastic astrocytoma) are more malignant and associated with poorer prognosis (8). Grade IV is assigned to the most malignant and mitotically active

tumors associated with extremely poor survival rates. Glioblastoma multiforme (GBM) is a grade IV glioma and is characterized high cellular proliferation, diffuse infiltration, necrosis, angiogenesis and resistance to apoptosis. The name "multiforme" signifies the vast intratumoral heterogeneity seen in the disease. GBM accounts for the majority (~ 50 %) of gliomas and together with astrocytoma account for about three–quarters of gliomas. Survival rates for patients with malignant gliomas are the worst among all brain tumors, less than 5 % of GBM patients survive for 5 years post diagnosis (1, 2).

A majority of GBMs are primary tumors that develop *de novo* in the brain without any evidence of a precursor tumor. Secondary GBMs are a relatively smaller fraction (~ 10 %) of GBMs that start as low-grade astrocytomas but subsequently progress to high-grade gliomas (9, 10). Progress in our understanding of the molecular pathogenesis of malignant gliomas has made it possible to distinguish between these two types of GBM based on the genetic aberrations and deregulated growth-factor pathways presented by the tumor. Primary GBMs are characterized by amplification of the epidermal growth factor receptor (EGFR) and its mutant EGFR vIII, loss of heterozygosity of chromosome 10q, amplification/overexpression of the MDM2 gene (mouse double minute 2), deletion of the phosphatase and tensin homologue (PTEN) and alterations in the RB1 and p53 signaling pathways. (9, 10). Secondary GBMs are characterized mainly by overexpression of the platelet derived growth factor receptor (PDGFR) and mutations of the *IDH1* gene and the p53 and RB1 signaling pathways (9, 10). Microarray analysis has also been used to identify several molecular subclasses of GBM based on expression of signature genes that correlate to hypoxia, ECM, proliferation and survival (10). Despite

the genetic differences, no differences in sensitivity to conventional chemotherapy between primary and secondary GBMs have been reported. The molecular and genetic aberrations in glioma have been extensively studied and highlight the remarkable heterogeneity of these tumors even within an individual tumor (11, 12). The enormous intra-tumoral variability combined with the complexity of the deregulated signaling pathways may be one of the reasons why most target-directed therapeutics are ineffective against the disease.

Despite aggressive treatment, essentially all malignant gliomas recur (13), eventually leading to death. The median survival of a glioblastoma patient after recurrence is approximately 5-7 months (5). Surgery remains one of the most effective treatments and almost all patients undergo surgery, unless the location of the tumor makes any degree of surgical debulking impossible (14). Studies have shown the existence of a correlation between the extent of surgical debulking and increased patient survival (15, 16). Unfortunately, the grim reality is that regardless of the extent of resection, tumor recurrence and death is almost always inevitable. Radiotherapy is another treatment option for GBM that has been proven to increase survival in patients post surgery (4). A recent study showed that bevacizumab in combination with radiotherapy was well tolerated and resulted in better overall survival (17). It is believed that anti-angiogenic therapy can potentiate the effects of radiation mainly by normalizing tumor blood vessels and enhancing oxygen delivery (18). Consequently, there are several ongoing clinical trials that are evaluating the effects of concurrent chemotherapy with radiotherapy in glioma. Chemotherapy is fast assuming an increasingly important role in the treatment of

malignant gliomas. Although many earlier studies failed to show benefit with adjuvant chemotherapy, the finding that temozolomide in combination with radiotherapy increases patient survival, dramatically changed chemotherapeutic treatment of glioma (4). Temozolomide is now the standard of care in glioma with almost every patient receiving the drug. However, reports of resistance to temozolomide have intensified the search for more effective target-directed therapies.

A potentially significant advancement in the treatment of gliomas is the development of molecularly targeted agents. There has been considerable progress in understanding the molecular pathogenesis of glioma and identification of key oncogenic pathways that can be targeted using small molecule inhibitors. This has led to the development of several small molecule agents that inhibit such deregulated signaling pathways in glioma. The recent success of such small molecule inhibitors in other cancers has propelled rapid development of similar therapies for treatment of malignant gliomas.

1A.3 Molecularly Targeted Therapy

Molecular abnormalities in signal transduction pathways are characteristic features of many brain tumors, including glioma, and result in uncontrolled tumor cell proliferation, survival and apoptotic resistance. The growth factor pathways that are commonly altered in malignant glioma include the epidermal growth factor (EGF) (19-21), platelet derived growth factor (PDGF) (22-24) and the vascular endothelial growth factor (VEGF) (24-26). Deregulation in receptors of these pathways (EGFR, PDGFR, VEGFR) results in constitutive activation of downstream effectors that regulate gene transcription ultimately

leading to the phenotype in malignant glioma (**Figure. 1.1**). Thus, an attractive approach to inhibit the aberrant signaling pathways in glioma is to use small molecule tyrosine kinase inhibitors (TKIs) that inhibit the activity of upstream receptors of these pathways.

1A.3.1 Targeting EGFR and PDGFR

Aberrant signaling through the EGFR pathway is one of the most common genetic alterations seen in glioma (19, 27) and therefore, several therapeutic strategies have used small molecule TKIs to target EGFR in glioma. Gefitinib (Iressa, Astra Zeneca) and erlotinib (Tarceva, OSI Pharmaceuticals) were some of the first TKIs to show potent inhibitory effect on EGFR, prolonging survival in preclinical models of brain tumors (28-31). However, neither of these two promising drugs showed any significant survival benefit in GBM patients (32-38). PDGFR is another attractive therapeutic target in glioma (**Figure 1.1**) since it is commonly overexpressed in glioma and is thought to contribute to the aggressive phenotype of the tumor (22, 23). Imatinib (Gleevec, Novartis), a potent inhibitor of the tyrosine kinases Bcr-Abl, c-Kit (KIT) and PDGFR, was the first selective tyrosine kinase inhibitor to be approved for the treatment of cancer (39, 40). Imatinib showed encouraging anti-glioma activity in preclinical studies raising hopes in clinical trials that followed (41-43). However, the preclinical success did not translate into significant clinical benefit with phase II trials reporting insignificant antitumor effects in glioma patients (44, 45). Dasatinib (Sprycel, Bristol-Myers Squibb) is another PDGFR inhibitor with additional inhibitory effect on the Src family of kinases. It has also been shown that dasatinib can inhibit the growth and migration of glioma cells and induce cellular apoptosis, again warranting clinical investigation in glioma (46),

however there is no published literature on the clinical efficacy of dasatinib in glioma (**Table 1.1**).

1A.3.2 Targeting VEGFR

Angiogenesis, the process of vascular proliferation due to formation of new blood vessels, is a histopathological hallmark of malignant glioma. The angiogenic effect is mediated primarily through the VEGFR pathway which is frequently upregulated in GBM making it a prime target for growth inhibition and therapeutic efficacy (25, 26). Numerous small molecule VEGFR inhibitors such as cediranib, sunitinib, sorafenib, vatalanib and vandetanib have shown promising results in preclinical glioma models. Cediranib (Recentin, AstraZeneca), a pan inhibitor of the VEGFR tyrosine kinase, is one of the most exciting prospects for anti-angiogenic therapy in glioma. It has demonstrated significant effects in mouse glioma models, decreasing edema via vascular normalization in tumor leading to improvement in survival (47). These preclinical effects have been mirrored in the clinic where cediranib treatment results in normalization of tumor vessels, decreased vessel permeability and alleviation of vasogenic edema (48). Encouraging new data from a recently concluded phase II trial suggests that cediranib therapy results in significant radiographic response and increases progression free survival (49). Sunitinib (Sutent, Pfizer) and sorafenib (Nexavar, Bayer) are two multi-targeted tyrosine kinase inhibitors exhibiting both anti-proliferative and anti-angiogenic activity by simultaneously targeting VEGFR and PDGFR (50, 51). Separate studies have shown that both these compounds can increase survival in mouse glioma models at doses achievable in the clinic (52, 53). Several clinical trials are currently evaluating the efficacy of these

two agents in human malignant glioma. Vandetanib (Zactima, AstraZeneca) is a novel small molecule inhibitor that simultaneously targets VEGFR and EGFR (54). It has demonstrated potent anti-glioma effects in clinically relevant GBM models suppressing tumor cell proliferation and angiogenesis while inducing apoptosis via inhibition of EGFR (55). There are many ongoing clinical studies that are evaluating the efficacy and toxicity of vandetanib in glioma patients.

1A.3.3 Targeting PI3K–AKT–mTOR

Other important molecularly targeted agents include inhibitors of the PI3k-AKT-mTOR pathway **(Figure 1.1)** that is thought to be highly activated in human GBMs, modulating key translational processes (56). Rapamycin (sirolimus) and its analogues, temsirolimus (CCI779) and everolimus (RAD001), are the three mTOR inhibitors that have undergone extensive preclinical and clinical evaluation for therapy in glioma. Clinical trials with mTOR inhibitors as a single agent in glioma have been largely unsuccessful, with no therapeutic benefits reported (35, 57, 58). However, several trials are currently evaluating mTOR inhibitors in combination with other tyrosine kinase inhibitors with an aim to shutdown multiple signaling cascades feeding the tumor.

1A.3.4 Improving Efficacy of Molecularly-Targeted Agents

Most promising molecularly targeted agents have failed to provide any survival benefit in malignant gliomas (**Table 1.1**). Given the dismal prognosis of patients with glioma, the quest to find newer effective therapeutic options have gained precedence over the need to find the reasons behind the failure of these agents, although the two goals are closely

linked. Some of the reasons for this lack of efficacy have been related to the genetic heterogeneity of gliomas and the complexity of signaling pathways such as negative feedback mechanisms and up regulation of alternative pathways. However, all these hypotheses are reliant on the *a priori* assumption that there is adequate drug delivery to the target. The lack of drug delivery to the target is an often overlooked, yet perfectly plausible explanation for a lack of efficacy. Would this delivery failure be detected in preclinical models that were used to justify the clinical trials? The answer is probably no if the preclinical model used was not established in the brain (e.g., flank model), or formed well-circumscribed brain tumors with a leaky BBB amidst no appreciable infiltrative growth to provide a pharmacologic sanctuary (discussed further below). The later well-circumscribed phenotype is the growth pattern of that majority of standard implanted models that are typically used for preclinical validation in the process of drug development (59). So the question germane to the efficacy of molecularly targeted agents in glioma is; are these drugs delivered to the tumor-infiltrated normal brain present after surgical removal of the bulk tumor mass at levels that are adequate to disrupt the function of their targets? Treatment of a brain tumor requires the drug to bypass several barriers and gain access to what is considered a 'sanctuary' in the CNS. The CNS is protected by a highly developed and well regulated interface that separates it from the peripheral circulation and maintains homeostasis in the brain (60). This interface also prevents most drugs and chemicals from entering the brain thereby rendering them ineffective. Once inside the brain, the drug faces additional barriers that further limit its delivery to the ultimate target. It is critical to recognize that the intracellular targets in question are in the

invasive glioma cell, i.e., cells left behind after resection. Discussion of these barriers that limit drug delivery to tumor and hence their efficacy is the essence of this review.

1A.4 Barriers Restricting Drug Delivery to Brain and Brain Tumor

1A.4.1 The Blood-Brain Barrier

The blood-brain barrier (BBB) is a natural defense mechanism in the CNS that separates the brain from the peripheral circulation. The barrier is formed by a dense network of blood capillaries supplying the brain wherein the endothelial cells are joined together by tight junctions such that most drugs and chemicals cannot readily cross into the brain parenchyma. The BBB thus shields the brain from exposure to circulating toxins and potentially harmful chemicals by preventing them from entering the brain. Besides the presence of tight junctions, a relative paucity of fenestrae and pinocytotic vesicles within the brain capillary endothelial cells along with the presence of the surrounding extracellular matrix, pericytes, and astrocyte foot processes further restrict brain uptake (60). As a result of the tight junctions in the BBB, circulating molecules gain access to the brain only via 1) passive diffusion of small nonpolar molecules through the BBB, or 2) active transport (61). Numerous studies have endeavored to correlate brain penetration and CNS activity of compounds to their physicochemical properties. These studies have used different approaches for predicting BBB permeability and reported that compounds that have activity within the CNS have high lipophilicity (log P ~4), few hydrogen bond donors (2-7), low polar surface area (PSA ~40 Å) and low molecular weight (MW ~ 400 Da) (62-65). It is not surprising that all these properties impart greater membrane permeability to the drug molecule resulting in enhanced transport to the brain (65).

However, several molecules with these favorable properties have been found to have a modest permeability into the brain, a result of active efflux transporters that further make the BBB impermeable (62, 66). The BBB is fortified by the presence of numerous drug transport proteins, many of which transport drugs out of the brain. It has been shown that ATP-dependent transporters can severely restrict brain penetration of therapeutic agents, even those molecules with favorable physicochemical properties that were predicted to cross the BBB with relative ease (62, 66). A majority of these transporters belong to two superfamilies - the ATP-binding cassette (ABC) and solute carrier (SLC). P-glycoprotein (P-gp, ABCB1), breast cancer resistance protein (BCRP, ABCG2) and multidrug resistance-associated proteins (MRPs, ABCC) are important members of the ABC. We will limit our discussion to P-gp, BCRP and MRPs in this review. The reader is directed to several excellent reviews that cover other drug efflux transporters in greater detail than possible within the scope of this review (67-73).

1A.4.1.A P-glycoprotein (ABCB1, MDR1, P-gp)

P-glycoprotein, the product of the multidrug resistance gene (*MDR1*), is by far the most extensively studied member of the ABC superfamily of transporters. It was originally discovered by Juliano et al. in 1976 while studying the mechanisms behind the resistance in tumor cell lines (74). The group noticed that cell membranes of the resistant cells expressed a 170 kDa protein, a surface glycoprotein capable of altering permeability of drugs and designated it as 'permeability glycoprotein' or 'P glycoprotein'. A decade later in 1986, the gene encoding the protein, *MDR1*, was discovered (75) and the complete primary structure of P-gp was determined (76). The existence of P-gp at the BBB was

first reported in 1989 when Cordon-Cardo et al. detected P-gp expression in the brain capillary endothelial cells and proposed that it played a role in regulating entry of drug molecules into the CNS (76). Shortly thereafter, Theibaut and colleagues reported the expression of P-gp at the rat BBB (77) followed by numerous studies showing presence of P-gp in brain capillaries of other species such as mice, rats, bovine and porcine (78-80). However, it was a seminal study by Beaulieu et al. that reported the localization of P-gp on the luminal side of the capillary endothelial cells and bolstered theories the transporter is involved in preventing drugs from entering the brain and development of multidrug resistance in cancer (81).

The most compelling first evidence of the protective role of P-gp at the BBB was a chance discovery when mice deficient in the *Mdr1a* gene (P-gp knockout) were found to be 100-fold more sensitive to the neurotoxin ivermectin compared to the normal wild-type mice (82). The study revealed elevated levels of ivermectin in the brains of the P-gp knockout mice, a finding confirming that P-gp protects the CNS by preventing drugs and chemicals from crossing the BBB. P-gp has since been implicated in restricting CNS penetration of hundreds of drugs including several chemotherapeutic agents in clinical practice. The development of the *Mdr1a/b*$^{-/-}$ double knockout (83) and *Mdr1a/1*$^{-/-}$*Bcrp1*$^{-/-}$ triple knockout mice (84) has provided researchers with powerful tools to examine the influence of P-gp in transport of drugs to the brain. Studies exploring the interaction of chemotherapeutic agents with P-gp have used these in vivo models to illustrate how potent anti-cancer drugs and many molecularly targeted TKIs are avid P-gp substrates and how this limits their distribution to the CNS (**Table 1.2)**.

1A.4.1.B Multidrug Resistance Associated Proteins (ABCC, MRP):

The discovery of p-glycoprotein as a transporter capable of effluxing drugs out of tumor cells led to an augmented interest among researchers to find other proteins involved in drug transport and resistance. In 1987 Cole and coworkers noticed that an adriamycin - selected lung cancer cell line was resistant to drugs such as colchicine, vinca alkaloids and anthracycline analogues (85). These cells were known not to overexpress P-gp, leading researchers to believe that the observed resistance might be due to a different mechanism that was similar to P-gp. Molecular analysis revealed the presence of a cDNA encoding a 190 kDa protein that was later confirmed to be present in several multidrug resistance cell lines that did not express P-gp. This protein was called the multidrug resistance-associated protein (86), the first of 12 members of a subfamily of ABC transporters now designated as subfamily-C (ABCC). Cloning of MRP in 1992 resulted in a renewed enthusiasm for drug resistance investigations which were now focused at identifying additional transporters capable of transporting drugs out of cells. There is now evidence that nine of the twelve ABCC family members (MRP1-9) mediate some form of xenobiotic and/or drug resistance (87). Discovery of MRPs also resulted in several studies investigating the localization and role of these transporters at the BBB. However, studies on the expression of MRP transporters at the BBB have been controversial and often contradictory. Huai-Yun et al in 1998 demonstrated the functional expression of MRP1 in bovine brain microvessel endothelial cells (BBMEC) and suggested that the most likely localization of MRP1 at the BBB should be apical (88). In 2004, Zhang et al described the localization of various MRP analogues in bovine brain microvessel

endothelial cells, showing that MRP1 and MRP5, which are predominantly localized basolaterally in various tissues, were highly expressed on the apical side, whereas MRP2 was not detected (89). The group also reported equal localization of MRP4 on the apical and the basolateral plasma membranes in these cells. Nies and coworkers quantitatively studied the expression and localization of MRPs in several regions of adult human brain and showed the presence of MRP 1, 4 and 5 on the luminal side of the BBB, consistent with the findings in the bovine brain (90). In contrast to these earlier studies that report absence of MRP2 at the BBB, some studies have shown MRP2 expression at the luminal membranes of the human (91), rat and pig BBB (92). Although equivocally, expression of MRPs at the BBB have now been described in several studies. However, their exact localization and role at the BBB is still debated. There have been reports that demonstrate the influence of MRPs at the BBB wherein absence or inhibition of the transporter(s) results in enhanced brain penetration of substrate drugs (93-97). Recently it was shown that brain transport of topotecan to the brain was enhanced when MRP4 was absent in the MRP4 knockout mice (98). These studies strongly suggest that some of the MRPs act as an active drug efflux transporter at the BBB. However, further investigation is necessary to completely understand the function of these transporters at the BBB. The availability of newer tools such as knockout mice deficient in one or more of the MRPs can provide answers to questions that are still unanswered with respect to the protective role of MRPs at the BBB.

1A.4.1.C Breast Cancer Resistance Protein (ABCG2, BCRP)

Breast cancer resistance protein is another member of the ABC superfamily of

transporters that confers drug resistance in cancer by virtue of its ability to translocate drugs out of cells. BCRP was originally identified independently and almost simultaneously by three different groups studying non P-gp- and non MRP-mediated drug resistance in cancer cell lines (99-101). In 1999, Doyle and colleagues observed an ATP-dependent reduction in the intracellular accumulation of anthracycline anticancer drugs in MCF-7 breast cancer cells and were not able to ascribe this to overexpression of known multidrug resistance transporters, P-gp or MRP. RNA fingerprinting identified overexpression of a mRNA that encoded a 655 amino-acid protein in the resistant cells, a protein that they designated as the breast cancer resistance protein (99). A similar study investigating the occurrence of mitoxantrone resistance in cancer cell lines isolated a novel cDNA that encoded for an ATP-dependent transporter that was called as the mitoxantrone resistance protein (MXR) (100). Around the same time, Allikmets and co-workers identified a novel gene that was highly expressed in the human placenta. They showed that the gene encoded an ABC transporter protein which they termed as the ABCP (ABC transporter in the placenta) (101). When the sequences of genes from these three studies were eventually compared, they were recognized as essentially identical and belonging to a subfamily of ABC transporters not previously associated with drug resistance in humans (102). Subsequently, the Human Genome Nomenclature Committee assigned this gene the name ABCG2. Following the cloning of BCRP, its role in the efflux of drugs from multidrug resistant cells has been widely studied with several reports on BCRP-mediated resistance to chemotherapeutic agents (**Table 1.2)**.

The putative role of BCRP in the barrier function at the BBB has been controversial.

Several studies have reported that BCRP is localized on the luminal side of the capillary endothelial cells in the human (103) and rat brains (104). Others have reported enriched presence of BCRP in brain capillaries of mice (105) and pigs (106). However, this presence of BCRP at the BBB has not been unequivocally correlated to the low brain penetration of all BCRP substrates. Lee et al. conducted *in situ* brain perfusion studies using dehydroepiandrosterone sulfate and mitoxantrone, two drugs that are efficiently transported by BCRP, and reported no enhancement in brain penetration of the two compounds in the *Bcrp1*$^{-/-}$ mice (107). Similarly, another study showed that *in vitro* interaction of BCRP with substrate compounds rarely translates to visible effects at the BBB *in vivo* (108). The authors from both studies concluded that BCRP plays a minor role in the efflux of drugs at the BBB. In contrast, there have been several studies that demonstrate the role of BCRP in efflux of drugs at the BBB. Cisternino and colleagues showed that BCRP mediated efflux of prazosin and mitoxantrone at the BBB limits permeability of the brain to these prototypical substrates (105). Likewise, Enokizono et al. showed that brain partitioning of drugs increased significantly when BCRP was absent in the *Bcrp1*$^{-/-}$ mice (109). Breedveld et al. showed that brain penetration of imatinib was restricted by BCRP (110) and we recently reported that sorafenib transport to the brain was significantly increased in the *Bcrp1*$^{-/-}$ mice (111). There has been a recent increase in the number of studies investigating the role of BCRP-mediated active efflux in the transport of drugs out of the brain. This surge has been driven by reports suggesting a possible cooperative role of P-gp and BCRP in keeping drugs out of the brain (111-118). Several studies have shown that there is a dramatic increase in the brain penetration of

dual P-gp and BCRP substrates, when these two transporters are absent simultaneously in the *Mdr1a/b*$^{-/-}$*Bcrp1*$^{-/-}$ mice. First seen with topotecan (112), this phenomenon has now been reported for several other compounds including important TKIs such as lapatinib (113), dasatinib (114, 115), gefitinib (116), erlotinib (117) and sorafenib (111, 118). These findings, along with reports that there is extensive overlap in the expression pattern and substrate specificity of BCRP and P-gp (119), suggest that P-gp and BCRP work together at the BBB to limit brain penetration of dual substrates.

The BBB is a major bottleneck that limits drug delivery to the brain; a significant fraction of large and small molecules do not effectively cross the BBB (6). It is clear that drug efflux transporters, a key component of this barrier , can significantly restricts passage of drugs into the brain, even those with favorable physiochemical properties to cross biological membranes. The fact that there are multiple drug transporters at the BBB, some of which might be working in concert with each other, further complicates the problem. Effective targeting of tumors in the brain will require novel strategies to inhibit these gatekeepers so that promising drug candidates are not rendered ineffective due to their inability to enter the brain.

1A.4.1.D Is the BBB Compromised in Glioma?

Recently, the role of the BBB in limiting treatment efficacy in glioma has been questioned based on studies that report high concentrations of chemotherapeutic agents in tumor resections (120). These reports suggest that the BBB does not influence delivery in glioma. This has caused confusion in the clinical assessment of drug delivery when using

drug concentrations in tumor core (the resected tissue) as a guide for the adequacy of drug delivery. It is true that the BBB can be disrupted at or near the tumor since the central core of the tumor is highly angiogenic, containing new and leaky blood vessels (121). While drug delivery might be greatly enhanced in such areas of the tumor, surgery almost completely removes the central core of the tumor in the brain (contrast-enhancing area). Therefore concentrations in these areas do not represent those in the brain areas that are not removed by surgery. Moreover, the BBB is intact at the growing edge of the tumor and early in the development of the vascular niche of invasive glioma cells (122). The disruption of brain vasculature is directly related to tumor size, and the distance from the central core (121). Invasive glioma cells that are not removed by surgery reside in such areas that can be centimeters away from the main tumor (123) and have an intact BBB capable of restricting drug levels. Given the diffusely infiltrating growth of glioma, it is not surprising that the tumor eventually recurs from areas of the tumor rim that are not resected (13), where drug delivery is impaired due the BBB. Effective delivery of chemotherapeutics to the invasive glioma cells is therefore critical, and long-term efficacy will depend upon the ability of a molecularly targeted agent to penetrate an intact and functional BBB throughout the entire brain. This idea of glioma as a disease of the whole brain lends particular credence to the need to use the systemic circulation to effectively deliver drug across the BBB to encompass the central tumor, growing edge of the tumor, and invasive glioma cells. We present this problem in **Figure 1.2** where a hypothetical schematic of a brain tumor can be seen with a gradient of drug concentration around the tumor (**Figure 1.2A**). The tumor core, the area with a disrupted BBB, can

have high drug levels; however areas immediately surrounding the core can receive significantly less drug owing to an intact BBB. The tumor core is usually removed after surgery however glioma cells invade areas of restricted drug delivery away from the tumor (**Figure 1.2B)**. The goal of effective chemotherapy should be to effectively deliver drug in areas that can harbor the invasive glioma cells and not just the tumor core, the part of the tumor removed by surgery **(Figure 1.2C)**. This idea has been supported in a study by Fine et al., where the authors measured paclitaxel concentrations in resected tissue specimens from brain tumor patients and showed that concentrations in the normal brain surrounding the tumor were 10-fold lower than that in the tumor core (124). Furthermore, Pitz et all recently summarized clinical studies reporting anti-cancer drug concentrations in brain tumors and suggested that drug concentrations in contrast enhancing areas of tumor (tumor core) were relatively higher than that in non-contrast enhancing areas (tumor periphery/normal brain (125)).

1A.4.2 The Brain –Tumor Cell Barrier

In addition to the BBB, the brain-tumor cell barrier (BTB) is another barrier that the drug has to cross to reach its intracellular target. The tumor cell membrane, that forms this barrier, regulates the transport of nutrients, growth factors, drugs and other substances into and out of the cell. A considerable amount of work has been done studying the expression, regulation and activity of ABC transporters in cells from various tumors, including GBMs. There is increasing evidence that suggests that drug efflux transporters decrease intracellular drug uptake resulting in the multi-drug resistant phenotype often observed in glioma cells. P-gp is by far the most extensively studied efflux transporter in

glial tumors and its presence has been confirmed by several studies. Fattori and coworkers used immunohistochemistry to show that P-gp was heterogeneously expressed in about 82 % of GBMs (126). Similarly several other studies have reported enhanced expression of P-gp in tissue specimens from human gliomas (127, 128). However there have also been several conflicting reports indicating the absence of P-gp in GBM cells. These studies suggest that expression of P-gp in human glioma specimens is relatively low and rare (129). Decleves et al. showed that P-gp was not expressed in human glioma cells at either the gene or the protein level (130). These widely differing results on the expression of P-gp have been attributed in part to the assay technique used for detection of P-gp (131). Nevertheless, there have been recent reports confirming the presence of P-gp in glioma cells and its effect on accumulation of anti-cancer drugs in these cells. In contrast to P-gp, very few studies have investigated the expression of BCRP in tumor cells from glioma. Despite its original isolation from drug resistant breast cancer cell lines, expression of BCRP in many solid tumors have been found to be negligible (132). However, new evidence implicates this transporter with a special side-population of tumor cells that are believed to have stem cell like properties (133, 134). These precursor cells, responsible for driving tumor growth and proliferation, are thought to be drug resistant due to efflux by BCRP. In a mouse model of glioma, Bleau et al. recently demonstrated enhanced tumorigenicity of BCRP enriched stem-like cells (135). This evidence suggests a similar role of BCRP wherein the transporter confers resistance in glioma cells by virtue of its ability to pump drugs out of the cell. Other than P-gp and BCRP, MRPs have also been found to be expressed in glioblastoma cells (136).

Transporters of this family have been found to be expressed at levels that are in some cases greater than that of P-gp (129). Histochemical analysis of glioma specimens has revealed the presence of significant amounts of MRPs 1, 3, 4 and 5 (130, 137, 138). The influence of MRPs on chemoresistance in glioma has also been reported where non-specific inhibition of MRPs enhanced the cytotoxic effects of anti-cancer agents in glioma cell lines (139). In a recent study, Kuan and coworkers reported elevated expression of MRP3 in human GBMs in contrast to negligible presence in normal brain (140) and suggested the potential use of MRP3 as a prognostic marker and molecular target for GBM.

Expression of ABC transporters in human glioma cells and their role in acquired drug resistance has been reported by several studies in the past few years. Their findings have often been ambiguous and conflicting. While the genetic heterogeneity of the tumor in glioma can account for some of the variability in the reports, more research is clearly needed to elucidate the role of these transporters in tumor cells. Nonetheless, it is clear that the BTB can be a significant second barrier that has the ability to hamper drug delivery to the intracellular target.

1A.4.3 BBB and BTB: Multiple Barriers that Limit Delivery of TKIs to Glioma

The impact of the BBB and BTB on drug delivery to the target site can be significant especially when the drug is a substrate for transporters present at both the barriers (**Figure 1.3**). The recent surge in the development of molecularly targeted TKIs for CNS tumors have led to several investigations on their interaction with important efflux. The

availability of tools in the form of transgenic mouse models and transporter over-expressing cell lines have made it possible to study drug-transporter interactions with an aim to modulate these and enhance drug transport to the target tissue. Given that P-gp and BCRP are the two important transporters that limit drug delivery to the brain and tumor cells, most studies have investigated the interaction of TKIs with these two efflux pumps. Imatinib was the first TKI that was reported to be a substrate for drug effluxing transporters, when it was discovered that distribution of imatinib to the brain was restricted by P-gp mediated efflux (141). This was followed by a number of studies that reported that imatinib was effluxed by both P-gp and BCRP at the BBB (110, 142). The finding that imatinib does not effectively cross the BBB was crucial in explaining its lack of efficacy against brain relapses in chronic myeloid leukemia (143). Similarly Polli et al. showed that the EGFR inhibitor lapatinib was a substrate for both P-gp and BCRP (144) and then suggested in a study that these two transporters work together at the BBB to limit brain penetration of dual substrates (113). Thereafter we have shown that P-gp and BCRP work in concert to limit the brain penetration of several other TKIs such as dasatinib, gefitinib and sorafenib (111, 114, 116). Subsequent studies have shown that this is true for tandutinib and erlotinib as well (145, 146). An extremely important finding in most of these studies is that pharmacological inhibition of the two transporters together significantly enhanced brain levels of the TKIs, over and above individual inhibition of one of the transporters. These preclinical studies used elacridar (GF120918), a dual inhibitor of P-gp and BCRP, and demonstrated that it increases the transport of the concurrently administered TKI to the brain. This suggests that co-administration of an

inhibitor of P-gp and BCRP can be used as a strategy to enhance the delivery of these drugs to the brain.

Many promising TKIs are effective in treating non-CNS malignancies such as lung, breast and hepatic cancer. However, none of them show any clinical efficacy against the metastatic disease in the brain or against primary brain tumors such as glioma (**Table 1.1)**. The complication of delivery across an intact BBB has made it difficult to apply peripherally acting chemotherapeutic agents to invasive cancers of the brain. The problem is confounded by the fact that the BTB has the ability to further restrict intracellular delivery of drug into the invasive glioma cells. A more detailed understanding of these multiple barriers can help researchers devise strategies to overcome some of these barriers and thereby increase the effectiveness of these drugs against GBM.

1A.5 Clinical Implications

1A.5.1 Tyrosine Kinase Inhibitors in GBM: Hopes and Disappointments

In May 2001, the first TKI, imatinib, was approved for treatment of a human malignancy (CML), raising hopes within the oncology community of the promise of similar target directed chemotherapeutics for treating other devastating cancers such as GBM. However, to date, none of the TKIs have been able to show any clinical benefit against this disease. Imatinib's success in CML started a wave of clinical trials that evaluated different TKIs either alone or in combination for therapy in glioma. The trials were backed by significant data showing efficacy of the compounds in preclinical models of

GBM, however, most of them culminated in disappointing failures. The first clinical trial of a TKI in glioma tested gefitinib (34) with a hope that inhibition of the highly deregulated EGFR signaling pathway can translate into improved patient survival. Its failure was soon followed by the clinical inefficacy of the other major EGFR inhibitor, erlotinib. Identification of newer targets led to introduction of newer targeted therapies, the clinical outcomes however, did not change. Studies explaining the failure of these trials have suggested that some reasons for this could be the heterogeneous molecular characteristics of individual gliomas and the complexity of signaling cascades that feed the tumor. However, several questions remain: 1) Does the drug cross the BBB? 2) What are drug concentrations in the brain? 3) What are the concentrations in the tumor? 4) Is the concentration sufficient to inhibit the target? Answers to these questions can help us gain an insight into the possible reasons behind the failure of these drugs. If therapeutic agents do not reach their intended molecular target, regardless of their potency, they cannot possibly be effective. It is well accepted that the BBB was evolved to protect the brain and will be a barrier in the CNS delivery of most drugs. As discussed earlier, many of the TKIs are substrates for important transporters at the BBB and this significantly limits their concentrations in the brain. Whether these preclinical findings translate in humans and whether these transporters restrict penetration of drugs across a human BBB is still unknown. But there is no evidence to suggest otherwise and the inefficacy of these agents against brain tumors in humans adds further credence to the hypothesis.

1A.5.2 Drug Concentrations in the Brain and the Tumor

Many of the questions raised above can be explored if drug levels in the brain could be

measured in patients receiving chemotherapy. Unfortunately, very few studies have evaluated drug concentrations in brain tissues. This is due in part to the difficulty in sampling drug levels in the brain tissue and an uncertainty in the prediction of drug levels in brain from concentrations in surrogate tissues such as the cerebrospinal fluid (147). However, recently Hofer and colleagues presented a few case-reports where they investigated concentrations of chemotherapeutic agents in the brain and tumor. The group measured gefitinib concentrations in tissue specimens from 7 GBM patients and reported 10-fold higher concentrations in excised tumor tissue compared to plasma (120, 148). These findings were supported by preclinical reports describing gefitinib accumulation in tumor (149). The groups concluded that delivery of drugs (gefitinib) to the tumor is not restricted in patients since the BBB is overcome by residual damage from radiotherapy and/or by the pathological infiltrative characteristics of GBM that compromises the functional integrity of the BBB. In the 1980s, a few studies by Stewart and coworkers measured concentrations of cisplatin (150), vinblastine (151) and etoposide (152) in brain tumors. All these studies reported high drug levels in the tumor similar to the above report. But the group also presented a very interesting finding. Drug concentrations in regions immediately adjacent to the tumor were surprisingly lower than that in the tumor, the concentrations decreasing with increasing distance from the tumor. In a similar study, Blakeley et al. used microdialysis to show that penetration of methotrexate was significantly lower in the brain areas adjacent to the tumor (153). All these studies show significantly high drug levels in the tumor. So how does one explain the apparent contradiction that tumor distribution of drugs does not seem to be restricted by the BBB,

yet at the same time their efficacy against the tumor is minimal and that the recurrence of tumor after surgery, centimeters away from the original tumor, is inevitable even with intensive radio/chemotherapy?

1A.5.3 Glioblastoma: A Whole Brain Disease

Given its invasive and infiltrating nature, we consider glioma essentially a disease of the entire brain and this idea can help understand the answers to some of the questions raised above. In addition to being one of the most malignant, glioma is also one the most infiltrative tumors. Local invasion is a hallmark of glioma; typical tumors show an area of central necrosis surrounded by a highly cellular rim of viable tumor cells, with a variable zone of infiltrated adjacent brain tissue (154). Given the distant spread of the disease, frequently into the contralateral hemisphere, gliomas can hardly be called a local disease (7). Tumor cells that migrate into the surrounding brain parenchyma escape surgical resection and are the putative source of the recurrent tumor (**Figure 1.2,1.3)**. This pathological property of glioma can account for many of the pharmacokinetic findings mentioned above. Firstly, the central core of the tumor is a highly necrotic mass and the BBB is most likely disrupted in this area. This allows systemically delivered chemotherapy to easily traverse the impaired barrier and reach the tumor thus explaining the high concentrations seen in tumor by Hofer and Frei (120). This is almost always true since the very ability of contemporary imaging techniques to detect a brain tumor relies on the ability of the contrast agent (gadolinium) to leak through a disrupted BBB and enhance the tumor core (155). Nevertheless, this is also the part of the tumor that is removed by surgical debulking, rendering less relevant any correlations between drug

concentrations in this area to eventual efficacy or lack thereof.

Secondly, disruption of the BBB becomes increasingly insignificant in areas away from the tumor. This is a valuable finding in the studies by Stewart et al. and Blakeley et al. (150-153). The fact that drug exposure in areas immediately adjacent to the tumor was an order of magnitude lower than the exposure in tumor confirms the presence of a functional BBB in these areas, capable of restricting passage of drugs into the brain. This has been elegantly demonstrated by Lockman et al., where the authors show that the BBB remains sufficiently intact in satellite legions of the metastatic tumor to significantly restrict drug delivery to the tumor cells (156). This theory has also been supported by other recent studies that have shown that concentrations of paclitaxel (124) and temozolomide (157) in the tumor periphery were lower than that in the tumor core. A recent study by Pitz et al. summarized findings from clinical studies and show that concentrations of many anti-cancer drugs in contrast enhancing areas of tumor were several fold higher than that in plasma (125). More importantly, the study also reports that tissue-to-blood ratios were generally higher in contrast-enhancing regions than non-enhancing regions (125). Thus, in areas distant from the tumor core, where gadolinium does not cross the intact BBB, mechanisms that limit drug distribution (tight junctions and efflux transport) will still be operative and limit drug delivery. Consequently, less drug reaches these sites that harbor the infiltrated tumorigenic glioma cells, which continue to grow and ultimately reach a clinically significant size. Thus recurrence, an inevitable occurrence in glioma, may not only be due to tumor cells invading the adjoining brain areas but also due to a lack of drug delivery in such areas.

Finally, there is a growing body of literature that suggests that a subset of these invasive cells have stem like properties that allow them to repopulate the tumor (158). The cancer stem cell hypothesis asserts that tumor development and maintenance in GBM is controlled exclusively by these rare fractions of cells with unlimited proliferative and self renewing capacities (159). A basic tenet of this hypothesis is that these stem-like cells have an innate resistance to chemotherapy (160, 161) mainly due to the presence of drug transporters that efflux drugs out of the cells (162-165). This indicates that even if a drug crosses the BBB to reach brain parenchyma, its entry into an infiltrative tumor cell can be further restricted by drug efflux proteins present within such cells. These infiltrative cells, shielded by the BBB and the BTB, thus grow and eventually give rise to the recurrent tumor.

Thus, the two sequential barriers, the blood-brain barrier and the brain-tumor cell barrier, are two important factors that govern the passage of drug from systemic circulation to the target site. The clinical failure of molecularly targeted therapy suggests two fundamental realities. One is that the BBB and the BTB can significantly limit drug delivery to the target site. The other reality is that regardless of how potent our targeted agents are, they will continue to be ineffective until strategies are devised to improve their delivery across the BBB and the BTB into the invasive glioma cells. An excellent depiction of this predicament is given by Berens et al., where the authors explain that the clinical course of glioma patients after surgery is determined by residual, invasive tumor cells, *i.e.*, "*those left behind*" (7).

1A.6 Outstanding Research Questions

The realization of the impact that the BBB and the BTB can have on chemotherapy in glioma has resulted in a renewed interest among researchers to pursue strategies that can overcome these barriers and increase the delivery of drug to the tumor targets. Several innovative methods have been developed and used to circumvent the BBB and improve drug delivery to the brain. These techniques can be divided into three broad categories; administration of chemotherapy directly into the brain parenchyma, osmotic disruption of the BBB and inhibition of drug efflux. Direct administration into the CNS is achieved via use of biodegradable polymers, convection enhanced delivery or by intrathecal and intraventricular administration. In 2002, the United States FDA approved Gliadel® wafers for use as an adjunct to surgery in the treatment of malignant glioma. These are biodegradable polymeric wafers that slowly release BCNU in the space remaining after surgical resection and have been shown to be well tolerated and offer a survival benefit in GBM patients with concurrent chemotherapy (166, 167). However, new data indicate no survival benefit and significant adverse effects on treatment with these wafers (168). Clinical evaluation of CED for enhancing tumoral delivery of chemotherapy has yielded similar results (169). In a recent trial, CED afforded no survival benefit compared to Gliadel® (170) while a separate clinical trial reported that treatment was associated with severe neurological complications (171). Transient disruption of the BBB by intra-arterial infusion of hyperosmotic solution of mannitol (172) or the bradykinin analogue RMP-7 (173) is method used to enhance concentrations of chemotherapy in brain. Recent studies have shown that treatment with carboplatin, etoposide (174) and bevacizumab (175) after

disruption of the BBB resulted in prolonged time to progression and reduction in tumor volume. A primary drawback common to the above approaches is that these are complex techniques and are associated with a significant incidence of treatment-related complications. In contrast, modulation of drug transporters at the BBB is a possible method to improve delivery of chemotherapy to the brain. Compounds such as valspodar (PSC833), zosuquidar (LY335979) and elacridar (GF120918), potent inhibitors of drug transporters P-gp and/or BCRP, can significantly enhance systemic and brain concentrations of the concurrently administered chemotherapeutic agent (111, 112, 114-116). Consequently, a number of clinical trials have tested these chemical modulators with the aim to reverse multidrug resistance in hematological and solid tumors. The results from these clinical investigations have been disappointing with many studies reporting no enhancement in drug efficacy and significant toxicities related to administration of the reversal agent. Treatment with valspodar has been associated with severe toxicities and no improvement in efficacy of concurrent chemotherapy (176, 177). The P-gp inhibitor zosuquidar has been reported to be relatively nontoxic but has again failed to show any improvement in treatment (178, 179). In contrast, co administration of the dual P-gp and BCRP inhibitor elacridar resulted in significant enhancement in the oral bioavailability of topotecan and doxorubicin (180, 181). However, these effects were seen after high doses of elacridar which were often toxic. While most of these failures were in trials for peripheral solid tumors, the scenario might be different in brain tumors where a moderate enhancement in drug delivery across the BBB can dramatically increase relative drug concentrations in the brain. Furthermore, in many of the studies, it

was not clear if the observed toxicities were a result of the transport modulator or the simultaneously administered chemotherapeutic agent. Again, this may be different in brain tumors where the most common toxicity observed with the current TKIs is systemic and administration of an efflux inhibitor could even serve to reduce the chemotherapeutic dose if the desired brain concentrations were achieved at lower systemic doses. Clinical trials of modulation of MDR have been limited by two major factors: inability to achieve adequate non-toxic levels of the modulators to reverse drug resistance in patients and the presence of multiple mechanisms of resistance (182). Development of new, more potent inhibitors can help overcome some of these limitations. Further clinical studies are needed to better understand the benefit of increasing delivery of chemotherapeutic drugs to tumors in the brain. Additionally, preclinical studies that will be used to justify these clinical trials must employ intracranial models that exhibit appreciable tumor-infiltrated normal brain protected by the BBB in order to be most informative.

1A.7 Conclusion

The blood-brain barrier and the brain-tumor cell barrier are two important obstacles that restrict the passage of molecularly targeted agents to the tumor. Increase in our understanding of the molecular biology of glioma has resulted in new potent compounds which intervene in various signaling pathways that drive the tumor growth. However, regardless of their potency, if the therapeutic agents do not reach their intended molecular target, they cannot possibly be effective. Numerous strategies have been devised to circumvent some of these barriers and improve delivery of drug to the tumor cells in the brain. Although some of these strategies have shown promising results in the preclinical

setting, results in patients have thus far been poor. The molecular heterogeneity in glioma calls for the use of multi-targeted agents, 'dirty drugs' that can inhibit multiple signaling pathways simultaneously. However, we also need 'sharp needles' that can effectively deliver such drugs to the site of the invasive tumor. The next generation of clinical trials is exploring the use of multi-targeted TKIs or combination of single targeting TKIs. Further research investigating delivery of chemotherapeutics to the tumor will ensure that these clinical trials do not follow the same pattern as that of the previous trials. Approaching the treatment of glioma by assuming that the tumor is localized in the contrast-enhancing area (hence resection) will lead to continued failure. The dismal prognosis in glioma may remain unchanged until measures are taken to ensure that promising anti-cancer treatments are delivered effectively to the invasive glioma cells, those hiding behind an intact BBB. We must effectively treat "*those left behind*".

Table 1.1: Molecularly Targeted Agents for Tumors of the Central Nervous System.

COMPOUND	MOLECULAR TARGET	RESULTS FROM CLINICAL TRIALS FOR GBM	CLINCAL TRIALS
Cediranib	VEGFR	Median OS in 16 patients of 211 days (48) 6-month PFS 25.8 %, PR in 56.7 % (49)	6
Dasatinib	Bcr-Abl, C-kit,PDGFR, Src	No Published Results	4
Erlotinib	EGFR	6-month PFS 3.1% (35) Median survival 19.3 months (36) 6-month PFS of 3 %, 12-month survival of 57 % (37) Median PFS 2.8 months, median OS 8.6 months (38)	20
Everolimus	mTOR	Stable disease in 36%, PR in 14 % of patients (57)	11
Gefitinib	EGFR	Median EFS 8.1 weeks, median OS 39.4 weeks (34) Median time to progression 8.4 weeks, 6-month PFS 14.3%, Median OS 24.6 weeks (33)	4
Imatinib	Bcr-Abl, C-kit,PDGFR	6-month PFS 3% (44) 6-month PFS 16% (45) 6-month PFS 27%, median PFS 14.4 week (183) 24% progression-free at 6 months (184)	7
Lapatinib	EGFR2	No Published Results	3
Pazopanib	C-kit, PDGFR,VEGFR	No Published Results	1
Sirolimus	mTOR	6-month PFS of 3.1% (35)	4
Sorafenib	C-kit, PDGFR,Raf	Median PFS 6 months, median OS 16 months (185)	7

Table 1.1: Molecularly Targeted Agents for Tumors of the Central Nervous System (continued)

COMPOUND	MOLECULAR TARGET	RESULTS FROM CLINICAL TRIALS FOR GBM	CLINCAL TRIALS
Sunitinib	VEGFR, C-kit, PDGFR	Median TTP 1.5 months and OS 3 months (186)	8
Temsirolimus	mTOR	6-month PFS 7.8 %, median OS 4.4 months (58)	9
Vandetanib	EGFR, VEGFR	No Published Results	10
Vatalanib	C-kit, PDGFR,VEGFR	Partial Response in 29 % patients (187)	2

OS, overall survival; PFS, progression-free survival; PR, partial response; EFS, event-free survival; TTP, time to progression.

Number of clinical trials are determined from the clinical trials that have either been completed or are ongoing for therapy in glioma, searched on www.clinicaltrial.gov on 1st Dec 2010.

Table 1.2: ABC Transporters at the Blood-Brain Barrier and Brain-Tumor Cell Barrier and their Substrate Chemotherapeutic Agents

TRANSPORTER	GENE	LOCATION AT THE BBB	PRESENCE IN TUMOR CELLS	SUBSTRATE CHEMOTHERAPEUTIC AGENTS
P-glycoprotein (P-gp)	*ABCB1 (MDR1)*	Luminal (Ref. 79)	Yes (Refs. 124-126)	Vincristine, vinblastine, paclitaxel, docitaxel, doxorubicin, daunorubicin, mitoxantrone, etoposide, teniposide, methotrexate, topotecan, imatinib, dasatinib, lapatinib, gefitinib, sorafenib, erlotinib, tandutinib,
Breast Cancer Resistance Protein (BCRP)	*ABCG2 (MXR)*	Luminal (Ref. 101)	Yes (Refs. 131-133)	doxorubicin, daunorubicin, mitoxantrone, methotrexate, topotecan, SN-38 (active metabolite of irinotecan), gimatecan, imatinib, dasatinib, lapatinib, gefitinib, sorafenib, erlotinib, tandutinib,
Multi-Drug Resistance Associated Protein 1 (MRP1)	*ABCC1 (MRP1)*	Luminal, Apical (Ref. 87, 88)	Yes (Refs. 127,128,136)	Etoposide, teniposide, vincristine, vinblastine, paclitaxel, docitaxel, doxorubicin, daunorubicin, mitoxantrone, topotecan, irinotecan, methotrexate
Multi-Drug Resistance Associated Protein 2 (MRP2)	*ABCC2 (MRP2)*	Luminal (Ref. 89)	?	Cisplatin, etoposide, vincristine, vinblastine, doxorubicin, daunorubicin, topotecan, irinotecan, methotrexate, paclitaxel, docitaxel
Multi-Drug Resistance Associated Protein 3 (MRP3)	*ABCC3 (MRP3)*	?	Yes (Refs. 128,136, 138)	Etoposide, teniposide, vincristine, methotrexate

Table 1.2: ABC Transporters at the Blood-Brain Barrier and Brain-Tumor Cell Barrier and their Substrate Chemotherapeutic Agents (Continued)

TRANSPORTER	GENE	LOCATION AT THE BBB	PRESENCE IN TUMOR CELLS	SUBSTRATE CHEMOTHERAPEUTIC AGENTS
Multi-Drug Resistance Associated Protein 4 (MRP4)	*ABCC4 (MRP4)*	Luminal, Apical (Ref. 87, 88)	Yes (Refs. 128,135)	Methotrexate, topotecan, 6-mercaptopurine, thioguanine, cisplatin
Multi-Drug Resistance Associated Protein 5 (MRP5)	*ABCC5 (MRP5)*	Luminal, Apical (Ref. 87, 88)	Yes (Refs. 128, 135, 136)	6-mercaptopurine, thioguanine, gemcitabine

Figure 1.1: Molecularly Targeted Therapy for Malignant Glioma.

Several signaling pathways are aberrantly activated in glioma, the most common being signaling through EGFR, PDGFR, VEGFR and C-kit (Ref. 24). These pathways can be deregulated due to one or more mechanisms such as auto-activation, aberrant expression, mutations and decreased activity of phosphatases that turn off the signal. Signaling through these pathways can be shut down by targeted therapies that inhibit these receptors, thereby preventing the downstream effects that ultimately lead to growth and proliferation of the tumor. Such molecularly targeted therapeutic agents have been shown in the figure near the targets that they inhibit. EGFR – epidermal growth factor receptor; PDGFR – platelet derived growth factor receptor; VEGFR – vascular endothelial growth factor receptor; mTOR – mammalian target of rapamycin; PI3K – phosphatidylinositol 3-kinase; ERK - extracellular signal-regulated kinase; MEK – ERK kinase; Src - rous sarcoma oncogene cellular homolog; PI3K - phosphoinositide 3-kinase; AKT - AKT8 virus oncogene cellular homolog

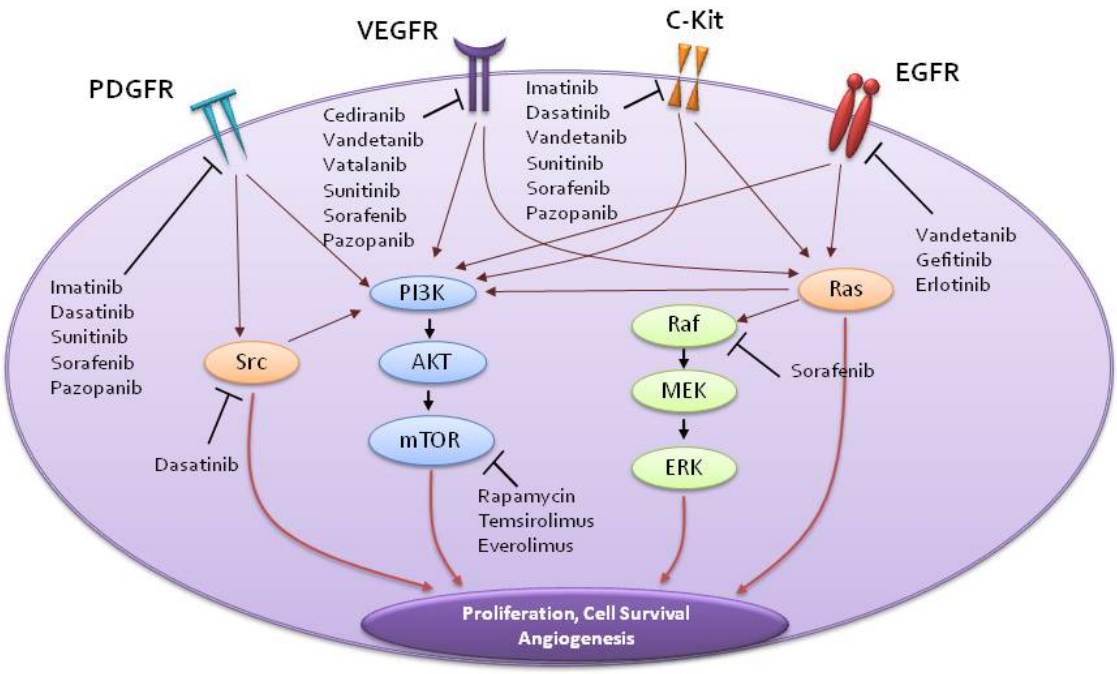

Figure 1.2: Hypothetical Schematic of Regional Drug Delivery in Glioma due to Invasive Nature of the Tumor.

(**A**) Schematic of a brain tumor with a simulated gradient of drug concentration around the site of tumor. The tumor core, the area with a disrupted BBB, can have high drug levels; however areas immediately surrounding the core can receive significantly less drug owing to an intact BBB. (**B**) The tumor core is usually removed after surgery however glioma cells invade areas of restricted drug delivery away from the tumor. These areas away from the tumor are the sites where the invasive glioma cells continue to grow and give rise to the recurrent tumor. (**C**) The goal of chemotherapy should be to effectively deliver drug in areas that can harbor the invasive glioma cells and not just the tumor core, the part of the tumor removed by surgery.

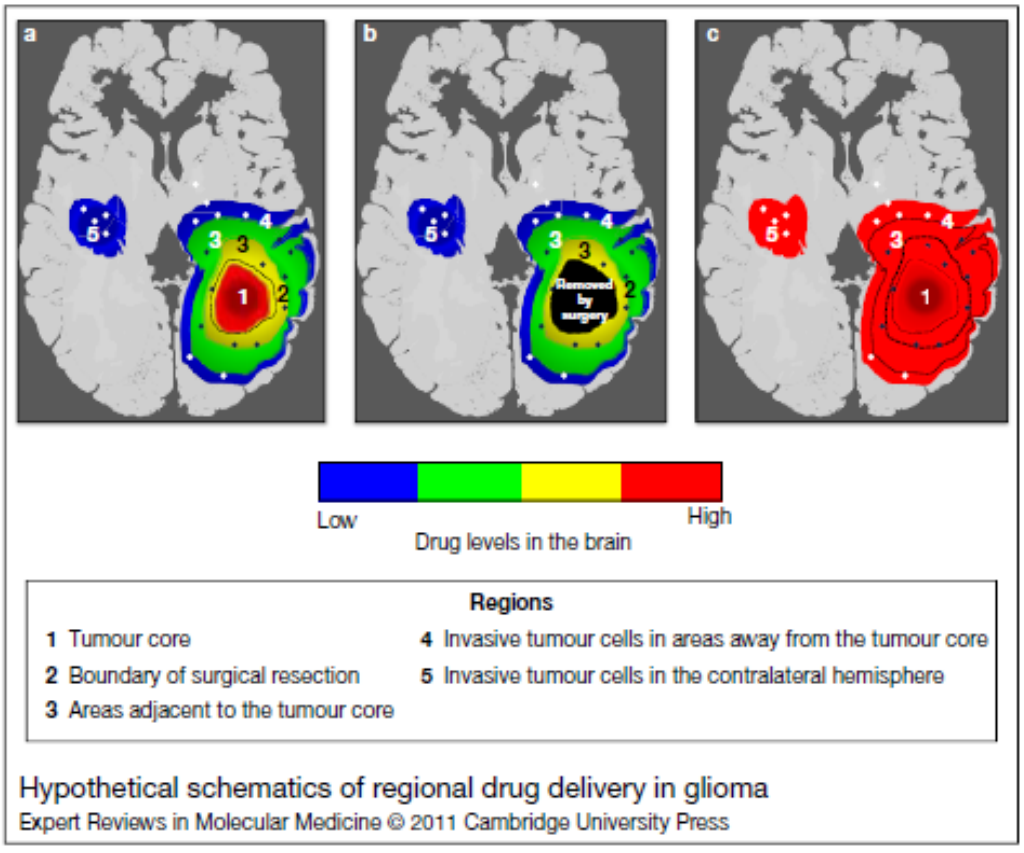

Figure 1.3: Multiple Mechanisms and Barriers That Limit Drug Delivery to Glioma.

The blood-brain barrier and the brain-tumor cell barrier form sequential barriers that a systemically administered drug must cross to reach the tumor. **A)** The BBB is often disrupted at the site of the tumor allowing for easy diffusion of drugs and small molecules into the tumor. However this is also the part of the tumor that gets removed after surgery. **B)** The BBB however is intact in areas centimeters away from the tumor core. Drug delivery across this barrier is restricted by the presence of tight junctions between endothelial cells and more importantly by drug efflux transporters that pump drugs back into the blood. Drug that gets across this barrier and reaches the brain is usually a fraction of what reaches the tumor core. **C)** Invasion of glioma cells from the tumor core into the normal brain parenchyma. These small nests of tumor cells are protected by the intact BBB and receive only a small amount of drug. These cells eventually give rise to the recurrent tumor after surgery **D)** The brain-tumor cell barrier represents the barrier between the brain parenchyma and the tumor cell. Drug efflux transporters present in the tumor cell are a major component of this barrier and restrict intracellular drug uptake. This second barrier is especially important for molecularly targeted agents since they target intracellular domains of receptor tyrosine kinases. P-gp – p-glycoprotein; BCRP –breast cancer resistance protein; MRP – multidrug resistance associated protein.

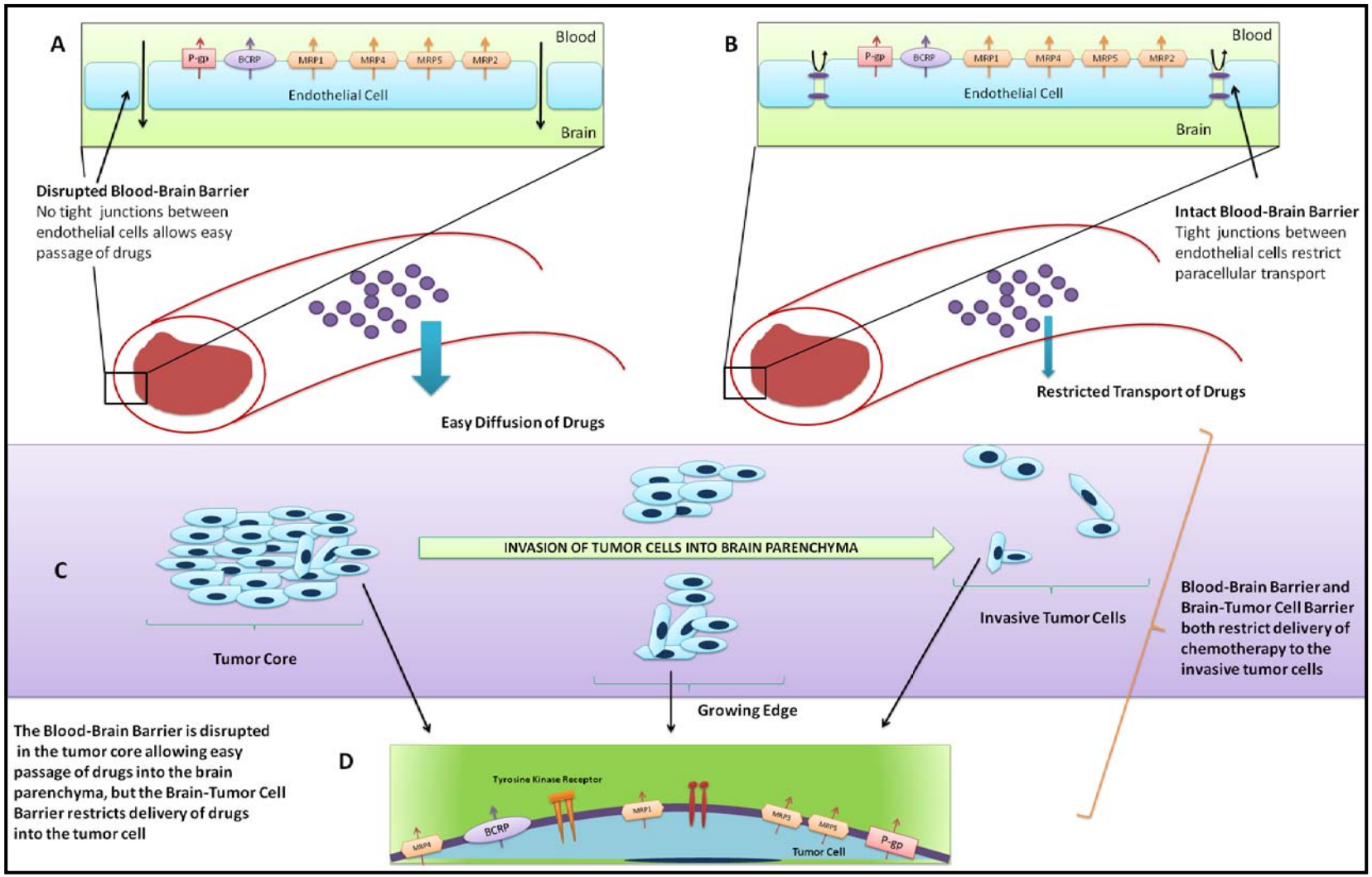
A
Blood
P-gp
BCRP
MRP1
MRP4
MRP5
MRP2
Endothelial Cell
Brain
Disrupted Blood-Brain Barrier
No tight junctions between endothelial cells allows easy passage of drugs
Easy Diffusion of Drugs
B
Blood
Endothelial Cell
Brain
Intact Blood-Brain Barrier
Tight junctions between endothelial cells restrict paracellular transport
Restricted Transport of Drugs
C
INVASION OF TUMOR CELLS INTO BRAIN PARENCHYMA
Tumor Core
Growing Edge
Invasive Tumor Cells
Blood-Brain Barrier and Brain-Tumor Cell Barrier both restrict delivery of chemotherapy to the invasive tumor cells
The Blood-Brain Barrier is disrupted in the tumor core allowing easy passage of drugs into the brain parenchyma, but the Brain-Tumor Cell Barrier restricts delivery of drugs into the tumor cell
D
Tyrosine Kinase Receptor
BCRP
MRP1
MRP3
MRP5
MRP4
P-gp
Tumor Cell

CHAPTER IB

BREAST CANCER RESISTANCE PROTEIN AND P-GLYCOPROTEIN IN BRAIN CANCER: TWO GATEKEEPERS TEAM UP

This chapter has been accepted for publication as a review article in a special edition of Current Pharmaceutical Design, 2011

Brain cancer is a devastating disease. Despite extensive research, treatment of brain tumors has been largely ineffective and the diagnosis of brain cancer remains uniformly fatal. Failure of brain cancer treatment may be in part due to limitations in drug delivery, influenced by the ABC drug efflux transporters P-gp and BCRP at the blood-brain and blood-tumor barriers, in brain tumor cells, as well as in brain tumor stem-like cells. P-gp and BCRP limit various anti-cancer drugs from entering the brain and tumor tissues, thus rendering chemotherapy ineffective. To overcome this obstacle, two strategies – targeting transporter regulation and direct transporter inhibition – have been proposed. In this review, we focus on these strategies. We first introduce the latest findings on signaling pathways that could potentially be targeted to down-regulate P-gp and BCRP expression and/or transport activity. We then highlight in detail the new paradigm of P-gp and BCRP working as a "cooperative team of gatekeepers" at the blood-brain barrier, discuss its ramifications for brain cancer therapy, and summarize the latest findings on dual P-gp/BCRP inhibitors. Finally, we provide a brief summary with conclusions and outline the perspectives for future research endeavors in this field.

1B.1 Introduction

The number of new cases of malignant brain cancers has significantly increased over the last two decades (1, 2). In 2010, an estimated 22,000 new patients were expected to be diagnosed and 13,000 patients were expected to die of brain cancer in the United States (1). Brain cancers can be divided into two categories: primary brain tumors and metastatic brain tumors. *Primary brain tumors* originate in the brain and usually do not metastasize. These tumors represent only 2% of all cancers but account for a disproportionate rate of morbidity and mortality (3). *Metastatic brain tumors* originate outside of the central nervous system (CNS) elsewhere in the body and spread to the brain as metastases (4). Metastatic brain tumors develop in 10–30% of cancer patients (5), and are the most common type of brain tumors with a more than four times greater annual incidence compared to primary brain tumors (6). The incidence of brain metastasis has increased over the last decade mainly due to improved treatment of primary peripheral cancers resulting in increased patient survival, as well as due the development of newer tools to image and detect tumors of the CNS. Despite extensive research, treatment of metastatic brain tumors has been largely ineffective and the diagnosis of brain cancer remains uniformly fatal (6).

One major challenge researchers face today is effective delivery of anti-cancer drugs to primary and metastatic cancers in the CNS. The primary impediment to successful drug delivery into the CNS is the blood-brain barrier (BBB). The BBB is an endothelial interface that separates the brain from the blood and shields the CNS from exposure to circulating toxins and potentially harmful chemicals (7). At the same time, this protective

barrier excludes therapeutic drugs from entering the brain, and thus, becomes an obstacle for drugs intended to treat CNS diseases, such as brain cancers.

At the molecular level, brain capillary endothelial cells that form the BBB are joined together by tight junctions that limit paracellular passage of solutes into the brain. Circulating solutes can therefore only gain access to the brain by passive diffusion, or uptake transport (8). The BBB is further fortified by ATP-binding cassette (ABC) efflux transporters that limit xenobiotics, including a large number of therapeutic drugs, from entering the brain. P-glycoprotein (P-gp, *ABCB1* or *MDR1*) and breast cancer resistance protein (BCRP, *ABCG2*) are two prominent members of the ABC transporter superfamily. Both have broad and partly overlapping substrate specificities that include a variety of structurally diverse drugs currently used in the clinic (9-11). These two "gatekeeper" transporters constitute a vital part of the protective defense mechanism at the BBB by limiting drugs from accessing the brain and thereby rendering them ineffective. Moreover, recent literature suggests that P-gp and BCRP team up and work together at the BBB to restrict brain penetration of drugs (12-16).

The present review is focused on this phenomenon and the challenge that these two transporters pose to chemotherapeutic delivery into the brain. We review P-gp and BCRP with respect to their roles and regulation at the BBB, and summarize recent findings on the P-gp/BCRP teamwork in restricting brain penetration of anti-cancer drugs.

1B.2 P-glycoprotein in Brain Cancer

1B.2.1 History

In 1976, Rudy Juliano and Victor Ling discovered a high molecular weight membrane glycoprotein in mutant cancer cells that appeared to alter membrane permeability for chemotherapeutics, and consequently named it P-glycoprotein ("permeability glycoprotein"; (17)). Shortly afterwards it became clear that P-glycoprotein (P-gp) is a highly potent ATP-driven efflux transporter that actively pumps its substrates out of cells, even against a concentration gradient (18). This discovery was groundbreaking because it provided the first explanation for treatment failure due to resistance to multiple chemotherapeutics, which is a frequently observed phenomenon in cancer.

Several years later, in 1989, P-gp protein expression was detected at the human blood-brain barrier (19, 20) and subsequent studies confirmed the presence of P-gp in the luminal (apical) membrane at the blood-brain barrier of dogfish, killifish, mouse, rat, cat, dog, monkey, pig, and cow (20-30). In addition, P-gp was found in primary brain tumors and is now recognized to be a critical transporter that conveys resistance to a large number of anti-cancer drugs, for example taxanes, vinca-alkaloids, etoposide and analogues, anthracyclines, lanafarnib, imatinib, and topotecan (31, 32). Thus, P-gp has been a focus of blood-brain barrier, brain tumor, and drug delivery research for almost two decades.

1B.2.2 P-glycoprotein Inhibition in Brain Cancer

One strategy to improve brain delivery of anti-cancer drugs is to directly block P-gp transport function at the blood-brain barrier by using transporter inhibitors. The first P-gp

inhibitor was found by serendipity in 1981 by Tsuruo *et al.*, who showed that verapamil, a calcium channel blocker, inhibits P-gp-mediated drug efflux in resistant tumor cells, thereby overcoming drug resistance (33). As a result, over the years numerous chemicals have been screened for their potential to inhibit P-gp, and a variety of inhibitors were developed that differ in potency, selectivity, and side effects (34, 35). However, only a few compounds have been tested for their potential to enhance drug delivery to the brain. The first proof-of-principle that P-gp inhibition can be used to treat brain cancer came from a study in nude mice with intracerebrally implanted human U-118 MG glioblastoma (36). In this study, Fellner *et al.* identified P-gp as the major factor in limiting the anti-cancer therapeutic paclitaxel from crossing the blood-brain barrier and permeating into the CNS (36). Consistent with this, treating glioblastoma-bearing mice with paclitaxel had no effect on tumor size but pretreating mice with the P-gp inhibitor PSC833 (valspodar) increased paclitaxel brain levels and reduced tumor size by 90% (36). Subsequent studies using the P-gp inhibitors cyclosporine A, elacridar (GF120918), tariquidar (XR9576), and zosuquidar (LY335979) confirmed these findings and demonstrated that P-gp inhibition increases paclitaxel brain levels (37-40). A recent study also demonstrated that oral, bi-weekly co-administration of the new P-gp inhibitor HM30181A with paclitaxel decreased tumor volume of K1735 melanoma brain metastases and U-87 MG glioblastoma in cancer animal models (41).

Thus, direct P-gp inhibition improves brain drug delivery of some anti-cancer drugs and treatment of brain tumors in animal models. However, this approach has never been tested in humans and it remains to be demonstrated if the translation can be made.

1B.2.3 Targeting P-gp Regulation

In this review, we will also comment on signaling pathways that affect P-gp and BCRP at the blood-brain and blood-tumor barriers, in brain tumors and brain cancer stem cells and that could potentially be used to improve delivery of chemotherapeutics. In this context, the goal of targeting transporter regulation is to down-regulate transporter expression and/or functional activity, thereby reducing drug efflux and overcoming drug resistance.

The field of blood-brain barrier transporter regulation is relatively new and only few studies have been conducted. The first study demonstrating P-gp down-regulation at the blood-brain barrier was published in 2004. This study focused on ET-1 signaling through the ETB receptor, NOS, and PKC, which rapidly decreased P-gp activity in isolated rat brain capillaries (42). Another report showed that blood-brain barrier P-gp is regulated by the inflammatory mediators LPS, TNF-α, and ET-1, which activated TLR4, TNFR1, ETB receptor, NOS, and PKC, leading to reduced P-gp activity (43). In a follow-up study, Rigor *et al.* identified PKC beta (I) as the responsible PKC isoform for down-regulation of P-gp activity in this pathway (44). Importantly, this study provides proof-of-principle that targeting PKC beta (I) increases brain uptake of the P-gp substrate verapamil.

In another study, Hawkins *et al.* made a similar observation using vascular endothelial growth factor (VEGF; (45)). It was shown that VEGF decreased P-gp activity in rat brain capillaries via activation of flk-1 and Src, likely through Src-mediated phosphorylation of caveolin-1. This finding implies that P-gp activity could be acutely diminished in pathological conditions associated with increased brain VEGF expression and that VEGF/Src signaling at the BBB could be targeted to decrease P-gp activity (45).

Together, two signaling pathways have been identified that could potentially be used to down-regulate P-gp transport activity at the blood-brain barrier; one involves signaling of inflammatory mediators through PKC beta(I), the other one involves VEGF signaling though flk-1 and Src. It remains to be demonstrated if targeting these pathways improves delivery of chemotherapeutics across the BBB and into brain tumors.

1B.3 BCRP in Brain Cancer

1B.3.1 History

In 1998, more than 20 years after the discovery of P-gp, Doyle *et al.* cloned the ABC transporter breast cancer resistance protein (BCRP, MXR: mitoxantrone resistance protein, ABCP1) from a multidrug-resistant human breast cancer cell line (46). Four years later, in 2002, two groups found BCRP to be physiologically expressed in brain capillary endothelial cell cultures and BCRP was localized at the luminal membrane of rat and human brain capillaries (47-49). BCRP has also been detected at the human, cow, rat, and mouse blood-brain barrier (49-52). In addition, BCRP is highly expressed at the plasma membrane of tumor stem cells (53, 54), where it could be involved in stem cell differentiation, protection against xenobiotics, and cancer cell survival under hypoxic conditions (55). Little is known about BCRP expression in brain cancer. In primary CNS lymphoma, BCRP protein expression and transport activity have been shown to be down-regulated (56). In contrast, in neuroepithelial tumors such as ependymomas and in glioma tumor stem-like cells BCRP protein and activity are highly up-regulated, causing multidrug resistance (57-59).

At the functional level, BCRP is a half transporter that works as a homodimer and

possibly as a heterodimer with other ABCG half transporter isoforms (48). A significant overlap in substrate specificity between P-gp and BCRP has been demonstrated (60, 61), and anti-cancer drugs handled by BCRP include tyrosine kinase inhibitors (imatinib, nilotinib, gefitinib, erlotinib, dasatinib, sorafenib, lapatinib, apatinib, and tandutinib; (12, 13, 62-65), topotecan, irinotecan, epirubicin, doxorubicin, daunorubicin, and mitoxantrone (66, 67). Studies show that BCRP restricts these chemotherapeutics from permeating across the blood-brain barrier and penetrating into brain tumors. As with P-gp, BCRP-mediated drug resistance in brain tumors is in part due to transporter up-regulation at the blood-tumor barrier contributing to reduced delivery and efficacy of anti-cancer drugs (59).

1B.3.2 BCRP Inhibition in Brain Cancer

Few compounds have been identified that specifically inhibit BCRP. Fumitremorgin C (FTC), a fungal toxin, was the first reported BCRP inhibitor (68), but is not suitable for *in vivo* studies due to severe neurotoxic side effects. This lead to the development of the FTC-derivatives Ko132, Ko134, and Ko143 that are 2-3-fold more potent, less toxic, and designed for use *in vivo* (69). Recent efforts focused on tyrosine kinase inhibitors such as imatinib, nilotinib, gefitinib, and erlotinib that directly interact with BCRP at the substrate binding site and that block ATPase activity of the transporter (64). These compounds have a unique pharmacologic profile in that they are effective chemotherapeutics, as well as potent BCRP inhibitors and transporter substrates. In this regard, *in vivo* studies showed that BCRP, together with P-gp, limited brain uptake of imatinib and that BCRP inhibition significantly increased imatinib brain penetration (70).

In a similar study, Breedveld *et al.* demonstrated that inhibition of BCRP with pantoprazole increased imatinib brain levels 1.8-fold (71). However, co-administration of the P-gp and BCRP inhibitor elacridar improved brain penetration of imatinib by 4.2-fold (71). The same group also showed that dual BCRP/P-gp inhibition using elacridar improved oral bioavailability and CNS penetration of anti-cancer drugs (72). While these studies demonstrate the importance of blood-brain barrier BCRP for brain uptake of anti-cancer drugs, they also show that for some compounds inhibition of either BCRP or P-gp alone is not sufficient to increase delivery into the brain.

1B.3.3 Targeting BCRP Regulation

Various signaling pathways have been shown to down-regulate BCRP, which is expected to improve anti-cancer drug delivery into brain tumors. In this regard, it was demonstrated that estrogens play a role in BCRP regulation. Imai *et al.* showed that estrone and 17β-estradiol (E2) reverse BCRP-mediated drug resistance (73) and that E2 triggers post-transcriptional down-regulation of BCRP in human breast cancer cell lines (73). Ee *et al.* identified an estrogen response element (ERE) in the BCRP promotor region and showed ERE activation by binding of the E2/estrogen receptor α complex, which up-regulated BCRP mRNA expression (74). From this study, however, it is unclear if BCRP protein expression and/or transport activity were also affected by ERE activation.

Other studies that were conducted in various tissues reported BCRP regulation through the PI3K/Akt signaling pathway (75, 76). In these studies, PI3K/Akt signaling triggered BCRP internalization and translocation from the plasma membrane to the cytoplasmic

compartment in stem cells and renal epithelial cells and was involved in regulating BCRP expression (75, 76).

With regard to brain cancer, Bleau *et al.* published a study showing PTEN/PI3K/Akt regulation of BCRP activity in glioma tumor stem-like cells (57, 58). In these cells, activation of Akt lead to BCRP translocation from the cytoplasm to the plasma membrane and increased BCRP-mediated efflux of anti-cancer drugs, which contributed to drug resistance and tumorigenicity. These findings are interesting considering recent studies where we demonstrated E2-mediated BCRP regulation in isolated brain capillaries and established a link between E2 and PTEN/PI3K/Akt signaling (50, 77). We showed that E2 signaling through ERβ, PTEN/PI3K/Akt and GSK3 triggered BCRP internalization from the brain capillary plasma membrane, which was followed by proteasomal degradation of the transporter and reduced BCRP functional activity and protein expression (50, 77). These findings suggest that PTEN/PI3K/Akt-mediated up-regulation of BCRP activity in glioma tumor stem-like cells that Bleau *et al.* observed (57, 58) could potentially be blocked, which may be one possibility to reduce BCRP-mediated resistance to chemotherapeutics at the level of the blood-brain and blood-tumor barriers. However, despite these studies it remains to be demonstrated if targeting BCRP regulation at the blood-brain barrier, in brain tumors, and/or in brain tumor stem cells is a valid strategy to improve drug delivery of chemotherapeutics into the CNS.

1B.4 P-gp and BCRP in Brain Cancer

1B.4.1 Two Gatekeepers Team Up at the Blood-Brain Barrier

The discovery of BCRP in brain endothelial cells changed the long standing opinion that P-gp is the sole important transporter responsible for efflux of drugs at the blood-brain barrier. However, BCRP expression at the BBB has not been unequivocally correlated to low brain penetration of all BCRP substrates. For example, Lee *et al.* conducted *in situ* brain perfusion studies using the BCRP substrates dehydroepiandrosterone sulfate and mitoxantrone and reported that brain penetration of the two compounds was not increased in *Bcrp1*$^{-/-}$ (BCRP knockout) mice (78). Similarly, Giri and coworkers showed that BCRP mediated efflux of the antiretroviral drugs abacavir and zidovudine *in vitro* (79). However, despite the absence of BCRP, brain uptake of these two compounds was not elevated in *Bcrp1*$^{-/-}$ mice (80). One conclusion drawn from these studies was that BCRP played a minor role in drug efflux at the BBB and another study showed that interaction of BCRP with substrates *in vitro* rarely translates to visible effects at the blood-brain barrier *in vivo* (81).

In contrast, other studies demonstrated BCRP transport activity at the BBB. Cisternino and colleagues showed that BCRP limits prazosin and mitoxantrone, two prototypical BCRP substrates, from penetrating into the brain (82). Likewise, Enokizono *et al.* and Breedveld *et al.* reported that brain distribution of drugs increased significantly in *Bcrp1*$^{-/-}$ mice (71, 83). Moreover, we recently reported that sorafenib transport into the brain was significantly increased in *Bcrp1*$^{-/-}$ mice (13).

Taken together, conflicting results on BCRP-mediated drug efflux from the brain initiated a controversy on the role of this transporter at the blood-brain barrier that lead to further studies. With the development of the P-gp/BCRP knockout mouse (*Mdr1a/1b*$^{-/-}$ *Bcrp1*$^{-/-}$; (84)), researchers have been provided with the opportunity to study the combined impact of these two efflux transporters on the delivery of drugs across the BBB. de Vries *et al.* showed that brain uptake of topotecan, a substrate for both P-gp and BCRP, was not increased in mice lacking BCRP (*Bcrp1*$^{-/-}$)(15). In P-gp knockout mice (*Mdr1a/1b*$^{-/-}$) topotecan brain levels increased slightly by 1.5-fold. In contrast, in mice lacking both P-gp and BCRP (*Mdr1a/1b*$^{-/-}$*Bcrp1*$^{-/-}$), topotecan brain uptake was increased by more than 12-fold. Thus, absence of both P-gp and BCRP resulted in an effect that was significantly larger than the combined effects from the single transporter knockout mice. This finding was confirmed by Polli *et al.* using lapatinib in P-gp/BCRP knockout mice (16). We have shown the same with dasatinib (14), gefitinib (12) and sorafenib (13). Even though these drugs are substrates for both P-gp and BCRP, absence of only one of the transporters did not significantly increase delivery of either drug to the brain, but the greatest enhancement in brain penetration was seen when both transporters were absent or inhibited at the BBB. Several studies now show that this is true for other dual P-gp and BCRP substrates as well (**Table 1.3,** (65, 85, 86)). **Figure 1.4** summarizes recent data by Kawamura *et al.* (87) that demonstrate this phenomenon. These findings suggest that inhibition of either P-gp or BCRP can be compensated by the respective other transporter, and that both transporters "cooperate" with each other in preventing chemotherapeutic drugs from entering the brain.

P-gp and BCRP cooperation implies that absence of either P-gp or BCRP alone does not result in an appreciable increase in brain penetration of dual substrates. In BCRP knockout mice (where P-gp is present), P-gp alone is sufficient to prevent drugs from penetrating into the brain. Likewise, in P-gp knockout mice (where BCRP is present) BCRP alone is sufficient to limit drug uptake into the brain. The greatest enhancement in brain penetration of dual substrates is always seen when both P-gp and BCRP are absent in the combined P-gp/BCRP knockout mice (**Figures 1.4 and 1.5**).

An insight into the mechanism of P-gp/BCRP cooperation can be gained by looking at relative transporter affinities of substrate drugs and relative transporter expression levels at the BBB (assuming protein expression correlates with transport capacity for both transporters). In this regard, Kamiie *et al.* used LC-MS to quantify membrane transporter expression at the mouse BBB and found approximately 5-fold higher P-gp protein levels compared to those of BCRP (88). Significantly higher protein expression levels at the BBB make P-gp appear to be the dominant efflux transporter for many dual substrates that have similar affinities to both P-gp and BCRP. In comparison, due to lower protein expression levels, BCRP-mediated efflux appears to be minor and becomes apparent only when P-gp or both transporters are absent. For example, for a compound with moderate P-gp affinity, higher P-gp expression levels (higher P-gp transport capacity) will compensate for lower transporter affinity, resulting in a pronounced P-gp effect on the efflux of this compound at the BBB. This is true for almost all anti-cancer drugs mentioned above (**Table 1**), with the exception of sorafenib and dantrolene. Both these compounds have a significantly higher affinity for BCRP than for P-gp (13, 86).

Therefore, BCRP is the dominant transporter in keeping these drugs out of the brain and an effect of P-gp on drug penetration is only noticeable in BCRP and P-gp/BCRP knockout mice. Kodaira *et al.* explained P-gp/BCRP cooperation by determining the net contribution of each transporter to the overall efflux of various drugs at the BBB (86). The authors showed that for many dual substrates, P-gp-mediated efflux out of the brain was greater than that by BCRP. On the other hand, P-gp-mediated efflux of dantrolene (high affinity BCRP substrate) was 10-fold lower than BCRP-mediated dantrolene efflux. P-gp/BCRP cooperation at the BBB suggests two fundamental realities. First, these two transporters can significantly affect drug delivery to the brain, thereby influencing drug efficacy. Second, combined inhibition of both P-gp and BCRP is potentially an attractive therapeutic strategy to improve delivery and thus efficacy of substrate drugs in the CNS. Many of the chemotherapeutic drugs mentioned above have been clinically unsuccessful in treating brain cancers. Even though P-gp- and BCRP-mediated cooperative efflux transport is not limited to anti-cancer agents, combined inhibition of both transporters might have the biggest impact in the treatment of brain cancers, where a small increase in drug brain uptake might dramatically improve anti-cancer efficacy.

In summary, absence of either P-gp or BCRP alone does not enhance brain distribution of dual substrates, but genetic or chemical knockout of both transporters is required to significantly increase brain uptake of dual P-gp/BCRP substrate anti-cancer drugs. Thus, current research indicates that P-gp and BCRP team up at the BBB and "cooperate" in preventing dual substrates from entering the brain. This finding has lead to a paradigm shift in the field of BBB transporter research.

1B.4.2 Dual Inhibition of P-gp and BCRP at the BBB

Given the cooperation of P-gp and BCRP at the BBB, developing compounds that are potent inhibitors of both transporters may prove beneficial. Elacridar (GF120918) is a dual P-gp/BCRP inhibitor that has undergone extensive preclinical and clinical evaluation (89). Elacridar has been used in several preclinical studies to inhibit P-gp and BCRP at the BBB with the purpose of enhancing brain distribution of simultaneously administered compounds (40, 90-93). These studies demonstrated that the greater than additive increase in brain penetration is not restricted to P-gp/BCRP knockout animals, but can also be observed with dual P-gp/BCRP inhibitors. For example, Chen *et al.* showed that brain penetration of dasatinib increased dramatically with co-administration of elacridar (14). Likewise, we showed that elacridar significantly enhanced gefitinib and sorafenib brain uptake (12, 13), and de Vries *et al.* published similar findings for topotecan (15). Thus, in preclinical studies, elacridar significantly increased brain penetration of drugs that are dual P-gp/BCRP substrates.

Apart from these compounds that were developed for use as multi-drug resistance reversal agents, several studies examined drugs that are dual P-gp/BCRP substrates to competitively inhibit both transporters. These include several anti-cancer tyrosine kinase inhibitors that have been shown to be substrates for both P-gp and BCRP. *In vitro* studies show that tyrosine kinase inhibitors like erlotinib (94), gefitinib (95), lapatinib (96) and sunitinib (97) inhibit ABC transporters, mainly P-gp and BCRP, and suggest the potential use of these agents as combination therapy to improve drug pharmacokinetics. In 2006, Zhuang *et al.* showed that concurrent administration of gefitinib results in a significant

increase in brain penetration of topotecan (98). The same group showed that gefitinib also increased intracellular tumor exposure to topotecan in a mouse model of glioma (99). In a recent clinical trial, Furman and coworkers used gefitinib to inhibit intestinal P-gp and BCRP and showed that it increased oral bioavailability of irinotecan (100). An interesting study by Nakanishi *et al.* in 2006 showed that imatinib attenuated its BCRP-mediated resistance by suppressing BCRP expression (101). The underlying mechanism for these differential responses involved downstream effects of imatinib leading to decreased phosphorylation of Akt, subsequently leading to reduced BCRP expression (101). Many tyrosine kinase inhibitors have an inhibitory effect on the PTEN/PI3K/Akt signaling pathway. These drugs can thus reduce functional activity and protein expression of ABC transporters, especially BCRP, by blockade of PI3K/Akt signaling. Combination of tyrosine kinase inhibitors with other anti-cancer drugs can therefore have a bimodal effect on ABC transporters, wherein decreased transporter expression/function coupled with competitive inhibition can result in significantly increased drug penetration across the BBB and potentially substantially increased drug levels in brain tumors.

In summary, concurrent treatment with dual P-gp/BCRP inhibitors can improve delivery and thus efficacy of substrate drugs in the CNS. Recent data imply that the use of tyrosine kinase inhibitors to inhibit P-gp/BCRP could have multiple benefits, especially if the anti-cancer agent enhances its own delivery to the brain.

1B.5 Summary, Conclusions and Future Perspectives

Recent brain cancer research demonstrates that the BBB drug efflux transporter BCRP is, in addition to P-gp, another obstacle for delivering chemotherapeutic drugs into the brain. It is now clear that both BCRP and P-gp are important elements of barrier function and their expression and transport activity are regulated by distinct signaling pathways. For many anti-cancer drugs it was shown that inhibition of one of the two transporters is not sufficient to deliver drugs into the brain because of compensation by the respective other transporter. These findings lead to the currently accepted paradigm that P-gp and BCRP work as a "cooperative team of gatekeepers" at the BBB. Such P-gp/BCRP teamwork efficiently protects the brain, but at the same time prevents effective CNS therapy, which poses a tremendous clinical problem for the treatment of brain cancers. Two strategies have been developed to circumvent P-gp and BCRP at the BBB and improve drug delivery to the brain. One strategy is to target signaling pathways that control P-gp and BCRP with the goal of down-regulating transporter function and/or expression. Several pathways have been identified for P-gp and one has recently been found for BCRP. However, a common pathway for both transporters that could potentially be targeted for therapeutic purposes has not been identified yet. A second strategy is combined inhibition of both P-gp and BCRP at the BBB that has been demonstrated to significantly increase brain uptake of chemotherapeutics that are dual P-gp/BCRP substrates. These findings are remarkable and provide a glimpse of hope, but also raise the question: Where do we go from here?

Future research in this field will have to address several points. First, it will be critical to determine if increases in anti-cancer drug brain levels by combined P-gp/BCRP inhibition or down-regulation of transporter function halts brain tumor growth and reduces tumor size. Second, it will also be important to assess if therapeutic effects on brain tumor growth and size translate into prolonged survival. Third, studies will have to demonstrate if inhibiting or down-regulating P-gp/BCPR is a valid therapeutic strategy that can be used chronically over the long term. Fourth, it will have to be tested if P-gp/BCRP inhibition or down-regulation leads to sustained treatment success or if other drug resistance mechanisms will evolve and undo any therapeutic progress made. Lastly, it will have to be shown if an arrest in tumor growth can be treated as a chronic disease or if brain tumors and brain tumor stem-like cells can be completely eradicated. These challenging questions will have to be answered in brain tumor animal models first before translation to patients can occur.

1B.6 Footnotes

We sincerely thank Dr. Bjoern Bauer and Dr. Anika Hartz for their immense contribution towards writing this review article. We thank Britt Johnson for editorial assistance.

Figure 1.4.A. ***Transaxial PET images showing [11C] GF120918 in the brain of a (A) wild-type, (B) P-gp knockout , (C) Bcrp knockout and (D) P-gp/Bcrp knockout mouse***. GF120918 is a substrate for and inhibits both P-gp and BCRP. The radioactivity level is low in the wild-type and BCRP knockout mouse, and increases slightly in the P-gp knockout mouse. The greatest increase in brain radioactivity is seen when both P-gp and BCRP are absent in the P-gp/Bcrp knockout mouse. **Figure 1.4B** shows the quantification of brain radioactivity in the four mouse types.

Figures reproduced with permission from Kawamura et al., Mol Imaging Biol (2010), DOI: 10.1007/s11307-010-0313-1

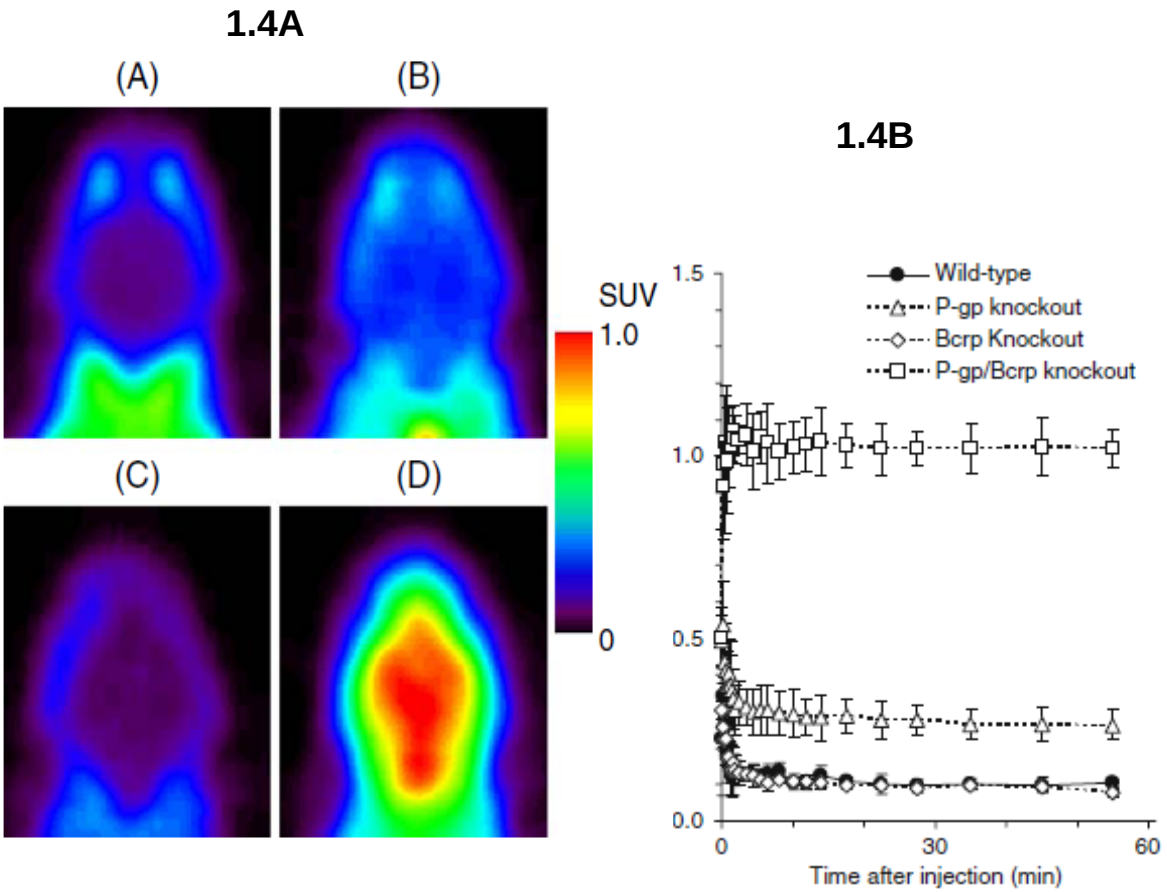

Figure 1.5A. Cooperation of P-gp and BCRP at the Blood-Brain Barrier.

P-gp and BCRP work together at the BBB and restrict brain penetration of dual substrates. Absence of either P-gp or BCRP alone may not result in a significant increase in brain penetration of dual substrates. In BCRP knockout mice (where P-gp is present), P-gp alone is sufficient to prevent drugs from penetrating into the brain. Likewise, in P-gp knockout mice (where BCRP is present), BCRP also is sufficient to limit drug uptake into the brain. The greatest enhancement in brain penetration of dual substrates is always seen when both P-gp and BCRP are absent in the combined P-gp/BCRP knockout mice.

Figure 1.5B. Impact of P-gp/BCRP Cooperation on Brain Distribution of Three Hypothetical Dual Substrates.

Note: for both transporters it is assumed that protein expression correlates with transport capacity.

i. For drugs with similar affinity for both P-gp and BCRP, P-gp is the dominant transporter due to higher P-gp protein expression levels at the BBB (higher transport capacity). Thus, P-gp-mediated drug efflux out of the brain is larger compared to BCRP-mediated efflux. As a result, the drug brain-to-plasma ratio is slightly increased in P-gp knockout mice, but unchanged in BCRP knockout mice. Absence of both P-gp and BCRP in P-gp/BCRP knockout mice results in drug brain levels that are significantly larger than the combined levels from the single transporter knockout mice. This phenomenon has been reported for drugs like dasatinib (14), gefitinib (12), topotecan (15), and lapatinib (16).

ii. For drugs with significantly higher affinity for BCRP than P-gp, BCRP is the dominant transporter in keeping these drugs out of the brain. The P-gp effect is only noticeable in BCRP knockout and combined P-gp/BCRP knockout mice. This has been observed for drugs like sorafenib (13) and dantrolene (86).

iii. For drugs with higher affinity for P-gp than BCRP, larger P-gp expression combined with high transporter affinity results in substantial P-gp-mediated efflux. In BCRP knockout mice, where P-gp is still present, drug brain-to-plasma ratio is unchanged. This has been reported for quinidine (86).

In all three scenarios the largest increase in drug brain-to-plasma ratio is seen when both P-gp and BCRP are absent at the BBB.

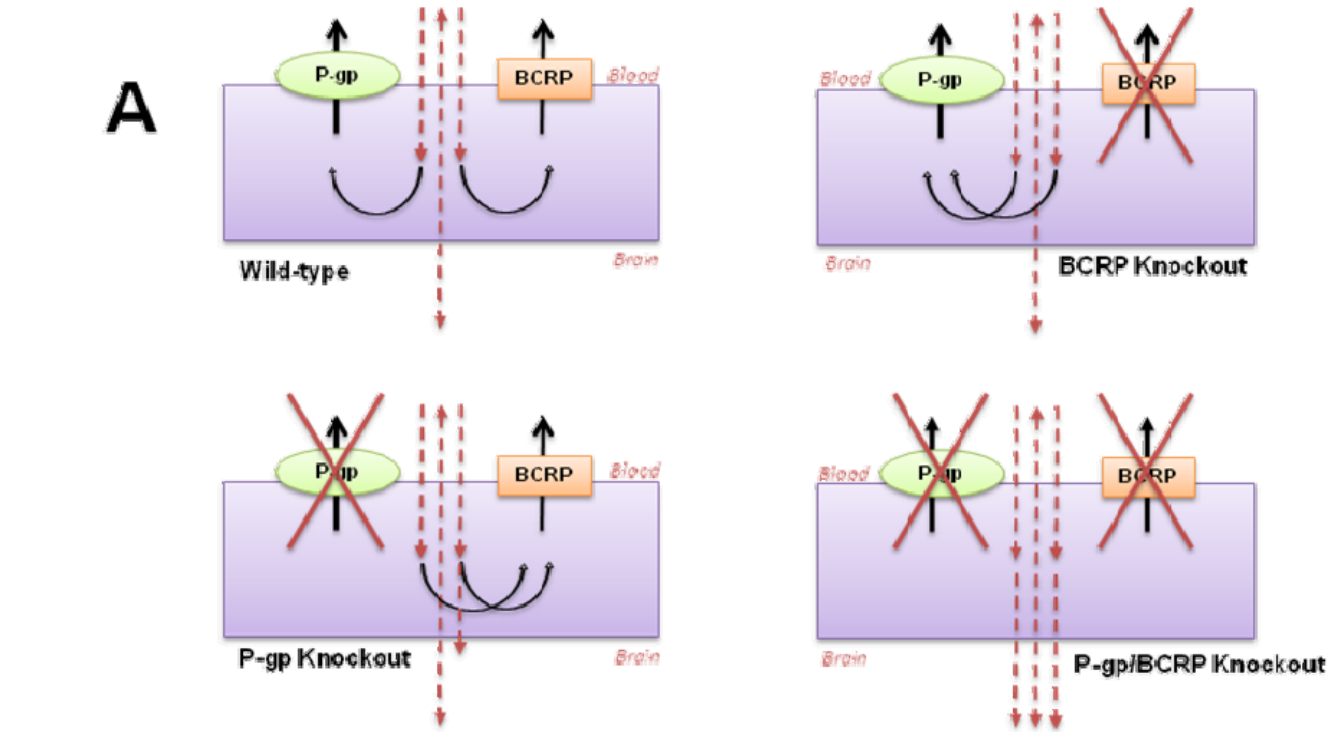
A
P-gp
BCRP
Blood
Brain
Wild-type
BCRP Knockout
P-gp Knockout
P-gp/BCRP Knockout

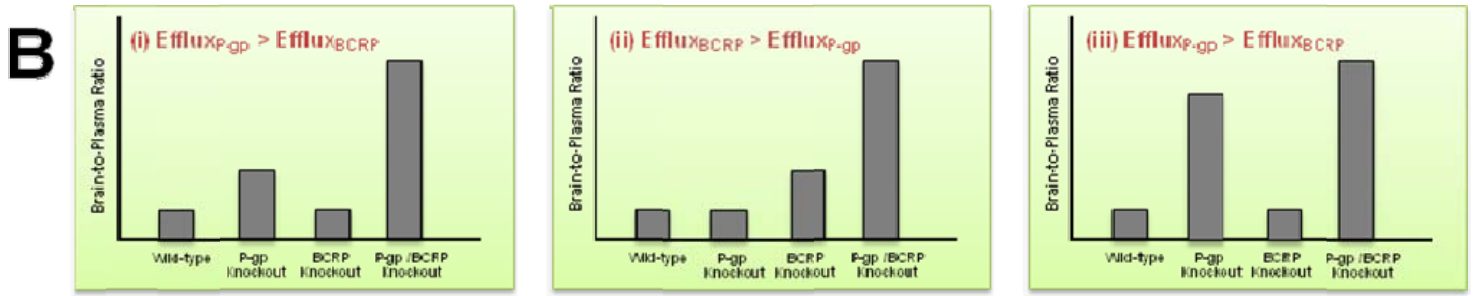
B
(i) Efflux P-gp > Efflux BCRP
(ii) Efflux BCRP > Efflux P-gp
(iii) Efflux P-gp > Efflux BCRP
Brain-to-Plasma Ratio
Wild-type
P-gp Knockout
BCRP Knockout
P-gp /BCRP Knockout

Table 1.3: Brain Distribution of Dual P-gp and BCRP Substrates

The brain-to-plasma ratio does not significantly increase in single P-gp or BCRP knockout mice, where the other transporter is still present and restricts brain penetration. In combined P-gp/BCRP knockout mice, where both P-gp and BCRP are absent, brain penetration of all compounds is dramatically increased.

Drug	**Fold Increase in Brain/Plasma Ratios Relative to Wild-Type Mice**			**Reference**
	P-gp Knockout	**BCRP Knockout**	**P-gp/BCRP Knockout**	
Topotecan	1.5	1.5	12	de Vries *et al.* (15)
Dasatinib	4	1	9	Chen *et al.* (14)
Gefitinib	31.1	13.7	108	Agarwal *et al.* (12)
Sorafenib	1	4	10	Agarwal *et al.* (13)
Erlotinib	2.9	1.2	8.5	Kodaira *et al.* (86)
Imatinib	1	1	12.6	Breedveld *et al.*(71)
Tandutinib	2	1	13	Yang *et al.* (65)
Lapatinib	4	1	42.5	Polli *et al.* (16)
Flavoperidol	3.4	1.2	14.2	Kodaira *et al.* (86)
Mitoxantrone	1.7	1.4	8	Kodaira *et al.* (86)

STATEMENT OF THE PROBLEM

Treatment of glioblastoma multiforme is at a crossroads. One one hand, novel molecularly-targeted agents are being discovered, while on the other, clinical trials evaluating them in GBM are culminating in disappointing failures. Investigations of the repeated failure of potent molecularly-targeted agents have often been focused on the target (changes in the intracellular receptors) or on the therapeutic agent (ineffective drug). However, there has been little emphasis on delivery of the drug to its target, which in essence, is the prerequisite to therapeutic effect. Certainly, restricted drug delivery to the target is a possible explanation for the inefficacy of otherwise potent molecularly-targeted agents in GBM.

The fact that the tumor resides in the brain, a tissue guarded by the blood-brain barrier, makes treatment particularly challenging. The blood-brain barrier, through a combination of protective mechanisms, like tight junctions and efflux transporters, restricts the transport of most large and small molecules into the brain. Unfortunately, many molecularly-targeted tyrosine kinase inhibitors are substrates for two dominant drug efflux transporters, p-glycoprotein and breast cancer resistance protein, and as a result they do not distribute into the brain to a significant extent. Thus potent therapeutic agents often fail to achieve effective concentrations in the target tumor cells that reside within the brain. Therefore therapeutic efficacy will depend on the ability of molecularly-targeted agents to traverse an intact BBB and reach their target in the glioma cells.

Moreover, the infiltrative growth pattern of the tumor in GBM makes it particularly lethal and virtually incurable. GBM is one of the most invasive tumors; tumor cells migrate and infiltrate normal brain tissue centimeters away from the primary tumor. These small nests of cells remain shielded from chemotherapy due to an intact BBB and eventually grow and give rise to the recurrent tumor. Thus it is imperative that these invasive cells are effectively targeted by chemotherapy.

Therapeutic treatment of glioblastoma multiforme thus is limited by two major problems: 1) restricted delivery of potent molecularly-targeted agents to the brain due to active efflux at the BBB, and 2) diffuse infiltration of the tumor into normal brain tissue, where an intact BBB shields the invasive glioma cells from chemotherapy. Improving drug delivery to the invasive glioma cells can lead to increased efficacy of molecularly-targeted agents, thereby improve treatment of gliomas.

RESEARCH OBJECTIVE

The objectives of this project were to:

1. investigate the role of p-glycoprotein and BCRP in limiting the targeted bioavailability of molecularly-targeted agents to the brain, and especially, to the invasive glioma cells.
2. examine strategies to enhance delivery of molecularly-targeted agents to the brain and brain tumor.
3. demonstrate that the blood-brain barrier is intact in growing regions of the tumor and continues to restrict drug delivery to the invasive glioma cells
4. study the influence of drug delivery on efficacy using a novel spontaneous mouse model of glioma.

RESEARCH PLAN

1. We first examined the role of ABC transporters, p-glycoprotein (P-gp) and breast cancer resistance protein (BCRP), on delivery of the tyrosine kinase inhibitors, gefitinib and sorafenib, to the brain (***Chapter II, III***).

2. Based on the findings of the first study, we investigated the cooperation of P-gp and BCRP on the efflux of dual substrates at the BBB and used the brain efflux index method to study the clearance of sorafenib from the brain (***Chapter IV***).

3. We then studied the heterogeneous disruption of the blood-brain barrier in a xenograft model of glioblastoma. We evaluated the delivery of the P-gp/BCRP substrate erlotinib across the BBB to different regions of the brain and its impact on efficacy. We then examined strategies to enhance delivery via pharmacological inhibition of P-gp and BCRP, and studied its effect on erlotinib efficacy at the target (***Chapter V***).

4. Finally, we examined the influence of drug delivery on efficacy of a molecularly-targeted agent in a spontaneous mouse model of glioma. We studied the efficacy of the tyrosine kinase inhibitor, dasatinib, against glioma in transgenic mice that were deficient in P-gp and BCRP (***Chapter VI***).

CHAPTER II

DISTRIBUTION OF GEFITINIB TO THE BRAIN IS LIMITED BY P-GLYCOPROTEIN (ABCB1) AND BREAST CANCER RESISTANCE PROTEIN (ABCG2) MEDIATED ACTIVE EFFLUX

This chapter has been published as a manuscript in Journal of Pharmacology and Experimental Therapeutics, July 2010 vol. 334 no. 1 147-155

Gefitinib is an orally active inhibitor of the epidermal growth factor receptor (EGFR) approved for use in patients with locally advanced or metastatic non-small-cell lung cancer. It has also been evaluated in several clinical trials for treatment of brain tumors such as high-grade glioma. In this study, we investigated the influence of p-glycoprotein (P-gp) and breast cancer resistance protein (BCRP) on distribution of gefitinib to the central nervous system. *In vitro* studies conducted in MDCKII cells indicate that both P-gp and BCRP effectively transport gefitinib limiting its intracellular accumulation. *In vivo* studies demonstrated that transport of gefitinib across the blood-brain barrier (BBB) is significantly limited. Steady-state brain-to-plasma (B/P) concentration ratios were 70-fold higher in the *Mdr*1a/*b*$^{-/-}$*Bcrp1*$^{-/-}$ mice (ratio ~7) compared with wild-type mice (ratio ~ 0.1). The B/P ratio after oral administration increased significantly when gefitinib was co-administered with the dual P-gp and BCRP inhibitor elacridar. We investigated the integrity of tight junctions in the *Mdr*1a/*b*$^{-/-}$*Bcrp1*$^{-/-}$ mice and found no difference in the brain inulin and sucrose space between the wild-type and *Mdr*1a/*b*$^{-/-}$*Bcrp1*$^{-/-}$ mice. This suggested that the dramatic enhancement in the brain distribution of gefitinib is not due to a leakier BBB in these mice. These results show that brain distribution of gefitinib is restricted due to active efflux by P-gp and BCRP. This finding is of clinical significance for therapy in brain tumors such as glioma, where concurrent administration of a dual inhibitor like elacridar can increase delivery and thus enhance efficacy of gefitinib.

2.1 Introduction

Malignant gliomas account for approximately 70% of all new cases of malignant primary brain tumors diagnosed in the United States every year. Glioblastoma Multiforme (GBM) is the most common type of glioma, accounting for approximately 60 to 70% of malignant gliomas (1, 2) and claiming 12,000 lives every year (3). Epidermal growth factor receptor (EGFR) and its variant EGFRvIII play a critical role in the development of an aggressive phenotype of GBM; EGFR amplification, mutation and overexpression are associated with poor prognosis and resistance to therapy (4). Several therapeutic strategies targeting EGFR in GBM have been proposed, including the use of monoclonal antibodies against EGFR or EGFRvIII, vaccine therapies, bispecific antibodies, toxin-linked conjugates and small molecule tyrosine kinase inhibitors (5).

In recent years, several small molecule inhibitors targeting the tyrosine kinase EGFR have been introduced in clinical practice. Gefitinib (Iressa, ZD1839, AstraZeneca Pharmaceuticals) is an orally active compound that is a reversible inhibitor of the tyrosine kinase activity associated with EGFR, blocking EGFR signal transduction pathways (6-8). Despite equivocal results in phase III clinical trials (9, 10), gefitinib was the first drug of its kind to be approved by the United States Food and Drug Administration for monotherapy in patients with locally advanced or metastatic non-small-cell lung cancer after failure of at least one prior chemotherapy regimen. However, results from studies evaluating the use of gefitinib for treatment in GBM have been disappointing. In phase II trials of gefitinib, patients with recurrent or progressive high-grade glioma showed no objective response, with a progression-free survival at 6-months of 13 to 14% (11, 12).

Similarly, no improvement in overall survival was observed in GBM patients at first relapse.

Studies explaining the failure of gefitinib have suggested that the reasons for this lack of efficacy could be related to the heterogeneous molecular characteristics of individual gliomas (13-15) or due to the complexity of signaling pathways such as negative feedback mechanisms and up regulation of alternative pathways (16). However, all of these hypotheses are based on the *a priori* assumption that there is adequate delivery of drug to the invasive tumor cells that can be found several centimeters away from the core tumor mass (17, 18). It is well known that ATP-binding cassette (ABC) transporter proteins, including p-glycoprotein (P-gp/ABCB1) and the breast cancer resistance protein (BCRP/ABCG2), cause multidrug resistance in tumors and actively extrude targeted therapeutics from the brain (19-21). Certainly, the lack of gefitinib delivery to the invasive tumor cells residing in the CNS behind an intact blood-brain barrier (BBB) is a plausible partial explanation for the lack of efficacy seen in GBM. There have been no published reports that indicate that transport of gefitinib across the intact BBB to the brain is limited. Several groups have studied the interaction of gefitinib with drug transport proteins *in vitro* and reported contrasting results. Elkind et al. reported in 2005 that BCRP actively pumps gefitinib and prevents its tyrosine kinase inhibitor activity (22). However shortly thereafter, Leggas et al. reported that gefitinib at clinically relevant concentrations is a potent inhibitor of BCRP and P-gp (23). Given the lack of evidence to prove that gefitinib can cross the BBB to produce therapeutic concentrations in the brain, it is important to study the brain distribution kinetics of gefitinib, and the mechanisms

that may influence adequate delivery of gefitinib to the target invasive tumor cells. Here we have used *in vitro* cell models to demonstrate that gefitinib is a substrate for the ATP transporters P-gp and BCRP. We have also used transporter deficient mice to study the brain distribution of gefitinib. The objective of this study was to establish the interaction of gefitinib with two important transporters of the ABC super family, P-gp and BCRP, and to show that distribution of gefitinib across an intact BBB is limited due to active efflux by these two transport proteins.

2.2 Methods

2.2.1 Chemicals and Reagents

[^{14}C] Gefitinib was kindly provided by AstraZeneca Pharmaceuticals (Chesire, U.K.). Unlabelled gefitinib and dasatinib were purchased from LC Laboratories (Woburn, MA). [^{14}C] Sucrose and [^{3}H] vinblastine were obtained from Moravek Biochemicals (La Brea, CA). [^{3}H] Prazosin was purchased from Perkin Elmer (Waltham, MA). [^{14}C] inulin was purchased from American Radiolabeled Chemicals, Inc. (St. Louis, MO). Elacridar (GF120918, N-[4-[2-(6, 7-Dimethoxy-3, 4-dihydro-1H-isoquinolin-2-yl) ethyl]-5-methoxy-9-oxo-10H-acridine-4-carboxamide) was purchased from Toronto Research Chemicals Inc. (Ontario, Canada). Ko143 (Allen et al., 2002) was kindly provided by Dr. Alfred Schinkel (The Netherlands Cancer Institute, Amsterdam, The Netherlands) and zosuquidar (LY335979, (*R*)-4-((1a*R*,6*R*,10b*S*)-1,2-difluoro-1,1a,6,10b-tetrahydrodibenzo-(*a*,*e*) cyclopropa(*c*) cycloheptan-6-yl)-α-((5-quinoloyloxy) methyl)-1-piperazine ethanol, trihydrochloride) was a gift from Eli Lilly and Co. (Indianapolis, IN). All other chemicals used were obtained from Sigma Chemical Co. (St. Louis, MO).

2.2.2 In vitro studies

Epithelial Madin Darby Canine Kidney (MDCKII) cells were used in all *in vitro* studies. Wild-type (WT) and MDR1-transfected cells were a gift from Dr. Piet Borst (Netherlands Cancer Institute), WT and Bcrp1-transfected cells were kindly provided by Dr. Alfred H. Schinkel (The Netherlands Cancer Institute, Amsterdam, The Netherlands). Cells were cultured in DMEM media supplemented with 10% fetal bovine serum (Sigma-Aldrich, St. Louis, MO), penicillin (100U/ml), streptomycin (100µg/ml) and amphotericin B 250 ng/mL (Sigma-Aldrich, St. Louis, MO) and maintained at 37°C with 5% CO_2 under humidifying conditions.

Intracellular Accumulation Studies in MDCKII Cells

The accumulation studies were done in 24-well polystyrene plates (Thermo Fisher Scientific, Rochester, NY). The wild-type and MDR1 or Bcrp1 transfected cells were seeded at a density of 2×10^5 cells/well. The medium was changed on alternate days until the cells formed confluent monolayers. On the day of the experiment, the medium was aspirated and the monolayer was washed twice with 1 mL prewarmed (37°C) assay buffer. The cells were preincubated with 1 ml of assay buffer for 30 min following which the buffer was aspirated and the experiment was initiated by adding 1 ml of a tracer solution of radiolabeled [^{14}C] gefitinib to each well. The plates were continuously agitated at 60 rpm in an orbital shaker maintained at 37°C for the duration of the experiment. At the end of the 1-hour accumulation period, the assay buffer containing the radiolabeled drug was aspirated from all wells and the cells were washed twice with 1 ml of ice-cold phosphate-buffered saline. Cells were then solubilized using 0.5 ml of a 1%

Triton X100 solution. A 150 μl sample of solubilized cell fractions was drawn from each well in duplicate, 4 ml of scintillation fluid (ScintiSafe Econo cocktail; Fisher Scientific Co., Pittsburgh, PA) was added, and the radioactivity associated with the cell fractions was determined by liquid scintillation counting (LS-6500; Beckman Coulter, Inc., Fullerton, CA). The BCA protein assay (Pierce Biotechnology, Inc., Rockford, IL) was used to determine the protein concentration in the cell fractions and was used to normalize the radioactivity in each well. Drug accumulation in cells was expressed as percentage of the accumulated radioactivity measured in the wild-type control cells (DPM) per microgram of protein. For inhibition studies, the cells were treated with the selective inhibitor (1 μM LY335979 for P-gp; 200 nM Ko143 for BCRP (24, 25)) during both the preincubation and accumulation periods. The stock solutions for all the inhibitors used were prepared in dimethyl sulfoxide (DMSO) and diluted using assay buffer to obtain working solutions, so that the final concentration of

DMSO was less than 0.1%.

2.2.3 Directional Flux across MDCKII Monolayers

Six-well transwells (Corning Inc., Corning, NY) were used in the permeability studies. Cells were seeded at a density of 2×10^5 cells/well on the polyester semipermeable membrane supports and the medium was changed on alternate days until the cells formed confluent monolayers. On the day of experiment, the monolayers were washed with 2 mL prewarmed (37°C) assay buffer. After a 30-min preincubation period, the experiment was initiated by adding a tracer solution of radiolabeled drug (^{14}C-gefitinib) in assay buffer to the donor side (apical side, 1.5 ml; basolateral side, 2.6 ml). Fresh assay buffer was added

to the receiver side and 200 µl was sampled from the receiver compartment at 0, 10, 20, 30, 45, 60, and 90 min. The volume sampled was immediately replaced with fresh assay buffer. Additional samples were drawn at 0 and 90 min from the donor compartment. The amount of radioactivity in the samples was determined using liquid scintillation counting. The apical compartment represented the donor for determination of apical-to-basolateral (A-to-B) flux, whereas for determination of basolateral-to-apical (B-to-A) flux, the donor was the basolateral compartment and the apical compartment was sampled at the aforementioned times. When an inhibitor was used in the flux study, the cell monolayers were preincubated with the inhibitor (1 µM LY335979 or 200 nM Ko143) for 30 min, followed by determination of A-to-B and B-to-A flux with the inhibitor present in both compartments throughout the course of the experiment. The apparent permeability (P_{app}) was calculated by the following equation

$$P_{app} = \frac{\left(\frac{dQ}{dt}\right)}{A * C_0} \qquad \text{..... (1)}$$

where dQ/dt is the mass transport rate (determined from the slope of the amount transported vs. time plot), A is the apparent surface area of the cell monolayer (4.67 cm^2), and C_0 is the initial donor concentration. The efflux ratio was defined as the ratio of P_{app} in the B-to-A direction to the P_{app} in the A-to-B direction and gives an indication of the magnitude of P-gp or BCRP-mediated efflux. The corrected flux ratio (CFR) was determined by dividing the efflux ratio in the Bcrp1 or MDR1 transfected cells by the efflux ratio in the corresponding wild-type cells.

2.2.4 In vivo studies

Animals

All animals used in this study were from Taconic Farms, Inc. (Germantown, NY). Animals used were male *Mdr1a/b*$^{-/-}$ (P-gp knockout), *Bcrp1*$^{-/-}$ (Bcrp1 knockout), *Mdr1a/b*$^{-/-}$*Bcrp1*$^{-/-}$ (triple knockout) and wild-type mice of a FVB/N genetic background and were 8 to 10 weeks old at the time of the experiment. Animals were maintained under temperature-controlled conditions with a 12-h light/dark cycle and unlimited access to food and water. All studies were conducted according to the guidelines set by the *Principles of Laboratory Animal Care* (National Institutes of Health) and were approved by The Institutional Animal Care and Use Committee (IACUC) of the University of Minnesota.

2.2.5 Brain Distribution of Gefitinib in FVB Mice

The dose formulation of gefitinib was prepared on the day of experiment at a concentration of 5 mg/ml. Gefitinib was suspended in 1% polysorbate 80 solution in saline or in a vehicle consisting of 10% DMSO, 35% propylene glycol, 5% ethanol and 50% saline. All mice received a 25 mg/kg oral dose of gefitinib via oral gavage.

In the first study, wild-type and *Mdr1a/b*$^{-/-}$*Bcrp1*$^{-/-}$ mice were administered an oral dose of gefitinib (1% polysorbate 80) following which blood and brain were sampled at 15, 30, 60, 90, 120 and 240 minutes post-dose, n=4 at each time point. At the desired time point, animals were euthanized using a CO_2 chamber. Blood was collected by cardiac puncture and transferred to heparinized tubes. Plasma was isolated from blood by centrifugation at 3000 rpm for 10 min at 4°C. Whole brain was immediately removed from the skull,

rinsed with cold saline and flash frozen in liquid nitrogen. Plasma and brain specimens were stored at -80°C until analysis by LC-MS/MS.

In another study, wild-type mice received an oral dose of gefitinib (10% DMSO, 35% propylene glycol, 5% ethanol and 50% saline) with or without an intravenous dose of 10 mg/kg elacridar (GF120918) 30 minutes prior to administration of gefitinib. Blood and brain were sampled at 15, 30, 60, 90 and 120 minutes post-dose as described above (n=4 at each time point). Gefitinib brain distribution was also studied after oral administration in a group of wild-type, *Mdr1a/b*$^{-/-}$, *Bcrp1*$^{-/-}$ and *Mdr1a/b*$^{-/-}$*Bcrp1*$^{-/-}$ mice and in wild-type mice which received 25 mg/kg LY335979 (20% ethanol, 80% saline), 10 mg/kg Ko143 (20% DMSO, 80% saline) or 10 mg/kg GF120918 (40% propylene glycol, 30% DMSO and 30% saline) intravenously 30 minutes before an oral gefitinib dose. Blood and brain were sampled at 90 minutes post-dose, n=4 at each time point.

2.2.6 Steady State Brain Distribution of Gefitinib

Alzet osmotic mini pumps (Durect Corporation, Cupertino, CA) were used to study the steady state brain and plasma levels of gefitinib. A 70 mg/ml solution of gefitinib in DMSO was filled in the minipumps (model 1003D) and the pumps were equilibrated by soaking them overnight in sterile saline solution at 37°C. The pump operated at a flow rate of 1 μL/hr yielding an infusion rate of 70 μg/hr. Wild-type, *Mdr1a/b*$^{-/-}$, *Bcrp1*$^{-/-}$ and *Mdr1a/b*$^{-/-}$*Bcrp1*$^{-/-}$ mice were anesthetized by intraperitoneal administration of 100 mg/kg ketamine and 10 mg/kg xylazine (Boynton Health Service Pharmacy, Minneapolis, MN). The abdominal cavity was shaved and cleaned. Next, a small midline incision was made in the lower abdomen under the rib cage. A small incision was then made in the

peritoneal wall directly beneath the cutaneous incision and the primed pump was inserted into the peritoneal cavity. The musculoperitoneal layer was closed with sterile absorbable sutures and the skin incision was closed using sterile wound clips. The animals were allowed to recover on a heated pad. Gefitinib half-life in mice has been reported to be approximately 1 hour (26), so an infusion lasting 24 hours was considered to be sufficient to attain steady-state in both brain and plasma. The animals were euthanized 24 and 48 hours post surgery followed by collection of brain and blood as described earlier.

2.2.7 Determination of Gefitinib Concentrations in Plasma and Brain by LC-MS/MS

Prior to analysis, frozen samples were thawed at ambient temperature. Brain samples were homogenized using 3 volumes of 5% bovine serum albumin in phosphate-buffered saline using a tissue homogenizer (Fisher Scientific, Pittsburgh, PA). A 50 µL aliquot of plasma and a 100 µL aliquot of brain homogenate were used for analysis. Plasma and brain samples were spiked with 10 ng of dasatinib (IS) as internal standard followed by liquid-liquid extraction using 200 µL buffer of pH 11 (sodium hydroxide: sodium bicarbonate, 50:50) and 1 mL of ice cold ethyl acetate. Samples were shaken vigorously on a mechanical shaker for 10 minutes and centrifuged at 5000 rpm for 15 minutes at 4°C to separate the organic layer. A volume of 750 µL of the top organic layer was transferred to fresh polypropylene tubes and dried under nitrogen. Samples were reconstituted in 100 µL mobile phase and transferred to glass auto sampler vials. A volume of 5 µL sample was injected in the HPLC system using a temperature controlled autosampling device maintained at 10°C. Chromatographic analysis was performed using an Agilent Model

1200 separation system (Santa Clara, Ca, USA). Separation of analytes was achieved using an Agilent Eclipse XDB-C18 RRHT threaded column (4.6mm ID x 50mm) packed with a 1.8-µm ZORBAX Rx-SIL silica stationary phase (Santa Clara, CA, USA). The mobile phase used for the chromatographic separation was composed of acetonitrile: 20mM ammonium formate (containing 0.1% formic acid, pH adjusted to 4 with ammonium hydroxide) (32:68 v/v), and was delivered at a flow rate of 0.25 mL/min. The column effluent was monitored using a Thermo Finnigan^{TM} TSQ$^{®}$ Quantum 1.5 detector (San Jose, CA, USA). The instrument was equipped with an electrospray interface, and controlled by the Xcalibur version 2.0.7 data system. The samples were analyzed using an electrospray probe in the positive ionization mode operating at a spray voltage of 4500V for both gefitinib and dasatinib (internal standard). Samples were introduced into the interface through a heated nebulized probe at 300°C. The spectrometer was programmed to allow the $[MH]^+$ ion of gefitinib at *m/z* 446.9 and that of internal standard at *m/z* 488 to pass through the first quadrupole (Q1) and into the collision cell (Q2). The collision energy was set at 9V for gefitinib and 16V for dasatinib. The product ions for gefitinib (*m/z* 128.1) and the internal standard (*m/z* 401) were monitored through the third quadrupole (Q3). The scan width and scan time for monitoring the two product ions were 1.5 *m/z* and 0.5s, respectively. The sensitivity of our assay was at least 7.5 ng/ml with a corresponding CV of ~ 10%.

2.2.8 Evaluating Blood-Brain Barrier Integrity in FVB Wild-type and *Mdr1a/b*$^{-/-}$*Bcrp1*$^{-/-}$ mice

A group of FVB wild-type and *Mdr1a/b*$^{-/-}$*Bcrp1*$^{-/-}$ mice received an intravenous dose of 5

μCi [^{14}C] sucrose (n=4). Another group received an intravenous dose of 2.5 μCi [^{14}C] inulin (n=4). Blood and whole brain were harvested at 10 minutes post dose. Brains were homogenized as described earlier. 4 ml of scintillation fluid (ScintiSafe Econo 1 cocktail; Fisher Scientific Co., Pittsburgh, PA) was added to 100 μL of brain or 20 μL plasma specimens and counted using liquid scintillation counting (LS-6500; Beckman Coulter Inc., Fullerton, CA) to determine the radioactivity associated with sucrose and inulin in the samples. Sucrose and inulin concentrations in brain and plasma were determined. Brain space was calculated as the ratio of the brain concentration (nCi/gm) to the plasma concentration (nCi/ml) and expressed as the percentage of brain volume (μL) exposed to the two compounds.

2.2.9 Statistical Analysis

Statistical analysis was conducted using SigmaStat, version 3.1 (Systat Software, Inc., Point Richmond, CA). Statistical comparisons between two groups were made by using two-sample t-test at $p < 0.05$ significance level. Multiple groups were compared by one way analysis of variance with the Holm-Sidak post-hoc test for multiple comparisons at a significance level of $p < 0.05$.

2.3 Results

2.3.1 Intracellular Accumulation of Gefitinib

Accumulation of gefitinib in MDCKII wild-type (WT) and P-gp or Bcrp1-transfected cells was studied. A positive control, ([^{3}H] vinblastine for P-gp or [^{3}H] prazosin for BCRP) was used in all accumulation experiments. As seen in **Figure 2.1A**, [^{3}H] prazosin

accumulation in the Bcrp1-transfected cells was significantly lower compared to the wild-type cells (*p<0.001*). Similarly, accumulation of [^{3}H] vinblastine was significantly lower in the MDR1-transfected cells (*p<0.001*) compared to WT (**Figure 2.1B**). Accumulation of gefitinib in the Bcrp1-transfected cells was significantly lower than that in the wild-type cells (~ 3% of WT control, *p<0.001*). This difference in accumulation between the two cell types was abolished upon treatment with the BCRP specific inhibitor Ko143 (200 nM) (**Figure 2.1A**). In the MDR1-transfected cells, accumulation of gefitinib was 50% lower than that in the wild-type cells (*p<0.001*). Treatment with the P-gp inhibitor LY335979 (1μM) decreased the difference in accumulation (**Figure 2.1B**).

2.3.2 Directional Permeabilites of Gefitinib across MDCKII Monolayers

MDCKII wild-type and Bcrp1 or MDR1-transfected cells were used to determine the directional flux of [^{14}C] gefitinib. **Figure 2.2A** demonstrates the directionality in permeability of gefitinib across wild-type and Bcrp1 monolayers. The B-to-A permeability of gefitinib in the Bcrp1 cells was significantly greater than the permeability in the A-to-B direction *(p<0.001)* yielding an efflux ratio of 55. This directionality in transport was abolished when the cells were treated with Ko143 (200 nM), such that there was no significant difference between the A-to-B and B-to-A permeabilities (efflux ratio = ~ 1). In the wild-type cells, there was no difference in the permeability of gefitinib in either direction, with an efflux ratio of ~ 1 in the control (no Ko143 treatment) and the KO143 treated cells. The corrected efflux ratio was about 34 in the control and 1.2 in the cells treated with the BCRP inhibitor Ko143. In the MDR1-transfected cells, the permeability was significantly enhanced in the B-to-A direction compared to the A-to-B

permeability *($p<0.001$)* with an efflux ratio of 8.4 (**Figure 2.2B**). The P-gp inhibitor LY335979 reversed the directionality in flux due to P-gp, such that there was no significant difference in the permeability of gefitinib in both directions, and the efflux ratio decreased to 1. Again, the B-to-A and A-to-B permeability was similar in the corresponding wild-type cells. The corrected efflux ratio was approximately 5.1 in the control and 0.9 in the cells treated with LY335979.

2.3.3 Brain Distribution of Gefitinib in Wild-type and *Mdr1a/b$^{-/-}$ Bcrp1$^{-/-}$* mice

We investigated the effect of p-glycoprotein and BCRP on the brain distribution of gefitinib using wild-type and transgenic mouse models. Brain distribution after a 25 mg/kg oral dose of gefitinib was determined in FVB wild-type and *Mdr1a/b$^{-/-}$Bcrp1$^{-/-}$* mice. Brain concentrations of gefitinib were significantly lower than the plasma concentrations in the wild-type mice ($p<0.05$), resulting in a brain-to-plasma (B/P) concentration ratio of less than 0.15 at all measured time points (**Figure 2.3**). However, gefitinib brain concentrations were significantly enhanced in the *Mdr1a/b$^{-/-}$Bcrp1$^{-/-}$* mice compared to those in the wild-type mice ($p<0.05$, **Figure 2.4A**). The brain-to-plasma concentration ratio was significantly greater in the *Mdr1a/b$^{-/-}$Bcrp1$^{-/-}$* mice at all the measured time points ($p<0.001$). The B/P ratio was on average 16-fold higher in the *Mdr1a/b$^{-/-}$Bcrp1$^{-/-}$* mice compared to the wild-type mice (**Figure 2.4B**). Plasma concentrations of gefitinib in the *Mdr1a/b$^{-/-}$Bcrp1$^{-/-}$* mice were not significantly different compared to the plasma concentrations in the wild-type mice.

2.3.4 Dual P-gp and BCRP Inhibitor Elacridar Enhances Brain Distribution of Gefitinib

We investigated if pharmacological inhibition of P-gp and BCRP at the blood-brain barrier enhances the brain exposure of gefitinib in FVB wild-type mice. The dual P-gp and BCRP inhibitor elacridar (GF120918) was used for this purpose. Brain gefitinib concentrations were significantly greater in the elacridar treated group compared to control (**Figure 2.5A**). The brain-to-plasma concentration ratio (B/P) was significantly greater in the elacridar treated wild-type mice compared to the control (*$p<0.05$*; **Figure 2.5B**). The brain-to-plasma ratio increased by more than 4–fold when elacridar was administered along with gefitinib, reaching values greater than 1 at the later time points. This indicates that brain distribution of gefitinib can be significantly improved by concurrent administration of a dual inhibitor like elacridar.

2.3.5 Effect of Pharmacological Inhibition and Genetic Deletion of P-gp and BCRP

We studied the brain distribution of gefitinib in wild-type, *Mdr1a/b*$^{-/-}$, *Bcrp1*$^{-/-}$ and *Mdr1a/b*$^{-/-}$*Bcrp1*$^{-/-}$ mice and in wild-type mice that were pretreated with pharmacological inhibitors of P-gp (LY335979), BCRP (Ko143) and the dual P-gp/BCRP inhibitor elacridar. **Figure 2.6** shows the brain-to-plasma ratios of gefitinib when P-gp and BCRP were pharmacologically inhibited or genetically deleted. Use of LY335979 and Ko143 did not result in any significant change in the B/P ratio of gefitinib, however the B/P ratio increased by ~6-fold in the wild-type mice that were pretreated with the dual inhibitor elacridar *($p<0.05$)*. Similarly, in the gene knockout group, the B/P ratio increased by

approximately 4-fold in the *Mdr1a/b*$^{-/-}$ mice *($p<0.05$)*. While there was no change in the B/P ratio in the *Bcrp1*$^{-/-}$ mice, the ratio increased by greater than 18-fold in the *Mdr1a/b*$^{-/-}$ *Bcrp1*$^{-/-}$ mice *($p<0.001$)*.

2.3.6 Steady-State Brain Distribution of Gefitinib

Table 2.1 summarizes the results from steady state brain and plasma distribution of gefitinib after a continuous intraperitoneal infusion. In the wild-type mice, steady-state brain concentrations of gefitinib were 15-fold lower than the corresponding plasma concentrations *($p<0.001$)*. Steady-state brain concentrations increased by 3-fold in the *Bcrp1*$^{-/-}$ and by 9-fold in the *Mdr1a/b*$^{-/-}$mice. In the *Mdr1a/b*$^{-/-}$*Bcrp1*$^{-/-}$ mice, where P-gp and BCRP both were absent, brain concentrations increased dramatically by over 50-fold. The brain-to-plasma ratio was approximately 0.07 ± 0.05 in the wild-type mice, indicating a brain tissue partition coefficient of 10%. The ratio increased to 0.92 ± 0.21 (13-fold) in the *Bcrp1*$^{-/-}$ and to 2.10 ± 0.22 (31-fold) in the *Mdr1a/b*$^{-/-}$mice (*$p<0.001$*. Steady state brain concentrations in the *Mdr1a/b*$^{-/-}$*Bcrp1*$^{-/-}$ mice increased more than 100-fold compared to that in the wild-type mice to reach a value of 7.32 ± 1.11 *(***Figure 2.7***, $p<0.001$*).

2.3.7 Blood-Brain Barrier Integrity in FVB *Mdr1a/b*$^{-/-}$*Bcrp1*$^{-/-}$ mice

The integrity of the BBB in the *Mdr1a/b*$^{-/-}$*Bcrp1*$^{-/-}$ mice was evaluated to ensure that the dramatic increase in brain distribution of gefitinib observed in the triple knockout mice was not a result of a leaky blood-brain barrier (compromised tight junctions). This was done by determining the brain spaces of [^{14}C] sucrose and [^{14}C] inulin. At short time

points postdose, both inulin and sucrose are limited to the vasculature under normal physiological conditions and are therefore used as markers of intravascular space. The brain spaces of [^{14}C] sucrose and [^{14}C] inulin in the *Mdr1a/b*$^{-/-}$*Bcrp1*$^{-/-}$ mice were not statistically different than those in the wild-type mice. The brain sucrose space at 10 minutes was 2.2 ± 0.4 % in the wild-type mice compared to 1.9 ± 0.6 % in the *Mdr1a/b*$^{-/-}$ *Bcrp1*$^{-/-}$ mice. Similarly the brain space of [^{14}C] inulin was 2.0 ± 0.7 % in the wild-type and 2.1 ± 1.1% in the *Mdr1a/b*$^{-/-}$*Bcrp1*$^{-/-}$ mice (**Figure 2.8**). The finding confirmed that there was no change in the integrity of the tight junctions that form the BBB in the *Mdr1a/b*$^{-/-}$*Bcrp1*$^{-/-}$ mice. This suggests that the cumulative change in brain distribution of gefitinib in these mice is due to the simultaneous absence of both drug efflux systems.

2.4 Discussion

The epidermal growth factor receptor (EGFR) pathway has been an attractive target because it is deregulated in a significant fraction of malignant gliomas through overexpression, amplification and activating mutations (12). Moreover, recent studies have demonstrated that EGFRvIII is required for tumor maintenance in glioma (27). The EGFR tyrosine kinase inhibitor gefitinib has been evaluated in a number of clinical trials for GBM, however results have been disappointing (12, 28). The failure of gefitinib raises questions pertaining to delivery of drug to its target. Active efflux at the BBB could prevent drugs from attaining therapeutic levels in the brain and is likely one of the main reasons behind resistance to chemotherapy. It has been shown that several other tyrosine kinase inhibitors are avid substrates for P-gp and BCRP and that their brain distribution is limited due to active efflux out of the brain (29-32). Whether gefitinib

crosses the BBB to achieve therapeutic levels in the CNS is an important question that has remained unanswered. We have raised this question herein and demonstrated that gefitinib is a substrate of the ABC transporters P-gp and BCRP and that these two efflux proteins actively efflux gefitinib at the BBB, thereby limiting its brain penetration. We have further demonstrated that steady-state brain partitioning improved by greater than 70-fold due to absence of both P-gp and BCRP in the *Mdr1a/b*$^{-/-}$*Bcrp1*$^{-/-}$ mice and that inhibition of these two transporters by use of a dual inhibitor like elacridar can be a useful therapeutic strategy to improve brain distribution of gefitinib.

In vitro studies conducted in immortalized MDCKII cells that stably overexpress human P-gp or murine BCRP demonstrated that gefitinib is a substrate of the two efflux pumps. It has been reported that gefitinib is an inhibitor of P-gp and BCRP and that concurrent administration increases the bioavailability of topotecan (23). Our study conclusively shows that gefitinib is a substrate for these two transporters. One explanation for the inhibitory effect seen could be given by the high gefitinib concentrations used by Leggas et al. in the above mentioned study. It is also possible that gefitinib competes with other substrates to bind with P-gp and BCRP and saturates the transporters thus leading to their inhibition.

In vivo studies using FVB wild-type mice showed that CNS distribution of gefitinib across the blood-brain barrier is significantly limited. Brain concentrations were on average 18-fold higher in the *Mdr1a/b*$^{-/-}$*Bcrp1*$^{-/-}$ mice than in the wild-type mice. Steady-state brain-to-plasma ratios increased from ~ 0.07 in the wild-type mice to ~ 7 in the *Mdr1a/b*$^{-/-}$*Bcrp1*$^{-/-}$ mice. This dramatic 100-fold increase in the brain partitioning

indicates the significant impact the two transporters have on the brain distribution of gefitinib.

The dramatic increase in brain gefitinib concentrations in the *Mdr1a/b*$^{-/-}$*Bcrp1*$^{-/-}$ mice suggested that inhibition of P-gp and BCRP might be an effective way to improve brain distribution of gefitinib. Therefore, we studied the influence of the dual P-gp and BCRP inhibitor elacridar on the brain distribution of gefitinib in FVB wild-type mice. Treatment with elacridar resulted in enhanced brain levels of gefitinib in the wild-type mice. This finding demonstrates the improvement in delivery of gefitinib to the brain resulting from pharmacological inhibition of active efflux at the BBB. Interestingly, plasma concentrations of gefitinib were not increased in the *Mdr1a/b*$^{-/-}$*Bcrp1*$^{-/-}$ mice or in the elacridar-treated wild-type mice compared to control wild-type mice, suggesting that under these experimental conditions P-gp and BCRP do not limit oral uptake of gefitinib. This finding is in agreement with other studies which report that oral absorption of TKIs like dasatinib and erlotinib is not influenced by P-gp and BCRP (33, 34).

In the study to determine the relative contribution of P-gp and BCRP in active efflux of gefitinib, pharmacological inhibition of BCRP by Ko143 or genetic deletion in *Bcrp1*$^{-/-}$ mice did not result in any significant increase in brain levels of gefitinib. Brain concentrations and the brain-to-plasma ratios increased by greater than 3-fold when P-gp was absent in the *Mdr1a/b*$^{-/-}$ mice. More importantly, concomitant inhibition of P-gp and BCRP by elacridar resulted in a ~ 6-fold increase in the brain-to-plasma ratio while absence of both transporters in the *Mdr1a/b*$^{-/-}$*Bcrp1*$^{-/-}$ mice had an even greater effect with

the B/P ratio increasing by greater than 18-fold. This indicates that P-gp seems to be the dominant transporter when it comes to efflux of gefitinib from the brain. However, the fact that brain concentrations increase only marginally when P-gp is inhibited or absent, suggests that BCRP efflux may compensate for the loss of P-gp. Moreover, in the steady-state study, the brain-to-plasma ratio increased significantly even in the *Bcrp1*$^{-/-}$ mice. The combined effect of the two transporters is noticeable in the *Mdr1a/b*$^{-/-}$*Bcrp1*$^{-/-}$ mice where gefitinib brain-to-plasma ratio was the highest.

This is consistent with previous reports for dasatinib (30, 31) and other published reports for tyrosine kinase inhibitors, including imatinib and lapatinib (32, 35). The *in vivo* finding that BCRP by itself does not influence brain penetration of gefitinib is in agreement with reports for other TKIs. One explanation for this could be the presence of significantly low levels of BCRP in the rodent and human BBB compared to overexpressing cell lines as reported by Lee et. al. Difference in protein levels can account for the discrepancies between the *in vitro* cell and the *in vivo* models (36). It is also possible that there are differences in the capacities of the two transporters at the BBB where P-gp might seem to play a predominant role at the BBB.

Previous studies have reported similar findings where the brain concentrations of dual P-gp/BCRP substrates increased dramatically in the *Mdr1a/b*$^{-/-}$*Bcrp1*$^{-/-}$ mice (32). This raised questions about the validity of the triple knockout mice as a model system to study drug transport to the CNS. Some of these questions pertain to the integrity of the BBB in these mice. We decided to evaluate this by studying the brain distribution of sucrose and

inulin. Sucrose and inulin do not readily cross membranes and under normal conditions, shortly after systemic dosing, do not enter the brain to any significant extent. A leakier BBB in the *Mdr1a/b*$^{-/-}$*Bcrp1*$^{-/-}$ mice would result in higher brain levels of these two compounds compared to the wild-type mice. We observed no differences in the brain concentrations of [^{14}C] sucrose and [^{14}C] inulin between the wild-type and *Mdr1a/b*$^{-/-}$ *Bcrp1*$^{-/-}$ mice. The brain space was ~2 % for sucrose and inulin in both wild-type and the *Mdr1a/b*$^{-/-}$*Bcrp1*$^{-/-}$ mice. This confirmed that these mice have an intact blood-brain barrier and therefore the dramatically high brain concentrations of substrate drugs in these mice are most probably due to the simultaneous absence of P-gp and BCRP at the BBB, that would not allow for compensatory transport when one or the other is present.

Limited CNS distribution of gefitinib due to active efflux transport at the BBB can be of significance while trying to elucidate the reasons behind the lack of gefitinib efficacy seen in brain tumors like GBM. It has been suggested that delivery of gefitinib across the BBB might not be an issue in GBM since tumor concentrations 10- to 12-fold higher than plasma concentrations have been reported (37, 38). One explanation for this increased tumor penetration of gefitinib can be given by the breakdown of the BBB at the contrast-enhancing tumor core. Also, while the BBB may be disrupted at or near the core, there is increasing evidence to show that it is still intact near the growing edge of the infiltrative tumor (39, 40), the site where invasive tumor initiating cells reside. Tumor recurrence after surgical removal and radio-chemotherapy questions the delivery of drug to the non-tumor containing areas of brain that may only have limited access to the drug. Brain tumor initiating cells residing behind an intact BBB can pose significant delivery

problems and might be one of the main reasons behind the recurrence of tumor after surgery. Despite recent advances in therapy, malignant glioma remains essentially fatal, with a median survival of 10-12 months. There are no studies that examine the failure of gefitinib chemotherapy in GBM that address the lack of drug delivery to the intended molecular target in tumor-initiating cells that reside behind an intact BBB. This lack of adequate delivery may be an important reason for the ineffectiveness of gefitinib in brain tumors like GBM.

In conclusion, we have shown here that the ATP transporters P-gp and BCRP actively efflux gefitinib at the blood-brain barrier and limit its CNS distribution. We have highlighted that gefitinib is another example where P-gp and BCRP can work together to dramatically limit brain distribution of dual substrates. We have also shown that the tight junctions that form the BBB are intact in the *Mdr1a/b*$^{-/-}$*Bcrp1*$^{-/-}$ mice and that the enhanced CNS distribution seen in these mice is due to the absence of P-gp and BCRP. Finally, co administration of the dual P-gp/BCRP inhibitor elacridar was able to significantly enhance brain distribution of gefitinib. This can be of importance in therapy for GBM, where limited distribution to the target tumor cells, i.e., the invasive glioma cells behind an intact blood-brain barrier, might be one of the reasons behind the lack of efficacy seen with gefitinib.

2.5 Footnotes

This work was supported by National Institutes of Health - National Cancer Institute [CA138437] (William F. Elmquist, John R. Ohlfest) and a grant from the Children's Cancer Research Fund at the University of Minnesota (William F. Elmquist, John R. Ohlfest). Financial support for Sagar Agarwal was provided by the Edward G. Rippie Fellowship and the Ronald J. Sawchuk Fellowship in Pharmacokinetics from the Department of Pharmaceutics, University of Minnesota.

Table 2.1. Steady-state brain distribution of gefitinib in wild-type, Mdr1a/b$^{-/-}$, Bcrp1$^{-/-}$ and Mdr1a/b$^{-/-}$Bcrp1$^{-/-}$ FVB mice after a continuous intraperitoneal infusion of gefitinib.

Group	Time	N	Plasma C_{ss} (µg/ml)	Brain C_{ss} (µg/gm)	Brain-to-Plasma Ratio
Wild-type (control)	24 hour	5	0.49 ± 0.17	0.03 ± 0.02*	0.07 ± 0.04
Mdr1a/b$^{-/-}$	24 hour	5	0.14 ± 0.09	0.33 ± 0.20*	2.1 ± 0.2†
Bcrp1$^{-/-}$	24 hour	5	0.09 ± 0.07	0.11 ± 0.11	0.92 ± 0.21†
Mdr1a/b$^{-/-}$Bcrp1$^{-/-}$	24 hour	4	0.24 ± 0.14	1.7 ± 1.0*†	7.3 ± 1.1†
Wild-type (control)	48 hour	4	0.21 ± 0.09	0.01 ± 0.02*	0.10 ± 0.10^{ns}
Mdr1a/b$^{-/-}$Bcrp1$^{-/-}$	48 hour	4	0.19 ± 0.20	1.2 ± 1.2*†	7.1 ± 1.8$^{\dagger ns}$

Mean ± S.D.
** $p<0.05$ compared to plasma, † $p<0.05$ compared to wild-type, ns- not significant compared to 24 hr time point*)

Figure 2.1A. Intracellular accumulation of [^{14}C] gefitinib in MDCKII-Bcrp1 cells.

Accumulation in wild-type (black bar) and *Bcrp1*-transfected (gray bar) cells. Gefitinib accumulation in the *Bcrp1*-transfects was about 30-fold lower compared to that in wild-type cells (* $p<0.001$). This difference in accumulation was abolished when BCRP was inhibited using the specific inhibitor Ko143. Results presented as mean ± S.D., n = 18.

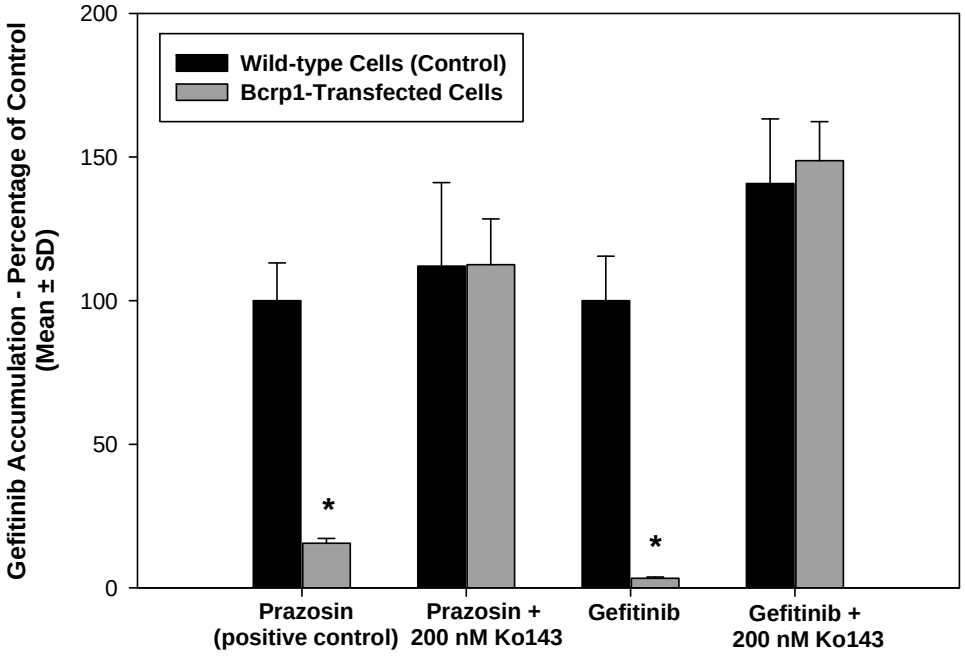

Figure 2.1B. Intracellular accumulation of [^{14}C] gefitinib in MDCKII-MDR1 cells.

Accumulation in wild-type (black bar) and *MDR1*-transfected (gray bar) cells. Gefitinib accumulation was significantly lower in the *MDR1*-transfected cells compared to wild-type (* $p<0.001$). Treatment with LY335979 reduced the difference in accumulation between the two cell types. Results presented as mean ± S.D., n = 18.

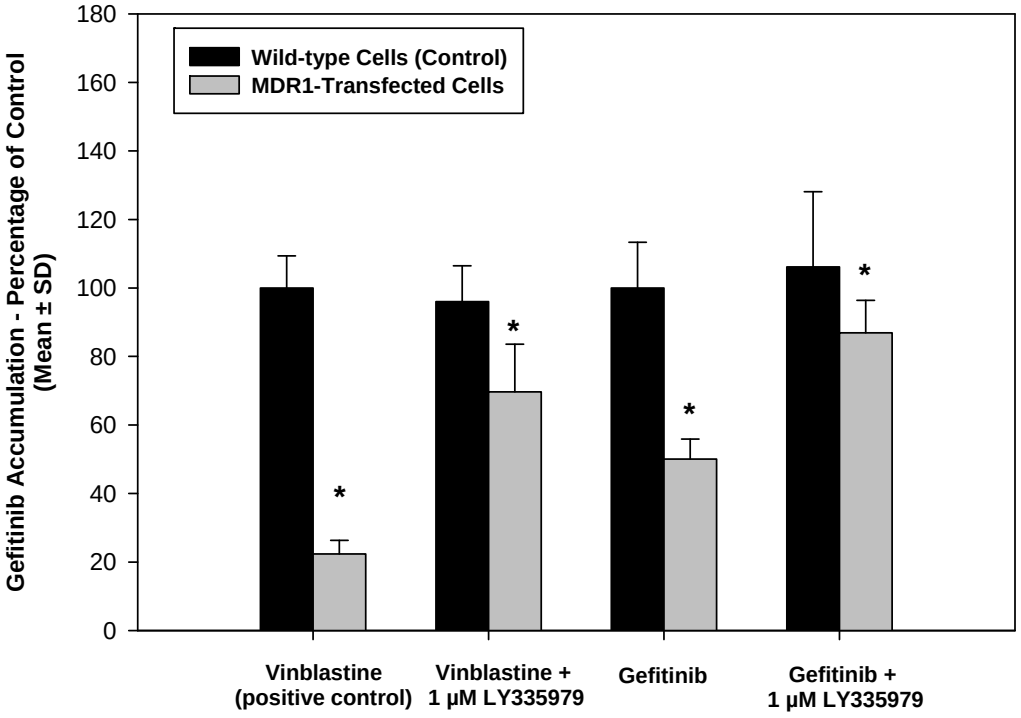

Figure 2.2A. Flux of [^{14}C] gefitinib across MDCKII-Bcrp1 cell monolayers.

Gefitinib permeability across wild-type and Bcrp1-transfected cells. In the Bcrp1-transfected cells, the B-to-A permeability (gray bar) of gefitinib was significantly greater than the A-to-B permeability (black bar) (* $p<0.001$). This directionality in transport was abolished when cells were treated with the BCRP specific inhibitor Ko143. Results presented as mean ± S.D., n = 9.

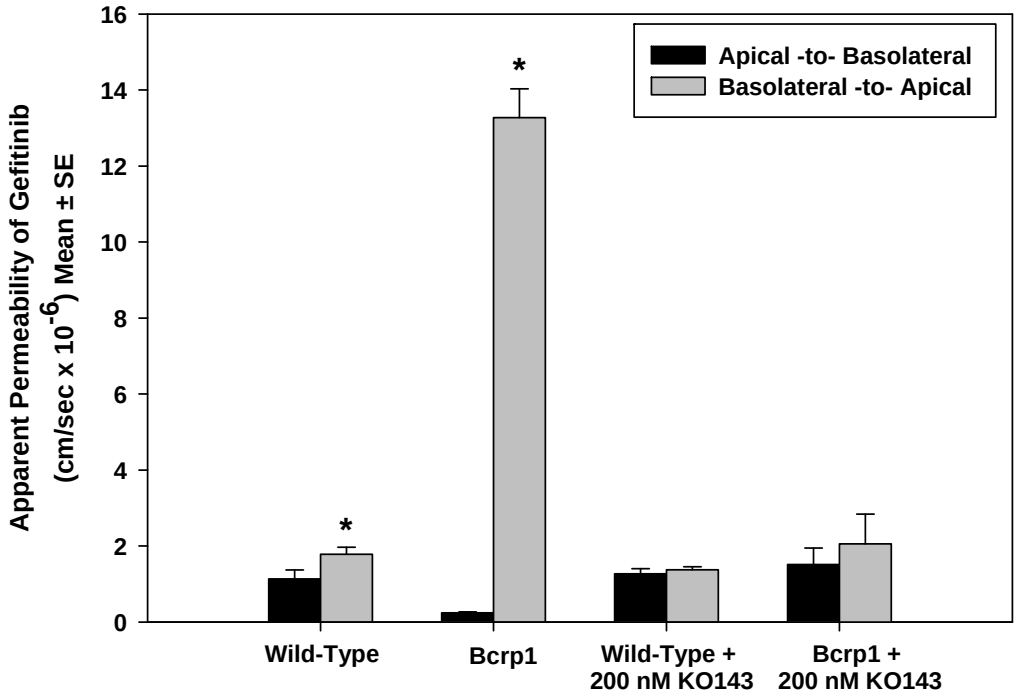

Figure 2.2B. Flux of [^{14}C] gefitinib across MDCKII-MDR1 cell monolayers.

Permeability across wild-type and MDR1-transfected cells. The B-to-A permeability (gray bar) was significantly greater than the A-to-B permeability (black bar) in the MDR1- transfected cells (* *p<0.001*). P-gp inhibition by LY335979 abolished this directionality in transport such that there was no difference in permeability between the two directions. Results presented as mean ± S.D., n = 9.

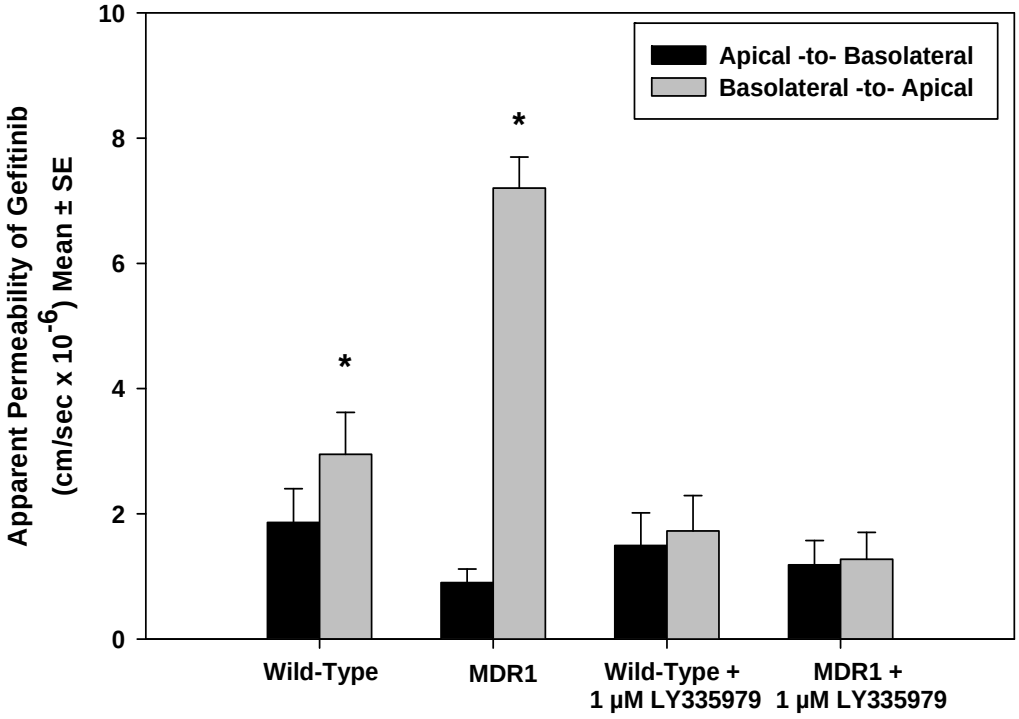

Figure 2.3. Brain and plasma concentrations of gefitinib in FVB wild-type mice after a 25 mg/kg oral dose of gefitinib.

Brain gefitinib concentrations (○) were significantly lower than the plasma concentrations (●) demonstrating the limited brain penetration of gefitinib. (mean ± S.D., n = 4, * *p<0.05 compared to wild-type control*)

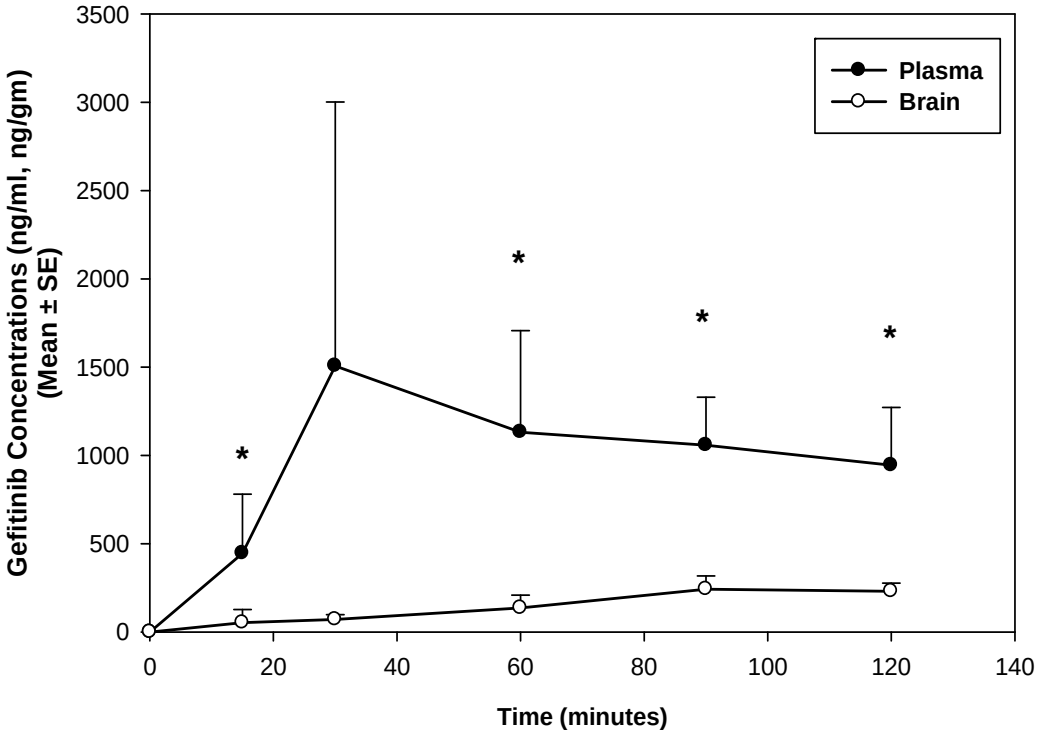

Figure 2.4A. Brain concentrations of gefitinib in wild-type and Mdr1a/b$^{-/-}$Bcrp1$^{-/-}$ FVB mice after an oral dose of 25 mg/kg gefitinib.

Brain concentrations of gefitinib in wild-type (●) and *Mdr1a/b$^{-/-}$Bcrp1$^{-/-}$* (▲) mice. Brain concentrations in the *Mdr1a/b$^{-/-}$Bcrp1$^{-/-}$* mice were significantly greater than the wild-type. Results are represented as mean ± S.D. *(* $p<0.001$, ** $p<0.05$ compared to wild-type control*).

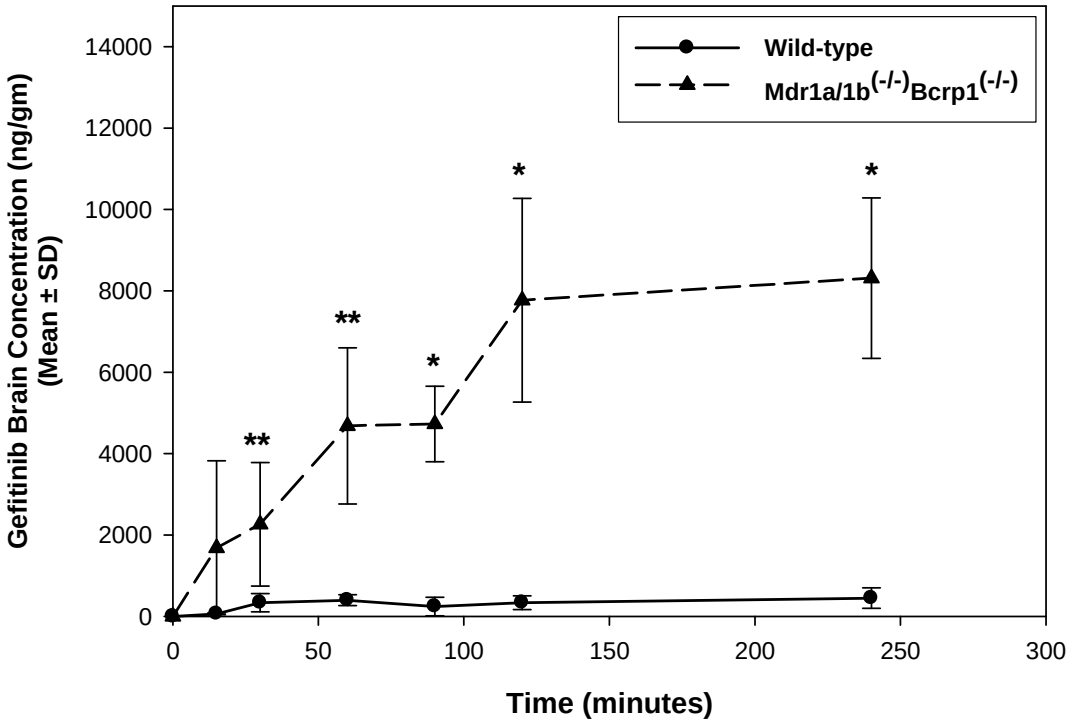

Figure 2.4B. Brain distribution of gefitinib in wild-type and Mdr1a/b$^{-/-}$Bcrp1$^{-/-}$ FVB mice after an oral dose of 25 mg/kg gefitinib.

Brain-to-Plasma (B/P) concentration ratios of gefitinib in wild-type (●) and *Mdr1a/b$^{-/-}$ Bcrp1$^{-/-}$* (▲) mice. The B/P ratios increased by greater than 16-fold in the *Mdr1a/b$^{-/-}$ Bcrp1$^{-/-}$* mice indicating the enhancement in brain distribution of gefitinib due to absence of P-gp and BCRP at the BBB. Results are represented as mean ± S.D. *(* $p<0.001$, ** $p<0.05$ compared to wild-type control*).

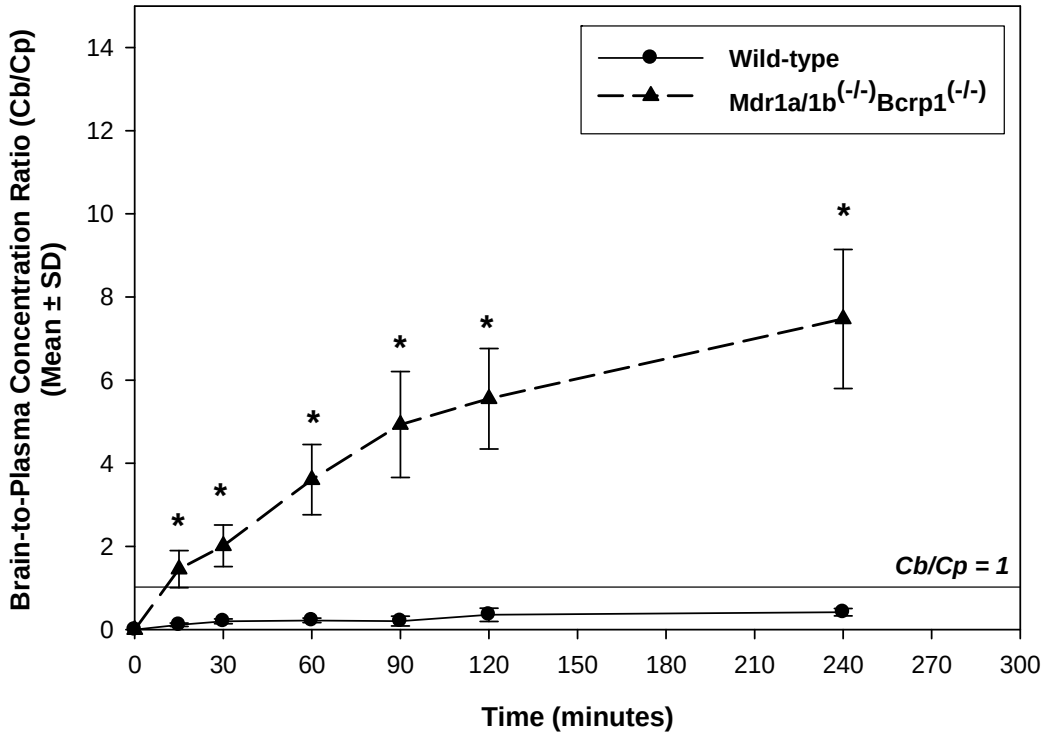

Figure 2.5A. Effect of P-gp & BCRP inhibition on brain concentrations of gefitinib.

Gefitinib brain concentrations in the vehicle treated (●) and elacridar treated (▲) wild-type mice. Brain concentrations increased in the wild-type mice when elacridar was administered prior to gefitinib. Results are represented as mean ± S.D. *(* $p<0.001$, ** $p<0.05$ compared to vehicle control*).

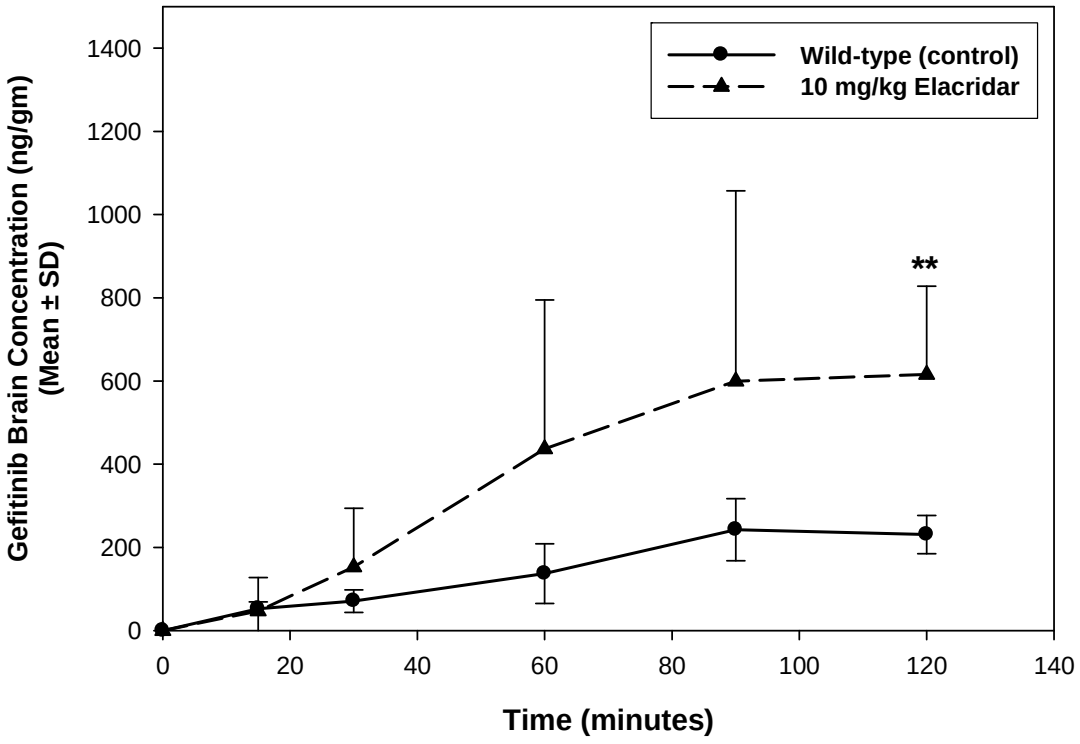

Figure 2.5B. Effect of P-gp & BCRP inhibition on brain distribution of gefitinib.

Brain-to-plasma (B/P) concentration ratios of gefitinib in the vehicle treated (●) and elacridar treated (▲) wild-type mice. The B/P ratios were also significantly greater in the elacridar treated group suggesting that dual inhibitors like elacridar can be used to improve brain penetration of substrate drugs. Results are represented as mean ± S.D. *(* $p<0.001$, ** $p<0.05$ compared to vehicle control*).

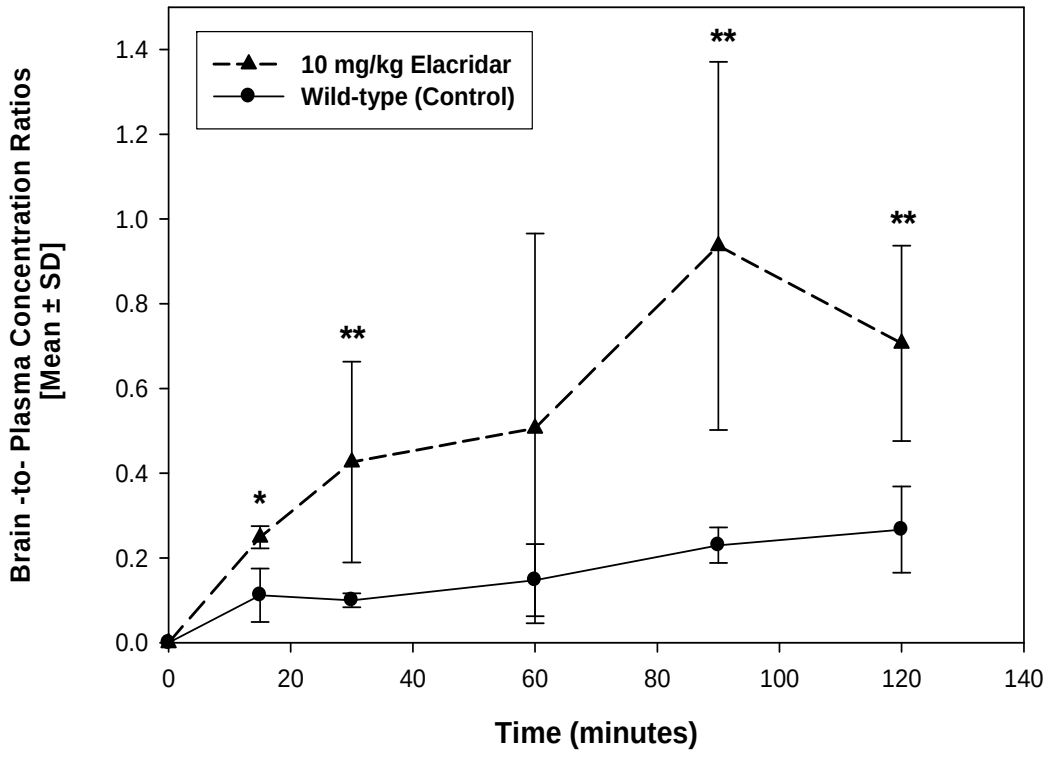

Figure 2.6A. Effect of pharmacological inhibition of drug efflux transporters on brain distribution of gefitinib in wild-type FVB mice.

Wild-type mice received 25 mg/kg gefitinib via oral gavage 30 minutes after i.v. administration of 25 mg/kg LY335979, 10 mg/kg Ko143 or 10 mg/kg GF120918 (elacridar). The values are presented as mean ± S.D. (** $p<0.05$, compared to wild-type control).

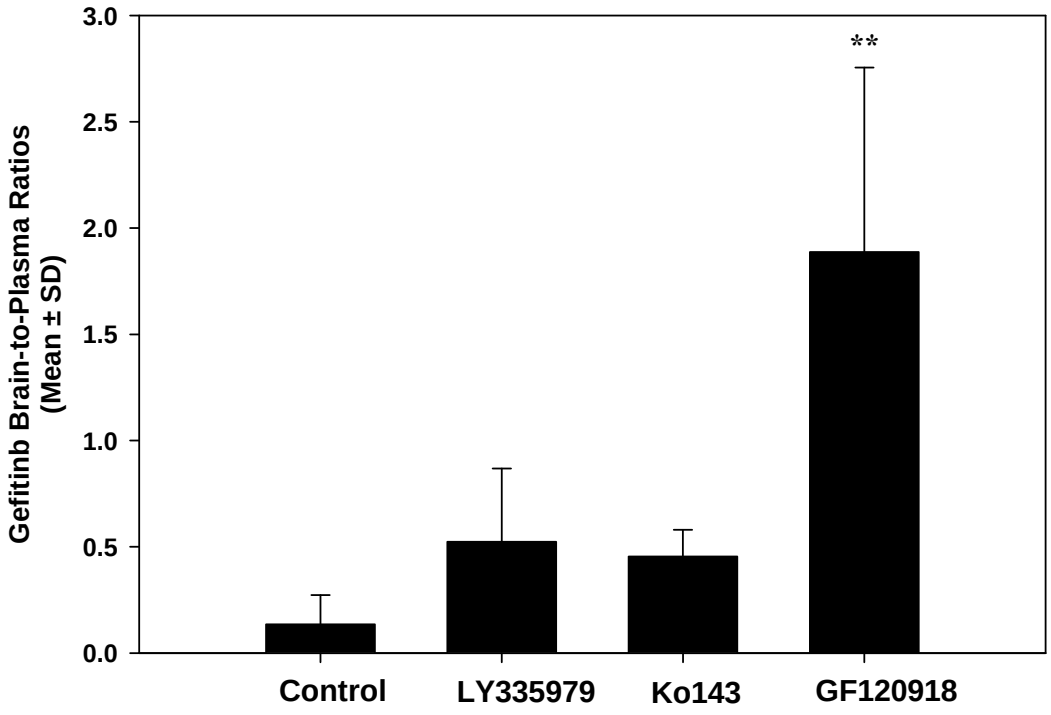

Figure 2.6B. Effect of genetic deletion of drug efflux transporters on brain distribution of gefitinib in FVB mice. Wild-type, *Mdr1a/b*$^{-/-}$, *Bcrp1*$^{-/-}$ and *Mdr1a/b*$^{-/-}$*Bcrp1*$^{-/-}$ mice were administered 25 mg/kg gefitinib. Whole brain tissue was collected at 90 minutes postdose (n=4 at each time point) and analyzed for gefitinib. The values are presented as mean ± S.D. *(** $p<0.05$, compared to wild-type*).

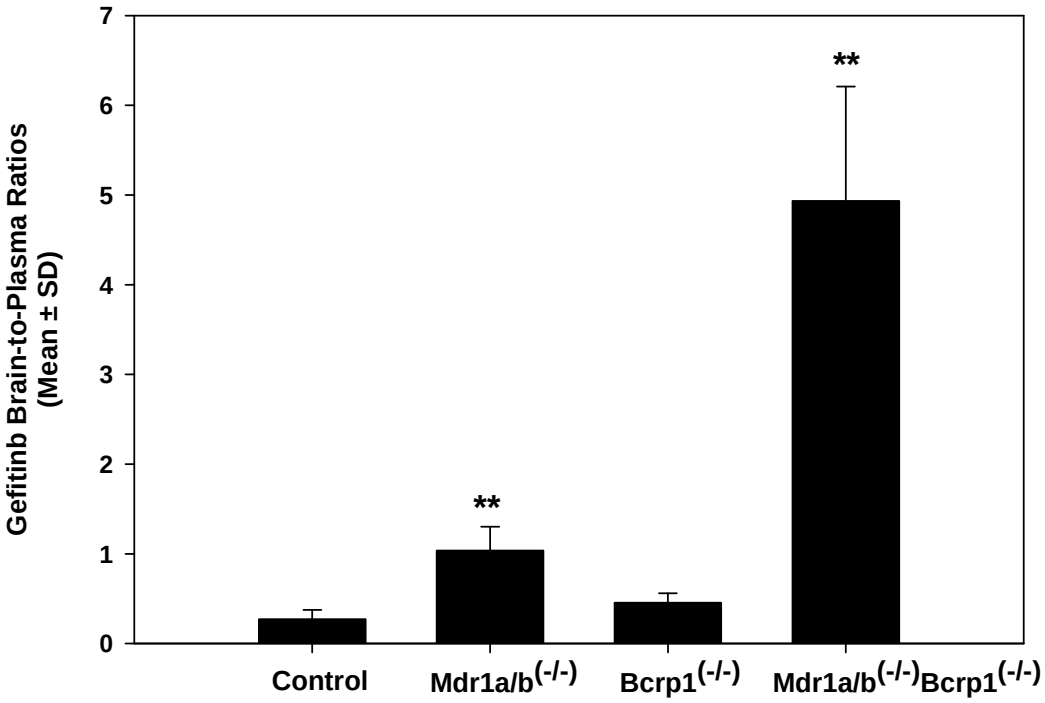

Figure 2.7. Steady-state brain distribution of gefitinib in wild-type, Mdr1a/b$^{-/-}$, Bcrp1$^{-/-}$ and Mdr1a/b$^{-/-}$Bcrp1$^{-/-}$ FVB mice. Steady-state brain-to-plasma ratios in wild-type, *Mdr1a/b$^{-/-}$, Bcrp1$^{-/-}$* and *Mdr1a/b$^{-/-}$Bcrp1$^{-/-}$* mice (n=4-5 per group) after a 70 µg/hr intraperitoneal infusion for 24 hours. The values are presented as mean ± S.D. *(* p<0.001, compared to wild-type*).

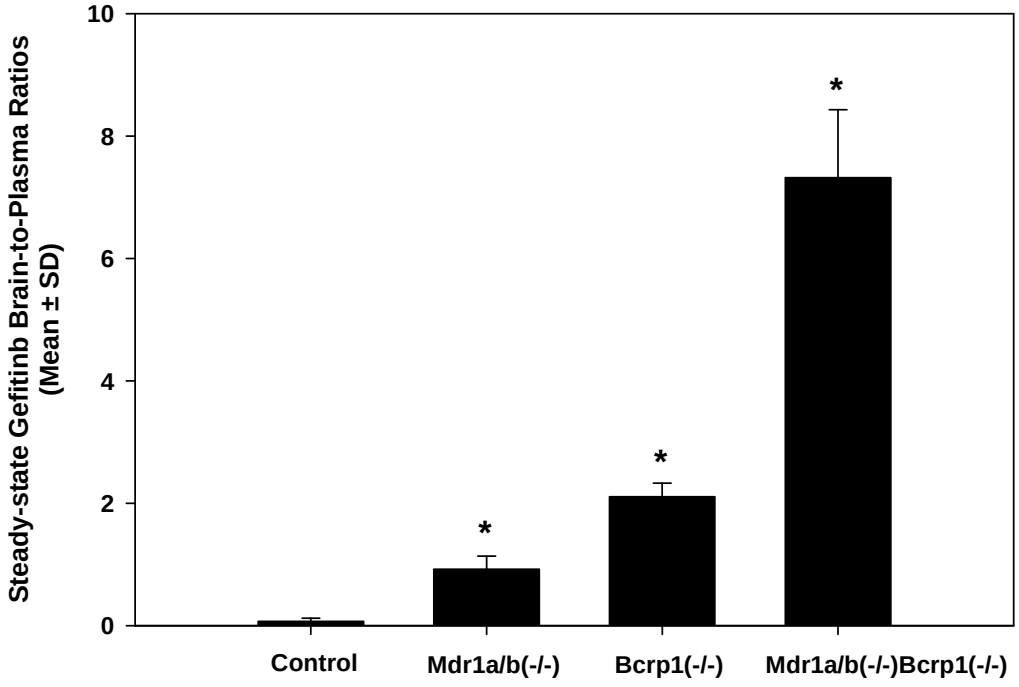

Figure 2.8. Integrity of the blood-brain barrier in Mdr1a/b$^{-/-}$Bcrp1$^{-/-}$ mice.

Brain spaces of sucrose and inulin in wild-type (black bar) and *Mdr1a/b$^{-/-}$Bcrp1$^{-/-}$* (gray bar) mice. The brain spaces of sucrose or inulin in the *Mdr1a/b$^{-/-}$Bcrp1$^{-/-}$* mice were similar to that in the wild-type mice indicating that the BBB is intact in these mice. The values are presented as mean ± S.D (n = 4).

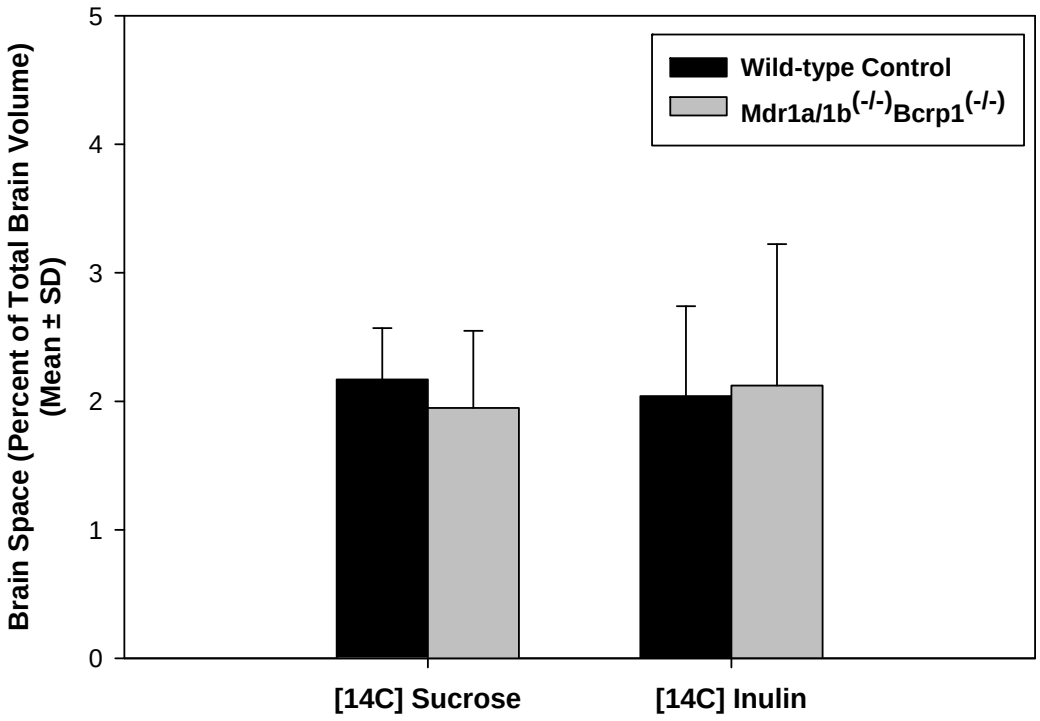

CHAPTER III

ROLE OF BREAST CANCER RESISTANCE PROTEIN (ABCG2/BCRP) IN THE DISTRIBUTION OF SORAFENIB TO THE BRAIN.

This chapter has been published as a manuscript in Journal of Pharmacology and Experimental Therapeutics, January 2011 vol. 336 no. 1 223-233

ATP-binding cassette transporters p-glycoprotein and breast cancer resistance protein have been shown to work in concert to restrict brain penetration of several tyrosine kinase inhibitors. It has been reported that P-gp is dominant in limiting transport of many dual P-gp/BCRP substrates across the blood-brain barrier. This study investigated the influence of P-gp and BCRP on the CNS penetration of sorafenib. In vitro studies showed that BCRP has a high affinity for sorafenib. Sorafenib inhibited P-gp, but did not appear to be a P-gp substrate in vitro. CNS distribution studies showed that transport of sorafenib to the brain was restricted due to active efflux at the BBB. The brain-to-plasma equilibrium-distribution coefficient (AUC_{brain}/AUC_{plasma}) was 0.06 in wild-type mice. Steady-state brain-to-plasma concentration ratio of sorafenib was approximately 0.36 ± 0.056 in the *Bcrp1*$^{-/-}$, 0.11 ± 0.021 in the *Mdr1a/b*$^{-/-}$ and 0.91 ± 0.29 in the *Mdr1a/b*$^{-/-}$*Bcrp1*$^{-/-}$ mice compared to 0.094 ± 0.007 in the wild-type mice. Sorafenib brain-to-plasma ratios increased on co administration of the dual P-gp/BCRP inhibitor elacridar such that the ratio in wild-type (0.76 ± 0.24), *Bcrp1*$^{-/-}$ (1.03 ± 0.33), *Mdr1a/b*$^{-/-}$ (1.3 ± 0.29) and *Mdr1a/b*$^{-/-}$*Bcrp1*$^{-/-}$ (0.73 ± 0.35) mice were not significantly different. This study shows that BCRP and P-gp together restrict brain distribution of sorafenib with BCRP playing a dominant role in the efflux of sorafenib at the BBB. These findings are clinically relevant to chemotherapy in glioma if restricted drug delivery to the invasive tumor cells results in decreased efficacy.

3.1 Introduction

ATP-binding cassette (ABC) transporters limit drug distribution to sites of action. P-glycoprotein (P-gp, *ABCB1*) and breast cancer resistance protein (BCRP, *ABCG2*) are two important members of the ABC-transporters that transport a variety of structurally diverse drugs that are currently used in the clinic (1-3). These two transporters constitute a vital part of the defense mechanism at the blood-brain barrier (BBB), where they prevent the passage of molecules into the brain by effluxing them back into the blood. While they help minimize the neurotoxic side effects of drugs that would otherwise penetrate the brain, they also limit brain distribution of drugs intended to target diseases of the central nervous system (CNS), such as brain tumors. There is considerable overlap in the substrate specificity between P-gp and BCRP (4) and a number of drugs have been reported to be dual substrates for P-gp and BCRP (5-8). Furthermore, it has been postulated that P-gp is the dominant transporter and that BCRP plays a minor role in the efflux of many dual substrates at the BBB (9, 10).

Tyrosine kinase inhibitors (TKI) inhibit tyrosine kinases that are a driving force for several aggressive tumors (11). Studies evaluating the interaction of tyrosine kinase inhibitors with ABC transporters have shown that several TKIs are substrates for and/or inhibit the function of both P-gp and BCRP (5, 6, 12-16). These interactions may alter selected pharmacokinetic processes and hence the tissue distribution of many drugs. This is important when the compounds are used for diseases in tissues such as brain, since active efflux at the blood-brain barrier can limit CNS distribution, thereby limiting their efficacy.

Sorafenib (Nexavar) is an oral, biaryl-urea RAF kinase inhibitor that acts against both vascular endothelial growth factor (VEGF) and platelet-derived growth factor (PDGF) receptors, simultaneously targeting both tumor cell proliferation and angiogenesis (17). It was the first multikinase inhibitor approved by the U.S. Food and Drug Administration for the treatment of patients with renal cell carcinoma (18) and was later granted approval for treatment of unresectable hepatocellular carcinoma. It also inhibits c-KIT, FLT-3 and several other tyrosine kinase receptors, making it a therapeutic option in several solid tumors such as breast, colon and non small cell lung cancer (19). Moreover, given its inhibitory action on STAT3 (20, 21) and its potent anti-angiogenic effect, it is being evaluated in clinical trials for brain tumors such as glioma (22-24). In contrast to other solid tumors, brain tumors reside in what is considered to be a pharmacological sanctuary site, separated from the systemic circulation by the blood-brain barrier. Glioma is highly invasive with tumor cells infiltrating normal brain areas several centimeters away from the tumor core (25, 26). This infiltrative growth pattern makes it difficult to target the invasive tumor cells that reside behind an intact BBB and receive low concentrations of drug due to efflux by P-gp and BCRP (27). Clearly, sorafenib efficacy against brain tumors like glioma depends in part on its ability to cross the BBB and achieve therapeutic concentrations in the brain, especially in the invasive tumor cells. This distribution process is also dependent on the interaction of sorafenib with drug efflux transporters present at the brain endothelial cells.

Results from studies investigating the interaction of sorafenib with efflux transporters have suggested that sorafenib is minimally transported by P-gp or BCRP and that

transporter-related interaction might not alter the systemic pharmacokinetics of sorafenib (15). In contrast, Lagas et al. recently reported that sorafenib is a substrate for both P-gp and BCRP that limit its brain accumulation (28). Furthermore, another recent study reported that P-gp does not affect plasma sorafenib exposure and might not limit transport of sorafenib across the BBB (29). Therefore, the interaction of sorafenib with transporters in the BBB is not fully elucidated. In the current study, we investigated whether sorafenib, like many other TKIs, is a substrate for P-gp and BCRP and whether these two transporters prevent sorafenib from traversing the BBB, thereby limiting its distribution to the CNS.

This aim of this study was to identify and better understand the interaction of the multikinase inhibitor sorafenib with P-gp and BCRP and to examine the effect of this interaction on the transport of sorafenib to the brain. This is of particular importance for treatment of invasive brain tumors like glioma, as subtherapeutic concentrations in the brain would limit the effectiveness of therapy at the invasive sites.

3.2 Materials and Methods

3.2.1 Chemicals and Reagents

[^{3}H] sorafenib (3.5 Ci/mmol, purity - 98.4 %), [^{3}H] mitoxantrone (3 Ci/mmol, purity - 95.1 %) and [^{3}H] vinblastine (18.2 Ci/mmol, purity - 97.4 %) were purchased from Moravek Biochemicals (La Brea, CA). [^{3}H] prazosin (70 Ci/mmol, purity - 97 %) was obtained from Perkin Elmer (Waltham, MA). Unlabelled sorafenib tosylate and tyrphostin (AG1478) was purchased from LC Laboratories (Woburn, MA). Elacridar

(GF120918, N-[4-[2-(6, 7-Dimethoxy-3, 4-dihydro-1H-isoquinolin-2-yl) ethyl]-5-methoxy-9-oxo-10H-acridine-4-carboxamide) was purchased from Toronto Research Chemicals, Inc. (Ontario, Canada). Ko143 ((3S,6S,12aS)-1,2,3,4,6,7,12,12a-Octahydro-9-methoxy-6-(2-methylpropyl)-1,4-dioxopyrazino[1',2':1,6] pyrido [3,4- b]indole-3-propanoic acid 1,1-dimethylethyl ester) was generously provided by Dr. Alfred Schinkel (The Netherlands Cancer Institute, Amsterdam, The Netherlands) and zosuquidar (LY335979, (*R*)-4-((1a*R*,6*R*,10b*S*)-1,2-difluoro-1,1a,6,10b-tetrahydrodibenzo-(*a*,*e*) cyclopropa(*c*) cycloheptan-6-yl)-α-((5-quinoloyloxy) methyl)-1-piperazine ethanol, trihydrochloride) was a gift from Eli Lilly and Co. (Indianapolis, IN). All other chemicals used were HPLC or reagent grade and were obtained from Sigma Chemical Co (St. Louis, MO).

3.2.2 In vitro Studies

In vitro studies were conducted in epithelial Madin-Darby Canine Kidney (MDCKII) cells expressing either human P-gp (MDCKII-*MDR1* cell line) or murine BCRP (MDCKII-*Bcrp1* cell line) and were generously provided by Dr. Piet Borst and Dr. Alfred H. Schinkel (The Netherlands Cancer Institute, The Netherlands). Cells were cultured in DMEM media supplemented with 10% fetal bovine serum (Sigma-Aldrich, St. Louis, MO), penicillin (100U/ml), streptomycin (100µg/ml) and amphotericin B (250 ng/mL) (all Sigma-Aldrich, St. Louis, MO) and maintained at 37°C with 5% CO_2 under humidifying conditions.

3.2.3 Intracellular Accumulation

Intracellular accumulation of sorafenib was examined in these cells using 24-well polystyrene plates (Thermo Fisher Scientific Inc., Rochester, NY). Cells were seeded at a density of 2 x 10^5 cells/well and confluent monolayers were obtained in three days. On the day of the experiment, growth media was aspirated and the cells were washed twice with prewarmed (37º C) cell assay buffer. The experiment was started after a 30-min preincubation during which the cells were equilibrated with 1 ml of cell assay buffer. 1 ml of a tracer solution (2 ng/ml) of [^{3}H] sorafenib was then added to the cells and the plates were incubated for 1 hour in an orbital shaker maintained at 37º C. At the end of the 1-hour accumulation, the experiment was ended by aspirating the radiolabeled drug solution from the wells and washing the cells with ice-cold phosphate-buffered saline. 0.5 ml of a 1 % Triton X100 solution was added to each well to solubilize the cells and the protein concentration in the solubilized cell fractions was determined by the BCA protein assay (Thermo Fisher Scientific Inc., Rockford, IL). Radioactivity associated with a 150 µL sample was determined by liquid scintillation counting (LS-6500, Beckman Coulter Inc., Fullerton, CA). The radioactivity in the cell fractions was normalized by the respective protein concentrations and drug accumulation in the cells was expressed as amount of accumulated radioactivity (DPM) per microgram of protein. [^{3}H] vinblastine and [^{3}H] prazosin were included in the accumulation studies as positive control for P-gp and BCRP respectively.

3.2.4 Directional Flux Studies in MDCKII Cells

Transport assays were carried out using 6-well Transwells (Corning Inc., Corning, NY).

The cells were seeded at a density of 2×10^5 cells/well until they formed confluent polarized monolayers. On the day of the experiment, the monolayers were washed with prewarmed (37º C) cell assay buffer, and after a 30-min preincubation, the experiment was initiated by addition of a tracer solution (2 ng/ml) of radiolabeled sorafenib in cell assay buffer to the donor side. The receiver compartment was sampled at predetermined times (0, 10, 20, 30, 45, 60, and 90 min) after addition of drug to the donor side. The volume sampled (200 µl) was immediately replaced with fresh assay buffer. The transport of sorafenib was measured in two directions; apical-to-basolateral (A-to-B) and basolateral-to-apical (B-to-A). When an inhibitor was used in the flux study, the inhibitor [1 µM LY335979 (30) or 200 nM Ko143 (31)] was added during the preincubation step, followed by determination of A-to-B and B-to-A flux with the inhibitor present in both compartments throughout the course of the experiment. [3H] Sorafenib was quantified using liquid scintillation counting. The apparent permeability of sorafenib was calculated as described below.

3.2.5 Permeability Calculations

The apparent permeability (P_{app}) was calculated by the following equation,

$$P_{app} = \frac{\left(\frac{dQ}{dt}\right)}{A \times C_0} \qquad \text{..... (1)}$$

where, dQ/dt is the mass transport rate (determined from the slope of the amount transported vs. time plot), A is the apparent surface area of the cell monolayer (4.67 cm^2), and C_0 is the initial donor concentration. The efflux ratio, defined as the ratio of P_{app} in the B-to-A direction to the P_{app} in the A-to-B direction, was used to estimate the

magnitude of P-gp or BCRP-mediated efflux.

3.2.6 Calculation of Km value

The affinity of BCRP for sorafenib (Km_{app}) was determined by calculating the basolateral-to-apical permeability in MDCKII-*Bcrp1* cells, with a range of concentrations (2 ng/ml to 30 µg/ml) applied to the donor side. The B-to-A permeability was plotted as a function of sorafenib concentration. Phoenix WinNonlin 6.1 (Mountain View, CA) was used to fit an inhibitory E_{max} model to the data,

$$E = E_{max}\left(1 - \frac{C}{Km_{app} + C}\right) \qquad \text{..... (2)}$$

where, E is the B-to-A permeability of sorafenib, E_{max} is the maximum permeability seen at the lowest sorafenib concentration, Km_{app} is the affinity constant determined by the concentration of sorafenib at which half-maximal inhibition is seen and C is concentration of sorafenib in the donor compartment.

3.2.7 P-gp and BCRP Inhibition Assays

Inhibition studies were conducted using prototypical probe substrates, [3H] vinblastine for P-gp and [3H] prazosin or [3H] mitoxantrone for BCRP. Intracellular accumulation of these substrates at 60 minutes was determined in MDCKII-*MDR1* or *Bcrp1* cells in presence of different concentrations of sorafenib spanning 20 ng/ml to 60 µg/ml. The increase in cellular accumulation relative to control (no sorafenib treatment) was measured as a function of sorafenib concentration. A sigmoid E_{max} model given by the following equation was fit to the data using Phoenix WinNonlin 6.1,

$$E = E_0 + (E_{max} - E_0)\frac{C^{\gamma}}{IC_{50}{}^{\gamma} + C^{\gamma}} \quad \text{..... (3)}$$

where, E is the fold increase in accumulation of substrate seen in presence of sorafenib relative to control (no sorafenib), E_0 is the accumulation of probe in absence of sorafenib normalized to unity, E_{max} is the maximum increase in accumulation of probe, IC_{50} is the concentration of sorafenib at which half-maximal effect is seen, C is concentration of sorafenib and γ is the shape factor that determines the slope of the curve.

In vivo Studies

In vivo studies were conducted in male FVB (wild-type), *Mdr1a/b*$^{-/-}$ (P-gp knockout), *Bcrp1*$^{-/-}$ (BCRP knockout) and *Mdr1a/b*$^{-/-}$*Bcrp1*$^{-/-}$ (triple knockout) mice of a FVB genetic background (Taconic Farms, Inc.). All animals were 8 to 10 weeks old at the time of experiment. Animals were maintained under temperature-controlled conditions with a 12-h light/dark cycle and unlimited access to food and water. All studies were carried out in accordance with the guidelines set by the *Principles of Laboratory Animal Care* (National Institutes of Health) and were approved by The Institutional Animal Care and Use Committee (IACUC) of the University of Minnesota.

3.2.8 Plasma and Brain Pharmacokinetics of Sorafenib

Sorafenib dosing solution was prepared on the day of the experiment in a vehicle containing DMSO, propylene glycol and saline (3:5:2 v/v/v) at a concentration of 5 mg/ml. FVB (wild-type) mice received an intravenous dose of 10 mg/kg sorafenib by injection into the tail vein. Blood and brain were sampled at 15 min, 0.5,1, 2, 4 and 6 hrs post-dose, n = 4 at each time point. At the desired time point, animals were euthanized

using a CO_2 chamber. Blood was collected by cardiac puncture and transferred to heparinized tubes. Plasma was isolated from blood by centrifugation at 3000 rpm for 10 min at 4°C. Whole brain was immediately removed from the skull, rinsed with cold saline and flash frozen in liquid nitrogen. Plasma and brain specimens were stored at -80°C until analysis by LC-MS/MS.

3.2.9 Steady-State Brain Distribution of Sorafenib in FVB Mice

Steady-state brain and plasma concentrations of sorafenib were determined in FVB wild-type, *Mdr1a/b*$^{-/-}$, *Bcrp1*$^{-/-}$ and *Mdr1a/b*$^{-/-}$*Bcrp1*$^{-/-}$ mice. Alzet osmotic minipumps (Durect Corp., Cupertino, CA) were used to maintain a constant rate infusion in the peritoneal cavity. The procedure was same as that previously employed (5). Briefly, a 50 mg/ml solution of sorafenib in DMSO was filled in the minipumps (model 1003D) and the pumps were equilibrated by soaking them overnight in sterile saline solution at 37°C. Mice were anesthetized by intraperitoneal administration of 100 mg/kg ketamine and 10 mg/kg xylazine (Boynton Health Service Pharmacy, Minneapolis, MN). The primed pumps were surgically inserted into the peritoneal cavity and the animals were allowed to recover for an hour on a heated pad. The animals were euthanized 48 hours post surgery followed by collection of brain and blood as described earlier. Plasma and brain specimens were stored at -80°C until analysis by LC-MS/MS. The pumps operated at a constant flow rate of 1 μL/hr resulting in an intraperitoneal infusion rate of 50 μg/hr (2 mg/hr/kg). Sorafenib half-life in plasma and brain after an intravenous dose was determined to be 1.6 hours and 0.9 hours, respectively. Therefore an infusion lasting 48 hours was considered to be sufficiently long to attain steady-state in plasma and brain.

3.2.10 Influence of Elacridar on Brain Distribution of Sorafenib

In a separate study, FVB wild-type, *Mdr1a/b*$^{-/-}$, *Bcrp1*$^{-/-}$ and *Mdr1a/b*$^{-/-}$*Bcrp1*$^{-/-}$ mice (n = 12 per group) were divided into 3 cohorts (n = 4) and administered 10 mg/kg sorafenib intravenously. One cohort (elacridar pretreatment) received 10 mg/kg elacridar (10:7:3 v/v/v DMSO, propylene glycol, saline) and a second cohort (vehicle control) was administered vehicle (10:7:3 v/v/v DMSO, propylene glycol, saline), via intravenous injection 30 minutes before sorafenib was administered. The third cohort did not receive any pretreatment and served as control. Blood and brain were collected at 60 minutes after the sorafenib dose and processed as described earlier. Sorafenib brain concentrations in the presence and absence of elacridar in the wild-type mice were compared with the three transgenic mouse groups.

3.2.11 Analysis of Sorafenib by Liquid Chromatography/Tandem Mass Spectrometry

The concentration of sorafenib in mouse plasma and brain homogenate was determined by high pressure liquid chromatography (HPLC) coupled with mass spectrometry. Prior to analysis, frozen samples were thawed at room temperature. Brain samples were homogenized using 3 volumes of ice-cold 5% bovine serum albumin in phosphate-buffered saline using a tissue homogenizer (Fisher Scientific, Pittsburgh, PA). A 50 μL aliquot of plasma and a 100 μL aliquot of brain homogenate were spiked with 20 ng of internal standard, tyrphostin (AG1478), and extracted by vigorous vortexing with 1 mL of ice cold ethyl acetate. Samples were centrifuged at 7500 rpm for 15 minutes at 4°C and a volume of 750 μL of the organic layer was transferred to fresh polypropylene tubes and

dried under nitrogen. Samples were reconstituted in 100 µL mobile phase and transferred to glass auto sampler vials. A volume of 10 µL was injected in the HPLC system using a temperature controlled autosampling device maintained at 10°C. Chromatographic analysis was performed using an Agilent Model 1200 separation system (Santa Clara, CA, USA). Separation of analytes was achieved using an Agilent Eclipse XDB-C18 RRHT threaded column (4.6 mm ID x 50mm, 1.8 µ) fitted with an Agilent C18 guard column (4.6 mm ID x 12.5mm, 5 µ) (Santa Clara, CA, USA). The mobile phase was composed of acetonitrile: 20mM ammonium formate (containing 0.1% formic acid) (68:32 v/v), and was delivered at a flow rate of 0.25 mL/min. The column effluent was monitored using a Thermo Finnigan™ TSQ® Quantum 1.5 detector (San Jose, CA, USA). The instrument was equipped with an electrospray interface, and controlled by the Xcalibur version 2.0.7 data system. The samples were analyzed using an electrospray probe in the positive ionization mode operating at a spray voltage of 4500V for both sorafenib and the internal standard. The spectrometer was programmed to allow the $[MH]^+$ ion of sorafenib at *m/z* 465.06 and that of internal standard at *m/z* 316.67 to pass through the first quadrupole (Q1) and into the collision cell (Q2). The collision energy was set at 30V for sorafenib and 9V for tyrphostin. The product ions for sorafenib (*m/z* 251.9) and the internal standard (*m/z* 300.9) were monitored through the third quadrupole (Q3). The scan width and scan time for monitoring the two product ions were 1.5 *m/z* and 0.5 s, respectively. The assay was sensitive over a range of 2.5 ng/ml to 1 µg/ml with the coefficient of variation being less than 15% over the entire range.

3.2.12 Pharmacokinetic Calculations

Pharmacokinetic parameters from the concentration-time data in plasma and brain were obtained by non-compartmental analysis (NCA) performed using Phoenix WinNonlin 6.1 (Mountain View, CA). We employed a built-in capability of NCA analysis which uses an extension of the Nedelman and Jia approach (32, 33) to analyze data from sparse sampling and estimate the variance in the area under the curve (AUC). The terminal rate constants (λz) for plasma and brain were determined from the last three data points of the respective concentration-time profiles. The areas under the concentration-time profiles for plasma (AUC_{plasma}) and brain (AUC_{brain}) from time zero to infinity were calculated using the linear trapezoidal method. The AUC from the last measured time point to infinity was estimated by dividing the last measured concentration by the respective terminal rate constant. The percentage of AUC extrapolated was less than 10% in both brain and plasma. In the case of plasma, the AUC from time zero to the first measured time point was obtained by back-extrapolation of the first two data points to time zero.

In the intraperitoneal infusion studies, the apparent plasma clearance (CL_{app}) was calculated by using the equation,

$$CL_{app} = \frac{k(0)}{C_{ss}} \qquad \text{..... (4)}$$

where, *k(0)* is the rate of infusion into the peritoneal cavity normalized to body weight (ng/hr/kg) and C_{ss} is the plasma concentration at steady-state (ng/ml).

3.2.13 Statistical Analysis

Comparison between groups were made using SigmaStat, version 3.1 (Systat Software,

Inc., Point Richmond, CA). Statistical difference between two groups was tested by using the two-sample t-test and significance was declared at $p < 0.05$. Multiple groups were compared by one way analysis of variance with the Holm-Sidak post-hoc test for multiple comparisons at a significance level of $p < 0.05$.

3.3 Results

3.3.1 Intracellular Accumulation of Sorafenib in MDCKII Cells

Intracellular accumulation of sorafenib was examined in polarized epithelial MDCKII cells that overexpressed the transporter proteins, P-gp or BCRP. Prazosin, a prototypical BCRP substrate, was included as a positive control and showed significantly lower accumulation in the MDCKII-*Bcrp1* cells compared to wild-type (~ 10 % of WT). Similarly, sorafenib accumulation in the *Bcrp1*-transfected cells was 5-fold lower compared to the wild-type cells ($p < 0.05$, **Figure 3.1A)**. This suggested that BCRP limits intracellular accumulation of sorafenib. In the *MDR1*-transfected cells, accumulation of the P-gp substrate vinblastine was significantly reduced compared to the wild-type (~ 10 % of WT). However, accumulation of sorafenib in the *MDR1*-transfected cells was not statistically different from that in wild-type cells indicating that P-gp might not be involved in efflux of sorafenib from the cells. (**Figure 3.1B)**

3.3.2 Directional Permeability of Sorafenib across MDCKII Cells

Transcellular transport of [3H] sorafenib was studied using MDCKII cells. In the MDCKII-*Bcrp1* cells, the rate of drug transported was significantly increased in the B-to-A direction compared to wild-type cells (**Figure 3.2A**, $p < 0.05$). The BCRP inhibitor

Ko143 completely inhibited BCRP mediated active transport in the *Bcrp1* cells such that there was no difference in the amount of sorafenib transported in the two directions (**Figure 3.2B**). The apparent permeability of sorafenib in the B-to-A direction was 15–fold greater than the A-to-B permeability in the *Bcrp1*-transfects ($p < 0.05$). This difference in permeability was abolished upon treatment with Ko143 (**Figure 3.3**). Directional flux experiments in the *MDR1*-transfected cells showed no signs of directionality in the transport of sorafenib, as there was no significant difference in the amount of sorafenib transported and the permeability between the A-to-B and B-to-A directions **(Figures 3.4A, 3.4B**). This indicated that sorafenib is not efficiently transported by P-gp in these cells. The in vitro studies suggest that while sorafenib is a substrate for BCRP, it is not effectively transported by P-gp. We determined the apparent affinity constant (Km_{app}) of BCRP for sorafenib by measuring the B-to-A permeability of sorafenib in the *Bcrp1*-transfected cells with varying concentrations of sorafenib applied to the donor (basolateral) side. The B-to-A permeability of sorafenib decreased with increasing sorafenib concentrations. An inhibitory E_{max} model fitted to the data estimated a Km_{app} of 5.5 ± 1.2 nM, indicating that sorafenib is a high affinity substrate for BCRP (**Figure 3.5**).

3.3.3 Sorafenib as a P-gp or BCRP Inhibitor

The ability of sorafenib to inhibit P-gp and BCRP was evaluated by studying the intracellular accumulation of prototypical probe P-gp and BCRP substrates (vinblastine for P-gp, prazosin and mitoxantrone for BCRP) in presence of varying concentrations of sorafenib. Treatment with sorafenib significantly increased intracellular accumulation of

vinblastine in the *MDR1*-transfected cells (**Figure 3.6A**). A sigmoidal E_{max} model was fit to the resulting data and the IC_{50} of sorafenib for inhibition of P-gp was estimated to be 25 ± 6 μM. Interestingly, sorafenib treatment did not increase accumulation of mitoxantrone or prazosin in the *Bcrp1*-transfected cells (**Figure 3.6B**). This suggests that while sorafenib is a high affinity substrate for BCRP, it did not inhibit BCRP mediated transport of the two common probe substrates. The fact that sorafenib is a substrate but does not inhibit BCRP in this particular case strongly suggests that sorafenib is transported via binding to a site that is different than that for prazosin or mitoxantrone.

3.3.4 Sorafenib Disposition in Plasma and Brain

We studied the brain and plasma pharmacokinetics of sorafenib in FVB wild-type mice. Sorafenib brain concentrations were significantly lower than the plasma concentrations at all the measured time points ($p < 0.05$, **Figure 3.7**) with brain-to-plasma ratios lower than 0.15 at all time points. Noncompartmental analysis of the brain and plasma data yielded a terminal half-life of 1.6 hours in plasma and 0.9 hours in the brain (**Table 3.1**). The total body clearance was estimated to be 5.8 ml/min/kg. The area under the curve (AUC) in plasma was 1.6 mg-min/ml, whereas the AUC in brain was 0.11 mg-min/ml. The AUC_{brain} to AUC_{plasma} ratio was 0.06 suggesting that sorafenib has limited distribution to the brain.

3.3.5 Steady-State Brain and Plasma Pharmacokinetics of Sorafenib

The influence of active efflux transport by P-gp and BCRP on the brain distribution of sorafenib was examined by determining the steady-state brain and plasma concentrations

in wild-type, *Mdr1a/b*$^{-/-}$, *Bcrp1*$^{-/-}$ and *Mdr1a/b*$^{-/-}$*Bcrp1*$^{-/-}$ mice. Sorafenib was delivered at a constant rate of 2 mg/hr/kg in the peritoneal cavity and brain and plasma concentrations were determined at 48 hours after the start of infusion. Given the plasma half-life (1.6 hours), an infusion lasting 48 hours was considered to be sufficient to attain steady-state in both plasma and brain. The steady-state concentrations (C_{ss}) in plasma ranged from 1.5 to 3 μg/ml in the four genotypes and were not statistically different from each other. Steady-state brain concentrations of sorafenib were significantly enhanced in the *Bcrp1 (-/-)* and *Mdr1a/b*$^{-/-}$*Bcrp1*$^{-/-}$ mice compared to wild-type mice ($p < 0.05$) (**Table 3.2**). There was no difference in steady-state brain sorafenib concentrations between the wild-type and *Mdr1a/b*$^{-/-}$ mice. The brain-to plasma ratio at steady-state (B/P_{ss}) in the wild-type mice was ~ 0.094 ± 0.007. This ratio was similar to the equilibrium distribution coefficient of 0.06 obtained from the i.v. study and indicates the limited CNS distribution of sorafenib. The B/P_{ss} ratio increased by approximately 4-fold in the *Bcrp1*$^{-/-}$ mice (0.36 ± 0.056) and 10-fold in the *Mdr1a/b*$^{-/-}$*Bcrp1*$^{-/-}$ mice (0.91 ± 0.29) ($p < 0.05$, **Figure 3.8**). This suggests that BCRP is the major transporter limiting brain penetration of sorafenib. The steady-state brain-to-plasma ratio in the wild-type mice was not statistically different than the ratio in the *Mdr1a/b*$^{-/-}$ mice (0.11 ± 0.021). This finding is similar to those by Lagas et al. and Gnoth et al., who also report a lack of P-gp mediated transport in vivo (28, 29). The apparent plasma clearance (CL_{app}) of sorafenib between the wild-type, *Mdr1a/b*$^{-/-}$ and the *Mdr1a/b*$^{-/-}$*Bcrp1*$^{-/-}$ mice were not significantly different from each other, however the CL_{app} increased significantly in the *Bcrp1*$^{-/-}$ mice compared to wild-type ($p < 0.05$).

3.3.6 Influence of Elacridar on Brain Distribution of Sorafenib

The influence of the dual P-gp and BCRP inhibitor elacridar on the distribution of sorafenib to the brain was investigated. The brain-to-plasma ratios at 60 minutes were 0.083 ± 0.020, 0.37 ± 0.035, 0.16 ± 0.11 and 0.86 ± 0.16 in the wild-type, *Bcrp1*$^{-/-}$, *Mdr1a/b*$^{-/-}$ and *Mdr1a/b*$^{-/-}$*Bcrp1*$^{-/-}$ mice respectively (**Figure 3.9**). These values were similar to the steady-state brain-to-plasma ratios in the wild-type (0.094), *Bcrp1*$^{-/-}$ (0.36), *Mdr1a/b*$^{-/-}$ (0.11) and *Mdr1a/b*$^{-/-}$*Bcrp1*$^{-/-}$ (0.91) mice (**Table 3.1**). The intravenous study indicated that around 60 minutes would represent a region where sorafenib is at a transient steady-state in the brain. This is evident from the similarity in the brain-to-plasma ratios at 60 min and at steady-state. Concurrent administration of the dual P-gp and BCRP inhibitor elacridar resulted in an enhancement in brain concentrations by 5-fold in the wild-type, 3-fold in the *Bcrp1*$^{-/-}$ and 4-fold in the *Mdr1a/b*$^{-/-}$ mice, compared to the control group ($p < 0.05$, **Table 3.3**). Pretreatment with elacridar had no significant effect on the brain concentrations of sorafenib in the *Mdr1a/b*$^{-/-}$*Bcrp1*$^{-/-}$ mice. Inhibition of P-gp and BCRP by elacridar increased the brain-to-plasma ratio to 0.76 ± 0.24 in wild-type, 1.03 ± 0.33 in the *Bcrp1*$^{-/-}$ and 1.3 ± 0.29 in the *Mdr1a/b*$^{-/-}$ mice ($p < 0.05$). Of interest, was the fact that the B/P ratio in the *Bcrp1*$^{-/-}$ also increased significantly upon treatment with elacridar. The brain-to-plasma ratios in the elacridar treated cohort in the four groups were not statistically different from each other (**Figure 3.9**). The brain-to-plasma ratios in the vehicle treated cohort were not statistically different from that in the control cohort, the values being 0.13 ± 0.037 in the wild-type, 0.30 ± 0.082 in the *Bcrp1*$^{-/-}$, 0.15 ± 0.045 in the *Mdr1a/b*$^{-/-}$ and 0.69 ± 0.15 in the *Mdr1a/b*$^{-/-}$*Bcrp1*$^{-/-}$ mice (T**able**

3.3). This confirmed that the enhanced brain penetration of sorafenib in the elacridar treated cohort was due to inhibition of P-gp and BCRP by elacridar. There was no significant difference in the plasma concentrations of sorafenib between the different mice groups except in the wild-type mice, where plasma levels were slightly higher compared to the other groups.

3.4 Discussion

Sorafenib is a potent inhibitor of several receptor tyrosine kinases and other regulators of tumor progression and tumor angiogenesis, e.g., VEGFR, PDGFR, cKIT and RAF (17, 19). This broad activity against critical targets makes sorafenib an attractive option for therapy in glioma, a tumor of the brain that is typically fatal (34). Efflux transporters present at the BBB can limit drug delivery to the brain, and therefore are one determinant of efficacy. This is especially relevant to an infiltrative disease like glioma, where invasive tumor cells that may reside behind an intact BBB might be deprived of a drug that is effluxed by P-gp and BCRP. Several studies have attempted to explain the interaction of sorafenib with P-gp and BCRP, two critical efflux transporters at the BBB (15, 28, 29). However, these studies fail to reach a consensus with respect to the role of the two proteins in limiting the CNS penetration of sorafenib. The current study investigated several questions that were hitherto unanswered with respect to transporter-mediated distribution of sorafenib to the brain. Our findings conclusively show that transport of sorafenib across the BBB is restricted by BCRP and the data suggest some involvement of P-gp. Sorafenib differs from many other tyrosine kinase inhibitors in that it is a higher affinity substrate for BCRP than for P-gp, and as a result, irrespective of

transporter capacity at the BBB, BCRP is the dominant transporter preventing sorafenib from entering the brain.

In vitro experiments showed that sorafenib is a high affinity substrate for BCRP with an affinity constant (Km) of 5nM. While it did not appear to be a substrate for P-gp from the in vitro data, sorafenib inhibited the transporter with an IC_{50} of 25 μM (**Figure 3.6A**). These findings can be clinically relevant since sorafenib plasma concentrations in humans with the currently accepted treatment regimen (100-400 mg b.i.d) have been reported to be in the range of 1-15 μM (35, 36). Inhibition of P-gp by sorafenib may alter tissue pharmacokinetics of concurrently administered drugs if the coadministered drug is a substrate for P-gp. Another interesting finding was that, while sorafenib inhibited the accumulation of vinblastine in the *MDR1*-transfected cells, it did not inhibit the accumulation of prazosin and mitoxantrone in the *Bcrp1*-transfected cells (**Figure 3.6B**). We have previously shown that there are differences in the inhibition of BCRP depending on both the inhibitor used and the substrate under evaluation (37). In the same study we raised the possible outcomes of in vitro screening related to multiple binding sites on BCRP for transport of drugs. The finding that sorafenib is transported by BCRP, but does not inhibit it, suggests that sorafenib might interact with BCRP by binding to sites that do not overlap with the binding sites of either prazosin or mitoxantrone, prototypical substrates often employed in drug screens.

The influence of P-gp and BCRP on transport of sorafenib across the BBB was examined by determining the steady-state brain-to-plasma (B/P) ratios in wild-type and transporter

knockout mice (**Table 3.2**). The steady-state brain-to-plasma ratio of sorafenib in the wild-type mice was approximately 10% indicating the restricted delivery of sorafenib across the BBB. Consistent with in vitro findings that sorafenib is a high affinity substrate for efflux mediated by BCRP, absence of BCRP resulted in a 4-fold increase in brain-to-plasma ratio of sorafenib in the *Bcrp1*$^{-/-}$ mice. This finding confirmed that sorafenib is actively effluxed by BCRP at the BBB and this limits its brain penetration. Interestingly, the steady-state brain-to-plasma ratio in the *Mdr1a/b*$^{-/-}$*Bcrp1*$^{-/-}$ mice was 10-fold greater than the B/P ratio in the wild-type mice and approximately 2.5-fold greater than the ratio in *Bcrp1*$^{-/-}$ mice (**Figure 3.8, Table 3.2**). The finding that the B/P ratio in the *Mdr1a/b*$^{-/-}$*Bcrp1*$^{-/-}$ mice was greater than the ratio in the *Bcrp1*$^{-/-}$ mice was unexpected, based on the fact that the B/P ratio was unchanged in the *Mdr1a/b*$^{-/-}$ mice and in vitro studies showed that sorafenib was not an avid P-gp substrate. This suggested that even though sorafenib does not appear to be transported by P-gp in vitro, the presence of P-gp at the BBB is important to restrict brain penetration of sorafenib, particularly when BCRP is also absent. Moreover, the results clearly show that BCRP plays the leading role in restricting the delivery of sorafenib across the BBB. This finding is different than reports for other TKIs, where P-gp appears to be the dominant transporter keeping dual substrates out of the brain (5, 6, 12, 38, 39).

The increased brain distribution of sorafenib when both P-gp and BCRP were absent in the *Mdr1a/b*$^{-/-}$*Bcrp1*$^{-/-}$ mice warranted further investigation into the potential role of P-gp in the efflux of sorafenib across the BBB. This was explored by administration of the dual P-gp and BCRP inhibitor in conjunction with sorafenib in the four genotypes. Co-

administration of elacridar increased the brain concentrations of sorafenib in the wild-type, *Bcrp1*$^{-/-}$ and *Mdr1a/b*$^{-/-}$ mice such that they were not different that the concentrations in the *Mdr1a/b*$^{-/-}$*Bcrp1*$^{-/-}$ mice (**Figure 3.9, Table 3.3**). This was a significant finding in light of the result that the steady-state brain concentrations of sorafenib did not increase when P-gp alone was absent in the *Mdr1a/b*$^{-/-}$ mice, and confirmed that even though sorafenib is a weaker substrate for P-gp compared to BCRP, P-gp may still be an influential determinant in the distribution of sorafenib to brain. Another intriguing possibility, yet to be confirmed, is that sorafenib brain distribution is limited by a different efflux system that is also inhibited by elacridar.

Our previous studies exploring the impact of drug efflux transporters on delivery of TKIs to the brain have postulated that P-gp and BCRP cooperate at the BBB to limit brain distribution of gefitinib and dasatinib (5, 6). This was first reported for the TKIs by Polli et al., where simultaneous absence of P-gp and BCRP in the *Mdr1a/b*$^{-/-}$*Bcrp1*$^{-/-}$ mice resulted in a greater than additive enhancement in the brain distribution of lapatinib (12). Similar findings have been reported for other TKIs such as imatinib and erlotinib (39, 40). All of these studies have suggested that P-gp is the dominant transporter limiting brain delivery of dual substrates. Sorafenib is different from these tyrosine kinase inhibitors in that BCRP plays the role of the dominant transporter in effluxing it at the BBB. Even so, it is similar to the other TKIs due to the fact that absence/inhibition of both P-gp and BCRP is necessary to see a maximal improvement in brain penetration. An understanding of the possible mechanisms behind this cooperation can be gained by looking at the relative expression of P-gp and BCRP (capacities of the two transporters)

at the BBB, as well as the relative affinity for substrate drugs. In a recent report, Warren et al. showed that the mRNA levels of P-gp in the brain vascular endothelial cells of mice was approximately 5-fold greater than the mRNA levels of BCRP (41). Likewise, Kamiie et al. quantified membrane transporter levels using LC-MS and reported approximately 5-fold higher levels of P-gp at the mouse BBB compared to BCRP (42). The significantly greater amount of P-gp at the BBB might be the reason behind it being dominant in the efflux of many dual substrates from the brain. The efflux mediated by BCRP can thus appear subdued and become apparent only when both transporters are absent or inhibited. This is of particularly important because most of the TKIs mentioned above demonstrate a significant BCRP mediated transport in vitro (5, 6, 8). The greater expression (capacity) of P-gp offsets the lower affinity, resulting in a pronounced P-gp effect on efflux of drugs at the BBB. However, for a drug like sorafenib, which has a significantly higher affinity for BCRP compared to a moderate affinity for P-gp (not detectable in vitro), it is BCRP that plays the role of the dominant transporter in keeping it out of the brain. The effect of P-gp is noticeable only in the *Bcrp1*$^{-/-}$ and the *Mdr1a/b*$^{-/-}$*Bcrp1*$^{-/-}$ mice. Recently, Kodaira et al. determined the net contribution of P-gp and BCRP to the overall efflux of various drugs at the BBB (39). This group showed that for many dual substrates the efflux clearance out of brain mediated by P-gp was greater than that mediated by BCRP. On the other hand, for dantrolene, the P-gp mediated efflux was 10-fold lower than the BCRP mediated efflux at the BBB. Similar to sorafenib, the P-gp mediated efflux of dantrolene was not detectable in vitro. Our study clearly shows that sorafenib is currently one of the select TKIs for which the role of BCRP in active efflux at the BBB is more than that of

P-gp. It is also one of the few cases in which the in vitro BCRP mediated transport correlates with limited brain penetration seen in vivo. Enokizono et al. and Zhao et al., in separate studies, have shown that this is true only for a handful of BCRP substrates such as dantrolene, prazosin and alfuzosin (9, 43).

In conclusion, we have shown that the brain distribution of sorafenib is restricted due to active efflux transport at the BBB. BCRP plays a dominant role in limiting the distribution of sorafenib to the brain. While we also present a possible mechanism behind the cooperative role of P-gp and BCRP at the BBB (simple compensation depending on relative expression and affinity), further studies in this direction are warranted. Finally, these results can be of clinical significance for therapy in glioma, since the ability of sorafenib to cross an intact BBB and achieve therapeutic concentrations in the tumor cells might determine efficacy against the invasive tumor cells that are out of the reach of surgical resection.

3.5 Footnotes

This work was supported by National Institutes of Health - National Cancer Institute [CA138437] (William F. Elmquist, John R. Ohlfest and a grant from the Children's Cancer Research Fund at the University of Minnesota (William F. Elmquist, John R. Ohlfest). Financial support for Sagar Agarwal was provided by the Doctoral Dissertation Fellowship from the University of Minnesota, the Edward G. Rippie Fellowship and the Ronald J. Sawchuk Fellowship in Pharmacokinetics from the Department of Pharmaceutics at the University of Minnesota.

Table 3.1 Plasma and brain pharmacokinetic parameters determined by noncompartmental analysis after the administration of a single i.v. bolus dose of sorafenib in wild-type mice.

Pharmacokinetic Parameter	**Plasma**	**Brain**
Terminal Rate Constant (hr^{-1})	0.42	0.73
Half life (hr)	1.6	0.9
Clearance (ml/min/kg)	5.8	-
Volume of Distribution (ml/kg)	840	-
$AUC_{0\rightarrow t\text{-}last}$ (mg.min/ml)	$1.5 \pm 0.1^{*}$	$0.11 \pm 0.008^{*}$
$AUC_{0\rightarrow inf}$ (mg.min/ml)	1.6	0.11
AUC_{brain}/AUC_{plasma}	0.06	

The ratio of AUC in the brain to that in plasma was estimated to be 0.06, signifying the restricted brain penetration of sorafenib. *Mean ± S.D. (standard error of the estimate)

Table 3.2. Steady-state plasma and brain concentrations of sorafenib in wild-type, Mdr1a/b$^{-/-}$, Bcrp1$^{-/-}$ and Mdr1a/b$^{-/-}$Bcrp1$^{-/-}$ mice after a constant intraperitoneal infusion of sorafenib at a constant rate of 2 mg/hr/kg

Genotype	N	Plasma Css	Brain Css	Brain-to-Plasma Ratio	Apparent Plasma Clearance (Cl_{app})
		µg/ml	µg/gm		ml/min/kg
FVB (wild-type)	4	2.5 ± 0.16	0.32 ± 0.18[a]	0.094 ± 0.007	11.5 ± 4.01
Bcrp1$^{-/-}$	4	1.5 ± 0.42[b]	0.51 ± 0.074[a]	0.36 ± 0.056[b]	24.3 ± 5.71[b]
Mdr1a/b$^{-/-}$	4	3.07 ± 0.91	0.34 ± 0.16[a]	0.11 ± 0.021	20.3 ± 7.07
Mdr1a/b$^{-/-}$Bcrp1$^{-/-}$	4	1.9 ± 0.17	1.7 ± 0.69[b]	0.91 ± 0.29[b]	17.3 ± 1.49

Data presented as mean ± S.D., $p < 0.05$
[a] compared to corresponding plasma concentration
[b] compared to wild-type group

Table 3.3. Plasma and brain concentrations of sorafenib at 60 minutes in wild-type, Mdr1a/b (-/-), Bcrp1$^{-/-}$ and Mdr1a/b$^{-/-}$Bcrp1$^{-/-}$ mice as influenced by treatment with the dual P-gp/BCRP inhibitor elacridar (elacridar was administered 30 minutes prior to the sorafenib dose).

Data presented as mean ± S.D., $p < 0.05$

[a] compared to corresponding plasma concentration

[b] compared to wild-type control group

[c] compared to corresponding control group

[d] not significant compared to *Mdr1a/b*$^{-/-}$*Bcrp1*$^{-/-}$ control group

[NS] no significant difference between the control and vehicle control groups of each genotype

Genotype	Cohort	Plasma Concentration	Brain Concentration	Brain-to-Plasma Ratio
		µg/ml	µg/gm	
FVB (wild-type)	Control	6.5 ± 1.5	0.52 ± 0.045[a]	0.083 ± 0.020
	Vehicle Control	5.04 ± 0.87[NS]	0.65 ± 0.091[a,NS]	0.13 ± 0.037[NS]
	Elacridar Treated	4.04 ± 0.69[b]	2.9 ± 0.46[b,c,d]	0.76 ± 0.24[b,c,d]
Bcrp1$^{-/-}$	Control	3.02 ± 1.03[b]	1.1 ± 0.35[a]	0.37 ± 0.035[b]
	Vehicle Control	3.6 ± 0.11[NS]	1.08 ± 0.29[a, NS]	0.30 ± 0.082[NS]
	Elacridar Treated	3.3 ± 1.7[b]	3.6 ± 1.9[b,c,d]	1.03 ± 0.33[b,c,d]
Mdr1a/b$^{-/-}$	Control	3.5 ± 2.1[b]	0.71 ± 0.78[a]	0.16 ± 0.11
	Vehicle Control	4.4 ± 0.36[NS]	0.67 ± 0.22[a, NS]	0.15 ± 0.045[NS]
	Elacridar Treated	2.4 ± 1.1[b]	3.01 ± 1.09[b,c,d]	1.3 ± 0.29[b,c,d]
Mdr1a/b$^{-/-}$*Bcrp1*$^{-/-}$	Control	4.7 ± 1.5[b]	3.9 ± 0.79[b]	0.86 ± 0.16[b]
	Vehicle Control	3.07 ± 1.8[NS]	2.08 ± 1.6[a, NS]	0.69 ± 0.15[NS]
	Elacridar Treated	4.1 ± 3.04[b]	3.4 ± 2.7[b,d]	0.73 ± 0.35[b,d]

Figure 3.1A. Intracellular accumulation of [3H]-sorafenib in wild-type and Bcrp1-transfected MDCKII cells.

Accumulation of the sorafenib in the *Bcrp1*-transfected cells (gray bars) was approximately 5-fold lower than that in the wild-type cells (black bars). (mean ± S.D., $n = 6$, *, $p < 0.05$)

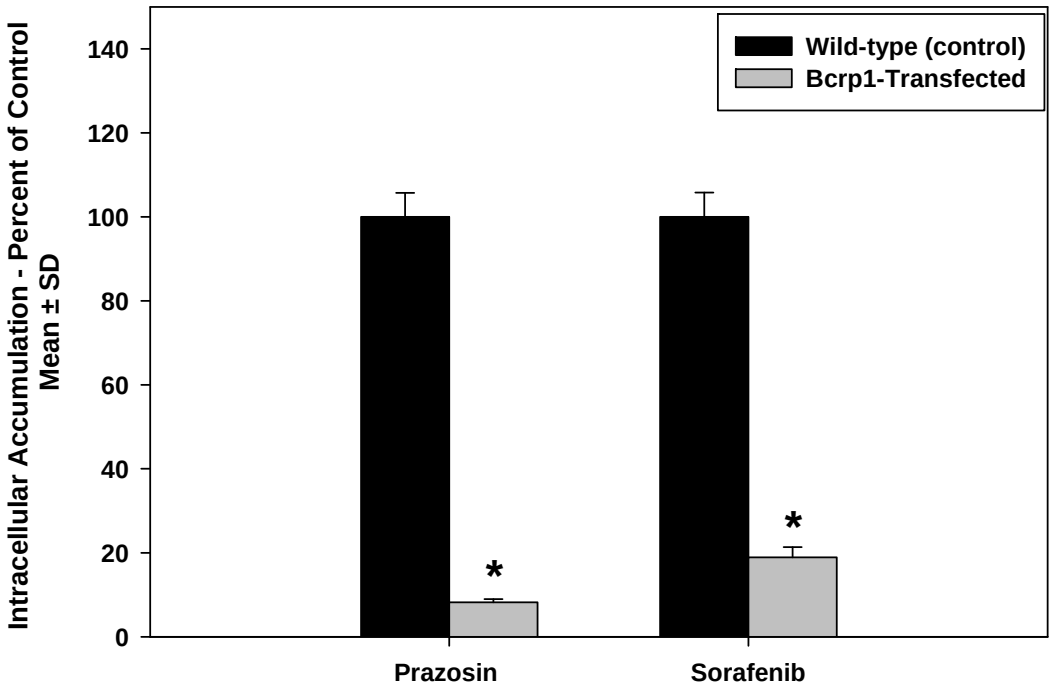

Figure 3.1B. Intracellular accumulation of [3H]-sorafenib in wild-type and MDR1-transfected MDCKII cells.

Accumulation of the prototypical substrate vinblastine in the *MDR1*-transfected cells (gray bars) was approximately 10-fold lower than that in the wild-type cells (black bars). In comparison, no such difference was seen in the accumulation of sorafenib between the two cell types. (mean ± S.D., $n = 6$, *, $p < 0.05$)

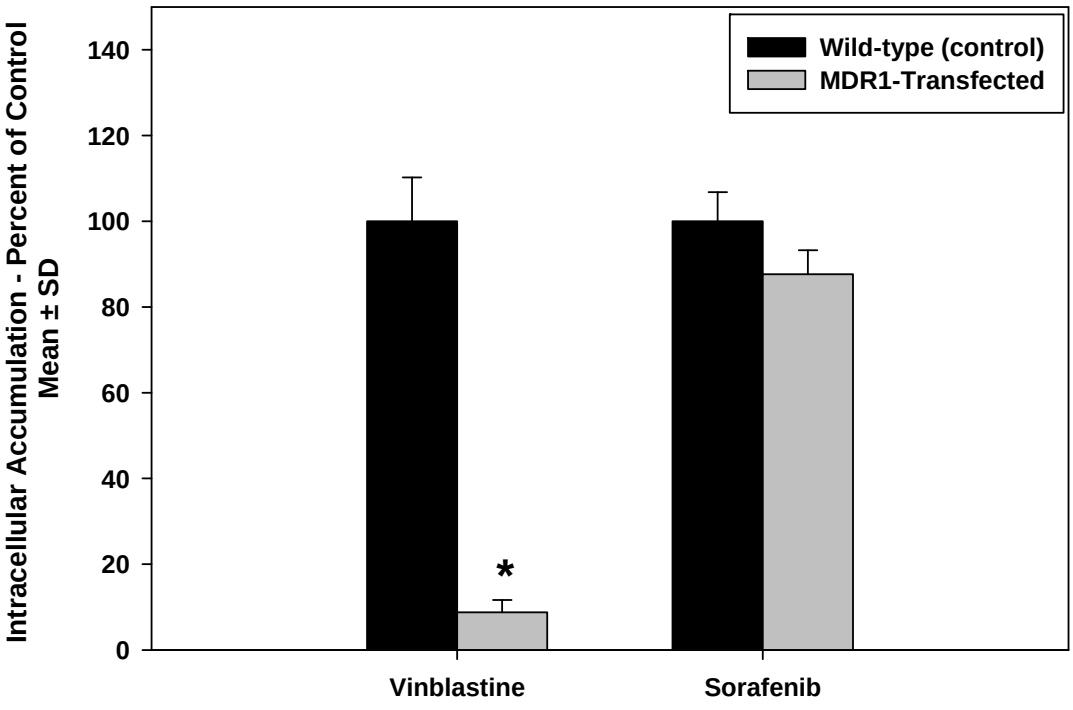

Figure 3.2A. Directional transport of [^{3}H] sorafenib across MDCKII-Bcrp1 cell monolayers.

Amount of sorafenib transported across wild-type (●, A-to-B transport; ○, B-to-A transport) and *Bcrp1*-transfected (▲, A-to-B transport; Δ, B-to-A transport) cells. There was significant directionality in transport of sorafenib across *Bcrp1* monolayers. (mean ± S.D., $n = 6$).

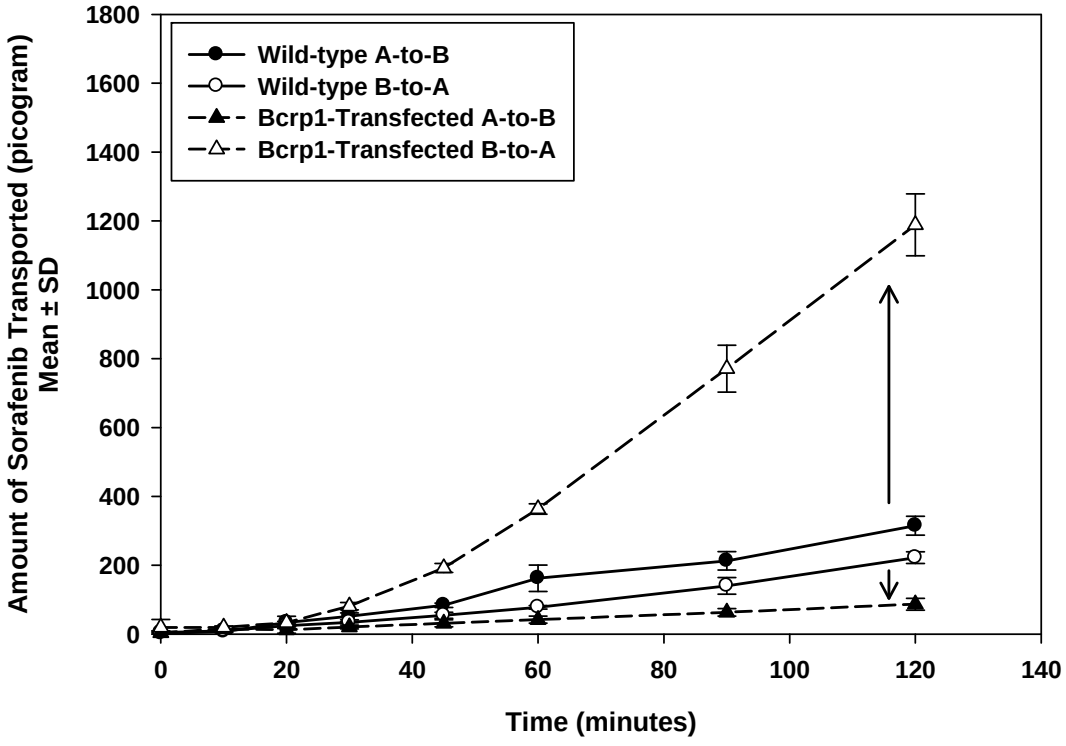

Figure 3.2B. Directional transport of [^{3}H] sorafenib across MDCKII-Bcrp1 cell monolayers.

Flux of sorafenib in *Bcrp1*-transfected cells in presence (●, A-to-B transport; ○, B-to-A transport) and absence (▲, A-to-B transport; Δ, B-to-A transport) of the BCRP inhibitor Ko143. This directionality was abolished when cells were treated with 200 nM Ko143. (mean ± S.D., n = 6).

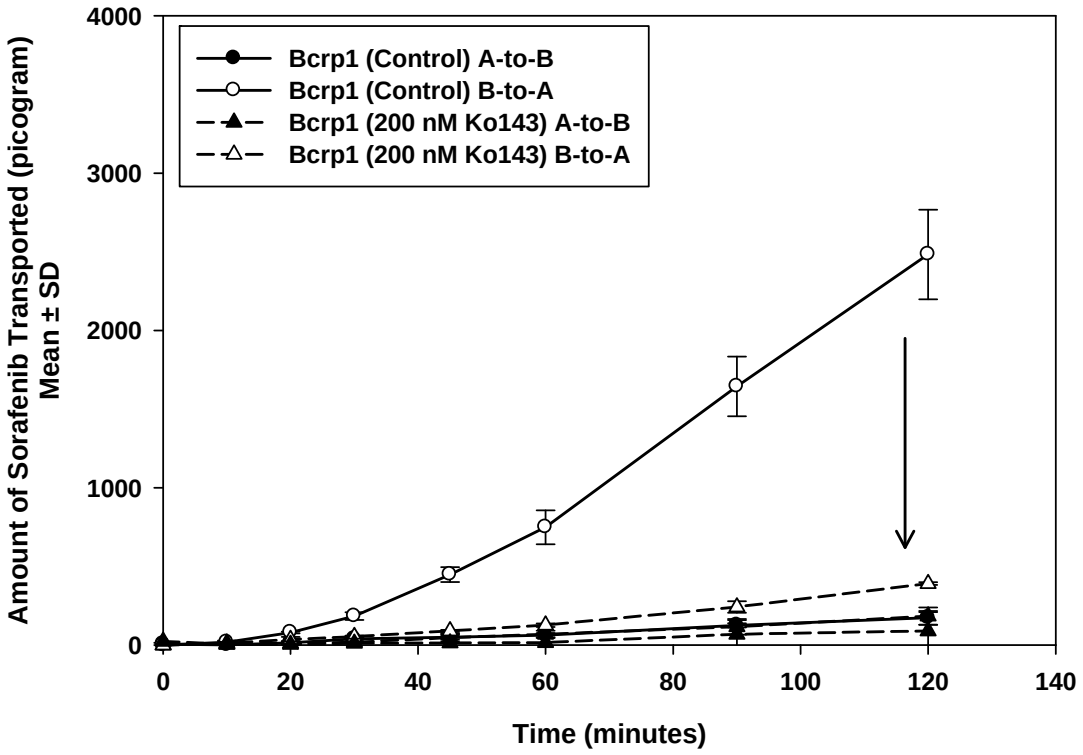

Figure 3.3. Apparent permeability of [^{3}H] sorafenib across MDCKII wild-type and Bcrp1-transfected cell monolayers.

In the *Bcrp1*-transfects, the B-to-A permeability (gray bar) was significantly greater than the A-to-B permeability (black bar). Treatment with Ko143 decreased the B-to-A permeability. No difference in apparent permeability was observed in the wild-type cells. (mean ± S.D., $n = 6$, *, $p < 0.05$)

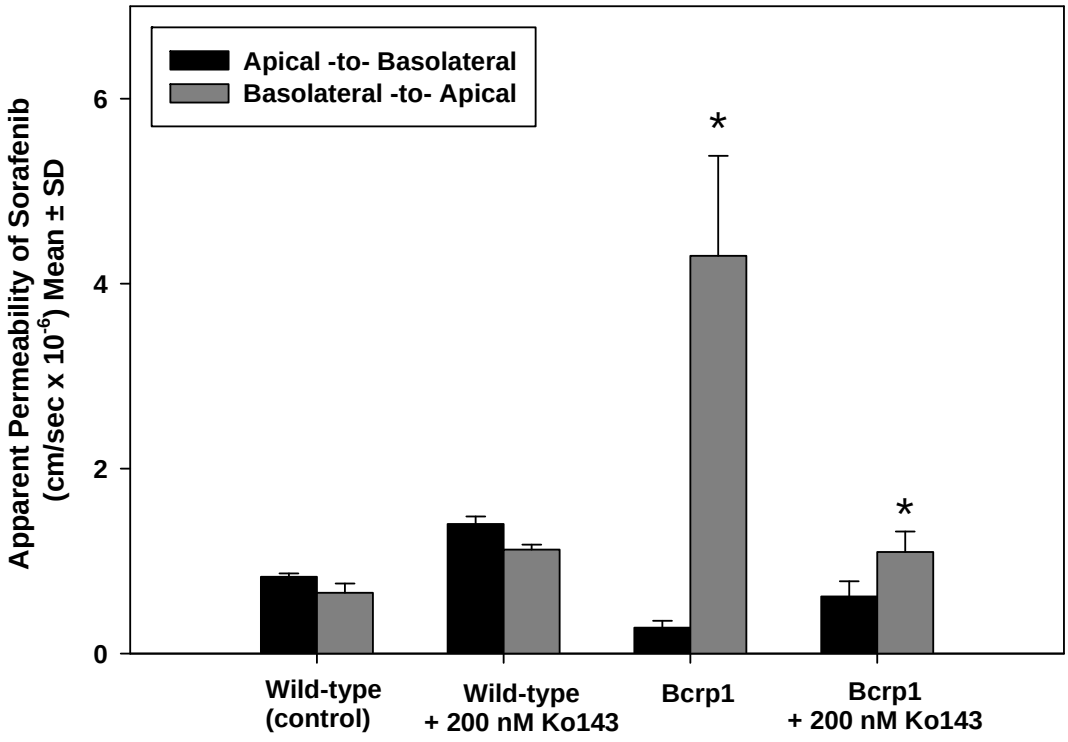

Figure 3.4A. Directional transport of [^{3}H] sorafenib across MDCKII-MDR1 cell monolayers.

Amount of sorafenib transported across wild-type (●, A-to-B transport; ○, B-to-A transport) and *MDR1*-transfected (▲, A-to-B transport; Δ, B-to-A transport) cells. (mean ± S.D., $n = 6$)

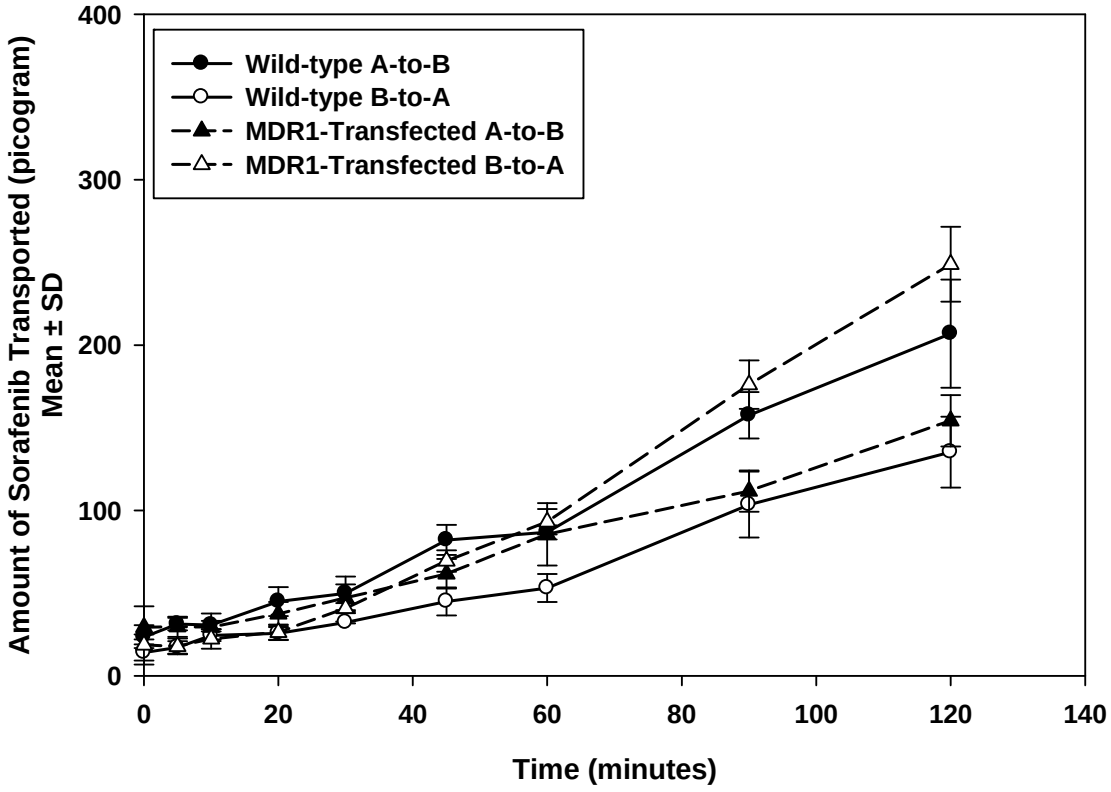

Figure 3.4B. Directional transport of [^{3}H] sorafenib across MDCKII cell monolayers.

Permeability of [^{3}H] sorafenib across MDCKII wild-type and *MDR1*-transfected cell monolayers. There was no difference in rate of sorafenib transported and apparent permeability of sorafenib between the A-to-B (black bar) and B-to-A (gray bar) directions, indicating lack of P-gp mediated efflux. (mean ± S.D., n = 6)

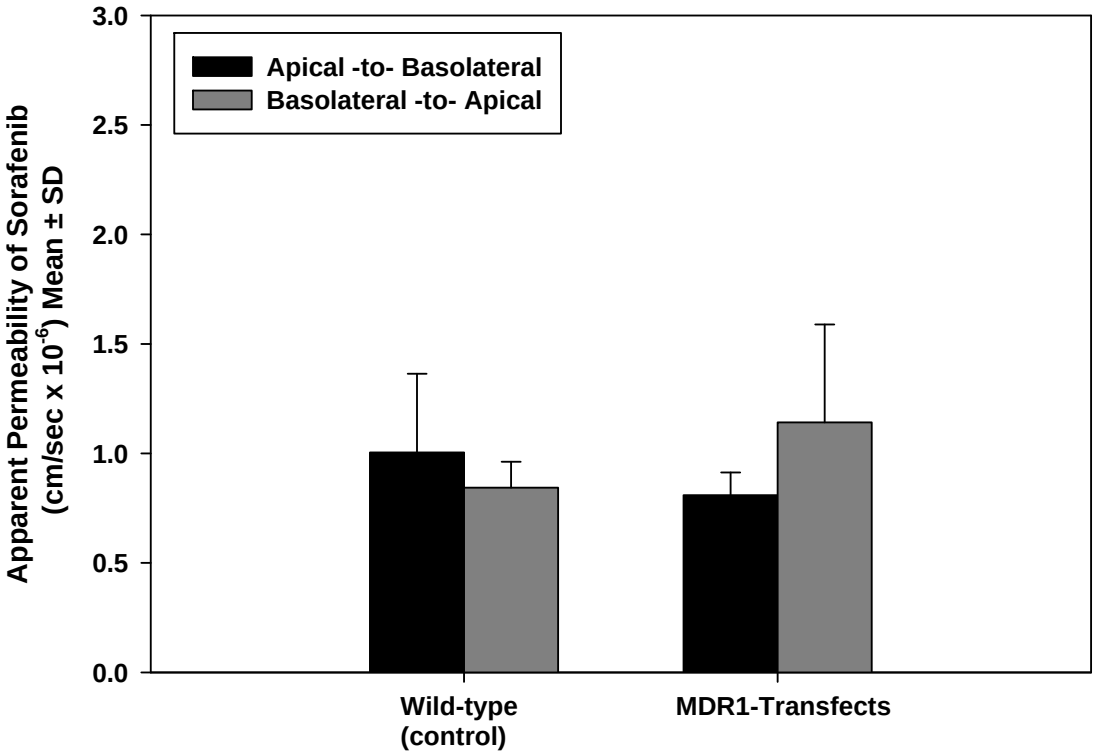

Figure 3.5. Affinity of sorafenib for BCRP.

The B-to-A permeability of sorafenib was determined in MDCKII-*Bcrp1* cells, with a range of concentrations (0.001 nM to 80 nM) applied to the donor side. A sigmoid inhibitory Emax model was fitted to the data and the affinity constant (Km_{app}) was determined to be 5 nM (●, observed data; - - -, model predicted curve; mean ± S.D., n = 3; parameter estimate reported as mean ± S.D. (standard error of the estimate)).

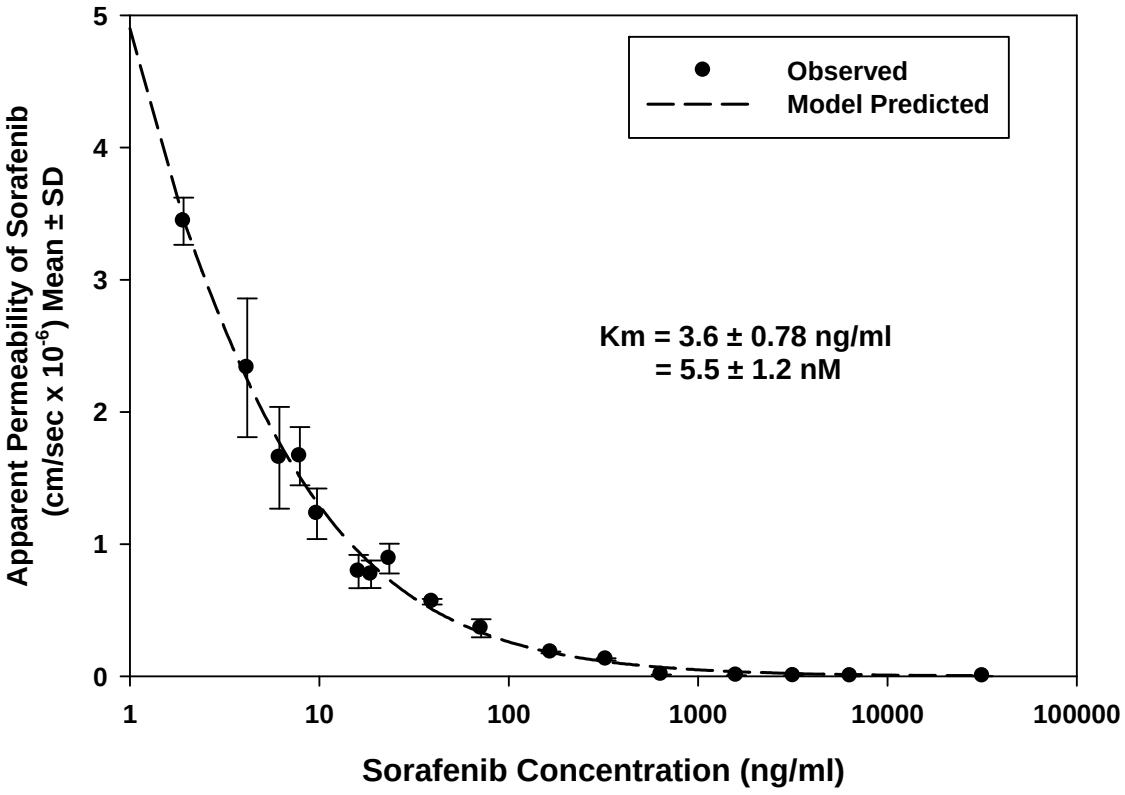

Figure 3.6A. Inhibition of P-gp by sorafenib.

Intracellular accumulation of the P-gp substrate, vinblastine, in MDCKII-*MDR1* cells in presence of increasing sorafenib concentrations. Sorafenib inhibited the accumulation of vinblastine with an IC_{50} of 25 µM (●, observed data; **- - -**, model predicted curve; mean ± S.D., $n = 4$; parameter estimate reported as mean ± S.D. (standard error of the estimate)).

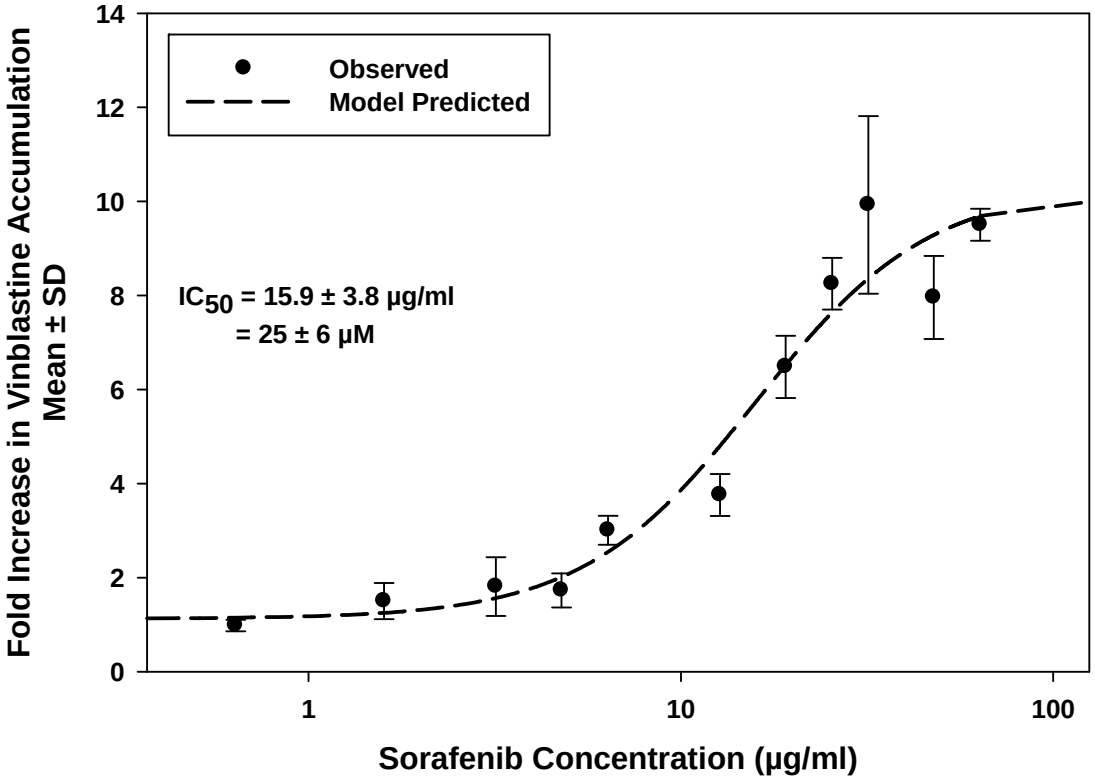

Figure 3.6B. Inhibition of BCRP by sorafenib.

Intracellular accumulation of BCRP substrates, prazosin (●) and mitoxantrone (▲), in MDCKII-*Bcrp1* cells in presence of increasing sorafenib concentrations. Sorafenib has no effect on accumulation of the two prototypical BCRP substrates (mean ± S.D., $n = 4$).

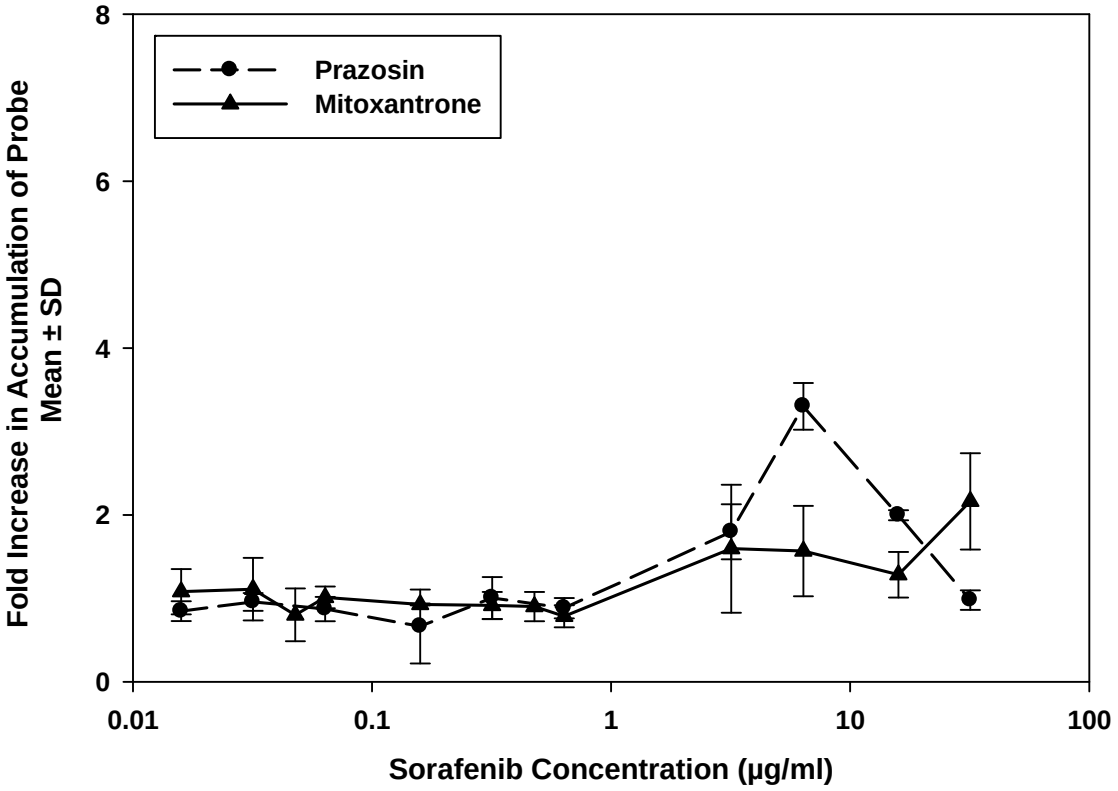

Figure 3.7. Sorafenib brain and plasma concentrations after a single intravenous dose of 10 mg/kg in FVB wild-type mice.

Brain concentrations were significantly lower than the plasma concentrations at all the measured time points suggesting limited delivery of sorafenib across the BBB (*, $p < 0.05$, mean ± S.D., $n = 4$).

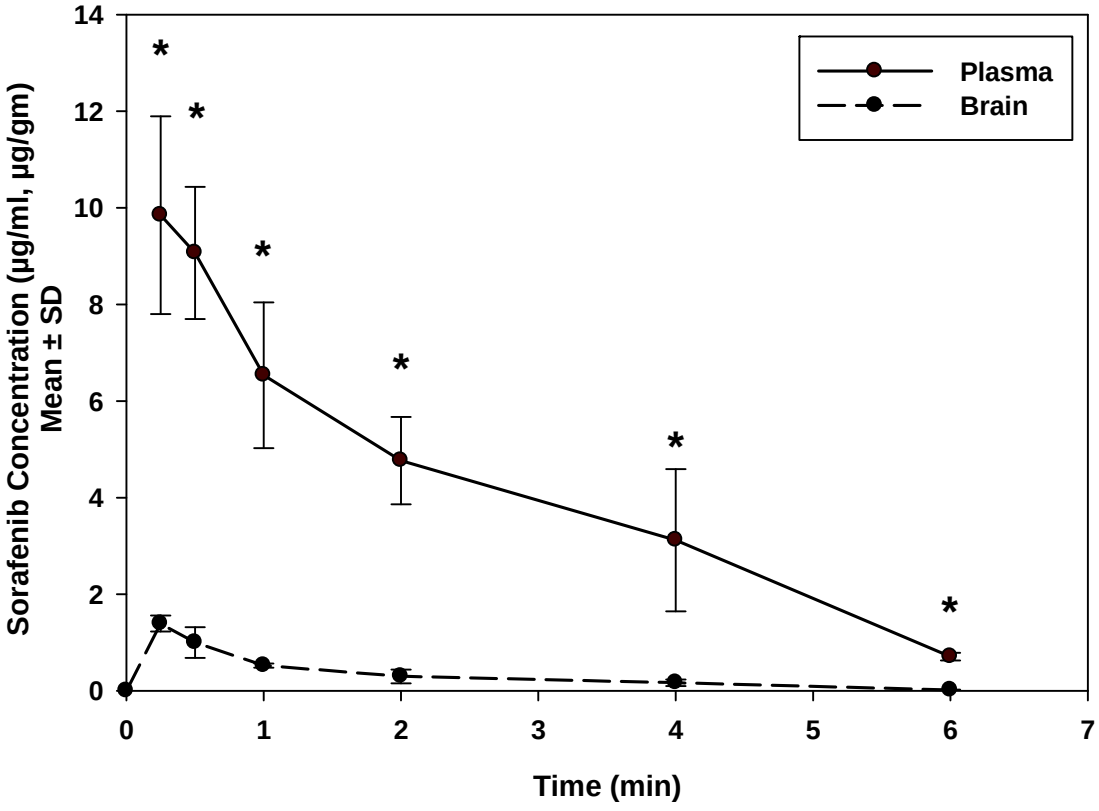

Figure 3.8. Steady-state brain distribution of sorafenib in wild-type, Mdr1a/b$^{-/-}$, Bcrp1$^{-/-}$ and Mdr1a/b$^{-/-}$Bcrp1$^{-/-}$ mice.

Sorafenib was delivered at a constant rate of 2 mg/hr/kg and ratio of the brain and plasma concentrations at steady-state (48 hrs) was determined. The B/P ratio in the *Bcrp1*$^{-/-}$ and *Mdr1a/b*$^{-/-}$*Bcrp1*$^{-/-}$ mice was significantly greater than that in wild-type mice suggesting the role of BCRP in efflux of sorafenib at the BBB (*, $p < 0.05$, compared to wild-type; †, $p < 0.05$, compared to *Bcrp1*$^{-/-}$ mice, mean ± S.D., $n = 4$).

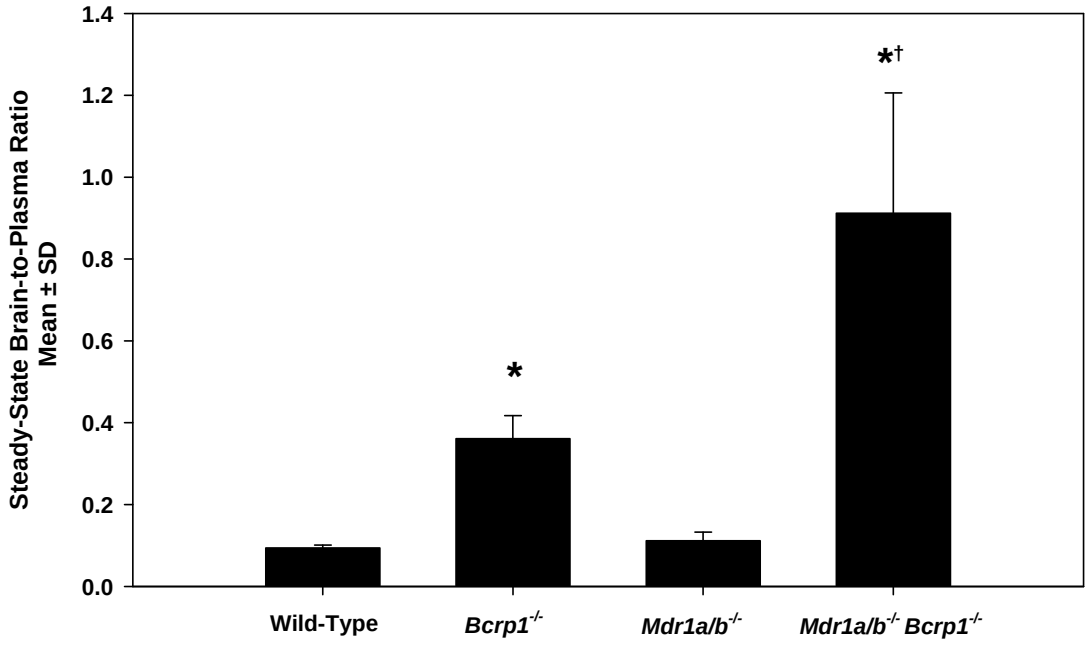

Figure 3.9. Influence of the dual inhibitor elacridar on the brain distribution of sorafenib.

10 mg/kg i.v. elacridar was given 30 minutes before the administration of 10 mg/kg sorafenib followed by determination of brain and plasma concentrations at 60 minutes. Administration of elacridar increased the B/P ratio in wild-type, *Bcrp1*$^{-/-}$ and the *Mdr1a/b*$^{-/-}$ mice such that they were not statistically different from the ratio in the *Mdr1a/b*$^{-/-}$*Bcrp1*$^{-/-}$ mice (*, $p < 0.05$, compared to wild-type control; †, $p < 0.05$, compared to corresponding control; #, no significant difference between the control and vehicle control groups of each genotype, mean ± S.D., $n = 4$).

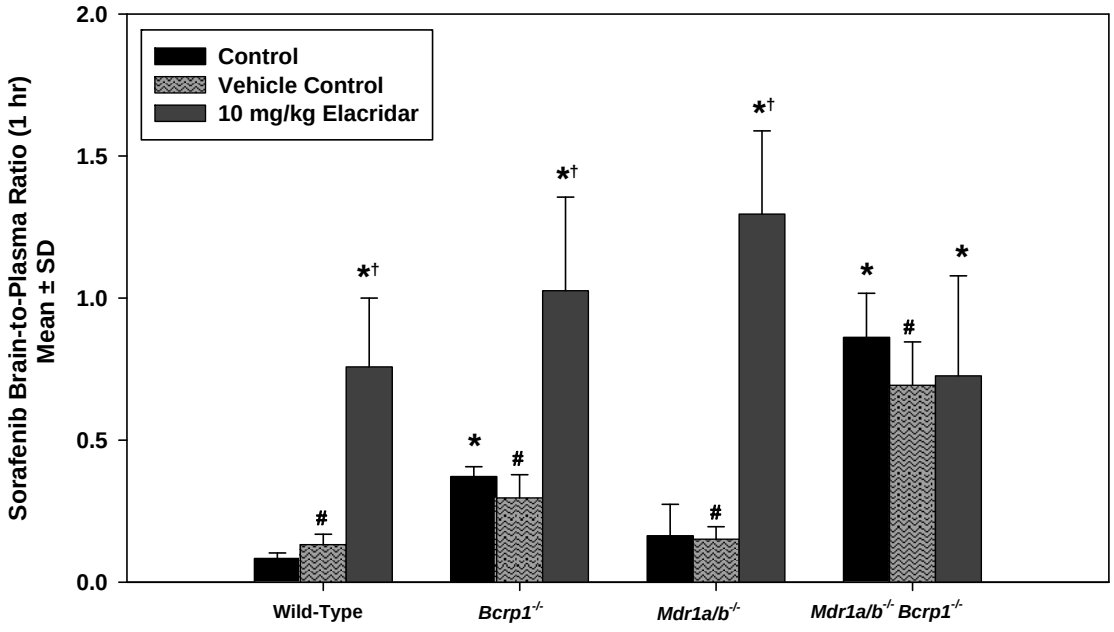

CHAPTER IV

INSIGHT INTO THE COOPERATION OF P-GLYCOPROTEIN (ABCB1) AND BREAST CANCER RESISTANCE PROTEIN (ABCG2) AT THE BLOOD-BRAIN BARRIER: A CASE STUDY EXAMINING SORAFENIB EFFLUX CLEARANCE

This chapter has been submitted for review in Drug Metabolism and Disposition, May 2011

The ATP-binding cassette transporters p-glycoprotein and breast cancer resistance protein have been shown to be critical determinants of drug transport across the BBB into the brain. Several therapeutic agents have been shown to be substrates for these two transporters, as a result they do not distribute to the brain to any significant extent. Recently, it has been shown that these two drug transporters cooperate at the BBB and brain penetration of dual substrates increase significantly only when both are absent. e.g., in the *Mdr1a/1b*$^{-/-}$*Bcrp1*$^{-/-}$ mice. The present study uses the brain penetration of sorafenib to investigate these findings and to attempt to explain the mechanistic basis of this cooperation with a simplistic theory based on affinity and capacity dependent carrier-mediated transport. The brain efflux index method , combined with the organotypic brain slices, were used to determine the net contribution of P-gp and BCRP to the total clearance of sorafenib out of the brain and show that its efflux at the BBB is mediated primarily by BCRP. Sorafenib clearance out of the brain decreased significantly in the *Bcrp1*$^{-/-}$ and *Mdr1a/1b*$^{-/-}$*Bcrp1*$^{-/-}$ mice. Clearance out of brain when P-gp was absent did not change significantly compared to wild-type. The affinity-capacity theory explains that due to a significantly greater expression at the BBB, P-gp appears to be the dominant transporter in efflux of many dual substrates at the BBB. It also explains why brain penetration of many of these compounds does not increase in the *Bcrp1*$^{-/-}$ mice. The study also investigated the expression of P-gp and BCRP at the BBB of the genetic knockout mice and show similar transporter levels between the wild-type and transporter deficient mice.

4.1 Introduction

The difficulty in delivering drugs to the central nervous system (CNS) is considered to be pivotal in the limited success of neurotherapeutics (1). The blood-brain barrier (BBB) is the most significant blood-CNS interface that restricts delivery of therapeutic agents to the brain (2). ATP binding cassette (ABC) transporters that prevent the passage of drugs into the brain by pumping them back into the blood form a vital component of this barrier (3). P-glycoprotein (P-gp) and the breast cancer resistance protein (BCRP) are two important ABC transporters at the BBB that have been extensively studied regarding their role in impeding drug penetration into the brain (4).

In the two decades following the discovery of P-gp at the BBB by Cordon-Cardo and colleagues (5), researchers have shown that P-gp plays a central role in the efflux of several neurotherapeutic agents from the brain (6). P-gp thus represents a critical gatekeeper governing the passage of drugs into the brain. In 2002, more than 20 years after the discovery of P-gp, BCRP was discovered at the BBB (7). It was believed that, similar to P-gp, BCRP was also involved in drug efflux at the BBB. This has been confirmed in several studies that show the impact of BCRP mediated efflux on brain penetration of substrate drugs (8-10).Thus BCRP is, in addition to P-gp, another obstacle for delivering chemotherapeutic drugs into the brain.

Recent research has led to a new paradigm suggesting that P-gp and BCRP work as a "cooperative team of gatekeepers" at the BBB. In 2007, de Vries et al. showed that brain uptake of topotecan, a substrate for both P-gp and BCRP, was not increased in mice

lacking BCRP (*Bcrp1*$^{-/-}$) and increased only slightly in P-gp deficient mice (*Mdr1a/1b*$^{-/-}$) (11). In contrast, topotecan brain uptake increased dramatically in mice lacking both P-gp and BCRP (*Mdr1a/1b*$^{-/-}$*Bcrp1*$^{-/-}$). Thus, absence of both P-gp and BCRP resulted in an effect that was significantly larger than the combined effects from the single transporter knockout mice. A similar phenomenon was reported by Polli et al. for lapatinib in P-gp/BCRP deficient mice (12). We have shown similar findings with other tyrosine kinase inhibitors, including dasatinib (13), gefitinib (14) and sorafenib (8). Even though these drugs are substrates for both P-gp and BCRP, absence of only one of the transporters did not significantly increase delivery of the drugs to the brain, but the greatest enhancement in brain penetration was seen when both transporters were absent at the BBB. Several studies now show that this is true for other dual P-gp and BCRP substrates as well (15-17).

These findings suggest that inhibition of either P-gp or BCRP can be compensated by the other transporter, and that both transporters "cooperate" with each other in preventing chemotherapeutic drugs from entering the brain (8). Kodaira et al. explained this cooperation of P-gp and BCRP by determining the net contribution of each transporter to the overall efflux of various drugs at the BBB (16). The authors concluded that for many dual substrates, P-gp-mediated efflux out of the brain was greater than that by BCRP. However, there are several questions that are still unanswered. Is the compensatory mechanism a result of changes in expression of other transporters in the genetic knockout mice? If so, changes in transporter-mediated active clearance can explain some of the findings in the transporter deficient mice.

The objective of this study was to examine the cooperation of P-gp and BCRP in an experimental paradigm that would explain the findings in the *Mdr1a/b*$^{-/-}$, *Bcrp1*$^{-/-}$ and the combined *Mdr1a/b*$^{-/-}$*Bcrp1*$^{-/-}$ mice. We use the brain efflux index method to determine the kinetics of sorafenib efflux out of the brain. We have previously demonstrated that P-gp and BCRP together limit the brain distribution of sorafenib (8). In this study we determine the contribution of P-gp- and BCRP-mediated efflux to the total clearance of sorafenib from the brain. Moreover, since the expression of P-gp and BCRP at the BBB in the genetic knockout animals remains to be carefully characterized, the present study used immunoblotting to show that P-gp and BCRP levels at the BBB are essentially unchanged in the knockout mice. Finally, we present a theory to explain the cooperation of P-gp and BCRP at the BBB. This hypothesis, based on differences in relative affinities and capacities of the two transporters, can reasonably explain the findings in the *Mdr1a/b*$^{-/-}$*Bcrp1*$^{-/-}$ mice.

4.2 Material and Methods

4.2.1 Chemicals and Reagents

[^{3}H] sorafenib (3.5 Ci/mmol, purity - 98.4) and [^{14}C] inulin (7.5 mCi/mmol, purity – 98.5 %) were purchased from Moravek Biochemicals (La Brea, CA). Elacridar (GF120918) was purchased from Toronto Research Chemicals (Ontario, Canada). Ko143 was kindly provided by Dr. Alfred Schinkel (The Netherlands Cancer Institute, Amsterdam, The Netherlands) and zosuquidar (LY335979) was a gift from Eli Lilly and Co. (Indianapolis, IN). All other chemicals were reagent grade and were purchased from Sigma Chemical Co (St. Louis, MO).

4.2.2 Brain Efflux Index (BEI) Study

FVB (wild-type), *Mdr1a/b*$^{-/-}$, *Bcrp1*$^{-/-}$ and *Mdr1a/b*$^{-/-}$*Bcrp1*$^{-/-}$ mice were from Taconic Farms, Inc. (Germantown, NY). All animals were 8 to 10 weeks old at the time of experiment. Animals were maintained under temperature-controlled conditions with a 12-h light/dark cycle and unlimited access to food and water. All studies were carried out in accordance with the guidelines set by the Principles of Laboratory Animal Care (National Institutes of Health) and were approved by The Institutional Animal Care and Use Committee (IACUC) of the University of Minnesota

The brain efflux index (BEI) technique was performed as described previously by Kakee and coworkers (18). Anesthetized mice were mounted on a stereotaxic device and a borehole was made 3.8 mm lateral to the bregma. The dosing solution was prepared by dissolving [^{3}H]-sorafenib (10 μCi/ml) and [^{14}C]-carboxyl-inulin (5 μCi/ml) in extracellular fluid (ECF) buffer (122 mM NaCl, 25 mM $NaHCO_3$, 3mM KCl, 1.4 mM $CaCl_2$, 1.2 mM $MgSO_4$, 0.4 mM K_2HPO_4, 10 mM D-glucose, and 10 mM HEPES, pH 7.4). Using a 2.5-μL microsyringe fitted with a 32 gauge needle (Hamilton, Reno, NE), 0.2 μL of the dosing solution was injected over 2 minutes at a depth of 2.5 mm. The injection process was controlled by a Quintessential® stereotaxic injector (Stoelting Co., IL, USA). Time zero was defined as the time when the injection was complete. The needle was left in place for additional 4 minutes to minimize the backflow of injected solution after which the mice were euthanized at designated time points post dose. The right (ipsilateral), left (contralateral) cerebrum and cerebellum were harvested, weighed and homogenized in 3 volumes of 5% bovine serum albumin solution. A 100-μL sample

of brain homogenate from the right, left cerebrum and cerebellum was mixed with 4 ml of scintillation fluid (ScintiSafe Econo cocktail; Thermo Fisher Scientific, Waltham, MA) and the associated radioactivity was measured in a liquid scintillation counter (Beckman Coulter, Fullerton, CA).

100-BEI (%) defined as the percentage of the amount of test drug remaining in the ipsilateral cerebrum, was calculated according to the following equation,

$$100 - BEI(\%) = \left(\frac{\text{amount of } [^3H] \text{ sorafenib in the brain} / \text{amount of } [^{14}C] \text{inulin in the brain}}{\text{amount of } [^3H] \text{ sorafenib injected} / \text{amount of } [^{14}C] \text{inulin injected}} \right) \text{x } 100$$

The apparent BBB efflux rate constant, k_{eff} , was obtained by linear regression of log (100-BEI) versus time.

4.2.3 Brain Slice Uptake Study

The volume of distribution of sorafenib in the brain was determined by using the brain slice uptake technique according to the procedure by Friden et al (19). In brief, whole brain was sliced to obtain 400 μm coronal slices using a Vibratome^{TM} (series 1000, The Vibratome Company, Bannockburn, IL). Slices were incubated in 3 ml of oxygenated ECF buffer containing [^{3}H]-sorafenib (0.1 μCi/ml) and [^{14}C]-inulin (0.05 μCi/ml) at 37 ˚C. The incubation solution was continuously aerated with a oxygen-CO_2 mixture (95:5) and shaken on an orbital shaker at 75 r.p.m. At designated time points, the slices were removed from the drug solution, dried on filter paper and weighed. The radioactivity associated with the slice was determined by liquid scintillation counting (Beckman Coulter, Inc., Fullerton, CA). The brain volume of distribution ($V_{d,brain}$) was calculated as

the amount of sorafenib in the brain slice divided by the concentration in the incubation solution

4.2.4 Isolation of Brain Capillaries and Membranes

Whole brain capillaries and crude membranes were prepared according to the method by Hartz et al. (20). Wild-type, *Mdr1a/b*$^{-/-}$, *Bcrp1*$^{-/-}$ and *Mdr1a/b*$^{-/-}$*Bcrp1*$^{-/-}$ mice were euthanized (n = 10 each) and whole brain was harvested. Brain tissue was carefully cleaned to remove all visible white matter and homogenized in ice-cold PBS buffer (2.7 mM KCl, 1.46 mM KH_2PO_4, 136.9 mM NaCl, 8.1 mM Na_2HPO_4, 0/9 mM $CaCl_2$ and 0.5 mM $MgCl_2$ supplemented with 5 mM D-glucose and 1 mM sodium pyruvate). The homogenate was mixed with Ficoll (final concentration 16 %) and centrifuged at 5800 *g* for 20 mins at 4 ºC. The resulting pellet was resuspended in PBS buffer containing 1 % BSA solution and passed over a 0.4 mm glass bead column. Capillaries adhering to the glass beads were collected by gentle agitation using 1 % BSA. Capillaries were washed three times with PBS buffer followed by centrifugation at 7000 *g* for 10 mins at 4 ºC to collect the capillary pellet. Pellets were then lysed using mammalian protein extraction reagent (Thermo Fisher Scientific, Rockford, IL) containing protease inhibitor cocktail (Thermo Fisher Scientific, Rockford, IL). The lysate was centrifuged at 15,000 *g* for 15 mins and the denucleated supernatant was used as brain capillary lysate for western blotting.

Crude membrane fractions were obtained from the brain capillaries by centrifugation of the denucleated supernatants at 100,000 *g* for 90 mins. Pellets of crude plasma

membranes were resuspended in mammalian protein extraction reagent and used for western blotting.

4.2.5 Western Blotting

Protein concentrations in the lysates from brain capillaries and the plasma membranes were determined by using the bicinchoninic acid (BCA) protein assay (Thermo Fisher Scientific, Rockford, IL). Lysates were diluted in a reducing sample buffer and separated on a 10 % SDS-PAGE gel, run at 100 volts for 1 hour. Gels were then transferred to a PVDF membrane at 100 volts for 1 hour at 4 ºC followed by blocking for 1 hour using 5 % milk. Membranes were incubated with primary antibody to BCRP (BXP-53, 1:50, 5 µg/ml; Enzo Life sciences, PA, USA), P-gp (2C19, 1:50, 2 µg/ml; Enzo Life sciences, PA, USA) or *β*-actin (1:1000, 1 µg/ml; Enzo Life sciences, PA, USA) overnight at 4 ºC. Membranes were then washed and incubated with horseradish peroxidase-conjugated secondary antibody (1:5000, ; Enzo Life sciences, PA, USA) for 1 hour. Blots were developed using the Pierce ECL western blotting substrate (Thermo Fisher Scientific, Rockford, IL). Densitometry calculations were done on unmodified images using the Image J software (NIH, Bethesda, MD).

4.2.6 Pharmacokinetic and Statistical Analysis

The efflux rate constant in the BEI studies was estimated by linear regression of the log transformation of percent remaining in brain (100 – BEI) vs. time. The regression line was not forced through 100 % at time zero which was included as a data point. In the brain slice uptake studies, the volume of distribution was calculated as the average ratio

of amount in brain slice to concentration in incubation solution after equilibrium had been reached (last two time points).

After direct intra cerebral injection using the brain efflux index technique, the brain represents a single compartment with drug eliminating out of the brain into the blood. It is assumed, that given the short experiment times, there is no redistribution of drug back from the blood into the brain. The kinetics of drug elimination are therefore explained by a one compartment system with k_{eff} being the first order elimination rate constant and $Cl_{app,efflux}$ being a first order clearance of drug out of the brain. The apparent efflux clearance out of brain ($Cl_{app,efflux}$) was thus calculated as the product of elimination rate constant (k_{eff}) obtained from the BEI study and brain distribution volume of distribution ($V_{d,brain}$).

$$CL_{app,efflux} = k_{eff} \times V_{d,brain}$$

The standard deviation of the efflux clearance was calculated according to the following formula.

$$\text{Standard Deviation}\left(CL_{app,efflux}\right) = k_{eff} \times V_{d,brain} \sqrt{\frac{(\text{std.dev.}k_{eff})^2}{k_{eff}^2} + \frac{(\text{std.dev.}V_d)^2}{V_d^2}}$$

Sigma Stat was used to make statistical comparisons using the t-test for comparison of two groups with significance declared at a *p value* less than 0.05. Multiple groups were compared by one way ANOVA, using the Holm-Sidak post hoc test for multiple comparisons.

4.3 Results

4.3.1 Kinetics of Sorafenib Efflux from the Brain

The brain efflux index method was used to study the kinetics of sorafenib elimination from the brain. Sorafenib was rapidly cleared out of the brain with an efflux rate constant of 0.17 ± 0.02 min^{-1} in the wild-type mice (**Figure 4.1**). The half-life in brain of wild-type mice was ~4 minutes. The rate constant was unchanged when P-gp was absent in the *Mdr1a/b*$^{-/-}$ mice, the value being 0.16 ± 0.03 min^{-1} and the half life was 4.3 minutes. This suggested that P-gp did not have any significant contribution to the efflux of sorafenib from the brain. However, sorafenib efflux from brain was significantly reduced when BCRP was absent in the *Bcrp1*$^{-/-}$ mice, the rate constant decreasing to 0.10 ± 0.01 min^{-1} and the half-life increasing to 6.93 mins (**Table 4.1, $p < 0.05$**). This indicated that BCRP plays a significant role in the efflux of sorafenib from the brain. Similarly, the efflux rate constant was significantly smaller in the *Mdr1a/b*$^{-/-}$*Bcrp1*$^{-/-}$ mice compared to wild-type ($p < 0.05$). The efflux rate constant and half-life in the *Mdr1a/b*$^{-/-}$*Bcrp1*$^{-/-}$ mice was 0.06 ± 0.02 min^{-1} and 11.5 minutes, respectively (**Figure 4.1, Table 4.1**).

4.3.2 Sorafenib Volume of Distribution in the Brain

Volume of distribution of sorafenib in brain was determined by studying sorafenib uptake in brain slices from wild-type, *Mdr1a/b*$^{-/-}$, *Bcrp1*$^{-/-}$ and *Mdr1a/b*$^{-/-}$*Bcrp1*$^{-/-}$ mice. After incubation with [3H]-sorafenib equilibrium was attained within 2 hours in slices from all four mouse groups (**Figure 4.2**). The volume of distribution was 62.71 ± 7.8 ml/gm in the wild-type, 91.10 ± 18.18 ml/gm in the *Mdr1a/b*$^{-/-}$, 55.7 ± 8.73 ml/gm in the *Bcrp1*$^{-/-}$ and 88.73 ± 12.33 ml/gm in the *Mdr1a/b*$^{-/-}$*Bcrp1*$^{-/-}$ mice (**Table 4.1**).

4.3.3 Sorafenib Clearance out of Brain

Sorafenib clearance out of brain was calculated as the product of the efflux rate constant from the BEI study and the volume of distribution from the slice uptake study (**Table 4.1**). The clearance of sorafenib out of brain from the wild-type brain was 10.78 ± 2.01 ml/min/gm. The clearance in the *Mdr1a/b*$^{-/-}$ mice was not significantly different at 14.57 ± 4.38 ml/min/gm. This suggested that P-gp did not contribute to the efflux of sorafenib and its absence at the BBB does not influence sorafenib clearance from the brain. However, when BCRP was absent, sorafenib efflux clearance decreased significantly to 5.57 ± 1.09 in the *Bcrp1*$^{-/-}$ mice and 4.3 ± 2.09 in the *Mdr1a/b*$^{-/-}$*Bcrp1*$^{-/-}$ mice. This confirms that BCRP significantly contributes to the efflux of sorafenib out of the brain.

4.3.4 Detection of P-gp and BCRP in Brain Capillaries

We used immunoblotting to examine expression of P-gp and BCRP in brain capillaries from FVB mice. **Figure 4.4A** illustrates western blotting results in isolated brain capillaries showing no difference in expression of P-gp between the wild-type and *Bcrp1*$^{-/-}$ mice. Likewise, BCRP expression was not different between the wild-type and *Mdr1a/b*$^{-/-}$ mice **(Figure 4.4B)**. **Figure 4.5A** shows western blots for P-gp and BCRP in plasma membranes of isolated brain capillaries. Again, there was little difference in the expression of P-gp and BCRP between the wild-type and the genetic knockout mice (**Figure 4.5B**). This suggests that there are no compensatory changes in expression of P-gp or BCRP in the genetic knockout mice where one transporter is absent.

4.4 Discussion

Recent research on the role of ABC transporters, P-gp and BCRP, at the BBB has led to a new paradigm that suggests a cooperative role of the two transporters in the efflux of drugs out of the brain (12-14). There are several reports that show a greater than additive increase in brain penetration of substrate drugs in *Mdr1a/b*$^{-/-}$*Bcrp1*$^{-/-}$ mice compared to the single knockout mice (11, 14-17). While there have been a couple of possibilities that explain this behavior of dual substrates in the combined P-gp/BCRP deficient mice, a clear understanding of the underlying mechanism is still absent. This study was undertaken with an objective to better understand the cooperation of P-gp and BCRP at the BBB and provide an explanation for the findings in the genetic knockout animals. We used the brain efflux index to study the magnitude of P-gp- and BCRP-mediated efflux on the clearance of a dual substrate from the brain. Sorafenib was chosen as the model substrate since we have previously shown that its brain penetration is restricted by both P-gp and BCRP.

In 2010, Kodaira et al. mathematically determined the net clearance by P-gp and BCRP at the BBB (16). Using several dual and single substrates for P-gp and BCRP, the group showed that P-gp was the major contributor to the efflux of dual substrates at the BBB. We used the brain efflux index method to determine the clearance of sorafenib due to P-gp and BCRP, and show that the above generalization is not true for all dual substrates. Sorafenib clearance out of the brain when P-gp was absent in the *Mdr1a/b*$^{-/-}$ deficient mice was similar to that in the wild-type mice (**Table 4.1**), indicating that lack of P-gp alone does not decrease the efflux of sorafenib at the BBB. This is consistent with our

previous report where brain penetration of sorafenib was unchanged in the *Mdr1a/b*$^{-/-}$ mice compared to wild-type mice. Interestingly, sorafenib clearance out of the brain decreased significantly when BCRP was absent at the BBB. There was no statistical difference between the clearances in the *Mdr1a/b*$^{-/-}$*Bcrp1*$^{-/-}$ and *Bcrp1*$^{-/-}$ mice (**Table 4.1, Figure 4.1**) further confirming a limited role of P-gp in the efflux of sorafenib at the BBB. Thus, in the case of sorafenib, it is BCRP that is the major contributor to its efflux at the BBB. This explains the findings in P-gp deficient mice where BCRP is still present and effluxes sorafenib out of the brain.

In 2004, Cisternino and colleagues reported that the BCRP mRNA was upregulated in the *Mdr1a*$^{-/-}$ mice and suggested that genetic knockout animals are susceptible to compensatory upregulation of ABC transporters (21). This finding, if true for all genetic knockout mice, can explain why brain penetration does not increase when a single transporter is absent at the BBB. Compensatory increase in levels of other transporters (P-gp or BCRP) can be a reason behind the lack of effect in the single knockouts and the greater than additive increase in brain penetration in the combined P-gp/BCRP knockout mice. We examined this in the FVB mouse model by immunoblotting for P-gp and BCRP in brain capillaries from wild-type, *Mdr1a/b*$^{-/-}$, *Bcrp1*$^{-/-}$ and *Mdr1a/b*$^{-/-}$*Bcrp1*$^{-/-}$ mice. There was no difference in protein levels of P-gp between the wild-type and BCRP deficient mice. Likewise, expression of BCRP protein in the P-gp deficient mice was unchanged compared to wild-type (**Figures 4.4, 4.5**). de Vries et al. reported similar findings that there was no difference in the levels of BCRP protein in the wild-type and *Mdr1a/b*$^{-/-}$ mice (11). These results suggest that there might be no compensatory

upregulation of P-gp in the BCRP deficient mice, and vice versa. However, the above discussion is limited to P-gp and BCRP only, and it is possible there are compensatory changes in regulation of other influx and efflux transporters in these mice. A detailed and precise study examining the levels of all relevant transporters at the BBB is therefore necessary and can provide a more accurate depiction of compensatory changes in transporter function in the gene knockout mice.

It has been shown that there is extensive overlap in the substrate specificities of BCRP and P-gp and that these two transporters co-localize at the BBB (22). This has led to extensive investigations on the role of BCRP at the BBB. Several studies have shown that BCRP effluxes several drugs in vitro. However, very few reports have shown the translation of this in vitro efflux to limited brain penetration in vivo. Lee *et al.* conducted *in situ* brain perfusion studies using the BCRP substrates dehydroepiandrosterone sulfate and mitoxantrone and reported that brain penetration of the two compounds was not increased in *Bcrp1*$^{-/-}$ mice (23) . Similarly, Giri and coworkers showed that BCRP mediated efflux of the antiretroviral drugs abacavir and zidovudine *in vitro* (24). However, despite the absence of BCRP, brain uptake of these two compounds was not elevated in *Bcrp1*$^{-/-}$ mice (25). One conclusion drawn from these studies was that BCRP played a minor role in drug efflux at the BBB. A study by Zhao et al. showed that interaction of BCRP with substrates *in vitro* rarely translates to visible effects at the blood-brain barrier in vivo (26).

Recently Kamiie *et al.* quantified expression of various membrane transporters at the

mouse BBB and reported approximately 5-fold higher P-gp protein levels compared to those of BCRP (27). Significantly higher protein expression levels at the BBB make P-gp appear to be the dominant efflux transporter for many dual substrates that have similar affinities to both P-gp and BCRP. In comparison, due to lower protein expression levels, BCRP-mediated efflux appears to be minor and becomes apparent only when P-gp or both transporters are absent. This may true for many drugs such as dasatinib, gefitinib, topotecan, lapatinib, erlotinib etc. However, in the case of sorafenib and dantrolene, both compounds have a significantly higher affinity for BCRP than for P-gp (16, 28). Therefore, BCRP is the dominant transporter in keeping these drugs out of the brain and an effect of P-gp on drug penetration is only noticeable in the P-gp/BCRP knockout mice. Differences in relative affinities of substrate drugs for P-gp and BCRP as well as different expression of the two transporters at the BBB can thus explain their cooperative role at the BBB. The above discussion is a simplistic theory that tries to explain the interplay of P-gp and BCRP at the BBB. Of course, it does not take into consideration role of other transporters that may be involved in the efflux of these compounds at the BBB.

It is important to consider the translation of this cooperation of active transporters to humans. Uchida et al. recently determined levels of various transporter proteins at the human BBB (29). Interestingly, the group reported significant higher levels of BCRP than P-gp. Furthermore, BCRP expression was 1.8-fold greater and P-gp expression was 2.3-fold lower at the human BBB in comparison to the mouse BBB. This suggests that in the cooperation of P-gp and BCRP at the human BBB, BCRP might play a more significant role. This is particularly important since many drugs show a significant

BCRP-mediated transport in vitro. As mentioned earlier, even though these drugs did not show a BCRP mediated efflux at the BBB in the mouse, the situation in the humans could be different due to the presence of significantly greater amount of BCRP.

In conclusion, the present study explains the cooperation of P-gp and BCRP at the BBB by using a simple affinity-capacity relationship that dictates the role of the individual transporter in drug efflux. We show that sorafenib is effluxed at the BBB mainly by BCRP but P-gp also plays a significant role and its effect if seen only in the P-gp/BCRP knockout mice. We also show that there might be no compensatory changes in expression of P-gp and BCRP in the genetic knockout mice. However more detailed investigations are warranted so that the exact levels of different influx and efflux transporters are determined and their influence on the transport of drugs to the brain can be ascertained.

4.5 Footnotes

The authors would like to thank Bjoern Bauer and Anika Hartz (University of Minnesota, Duluth) for their help and support in development of the brain capillary isolation method This work was supported by National Institutes of Health - National Cancer Institute [CA138437] (William F. Elmquist) and a grant from the Children's Cancer Research Fund at the University of Minnesota (William F. Elmquist). Financial support for Sagar Agarwal was provided by the Doctoral Dissertation Fellowship from the University of Minnesota.

Table 4.1 Efflux Clearance of Sorafenib from Brain in FVB wild-type, Mdr1a/b$^{-/-}$, Bcrp1$^{-/-}$ and Mdr1a/b$^{-/-}$Bcrp1$^{-/-}$ Mice.

Genotype	K_{eff} (min^{-1})	Vd (ml/gm)	$Cl_{app,efflux}$ (ml/min/gm)	Half-life (min)
Wild-type	0.17 ± 0.02	62.71 ± 7.8[b]	10.78 ± 2.01	4.07
Mdr1a/b$^{-/-}$	0.16 ±0.03	91.10 ± 18.18	14.57 ± 4.38	4.33
Bcrp1$^{-/-}$	0.10 ± 0.01[a]	55.7 ± 8.73[b]	5.57 ± 1.09[a,c]	6.93
Mdr1a/b$^{-/-}$Bcrp1$^{-/-}$	0.06 ± 0.02[a]	88.73 ± 12.33	4.3 ± 2.09[a,c]	11.55

[a] ***p < 0.05 compared to wild-type mice***

[b] ***p < 0.05 compared to Mdr1a/b$^{-/-}$ and Mdr1a/b$^{-/-}$Bcrp1$^{-/-}$mice***

[c] ***p < 0.05 compared to Mdr1a/b$^{-/-}$ mice***

Figure 4.1 Brain efflux index of sorafenib in FVB mice

Sorafenib was rapidly cleared out of the brain in wild-type and *Mdr1a/b*$^{-/-}$ mice with an efflux rate constant of 0.17 ± 0.02 and 0.16 ± 03 min^{-1} respectively. Sorafenib clearance out of brain decreased in the *Bcrp1*$^{-/-}$ and *Mdr1a/b*$^{-/-}$*Bcrp1*$^{-/-}$ mice with efflux rate constants of 0.1 ± 0.01 and 0.06 ± 02 min^{-1} respectively. Data presented as mean ± S.D. (*n = 3-5 per time point*)

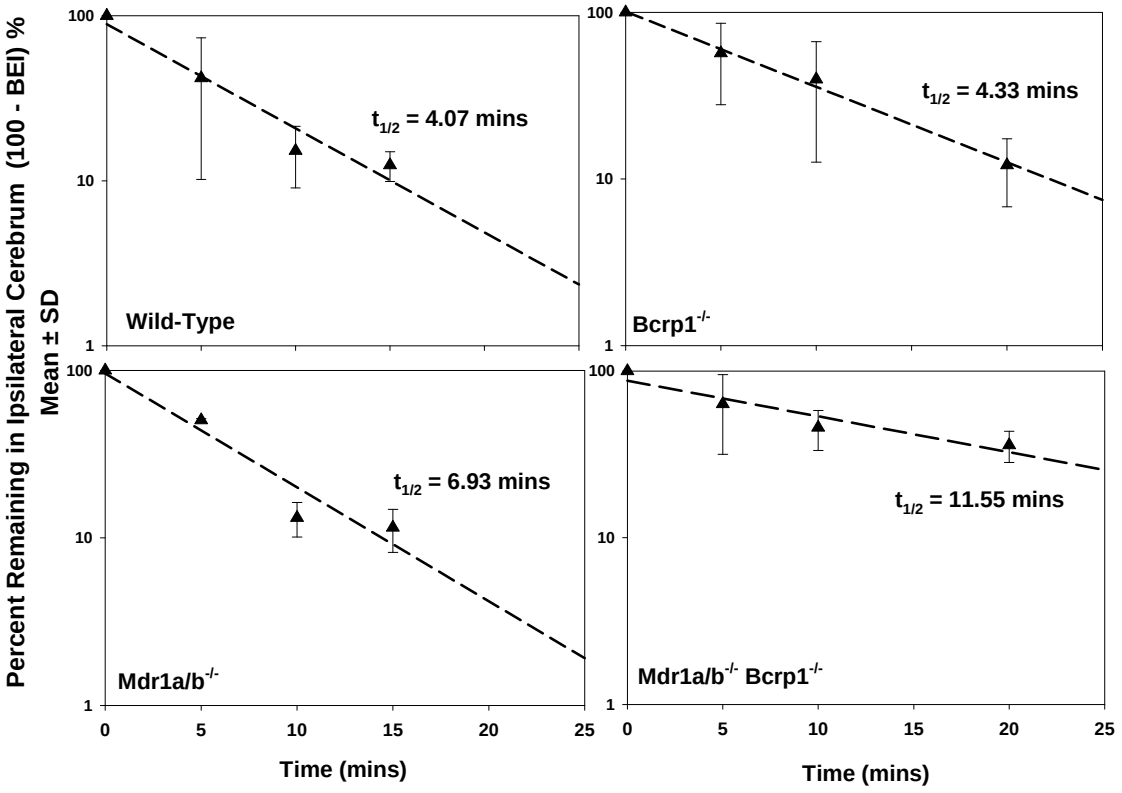

Figure 4.2 Volume of distribution of sorafenib in brain

Volume of distribution was determined by measuring uptake of [3H]-sorafenib in brain slices from wild-type, *Mdr1a/b*$^{-/-}$, *Bcrp1*$^{-/-}$ and *Mdr1a/b*$^{-/-}$*Bcrp1*$^{-/-}$ mice. Data presented as mean ± S.D. (*n = 3-5 per time point*)

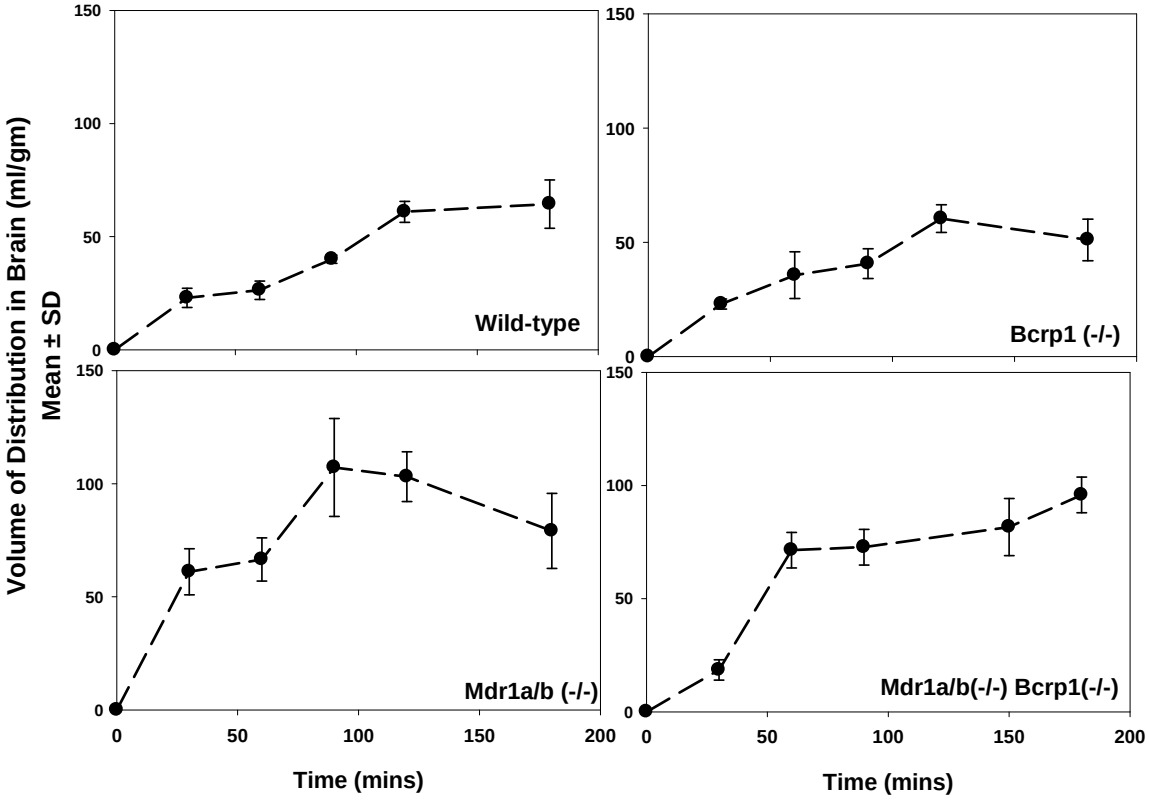

Figure 4.3 Photographs (400x) of freshly isolated mouse brain capillaries

Figure 4.4A Western blot analysis of P-gp and BCRP in isolated brain capillaries of wild-type, Mdr1a/b$^{-/-}$, Bcrp1$^{-/-}$ and Mdr1a/b$^{-/-}$Bcrp1$^{-/-}$ mice (pooled samples from 10 mouse brains)

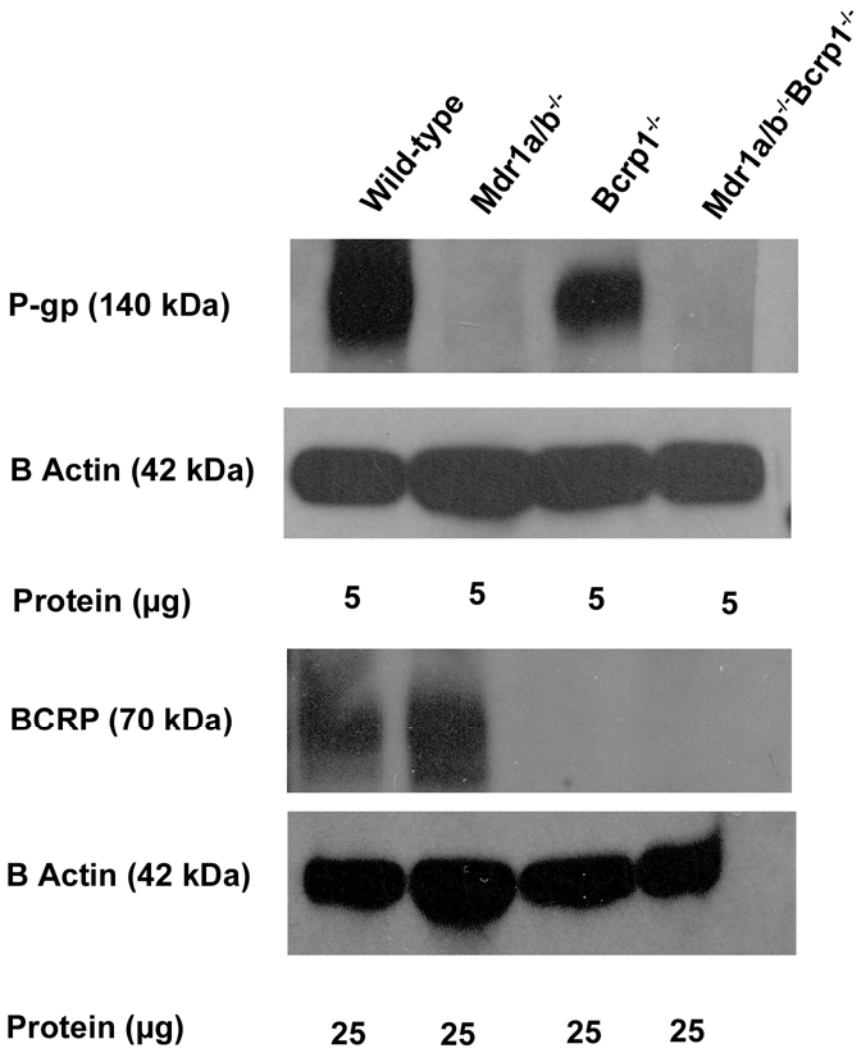

Figure 4.4B Quantification of western blots from brain capillaries

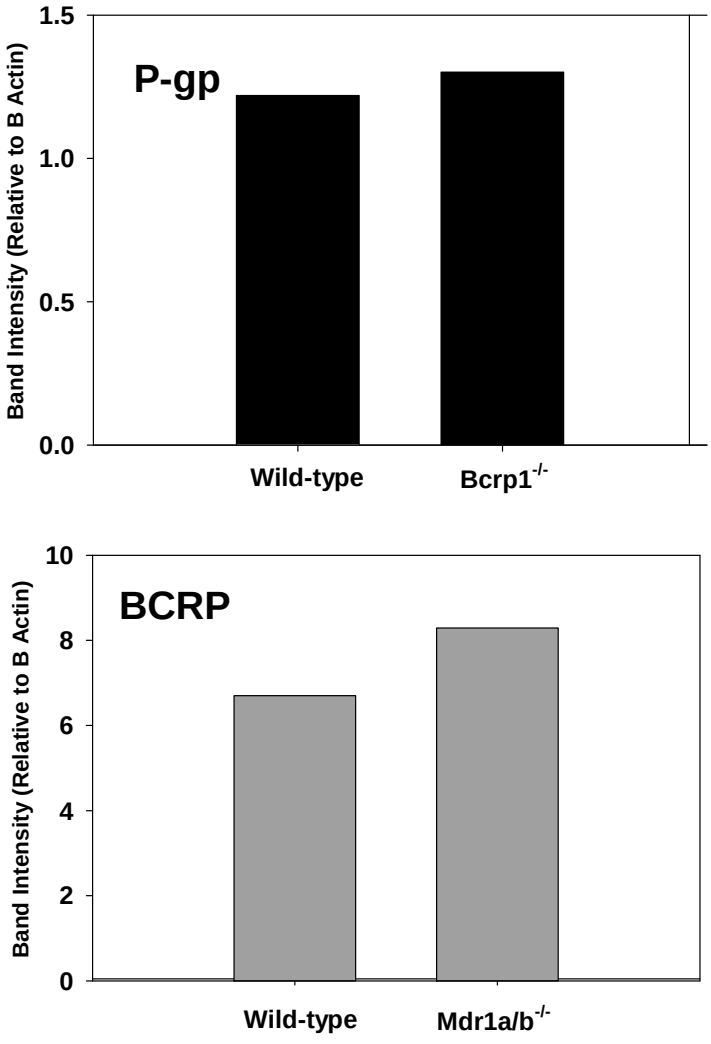

Figure 4.5A Western Blot Analysis of P-gp and BCRP in plasma membranes from brain capillaries of wild-type, Mdr1a/b$^{-/-}$, Bcrp1$^{-/-}$ and Mdr1a/b$^{-/-}$Bcrp1$^{-/-}$ mice (pooled samples from 10 mouse brains).

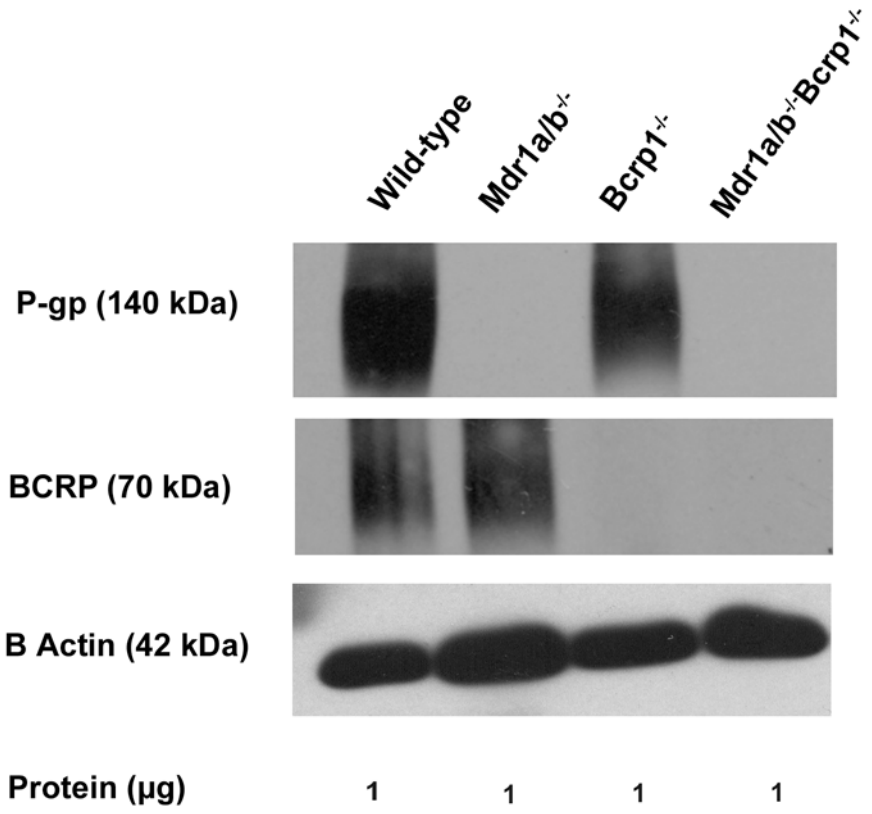

Figure 4.5B Quantification of western blots from plasma membranes

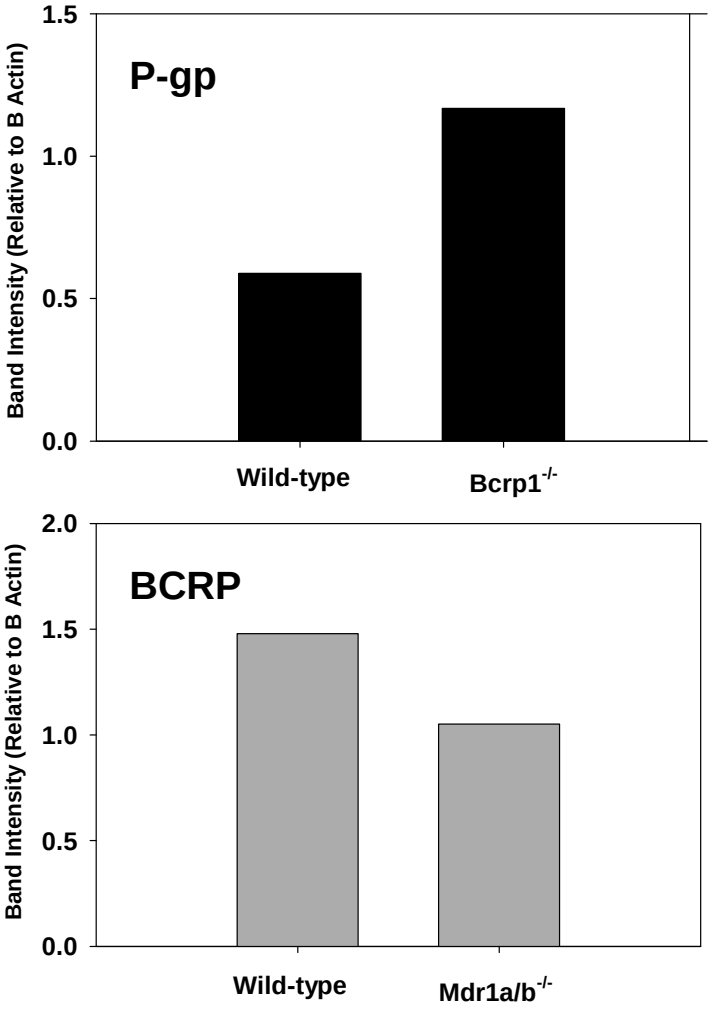

CHAPTER V

INHIBITION OF ACTIVE EFFLUX IMPROVES DELIVERY OF ERLOTINIB IN A ORTHOTOPIC XENOGRAFT MODEL OF GLIOMA

Despite aggressive treatment with radiation and chemotherapy, recurrence in glioblastoma multiforme (GBM) is inevitable. Infiltrative growth of the tumor into surrounding brain areas is a pathophysiological hallmark of GBM. The fact that recurrence occurs in areas away from the margins of surgical resection is indicative that invasive glioma cells in these areas are not being effectively targeted. One reason behind the inefficacy of molecularly-targeted agents in glioma might be inadequate delivery of drugs across the blood-brain barrier (BBB) to the invasive cells. The objective of this study was to show that the BBB, through a combination of tight junctions and efflux transporters, significantly restricts delivery of chemotherapeutic drugs to the tumor. We first show that erlotinib transport across the BBB is significantly restricted due to P-gp and BCRP-mediated efflux transport. We then address the issue of disruption of the BBB in glioma and show that the BBB is sufficiently intact in areas of brain away from the tumor where it significantly restricts erlotinib delivery. Inhibition of P-gp and BCRP by the dual inhibitor elacridar dramatically increased erlotinib delivery to the tumor core, rim and normal brain, indicating that this strategy can be used to enhance delivery of erlotinib to the brain and brain tumor. This study provides conclusive evidence of the impact of active efflux at the BBB on delivery of molecularly-targeted therapy in glioma. This finding is of clinical significance for therapy in glioma, where limited drug delivery to tumor cells residing behind an intact BBB can be an important reason behind the failure of potent molecularly targeted agents.

5.1 Introduction

Glioblastoma multiforme (GBM), due to its invasive nature, can essentially be regarded as a disease of the entire brain (1). Despite recent advances in surgery, radiotherapy, and chemotherapy, there exists no therapeutic cure for GBM, and the disease almost always results in patient death. The median survival of patients with GBM is only 16-19 months (2). Even after radical surgical approaches, such as complete removal of the tumor-bearing hemisphere (hemispherectomy), recurrence is inevitable, and has been discontinued (3). A fatal characteristic of GBM is invasive growth of tumor cells into normal brain tissue surrounding the core tumor mass, making complete surgical resection unfeasible. Tumor invasion in GBM has been reported as early as in 1938, when Hans – Joachim Scherer described the diffuse invasion of glioblastomas by defining secondary patterns that reflected growth of tumor in neighboring brain tissue (4). In 1961, Matsukado showed that more than 50% of untreated brain tumors spread into the contralateral hemisphere (5). Given this distant spread of the disease, glioma can hardly be called a local disease (1). Thus invasive glioma cells, that invade brain areas several centimeters away from the tumor and escape surgical resection, remain shielded by protective mechanisms such as the blood-brain barrier (BBB), and are the putative source of the recurrent tumor (1). It is therefore critical that these invasive glioma cells, left behind after surgery, are targeted by chemotherapy.

Advances in our understanding of the molecular pathogenesis in GBM have led to the development of many promising small molecule tyrosine kinase inhibitors (TKIs), that inhibit critical signaling pathways essential for growth and development of the tumor.

Aberrant signaling through growth factor pathways, such as through the epidermal growth factor receptor (EGFR), platelet derived growth factor receptor (PDGFR) and the vascular endothelial growth factor receptor (VEGFR), is a patho-physiological hallmark of GBM (6). It was hoped that inhibitors of these highly deregulated pathways would increase patient survival by inhibiting tumor growth and proliferation (7). However, clinical trials evaluating molecularly-targeted TKIs in GBM have mostly resulted in disappointing failures (8).

Amongst the various hypotheses developed to explain the failure of promising molecularly targeted agents in GBM, one that has often been overlooked is impaired delivery of drug to its intracellular target. The central nervous system (CNS) is protected by the blood-brain barrier (BBB) that restricts the passage of most small and large molecules into the brain (9). ATP-binding cassette (ABC) transporters, such as P-glycoprotein (P-gp, ABCB1) and the breast cancer resistance protein (BCRP, ABCG2), constitute a major component of this barrier and restrict drug penetration into the CNS by effluxing the drug out of the brain (10). Certainly, restricted drug delivery to the target can explain the inefficacy of otherwise potent molecularly-targeted agents in GBM. The invasive nature of GBM therefore complicates the drug delivery problem across the BBB. Recent studies have indicated that drug delivery to the tumor is not restricted in GBM (11). These studies suggest that the BBB is overcome by residual damage from radiotherapy, and/or by the pathological infiltrative characteristics of GBM that compromises the functional integrity of the BBB (11). These conclusions were based on the finding that drug concentrations in tumor (resected tissue) were 10-fold greater than

plasma concentrations. Similar findings have been reported in a recent study by Pitz and coworkers, who showed that concentrations of many anti-cancer drugs in contrast-enhancing areas of the tumor were generally higher than the corresponding plasma concentrations (12). Likewise, tumor concentrations of paclitaxel and temozolomide have also been reported to be higher than that in plasma (13, 14). All these studies suggest that the BBB is disrupted in the tumor and does not restrict drug delivery to the tumor. However, are drug concentrations in the resected tumor tissue representative of that in the entire brain? A significant finding in all of the above studies is, that drug concentrations in areas distant from the tumor core (non-contrast enhancing regions) were several fold lower than that in the tumor core (contrast-enhancing areas) (12-14). This suggests that while the BBB is disrupted at or near the tumor core, it most certainly is intact near the growing edge of the tumor, regions where invasive tumor cells may reside. An intact BBB along with its functional efflux transport systems can significantly impede drug delivery to the invasive tumor, which, in almost all cases, is more important to treat after resection of the primary tumor.

The objective of this study was to show that delivery of molecularly-targeted agents to glioma can be significantly limited due to the presence of an intact BBB, especially in sites away from the tumor core. Using a xenograft model of GBM, we show that active efflux at the BBB mediated by P-gp and BCRP restricts the delivery of erlotinib to the brain. Furthermore, we show that that increasing delivery across the BBB by inhibition of P-gp and BCRP results in a remarkable increase in drug concentrations in the brain, even in the tumor core where the BBB is thought to be disrupted.

5.2 Materials and Methods

5.2.1 Chemicals

Erlotinib hydrochloride and AG1478 were procured from LC Labs (Woburn MA). Elacridar (GF120918) was obtained from Toronto Research Chemicals (Ontario, Canada). Ammonium formate and acetonitrile were HPLC grade and were obtained from Sigma-Aldrich (St. Louis, MO).

5.2.2 Steady-State Brain Distribution of Erlotinib in FVB Mice

Steady-state brain distribution of erlotinib was examined in male FVB wild-type, *Mdr1a/b*$^{-/-}$*, Bcrp1*$^{-/-}$ *and Mdr1a/b*$^{-/-}$*Bcrp1*$^{-/-}$ mice of a FVB genetic background (Taconic Farms, Inc.). All animals were 8 to 10 weeks old at the time of experiment. Animals were maintained under temperature-controlled conditions with a 12-h light/dark cycle and unlimited access to food and water. All studies were carried out in accordance with the guidelines set by the Principles of Laboratory Animal Care (National Institutes of Health) and were approved by The Institutional Animal Care and Use Committee (IACUC) of the University of Minnesota.

Erlotinib was infused to steady-state using Alzet osmotic mini pumps (Durect Corporation, Cupertino, CA). A 15 mg/ml solution of erlotinib in DMSO was filled in the minipumps (model 1003D) and the pumps were equilibrated by soaking them overnight in sterile saline solution at 37ºC. The pump operated at a flow rate of 1 µL/hr yielding an infusion rate of 15 µg/hr (0.6 mg/hr/kg). Mice were anesthetized using 5 % isoflurane (Boynton Health Service Pharmacy, Minneapolis, MN) and were maintained under anesthesia using 2 % isoflurane in oxygen. The abdominal cavity was shaved and

cleaned and a small midline incision was made in the lower abdomen under the rib cage. An incision was made in the peritoneal wall directly beneath the cutaneous incision and the primed pump was inserted into the peritoneal cavity. The musculoperitoneal layer was closed with sterile absorbable sutures and the skin incision was closed using sterile wound clips. The animals were allowed to recover on a heated pad. Erlotinib half-life in mice has been reported to be approximately 1 hour (15), so an infusion lasting 48 hours was considered to be sufficient to attain steady-state in both brain and plasma. The animals were euthanized 72 hours post surgery by using a CO_2 chamber. Blood was collected by cardiac puncture and whole brain was harvested. Plasma was obtained by centrifuging the blood sample at 3500 rpm for 10 minutes. Plasma and brain specimens were stored at – 80 ºC until analysis by LC-MS/MS.

5.2.3 Glioblastoma cells

Human glioblastoma U87 cells transfected with wild-type EGFR were grown in short-term cell culture (7–14 days) at 37°C with 5% CO2 in DMEM supplemented with 10% fetal bovine serum, and 1% antibiotic/antimycotic (Invitrogen, Carlsbad, CA, USA). Immediately before inoculation, cells were harvested and suspended in PBS to a concentration of 5×10^4 cells/µl.

Orthotopic Xenograft Model

All experiments were performed on a protocol approved by the Cleveland Clinic Institutional Animal Care and Use Committee. Animals were fed a standard rodent diet, and maintained in a pathogen-free environment. Athymic nude rats (RNu, Charles River), 6-7 wks of age were obtained from Charles River Laboratories (Wilmington, MA) and

housed in the Biological Resources Unit of the Cleveland Clinic. Rats were anesthetized by an intraperitoneal injection of ketamine and xylazine and inoculated with U87 cells (2.5×10^5 cells in a total volume of 5 µl) by injection into the right frontal region using a stereotaxic frame (David Kopf Instruments, Tujunga, CA, USA). Tumor was allowed to grow for three weeks before being used for further studies.

5.2.4 Regional Tumor Distribution of Erlotinib

Tumor bearing rats were randomly assigned to one of the three groups (*n = 9 per group*); control (no erlotinib treatment), erlotinib treatment with perfusion, and erlotinib treatment without perfusion. The rats in the treatment groups received 20 mg/kg/day erlotinib (in 0.5% methylcellulose) by oral gavage for 5 days. All animals were sacrificed 30 minutes after the last erlotinib dose followed by collection of blood and brain tissue. Rats in the perfusion group were perfused with saline prior to collection of brain. Brain tissue was visually dissected into 3 parts: the tumor, the tissue adjacent to the tumor and the contralateral hemisphere. Plasma was separated by centrifuging the blood at 3500 rpm for 10 minutes. Tissue specimens were flash frozen in liquid nitrogen and stored at -80ºC until further analysis. Tissue specimens from 6 out of the 9 animals from each group were analyzed for erlotinib concentrations while the rest were used for western blotting.

5.2.5 Effect of Elacridar on Distribution of Erlotinib to the Tumor

In a separate study, tumor bearing rats were divided into three groups (*n = 7 per group*): control (no erlotinib treatment), erlotinib treatment, and treatment with erlotinib plus elacridar. The rats in the treatment groups received 20 mg/kg/day erlotinib (in 0.5%

methylcellulose) by daily gavage for 3 days. Rats in the erlotinib plus elacridar group received an additional dose of 10 mg/kg elacridar by intravenous administration into the jugular vein 30 minutes before each erlotinib dose. Animals were sacrificed 30 minutes after the last erlotinib dose followed by collection of blood. All rats were then perfused with saline and brain tissue was harvested. Plasma and brain tissue were processed as above. Tissues from 4 out of the 7 animals were analyzed for erlotinib concentrations while the rest was used for western blotting. All samples were stored at - 80ºC until further analysis

5.2.6 Quantification of Erlotinib in Brain and Plasma by LCMS-MS

The concentration of erlotinib in mouse plasma and brain homogenate was determined by high pressure liquid chromatography (HPLC) coupled with mass spectrometry. Prior to analysis, frozen samples were thawed at room temperature. Brain samples were homogenized using 3 volumes of ice-cold 5% bovine serum albumin in phosphate-buffered saline using a tissue homogenizer (Fisher Scientific, Pittsburgh, PA). 100 µL of specimen plasma and brain homogenate were spiked with 50 ng of internal standard, tyrphostin (AG1478), and alkalinized by addition of 100 µL of a pH 11 buffer (1 mM sodium hydroxide, 0.5 mM sodium bicarbonate). Samples were extracted by vigorous vortexing with 1 mL of ice cold ethyl acetate followed by centrifugation at 7500 rpm for 15 minutes at 4ºC. A volume of 750 µL of the organic layer was transferred to fresh polypropylene tubes and dried under nitrogen. Samples were reconstituted in 100 µL mobile phase and transferred to glass auto sampler vials. A volume of 10 µL was injected in the HPLC system using a temperature controlled autosampling device maintained at

10ºC. Chromatographic analysis was performed using an Agilent Model 1200 separation system (Santa Clara, CA, USA). Separation of analytes was achieved using an Agilent Eclipse XDB-C18 RRHT threaded column (4.6 mm ID x 50mm, 1.8 μ) fitted with an Agilent C18 guard column (4.6 mm ID x 12.5mm, 5 μ) (Santa Clara, CA, USA). The mobile phase was composed of acetonitrile: 20mM ammonium formate (containing 0.1% formic acid) (45:55 v/v), and was delivered at a flow rate of 0.25 mL/min. The column effluent was monitored using a Thermo Finnigan™ TSQ® Quantum 1.5 detector (San Jose, CA, USA). The instrument was equipped with an electrospray interface, and controlled by the Xcalibur version 2.0.7 data system. The samples were analyzed using an electrospray probe in the positive ionization mode operating at a spray voltage of 4500V for both erlotinib and the internal standard. The spectrometer was programmed to allow the [MH]+ ion of erlotinib at m/z 395.14 and that of internal standard at m/z 316.68 to pass through the first quadrupole (Q1) and into the collision cell (Q2). The collision energy was set at 14V for erlotinib and 9V for tyrphostin. The product ions for erlotinib (m/z 278.91) and the internal standard (m/z 300.9) were monitored through the third quadrupole (Q3). The scan width and scan time for monitoring the two product ions were 1.5 m/z and 0.5 s, respectively. The assay was sensitive over a range of 2.5 ng/ml to 1 μg/ml with the coefficient of variation being less than 15% over the entire range.

5.3 Results

5.3.1 P-gp and BCRP Mediated Efflux Restricts Erlotinib Transport to the Brain

The influence of P-gp and BCRP on the transport of erlotinib across the BBB was

examined by studying its steady-state brain distribution in FVB mice. After a continuous intraperitoneal infusion lasting for 48 hours, the steady-state plasma concentrations of erlotinib ranged from 72 ± 42 ng/ml in the wild-type mice to 99 ± 22 ng/ml in the *Mdr1a/b*$^{-/-}$*Bcrp1*$^{-/-}$ mice. Steady-state plasma concentrations were not significantly different from each other between the four mouse groups (**Table 5.1**). Steady-state brain concentrations was 3.3 ± 2.8 ng/ml in the wild-type, 12 ± 2.8 ng.ml in the *Mdr1a/b*$^{-/-}$, 4.9 ± 2.9 ng/ml in the *Bcrp1*$^{-/-}$, and 40 ± 8.1 ng/ml in the *Mdr1a/b*$^{-/-}$*Bcrp1*$^{-/-}$ mice. The corresponding steady-state brain-to-plasma ratios was 0.08 ± 0.11 in the wild-type mice and increased to 0.13 ± 0.03 (1.6-fold) in the *Mdr1a/b*$^{-/-}$, 0.07 ± 0.02 in the *Bcrp1*$^{-/-}$, and to 0.60 ± 0.35 (7.8-fold) in the *Mdr1a/b*$^{-/-}$*Bcrp1*$^{-/-}$ mice (**Figure 5.1**). This indicates a dramatic enhancement in brain distribution of erlotinib when P-gp and BCRP are absent at the BBB.

5.3.2 Regional Brain Delivery of Erlotinib in GBM Model

The impact of the BBB in restricting delivery of erlotinib to the tumor was investigated using the U87 rat xenograft model of GBM. Concentration of erlotinib in the tumor core was 2.78 ± 0.74 μg/gm and decreased significantly to 0.97 ± 0.27 μg/gm in the brain around the tumor (16) and to 0.77 ± 0.17 μg/gm in the contralateral hemisphere ($p < 0.001$, **Figure 5.2**). The tissue to plasma concentration ratio was 0.53 ± 0.14 in the tumor core and decreased significantly to 0.18 ± 0.03 in the tumor rim and 0.14 ± 0.03 in the normal contralateral hemisphere ($p < 0.001$). This indicates that while drug delivery is not completely restricted by the BBB in the core, efflux transporters at the intact BBB definitely limit transport of erlotinib to sites away from the tumor. We then studied the

effect of perfusion, prior to tissue collection, on the concentrations of erlotinib in the brain. Residual blood remaining in the brain vasculature can significantly contribute to drug concentration measurements in brain, resulting in significant error. Erlotinib concentrations in all three brain areas decreased significantly when brain was perfused with saline prior to harvesting (**Figure 5.3A, B**). Drug concentrations were approximately 34 % lower in the tumor core at 1.83 ± 0.54 μg/gm, while that in the tumor rim and normal brain decreased by more than 50 % to 0.39 ± 0.19 μg/gm and 0.37 ± 0.22 μg/gm, respectively ($p < 0.05$). These findings suggest that drug in residual blood in the brain vasculature can contribute significantly to total brain concentrations thereby introducing significant error to overall results.

5.3.3 Effect of P-gp and BCRP Inhibition on Regional Erlotinib Delivery

Inhibition of P-gp and BCRP using small molecule inhibitors is an attractive strategy to enhance brain penetration of substrate drugs. We investigated this by using the dual P-gp/BCRP inhibitor elacridar (GF120918) in combination with erlotinib. Erlotinib concentrations in all three brain regions increased dramatically in rats that were administered elacridar with erlotinib, compared to those which were treated with erlotinib alone (**Figure 5.4A**). Concentrations in the tumor core increased by 4-fold while that in the brain around tumor and normal brain increased by more than 12-fold compared to the vehicle treated group ($p < 0.001$). When elacridar was administered along with erlotinib, concentrations in all three brain regions were not statistically different from each other, the tissue-to-plasma ratio reaching a value of ~ 1 in all three regions (**Figure 5.4B**). This

indicates that inhibition of P-gp and BCRP by elacridar dramatically enhances erlotinib delivery, especially to the tumor periphery and normal tissue where the BBB is intact.

5.4 Discussion

Glioblastoma multiforme is an invasive disease of the whole brain. The infiltrative nature of the disease makes treatment particularly challenging, since surgery does not remove tumor cells that have invaded normal brain areas, and protective mechanisms such as the BBB shield and protect these invasive cells from cytotoxic chemotherapeutic agents. Recent studies have questioned the role of the BBB in limiting delivery and thus efficacy of chemotherapy, based on findings that drug concentrations in tumor (resected tissue) were several fold-higher than that in plasma (11, 17). However, these concentrations do not represent drug levels in other areas of the brain, especially those where the BBB can be intact and capable of restricting drug delivery. Given that GBM can be considered a disease of the entire brain, and the target in question includes invasive tumor cells away from the site of surgical resection, drug concentrations in these invasive sites are of paramount importance. We have raised this question herein and demonstrated that BBB restricts the delivery of erlotinib, a substrate for P-gp and BCRP, to the brain. Using a xenograft model of GBM, we show that drug concentrations in sites away from the main tumor, such as the tumor rim and the contralateral normal hemisphere, are several fold lower than that in the tumor core, and that inhibition of the two efflux transporters results in a dramatic increase in drug distribution to the entire brain. Furthermore, we show that inhibition of P-gp and BCRP dramatically enhanced delivery of erlotinib to the different brain regions.

A steady-state brain distribution study in FVB mice showed that erlotinib is a substrate for both P-gp and BCRP and together the two transporters significantly restrict its brain penetration (**Figure 5.1**). The impact of P-gp and BCRP on brain penetration of erlotinib has been previously shown by several other studies (18-20). Our results are consistent with these reports and show that erlotinib distribution to the brain increases dramatically when both P-gp and BCRP are absent at the BBB. Even though erlotinib is a substrate for both transporters, absence of either one of them alone does not enhance brain penetration of erlotinib. This finding is similar to our previous studies with other TKIs where we reported that P-gp and BCRP cooperate at the BBB and compensate functionally for each other's loss (21-23). Thus brain penetration of dual substrates increase only when both the transporters are absent simultaneously at the BBB.

We used the U87 rat xenograft model of GBM to show that the BBB restricts delivery of erlotinib to the brain, especially to areas away from the tumor core. After three days of erlotinib treatment, concentrations in the brain around the tumor and the normal brain were up to 7-fold lower than that in plasma (**Figure 5.2**). The resulting tissue-to-plasma concentration ratio of 0.14 in the normal brain and 0.17 in the rim were similar to the steady-state B/P ratio in the FVB wild-type mice and indicate that the BBB can be fully intact in areas away from the tumor. The tissue-to-plasma ratio of 0.52 in the tumor core suggests that the BBB is not completely disrupted even in the tumor core and restricts drug penetration to a small extent. Recently, there have been several studies that have investigated the impact of the blood-brain barrier in restricting drug delivery to the tumor (11-14, 17). All these studies determined drug concentrations in resected tumor tissue and

used that as a guide for adequacy of drug delivery to the entire brain. These studies reported significantly high concentrations of chemotherapeutic agents in the tumor and indicated that drug delivery to the tumor is not restricted in GBM. However, are drug concentrations in the resected tumor representative of that in the entire brain? Many of these studies also reported that drug concentrations in non-contrast enhancing regions of the brain (distant from the tumor core) were several fold lower than that in the contrast-enhancing tumor (12-14, 17). These findings imply that while the pathological characteristics of GBM compromises the integrity of the BBB in the tumor core, leading to high drug concentrations, the BBB it most certainly is intact near the growing edge of the tumor. Invasive cells residing in such areas remain shielded from chemotherapy and ultimately give rise to the recurrent tumor. Thus conclusions drawn on the basis of drug concentrations in a resected tumor can be highly misleading and do not represent the status of the BBB thought out the entire brain.

Drug remaining in residual blood inside the brain vasculature can contribute significantly to total brain concentrations thereby resulting in erroneous results. In brain concentration measurements done in mice, we have previously showed that total concentrations can be corrected for residual blood to eliminate this error (24). However to date, no such correction method has been reported for rats or humans. Perfusion remains the method of choice to wash out residual blood from brain capillaries. We studied the effect of perfusion on brain concentrations of erlotinib. Erlotinib brain concentrations in rats, perfused with saline prior to collection of tissue, were significantly lower compared to the non-perfused rats (**Figure 5.3**). This shows that drug concentration measurements in

brain tissues that are not perfused or corrected can be misleading and should be cautiously interpreted.

Many small molecule anti-cancer TKIs are substrates for P-gp and BCRP, and therefore they do not cross the BBB to a significant extent (21-26). Consequently, inhibition of these two transporters has been proposed as a possible strategy to enhance brain penetration of substrate drugs. Elacridar (GF120918) is a dual inhibitor of P-gp and BCRP that was developed to reverse multi-drug resistance seen in cancer (27). Several preclinical studies have evaluated concurrent treatment with elacridar with the goal to improve brain distribution of the substrate drugs. These studies have shown that brain distribution of dual P-gp/BCRP substrates increase dramatically when elacridar is administered concomitantly (21-23, 25, 28). We therefore used elacridar to investigate its influence on delivery of erlotinib to the brain and brain tumor.

When elacridar was administered concurrently with erlotinib, concentrations in all three brain regions increased significantly compared to the vehicle treated group (**Figure 5.4**). In the elacridar treated group, the tissue-to-plasma ratio in all three brain regions was approximately 1, indicating that when these two transporters are inhibited erlotinib crosses the BBB to enter the brain. The fact that elacridar increased erlotinib delivery to the tumor core as well, suggests that the BBB is not completely disrupted in the tumor core either, and is capable of restricting drug delivery. Thus, inhibition of P-gp and BCRP can be an attractive strategy to enhance delivery of substrate drugs across the BBB and thereby improve their efficacy.

Despite aggressive treatment with radiation and chemotherapy, recurrence in glioblastoma multiforme is inevitable. Several clinical trials have evaluating the EGFR inhibitor erlotinib have reported disappointing results (29-32). The fact that recurrence occurs in areas away from the margins of surgical resection is indicative that invasive glioma cells in these areas are not being effectively targeted. Confusion over the status of the BBB in glioma has stemmed from the fact that high drug concentrations in tumor have been used to represent drug delivery to the entire brain. This study shows that this practice can be highly misleading since the BBB is not disrupted in areas of brain away from the tumor and drug concentrations in these areas are significantly lower. Therefore, successful targeting of the invasive glioma cells will require enhanced delivery of chemotherapeutic agents across an intact BBB.

In conclusion, this study shows the impact of an intact BBB on the delivery and efficacy of a molecularly-targeted agent against glioma. We show that drug concentrations in the tumor core are not representative of that in the entire brain and should not be used as a guide for adequacy of drug delivery to the brain. Finally, we show that concurrent administration of a modulator of drug transporters, such as elacridar, can be used as a strategy to enhance delivery of substrate chemotherapeutic agents to the brain. This finding can be of significant importance in GBM chemotherapy since several molecularly-targeted agents are substrates for the ABC transporters P-gp and BCRP.

5.5 Footnotes

We would like to thank Dr. Michael Vogelbaum and Pooja Manchanda at the Cleveland Clinic, Cleveland, OH for their collaboration on this project. This work was supported by a grant from the National Institutes of Health - National Cancer Institute [CA138437]. Financial support for Sagar Agarwal was provided by the Doctoral Dissertation Fellowship from the University of Minnesota.

Table 5.1 Steady-state plasma and brain concentrations of erlotinib in wild-type, Mdr1a/b$^{-/-}$, Bcrp1$^{-/-}$ and Mdr1a/b$^{-/-}$Bcrp1$^{-/-}$ mice after a constant intraperitoneal infusion at a rate of 0.6 mg/hr/kg for 48 hours.

Genotype	N	Plasma Css	Brain Css	Brain-to-Plasma Ratio
		µg/ml	µg/gm	
FVB (wild-type)	4	0.07 ± 0.04	0.004 ± 0.005^{a}	0.02 ± 0.02
***Bcrp1*$^{-/-}$**	4	0.07 ± 0.03	0.005 ± 0.003^{a}	0.07 ± 0.02
***Mdr1a/b*$^{-/-}$**	4	0.08 ± 0.04	$0.011 \pm 0.002^{a,b}$	0.09 ± 0.06^{b}
***Mdr1a/b*$^{-/-}$*Bcrp1*$^{-/-}$**	4	0.09 ± 0.02	0.034 ± 0.017^{b}	0.62 ± 0.27^{b}

Data presented as mean ± S.D., $p < 0.05$
[a] compared to corresponding plasma concentration
[b] compared to wild-type group

Figure 5.1 Steady-state brain distribution of erlotinib in wild-type, Mdr1a/b$^{-/-}$, Bcrp1$^{-/-}$ and Mdr1a/b$^{-/-}$Bcrp1$^{-/-}$ FVB mice. Brain-to-plasma ratios after a 0.6 mg/hr/kg intraperitoneal infusion for 48 hours. The values are presented as mean ± S.D. (** p<0.001, compared to wild-type*)

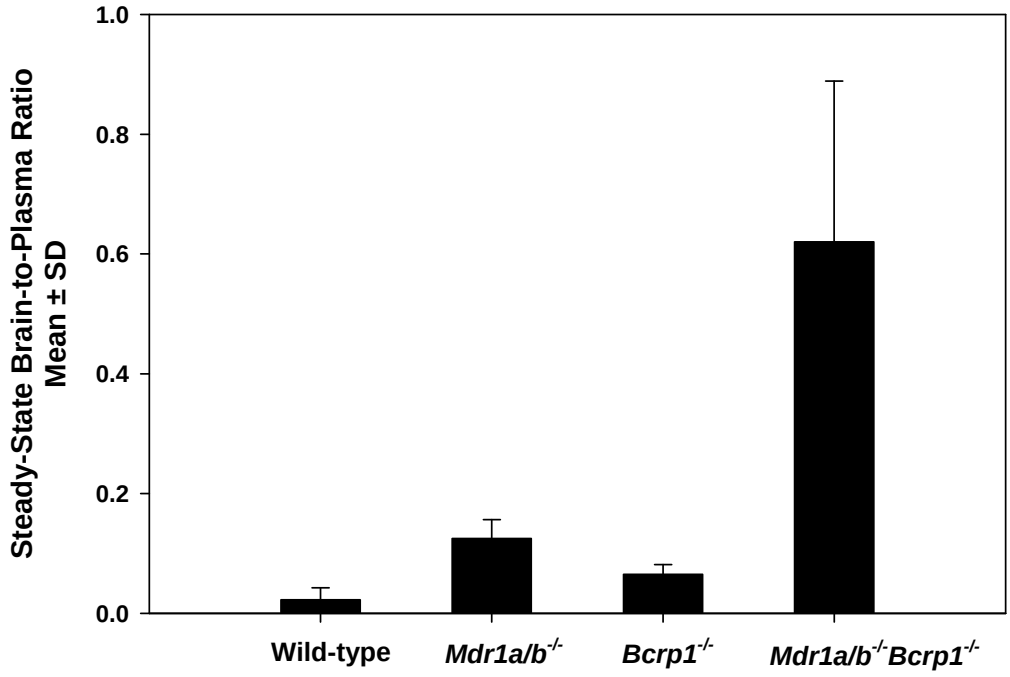

Figure 5.2 Regional Distribution of Erlotinib in the U87 Rat Xenograft Model.

Erlotinib concentrations in tumor core were significantly greater than those in the brain around the tumor (16) and normal brain (C/L hemisphere). The corresponding brain-to-plasma ratios (*inset*) show that the BBB is intact in areas away from the tumor and restricts delivery of erlotinib to the brain.

(** p<0.05, compared to tumor core*)

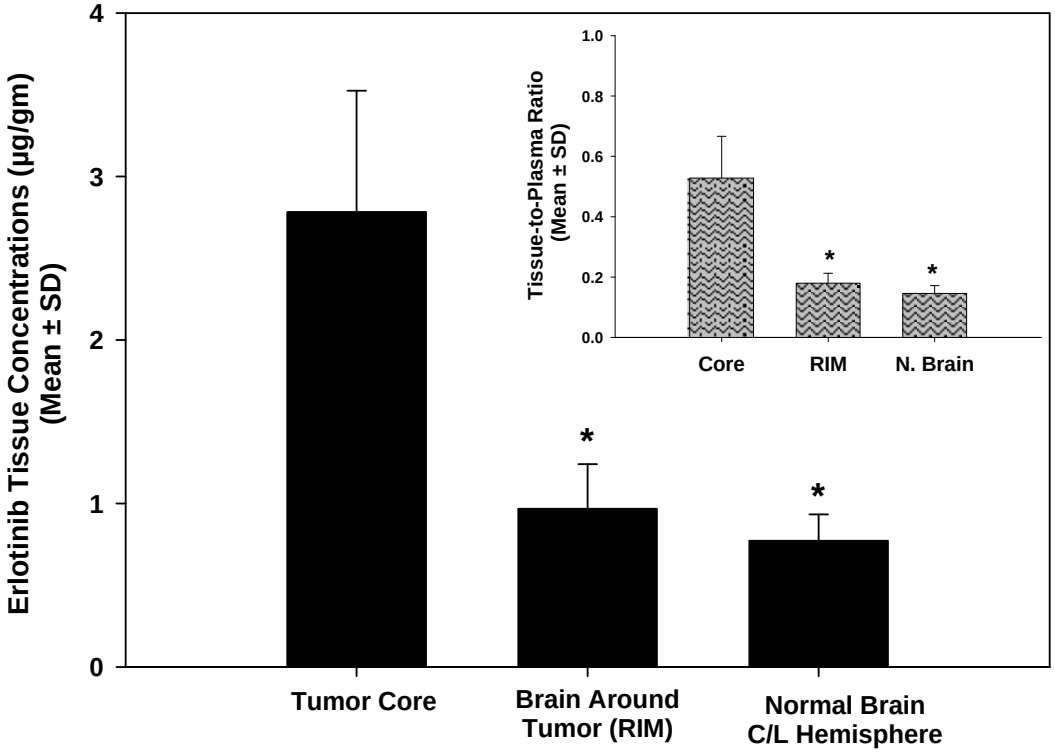

Figure 5.3A Effect of Perfusion on Regional Distribution of Erlotinib.

Erlotinib concentrations in tumor core, rim and normal brain were significantly lower in rats that were perfused with saline prior to collection of brain tissue (gray bars) compared to the non perfused rats (black bars). This indicates that residual drug in brain vasculature can contribute significantly to total brain levels.

(** p<0.05, compared to tumor core, † p<0.05 compared to non-perfused group*)

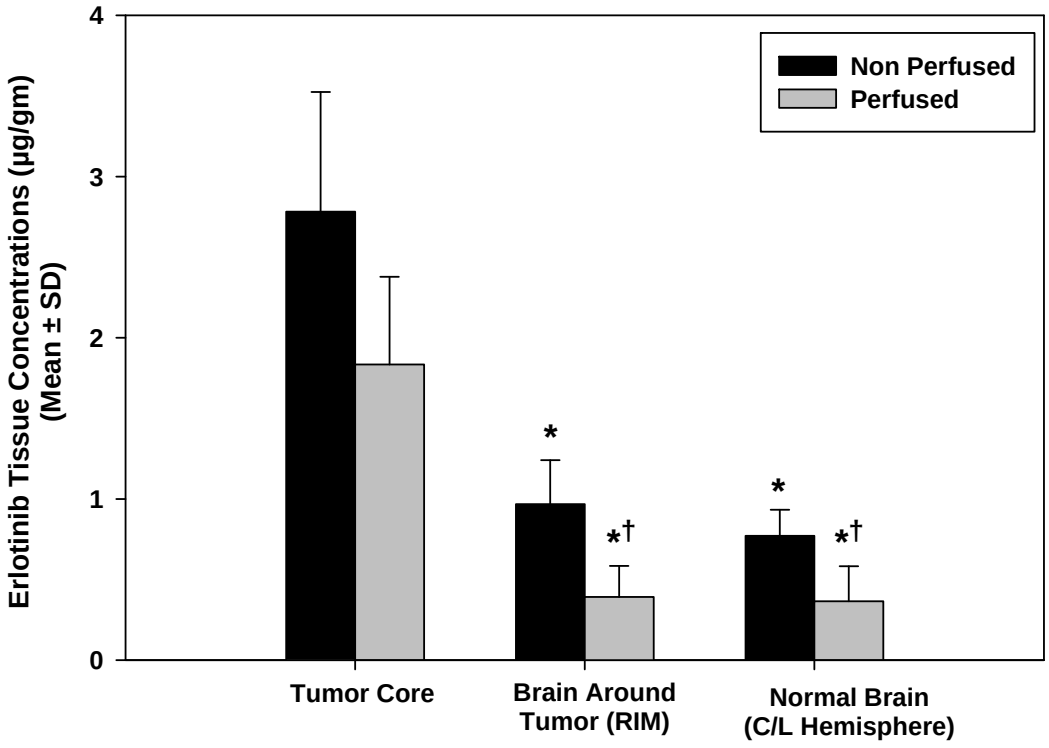

Figure 5.3B Effect of Perfusion on Regional Distribution of Erlotinib.

Erlotinib brain-to-plasma ratios in tumor rim and normal brain were significantly lower in rats that were perfused with saline prior to collection of brain tissue (gray bars) compared to the non perfused rats (black bars). This indicates that drug concentration measurements in brain tissues that are not perfused or corrected can be misleading and should be cautiously interpreted.

(** p<0.05, compared to tumor core, † p<0.05 compared to non-perfused group*)

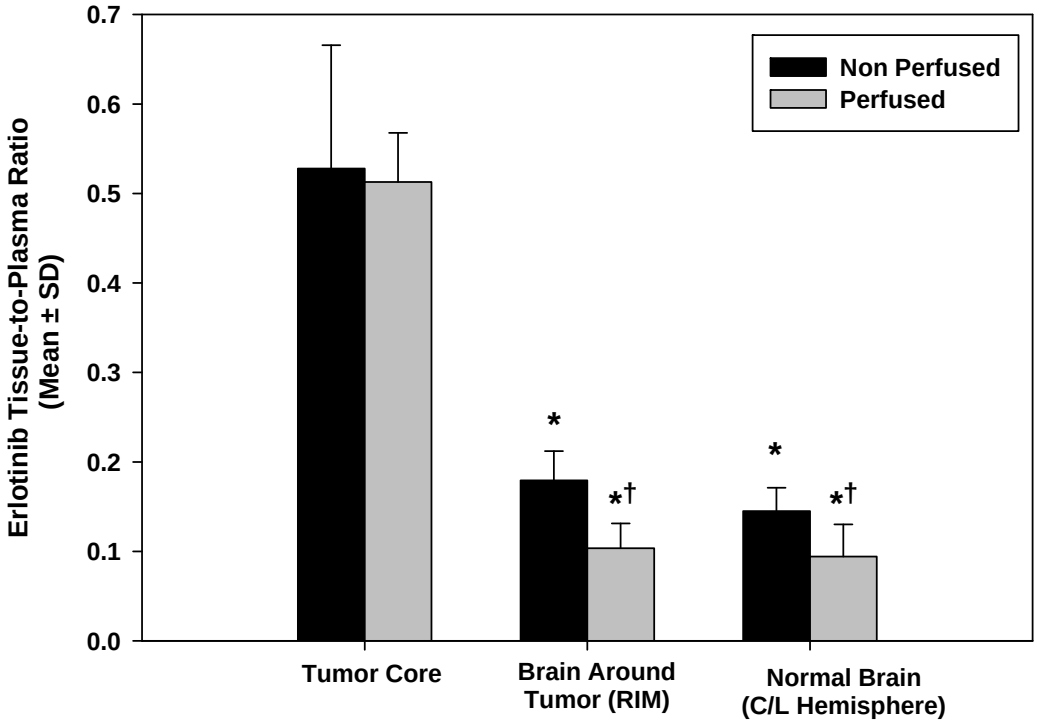

Figure 5.4A Influence of Elacridar on Regional Distribution of Erlotinib.

Erlotinib concentrations in tumor core, rim and normal brain increased significantly in the elacridar treated group (gray bars) compared to control (black bars). This indicates that inhibition of P-gp and BCRP can significantly enhance delivery of erlotinib to the tumor in the brain.

(** p<0.05, compared to tumor core, † p<0.05 compared to vehicle control group*)

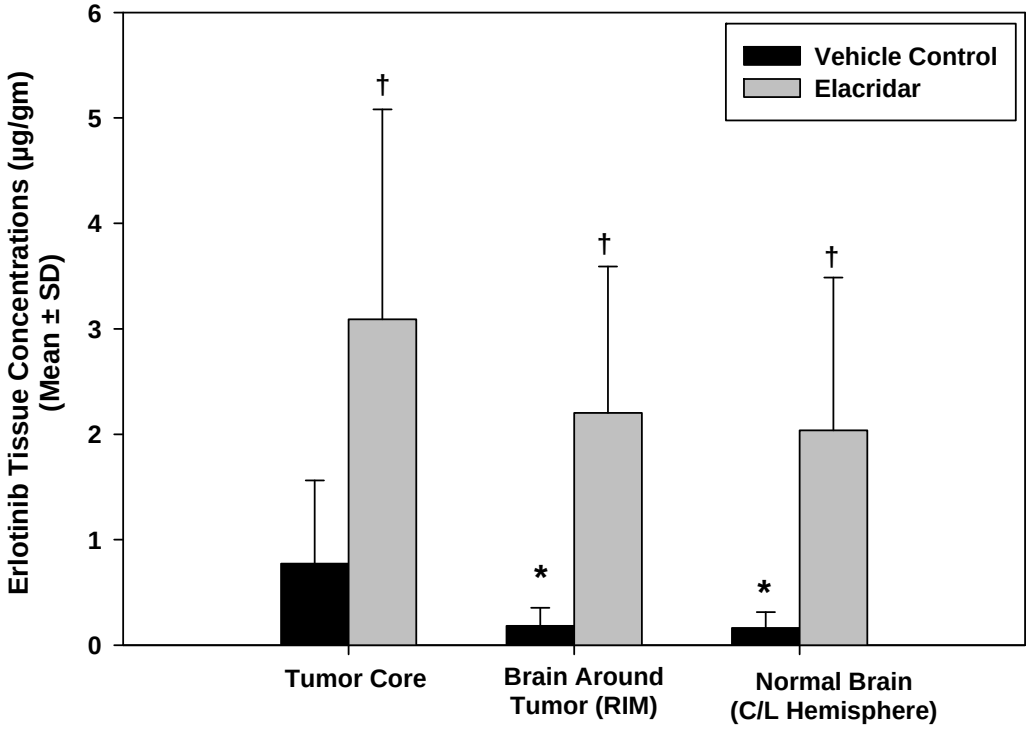

Figure 5.4B Influence of Elacridar on Regional Distribution of Erlotinib.

Erlotinib brain-to-plasma ratio increased significantly and was approximately 1 in all three brain regions, indicating that when these two transporters are inhibited there is no restriction to the delivery of erlotinib to the brain. This indicates that concurrent administration of a modulator of drug transporters, such as elacridar, can be used as a strategy to enhance delivery of substrate chemotherapeutic agents to the brain

(** p<0.05, compared to tumor core, † p<0.05 compared to vehicle control group*)

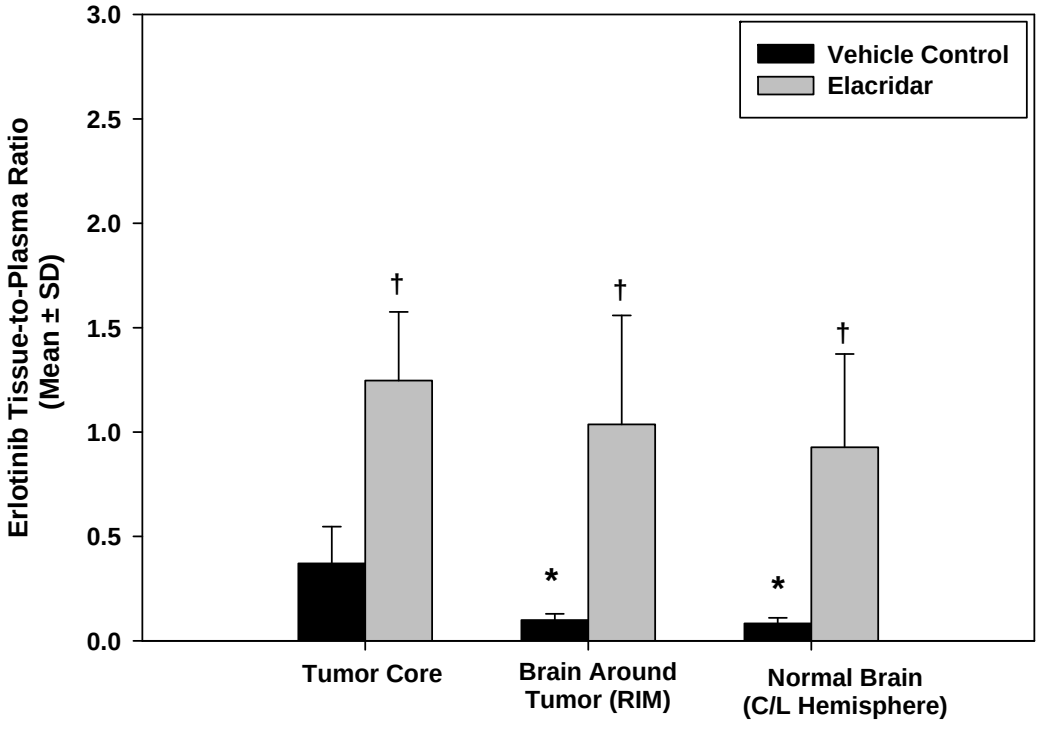

CHAPTER VI

INFLUENCE OF DRUG DELIVERY ON EFFICACY OF A MOLECULARLY-TARGETED AGENT IN A NOVEL MOUSE MODEL OF GLIOBLASTOMA MULTIFORME

There is increasing evidence that the inevitable relapse and lethality of glioblastoma multiforme, a devastating primary brain tumor, is due to a failure to effectively target the invasive glioma cells. Despite aggressive treatment, almost all gliomas recur and patient survival post recurrence is dismal at 5-7 months. The brain is a pharmacological and immunological sanctuary for several diseases of the central nervous system, and treatment of brain tumors requires efficient delivery of chemotherapeutic drugs across the BBB. The objective of this study was to examine the influence of active efflux at the blood-brain barrier on efficacy of potent molecularly-targeted agents in glioma. We show that efficacy of the dual P-gp/BCRP substrate dasatinib increases dramatically when the two transporters are absent at the BBB. Tumor bearing *Mdr1a/b*$^{-/-}$*Bcrp1*$^{-/-}$ mice survived for twice as long when treated with dasatinib compared to the wild-type mice. This study also investigated another issue central to chemotherapy in glioma, *i.e.*, disruption of the BBB in the tumor. Using GFP-guided tumor dissection, we show that concentration of the vascular marker dextran was greater in the tumor core as compared to the tumor rim and the contralateral normal brain. Furthermore, concentrations of dasatinib were also greater in the core compared to the other two regions of brain. This shows that while the BBB might be disrupted in the tumor core, it is sufficiently intact in areas away from the tumor. This intact BBB, through a combination of tight junctions and efflux transporters, restricted delivery of dasatinib. Immunoblotting results show that dasatinib efficacy in all regions increased dramatically when its delivery to the brain is enhanced in mice deficient in P-gp and BCRP. This study provides conclusive evidence of the impact of active efflux at the BBB on the efficacy of molecularly-targeted therapy in glioma. This

finding is of clinical significance for therapy in glioma, where limited drug delivery to tumor cells residing behind an intact BBB might be an important reason behind the failure of potent molecularly-targeted agents.

6.1 Introduction

Glioblastoma multiforme (GBM) is a devastating primary brain tumor that claims more than 12,000 lives each year in the United States (1). Despite aggressive treatment, essentially all malignant gliomas recur (2), eventually leading to patient death. The median survival of patients with GBM is only about 16-19 months (3), whereas survival after tumor recurrence is a dismal 5-7 months (4). Surgery remains the most effective treatment for GBM patients, and it has been shown that there is a correlation between the extent of resection and patient survival (5). However, regardless of the degree of debulking, death is inevitable.

Radiotherapy and chemotherapy are fast assuming an increasingly important role in the treatment of glioma. The current standard of care in glioblastoma multiforme is treatment with the DNA-alkylating agent temozolomide combined with radiation, a treatment that has been shown to prolong patient survival by only a few months (6). A significant advancement in cancer chemotherapy has been the development of molecularly-targeted agents. These small molecule inhibitors target signaling pathways critical for glioma growth and proliferation and have been extensively evaluated for therapy in GBM (7). Unfortunately, none of these have resulted in any significant clinical benefit (8).

A critical challenge in treatment of tumors of the brain is delivery of drugs into a pharmacological sanctuary within the central nervous system (CNS) (9) The blood-brain barrier (BBB) is a natural defense mechanism that separates the brain from peripheral circulation and thus protects it from harmful toxins and chemicals (10). The BBB thus restricts transport of most small and large drug molecules into the brain and can thereby render efficacious drugs ineffective in treating diseases of the CNS (10). Drug transporter proteins, such as the ATP-binding cassette (ABC) transporters P-glycoprotein (P-gp, ABCB1) and the breast cancer resistance protein (BCRP, ABCG2), constitute a major component of this barrier and restrict drug penetration into the brain by effluxing them back into the blood (11). It has been shown that these transporters significantly limit the distribution of a number of drug molecules to the brain, including several anti-cancer agents currently in clinic (12-19). We have shown that several molecularly-targeted tyrosine kinase inhibitors (TKI) are substrates for P-gp and BCRP, and as a result, they do not traverse the BBB to any significant extent (12-14).

Dasatinib (Sprycel, Bristol-Myers Squibb) is one such small molecule TKI that is also an avid substrate for P-gp and BCRP (14). It has potent inhibitory activity against PDGFR α/β, BCR-ABL, c-KIT and SRC (20, 21) and has been shown to inhibit growth and migration of glioma cells and induce cellular apoptosis in vitro (22). However no preclinical studies have been performed in animal models of GBM that can examine the impact that drug delivery across the BBB can have on the efficacy of dasatinib. We have raised this issue herein and hypothesize that restricted delivery of dasatinib to the brain can significantly limit its efficacy against the tumor. Using a spontaneous mouse model

of glioma, we show that increased delivery of dasatinib to the brain of a mice deficient in P-gp and BCRP, significantly enhances its efficacy against the tumor.

Moreover, we also raise another issue critical to the status of the BBB in GBM. Recent studies have suggested that drug delivery to the tumor is not restricted in GBM (23, 24). These studies further suggest that the BBB is overcome by residual damage from radiotherapy, and/or by the pathological infiltrative characteristics of GBM that compromises the functional integrity of the BBB (23, 24). However, GBM is extremely invasive making it essentially a disease of the entire brain. Invasive glioma cells invade brain areas several centimeters away from the tumor, escape surgical resection and remain shielded by protective mechanisms such as the BBB, and are the putative source of the recurrent tumor (25). Using a spontaneous model we show that in case of an invasive tumor like GBM, the BBB can be disrupted at the tumor core. But it is intact near the growing edge of the tumor, regions where invasive tumor cells may reside. We hypothesize herein that an intact BBB along with its functional efflux transport systems can significantly impede drug delivery to the invasive tumor therefore limiting dasatinib efficacy in these areas of the brain.

The objective of this study was to show that efficacy of dasatinib can be significantly enhanced by increasing its delivery across the BBB. We show dasatinib is significantly more efficacious against a spontaneous GBM when P-gp and BCRP are absent at the BBB. We also show that the BBB is intact in growing areas of the tumor and enhanced dasatinib delivery in such areas translates to improved efficacy against its targets.

6.2 Materials and Methods

6.2.1 Chemicals

Dasatinib and gefitinib were procured from LC Labs (Woburn MA). Elacridar (GF120918) was obtained from Toronto Research Chemicals (Ontario, Canada). Texas Red conjugated dextran was purchased from Invitrogen (Carlsbad, CA). Ammonium formate and acetonitrile were HPLC grade and were obtained from Sigma-Aldrich (St. Louis, MO).

6.2.2 Animal Care

All procedures were carried out in accordance with the guidelines set by the Principles of Laboratory Animal Care (National Institutes of Health) and were approved by The Institutional Animal Care and Use Committee (IACUC) of the University of Minnesota. FVB wild-type and *Mdr1a/b*$^{-/-}$*Bcrp1*$^{-/-}$ mice were from Taconic Farms, Inc. (Germantown, NY). Animals were maintained under temperature-controlled conditions with a 12-h light/dark cycle and unlimited access to food and water.

6.2.3 Spontaneous Glioma Model

We used a genetically engineered mouse model of spontaneous glioma that has been previously described by Wiesner et al. (26) Plasmid vectors containing sequences coding for mPDGFβ, eGFP and shp53RNA, and flanked by transposon inverted repeat/direct repeats (IR/DR's), were mixed with a transfection agent, in vivo-jetPEI™ (Polyplus-transfection Inc., NewYork, NY), and a sleeping beauty (SB) transposase vector containing the luciferase reporter, in the ratio 2:2:1 (PDGF:p53:SB, respectively).

Neonatal mice were placed on ice for three minutes to induce anesthesia and then secured in a cooled, "neonatal rat" stereotaxic frame (Stoelting, Wood Dale, IL) maintained at 4-8 ºC by a dry ice/ethanol reservoir. DNA-PEI complexes were injected into the right lateral ventricle (1 μg total DNA in 2 μL) using a 10 μL Hamilton syringe fitted with a 30 guage hypodermic needle (Hamilton Company, Reno, NV). Mice were allowed to recover on a heated pad before moving them back to their cages. Tumors spontaneously arising after three weeks were monitored by bioluminescent in-vivo imaging, and animals were enrolled in experiments when the signal was between 2 x 10^5 to 3 x 10^9 photons/sec/cm^2/ steradian.

6.2.4 Heterogeneous Brain Distribution of Dasatinib

Tumor bearing wild-type and *Mdr1a/b*$^{-/-}$*Bcrp1*$^{-/-}$ mice were administered 15 mg/kg dasatinib via oral gavage (n = 5 - 10 per group). Animals were sacrificed 90 minutes post dose and whole brain was harvested. With the aid of GFP visualization goggles (Biological Laboratory Equipment, Budapest, Hungary), the brain was immediately dissected into core, rim (brain around tumor) and normal brain. Since the tumor expresses GFP, the region of concentrated green fluorescence was deemed as the tumor core, the tissue surrounding the tumor was called as tumor rim and normal brain tissue was collected from the left (contralateral) hemisphere. Tissue specimens were flash frozen in liquid nitrogen and stored at - 80ºC until further analysis by LC-MS/MS for determination of dasatinib concentrations.

6.2.5 Regional Breakdown of the Blood-Brain Barrier

We investigated the integrity of the blood-brain barrier in a tumor bearing brain by injecting a vascular marker. Dextran (molecular weight 3 kDa) conjugated to Texas Red dye was used for this purpose. Tumor bearing wild-type and *Mdr1a/b*$^{-/-}$*Bcrp1*$^{-/-}$ mice were administered a 1 mg intravenous dose of Texas Red-Dextran by injection into the tail vein (n = 3 - 5 per group). Mice were sacrificed 10 minutes post injection, followed by perfusion of the brain using phosphate buffered saline. Whole brain was then harvested and dissected into core, rim (brain around tumor) and normal brain as described above. Tissue specimens were flash frozen in liquid nitrogen and stored at -80ºC until further analysis. Dextran concentrations in the tissue specimens were determined by measuring the Texas Red fluorescence at 595/615 nm using a 96-well plate reader and quantified by a calibration curve of Texas Red-Dextran in blank brain homogenate.

6.2.6 Efficacy by Target Inhibition

A separate group of wild-type and *Mdr1a/b*$^{-/-}$*Bcrp1*$^{-/-}$ mice (n = 2-4 per group) were treated with vehicle or dasatinib (15 mg/kg) for two days. Mice were sacrificed and whole brain was dissected into core, rim (brain around tumor) and normal brain using the GFP visualization goggles. Western blotting was conducted in the tissue specimens for determination of expression levels of AKT, phospho-AKT, SRC and phospho-SRC. Beta-actin was blotted as a control for protein loading. Tissue specimens were lysed in radioimmunoprecipitation assay buffer containing protease and phosphatase inhibitors. Protein concentration was determined using the bicinchoninic acid assay. Lysates were diluted in reducing sample buffer and 40 μg were loaded per lane on a 4% to 12% SDS-

PAGE gel and run at 170 volts for 1 hour. Gels were transferred to a nitrocellulose membrane at 5 volts overnight and blocked for 1 hour at room temperature using 5 % milk. Blots were then incubated with the primary antibodies to pSRC, SRC, pAKT, AKT and Actin (1:1000, Cell Signalling, MA) overnight at 4 ºC. Membranes were washed and incubated with horseradish peroxidase-conjugated secondary antibody (1:1000, Cell Signaling, MA) for 1 hour. Proteins were detected using Amersham ECL™ Advance Western Blotting Detection Kit (GE Life Sciences, NJ).

6.2.7 Efficacy of Dasatinib in the Spontaneous Glioma Model

Spontaneous tumor were developed in wild-type and *Mdr1a/b*$^{-/-}$*Bcrp1*$^{-/-}$ mice. After reaching the signal threshold, mice were randomly assigned to one of four groups (n = 5 - 7 per group); (1) wild-type mice treated with 15 mg/kg dasatinib by oral gavage twice a day for seven days, (2) wild-type mice treated with vehicle over the same duration, (3) *Mdr1a/b*$^{(-/-)}$*Bcrp1*$^{(-/-)}$ mice treated with dasatinib and (4) *Mdr1a/b*$^{-/-}$*Bcrp1*$^{-/-}$ mice treated with vehicle. Survival was monitored post treatment with the experimental endpoint being death or moribund status of the mice. Median survival time in each of the four groups was determined and compared using a t-test with $p < 0.05$ considered to be significant.

6.2.8 Quantification of Dasatinib by LCMS-MS

Dasatinib concentrations in the tissue specimens were determined by a rapid and sensitive LC-MS/MS method. Prior to analysis, frozen samples were thawed at ambient temperature. Brain samples were homogenized using 3 volumes of 5 % bovine serum

albumin in phosphate-buffered saline using a tissue homogenizer (Fisher Scientific, Pittsburgh, PA). A 100 µL aliquot of brain homogenate was used for analysis. Brain samples were spiked with 10 ng of gefitinib as internal standard and alkalinized by addition of 200 µL of a pH 11 buffer (1 mM sodium hydroxide, 0.5 mM sodium bicarbonate). The samples were then extracted by addition of 1 mL of ice cold ethyl acetate followed by vigorous vortexing on a mechanical shaker for 10 minutes and centrifuged at 7500 rpm for 15 minutes at 4°C to separate the organic layer. A volume of 750 µL of the top organic layer was transferred to fresh polypropylene tubes and dried under nitrogen. Samples were reconstituted in 100 µL mobile phase and transferred to glass auto sampler vials. A volume of 5 µL sample was injected in the HPLC system using a temperature controlled autosampling device maintained at 10°C. Chromatographic analysis was performed using an Agilent Model 1200 separation system (Santa Clara, CA, USA). Separation of analytes was achieved using an Agilent Eclipse XDB-C18 RRHT threaded column (4.6mm ID x 50mm) packed with a 1.8-µm ZORBAX Rx-SIL stationary phase (Santa Clara, CA, USA). The mobile phase used for the chromatographic separation was composed of acetonitrile: 20mM ammonium formate (containing 0.1% formic acid, pH adjusted to 4 with ammonium hydroxide) (32:68 v/v), and was delivered at a flow rate of 0.25 mL/min. The column effluent was monitored using a Thermo Finnigan™ TSQ® Quantum 1.5 detector (San Jose, CA, USA). The instrument was equipped with an electrospray interface, and controlled by the Xcalibur version 2.0.7 data system. The samples were analyzed using an electrospray probe in the positive ionization mode operating at a spray voltage of 4500V for both dasatinib and

gefitinib (internal standard). Samples were introduced into the interface through a heated nebulized probe at 300°C. The spectrometer was programmed to allow the $[MH]^+$ ion of dasatinib at *m/z* 488 and that of internal standard at *m/z* 446.9 to pass through the first quadrupole (Q1) and into the collision cell (Q2). The collision energy was set at 9V for gefitinib and 16V for dasatinib. The product ions for dasatinib (*m/z* 401) and the internal standard gefitinib (*m/z* 128.1) were monitored through the third quadrupole (Q3). The scan width and scan time for monitoring the two product ions were 1.5 *m/z* and 0.5s, respectively. The sensitivity of the assay was at least 2.5 ng/ml with a corresponding CV of ~ 10%.

6.3 Results

6.3.1 Spontaneous Mouse Model of Glioma

Figure 6.1A shows a schematic of the plasmid vectors used for generation of tumor along with an image of a representative tumor arising from the spontaneous mouse model (**Figure 6.1B**). The GFP tagged tumor can be seen to present a central core (**i**), along with an infiltrating rim (**ii**), branching out into normal brain areas. Areas of slight green (**iii**) in normal brain indicate invasive tumor cells that have infiltrated from the tumor core.

6.3.2 Heterogeneous Permeability of the BBB

The breakdown of the blood-brain barrier in the tumor and areas adjoining the tumor was investigated by examining the brain penetration of dextran. Dextran of molecular weight 3 kDa under normal circumstances does not cross the BBB and can therefore be regarded as a marker for intactness of the brain vasculature tight junctions. After intravenous

administration of Texas Red-conjugated dextran, concentrations in the brain were greater in the tumor core compared to that in the rim and normal brain (**Figure 6.2**). This difference however did not reach statistical significance. There was a similar trend in both the wild-type and *Mdr1a/b*$^{-/-}$*Bcrp1*$^{-/-}$ mice where concentrations in the core appeared to be greater than that in the tumor rim which in turn were greater than the normal brain concentrations. Higher dextran levels in the tumor core indicates that the BBB is disrupted near the core, however the lower levels in the rim and normal brain is suggestive of an intact BBB in these areas.

6.3.3 Differential Distribution of Dasatinib to the Brain

Given the heterogeneous disruption of the BBB near the tumor, we studied the ability of dasatinib to traverse the BBB in the three brain regions. In the wild-type mice, concentrations in the tumor core were greater than that in tumor rim and normal brain (**Figure 6.3**). Mean dasatinib concentrations in the tumor core were 2-fold higher than that in the normal brain and rim. However, again due to the high variability, the difference did not reach statistical significance. When P-gp and BCRP were absent in the *Mdr1a/b*$^{-/-}$*Bcrp1*$^{-/-}$ mice, brain concentrations increased by over 2-fold in the normal brain and by upto 3-fold in the tumor rim and core. This suggests that absence of the two transporters at the BBB can significantly enhance delivery of dasatinib, especially to the normal brain where the BBB is intact. Dasatinib concentrations increased even in the tumor core suggesting that the BBB is not completely disrupted in the core either and can restrict delivery to a small extent.

6.3.4 Efficacy of Dasatinib Measured by Signal Inhibition

We performed western blotting on tissue samples from tumor core, rim and normal brain to examine the efficacy of dasatinib in inhibiting phosphorylation of SRC and AKT. In the vehicle treated wild-type and *Mdr1a/b*$^{-/-}$*Bcrp1*$^{-/-}$ mice, high levels of phosphorylated SRC and AKT were detected in the tumor core, rim and normal brain tissue (**Figure 6.4A**). When wild-type mice were treated with dasatinib, levels of phosphorylated SRC decreased, with the lowest levels seen in the tumor core. Similarly, levels of phospho-AKT decreased in the tumor rim and normal brain. In the dasatinib treated *Mdr1a/b*$^{-/-}$ *Bcrp1*$^{-/-}$ mice, dasatinib was much more effective in preventing the phosphorylation of AKT and SRC. No phospho-SRC was detected in tumor core, rim or normal brain. Likewise, levels of phospho-AKT were also low in all three brain regions (**Figure 6.4B**). This indicates that dasatinib is much more effective in inhibiting its targets in the *Mdr1a/b*$^{-/-}$*Bcrp1*$^{-/-}$ mice, where absence of P-gp and BCRP at the BBB results in increased drug delivery to the targets in the brain.

6.3.5 Efficacy of Dasatinib in the Spontaneous Glioma Model

Efficacy of dasatinib against a spontaneous glioma was examined by monitoring survival in wild-type and *Mdr1a/b*$^{-/-}$*Bcrp1*$^{-/-}$ mice that were treated with dasatinib. The vehicle treated cohort of both mouse genotypes died rapidly after initiation of the study, with the median survival time being 7 days in the wild-type and 9 days in the *Mdr1a/b*$^{-/-}$*Bcrp1*$^{-/-}$ mice **(Figure 6.5)**. When treated with dasatinib, wild-type mice survived significantly longer, with a median survival time of 14 days compared to the untreated group.

Importantly, the most significant effect was seen in the *Mdr1a/b*$^{-/-}$*Bcrp1*$^{-/-}$ mice treated with dasatinib, where the mice survival increased dramatically to yield a median survival time of 33 days (***p < 0.001*, Figure 6.5**). These results conclusively indicate that dasatinib is much more effective against the tumor when drug delivery to the brain and hence the targets, is enhanced in the *Mdr1a/b*$^{-/-}$*Bcrp1*$^{-/-}$ mice.

6.4 Discussion

Despite decades of research, there is still no cure for glioblastoma multiforme. Scientific advances have led to powerful tools in the form of molecularly-targeted agents, however, none of the clinical trials with small molecule TKIs have yielded therapeutic benefit in GBM (8). One of the most significant challenges in treatment of brain tumors is delivery of drug into a pharmacological sanctuary that does not allow easy access to circulating drugs and chemicals. It has been shown that active efflux transporters at the BBB prevent transport of several TKIs to the brain. If therapeutic agents do not reach their intended molecular target, regardless of their potency, they cannot possibly be effective. However, there has been some controversy on the status of the BBB in brain tumors. Reports suggest that high drug concentrations measured in resected tumor tissue are indicative of a disrupted BBB (24), leading these studies to conclude that the BBB does not restrict drug delivery to the tumor in GBM (23). But unlike many other tumors, GBM is an extremely invasive disease of the entire brain. Given the infiltrative nature of the tumor, concentrations measured in the resected tumor tissue are not representative of that in other regions of the brain, areas where the BBB can be intact and capable of restricting drug delivery. In this study we raise this critical issue and show that restricted drug

delivery across the BBB into the brain can be a significant determinant of drug efficacy in treating glioma in this realistic model. Moreover, we show that the BBB is heterogeneously disrupted at the site of the tumor, but is intact in regions away from the brain and restricts delivery of dasatinib to these sites which contain invasive tumor cells. Finally we show that increased delivery of dasatinib when the two active transporters, P-gp and BCRP, are absent at the BBB results in a remarkable enhancement in efficacy of dasatinib.

We first investigated the critical question regarding the integrity of the BBB in glioma. Brain permeability studies with dextran showed that while the BBB might be disrupted at the tumor core, it most certainly is intact in regions away from the tumor (rim) as well as in the normal brain hemisphere (**Figure 6.2**). Moreover, the intact BBB significantly restricted delivery of dasatinib to areas away from the tumor (**Figure 6.3**). Furthermore, in the *Mdr1a/b*$^{-/-}$*Bcrp1*$^{-/-}$ mice, dasatinib concentrations increased in all three brain regions, signifying the impact of P-gp and BCRP at the intact BBB. The controversy over the integrity of the BBB in GBM has been driven by reports of high drug levels in tumor tissue that was resected from the brain (23). However, there are several studies that show that while drug levels in the tumor are high, concentrations are dramatically lower in brain tissue away from the tumor. Pitz et al. recently showed that concentrations of several anti-cancer agents in the non-contrast enhancing regions of the brain were significantly lower than that in the contrast enhancing tumor (27). Similarly, it has been shown that concentrations of paclitaxel (28) and temozolomide (29) in the tumor periphery were lower than that in the tumor core. Lockman et al. recently demonstrated

the heterogeneous permeability of the BBB in satellite legions of metastatic brain tumors and showed that it significantly restricts drug delivery to the tumor cells (30). Our results are consistent with these findings and show that drug concentrations in the tumor core are not representative of whole brain concentrations. The lower drug concentrations in growing areas of the tumor are indicative that the BBB is intact along with functional efflux mechanisms that can significantly restrict drug entry into the brain.

P-gp and BCRP are two dominant transporters that together restrict distribution of a number of anti-cancer drugs to the brain. More importantly, several molecularly targeted agents have been shown to be excluded from the brain due to efflux mediated by these two transporters (12-15, 18, 19). Dasatinib is one such small molecule TKI that is an avid substrate for P-gp and BCRP (14, 31). We have previously shown that delivery of dasatinib to the brain increases dramatically when P-gp and BCRP are absent at the BBB in the *Mdr1a/b*$^{-/-}$*Bcrp1*$^{-/-}$ mice (14). While the influence of these transporters in restricting distribution of dasatinib to the brain has been shown, their role in limiting efficacy of substrate drugs remains to be carefully characterized. We examined this first by studying the ability of dasatinib to inhibit two target proteins, SRC and AKT. Western blotting results show that dasatinib was much more effective in inhibiting the phosphorylation of SRC and AKT in the *Mdr1a/b*$^{-/-}$*Bcrp1*$^{-/-}$ mice (**Figure 6.4**). Complete inhibition of SRC phosphorylation in all three brain regions is consistent with the delivery data that show that drug delivery increases in the *Mdr1a/b*$^{-/-}$*Bcrp1*$^{-/-}$ mice. The most comprehensive evidence that restricted delivery to brain can limit drug efficacy was seen in the study monitoring survival in dasatinib treated mice. *Mdr1a/b*$^{-/-}$*Bcrp1*$^{-/-}$ mice that were treated

with dasatinib survived significantly longer than the wild-type mice. The median survival increased from 14 days in the wild-type to 33 days in the transporter knockout animals (**Figure 6.5**). These results conclusively show that enhancement in delivery of dasatinib to the brain dramatically increases its efficacy in treating the tumor.

Many promising molecularly-targeted TKIs have failed to show any clinical benefit in glioma. While studies investigating the failure of these agents have proposed various hypotheses, few have considered limited drug delivery to the tumor as a possible explanation. The objective of this study is to highlight two fundamental realities in treating an infiltrative tumor like glioblastoma multiforme; (1) the blood-brain barrier is not disrupted throughout the entire brain in GBM and can significantly restrict transport of drugs into the brain, (2) enhanced delivery across the BBB can significantly improve efficacy of molecularly targeted agents. First, a disruption in the BBB at the tumor core in GBM is conceivable due to the pathophysiological characteristics of the necrotic tumor that damages the surrounding tissue and blood vessels. The resulting high drug concentrations in the tumor, however, are essentially irrelevant to future recurrence since the tumor core is usually removed after surgery. Chemotherapeutic drug concentrations in the brains areas adjacent to the tumor are the most clinically relevant, since the tumor in GBM eventually recurs and in most cases recurrence occurs in areas very close to the margin of surgical resection (2). The BBB is intact in such areas where small nests of invasive tumor cells reside and ultimately grow to give rise to the recurrent tumor. This has been elegantly shown in a study by Blakeley et al, where in a human GBM patient, concentrations of methotrexate in areas centimeters away from the tumor were about an

order of magnitude lower than that in the tumor (32). The idea of glioma as a disease of the whole brain lends particular credence to the need to use the systemic circulation to effectively deliver drug across the BBB to encompass the central tumor, growing edge of the tumor, and invasive glioma cells.

Secondly, the finding that increasing drug delivery to the brain translates to improved efficacy can be valuable while choosing future combinatorial drug therapy in GBM. We have shown that inhibition of P-gp and BCRP using a small molecule inhibitor is a useful strategy to enhance brain penetration of substrate drugs (12, 13) including dasatinib (14). Elacridar is a well known dual inhibitor of P-gp and BCRP that has been tested extensively for use as a concurrent therapy to improve drug delivery to the brain. There are also reports suggesting the use of drugs that are dual P-gp/BCRP substrates to competitively inhibit both transporters. These include several TKIs that have been shown to be substrates for both P-gp and BCRP. In vitro studies show that erlotinib (33), gefitinib (34), lapatinib (35) and sunitinib (36) inhibit ABC transporters, mainly P-gp and BCRP, and suggest the potential use of these agents as combination therapy to improve drug pharmacokinetics. It has been shown that concurrent treatment with gefitinib results in a significantly increases brain (37) and tumor exposure to topotecan in a mouse model of glioma (38). Certainly, combination therapy with a molecularly-targeted agent and a modulator of ABC transporters can be a vital approach to counter one of the most significant challenges in glioma chemotherapy.

In summary, this study highlights the influence of restricted drug delivery across the BBB on efficacy of dasatinib in glioma. The heterogeneous permeability of the BBB in the

tumor suggests that clinical assessment of drug delivery by using the tumor core drug concentrations (in resected tissue) as a guide for the adequacy of drug delivery can be highly misleading. Inhibition of P-gp and BCRP can be explored in future clinical trials as a possible strategy to improve delivery and hence efficacy of molecularly-targeted agents.

6.5 Footnotes

We would like to thank Dr. John R. Ohlfest, Jose L. Gallardo and Randy Donelson at the Department of Pediatrics for their collaboration on this project. This work was supported by National Institutes of Health - National Cancer Institute [CA138437] (William F. Elmquist and John R. Ohlfest) and a grant from the Children's Cancer Research Fund at the University of Minnesota (William F. Elmquist and John R. Ohlfest). Financial support for Sagar Agarwal was provided by the Doctoral Dissertation Fellowship from the University of Minnesota

Figure 6.1A Schematic of the plasmid vector used for generation of the spontaneous mouse model of GBM

Plasmid vectors contained sequences coding for mPDGFβ, eGFP and shp53RNA. A sleeping beauty (SB) transposase vector containing the luciferase reporter allowed the use of bioluminescence imaging for monitoring tumor growth.

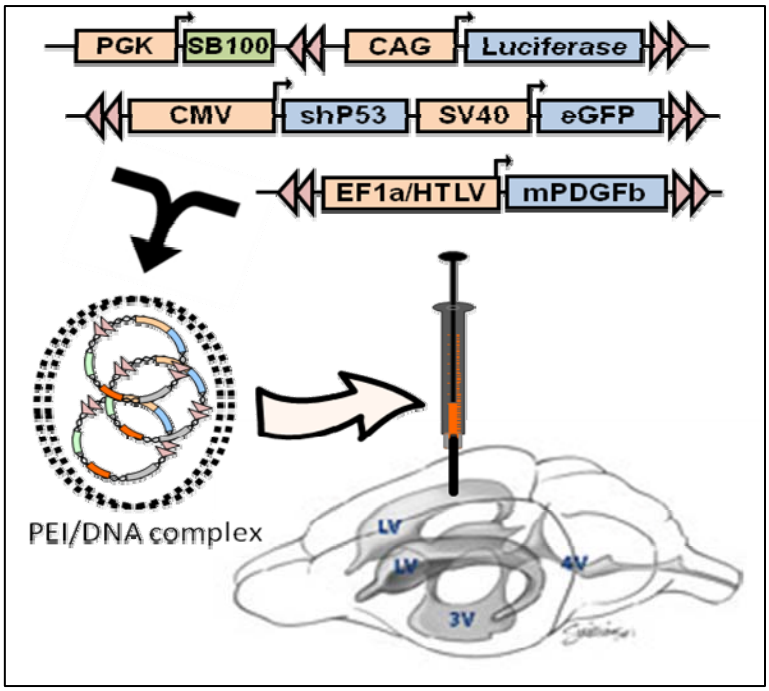

Figure 6.1B Image of a brain tumor from the spontaneous model as seen under GFP-visualization goggles.

The GFP-tagged tumor allows dissection of the brain into the tumor core, brain around tumor (rim) and normal brain in the mouse. Invasive tumor cells can be seen as areas of slight green fluorescence in the normal brain tissue.

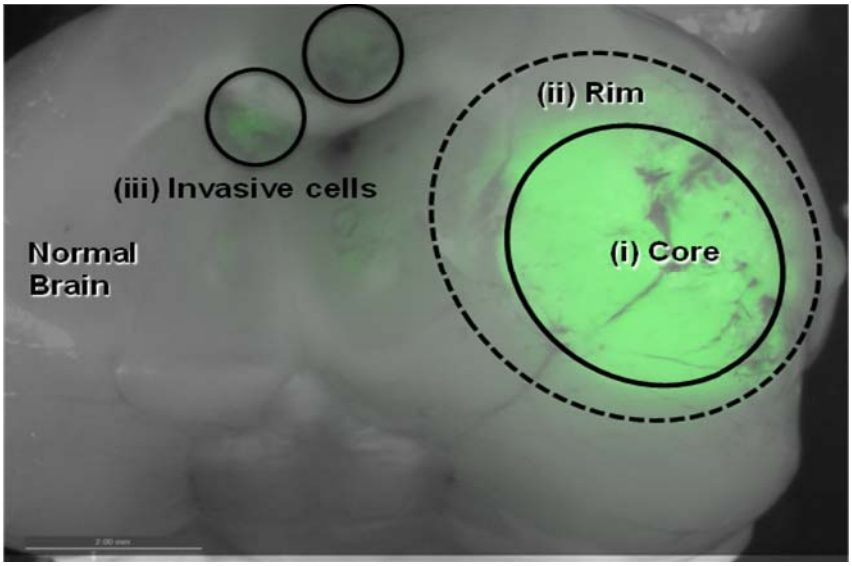

Figure 6.2 Heterogeneous permeability of the blood-brain barrier

Brain concentrations of Texas Red dextran in wild-type and *Mdr1a/b*$^{-/-}$*Bcrp1*$^{-/-}$ mice were higher in the tumor core as compared to the rim and normal brain (NB). This suggests that the BBB is disrupted at the tumor core, but also indicates the presence of an intact BBB in the brain around the tumor and the normal brain away from the tumor

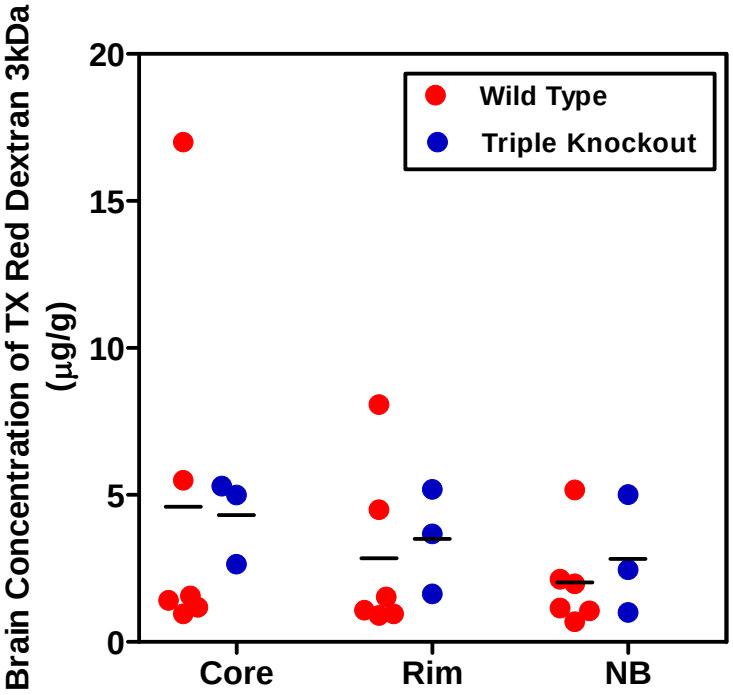

Figure 6.3 Regional delivery of dasatinib across the BBB

Brain concentrations of dasatinib in wild-type and *Mdr1a/b*$^{-/-}$*Bcrp1*$^{-/-}$ mice after an oral dose of 15 mg/kg. Concentrations were higher in the tumor core as compared to the rim and normal brain (NB) suggesting that the disrupted BBB at the tumor core does not limit drug delivery to the core. However, the low dasatinib concentrations in the rim and normal brain are suggestive of the restricted delivery due to the intactness of the BBB in these areas.

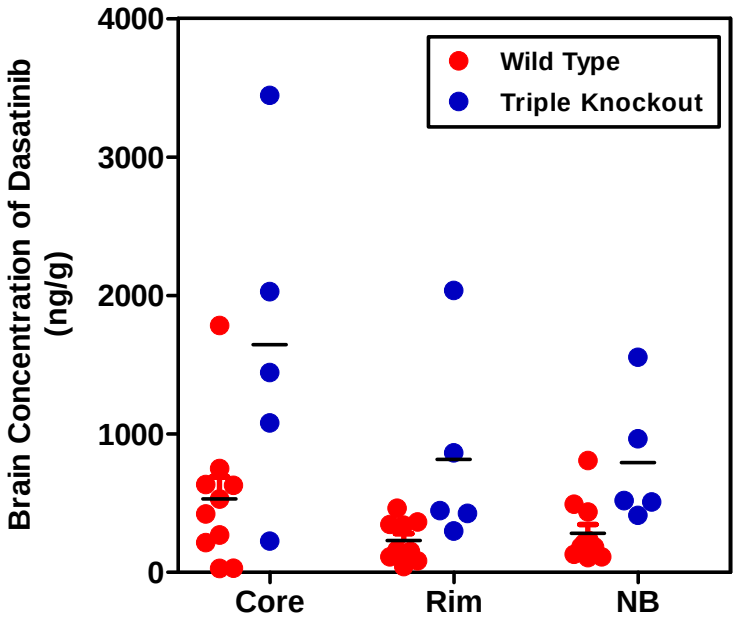

Figure 6.4 Efficacy of dasatinib against target proteins in wild-type and Mdr1a/b$^{-/-}$ Bcrp1$^{-/-}$ mice

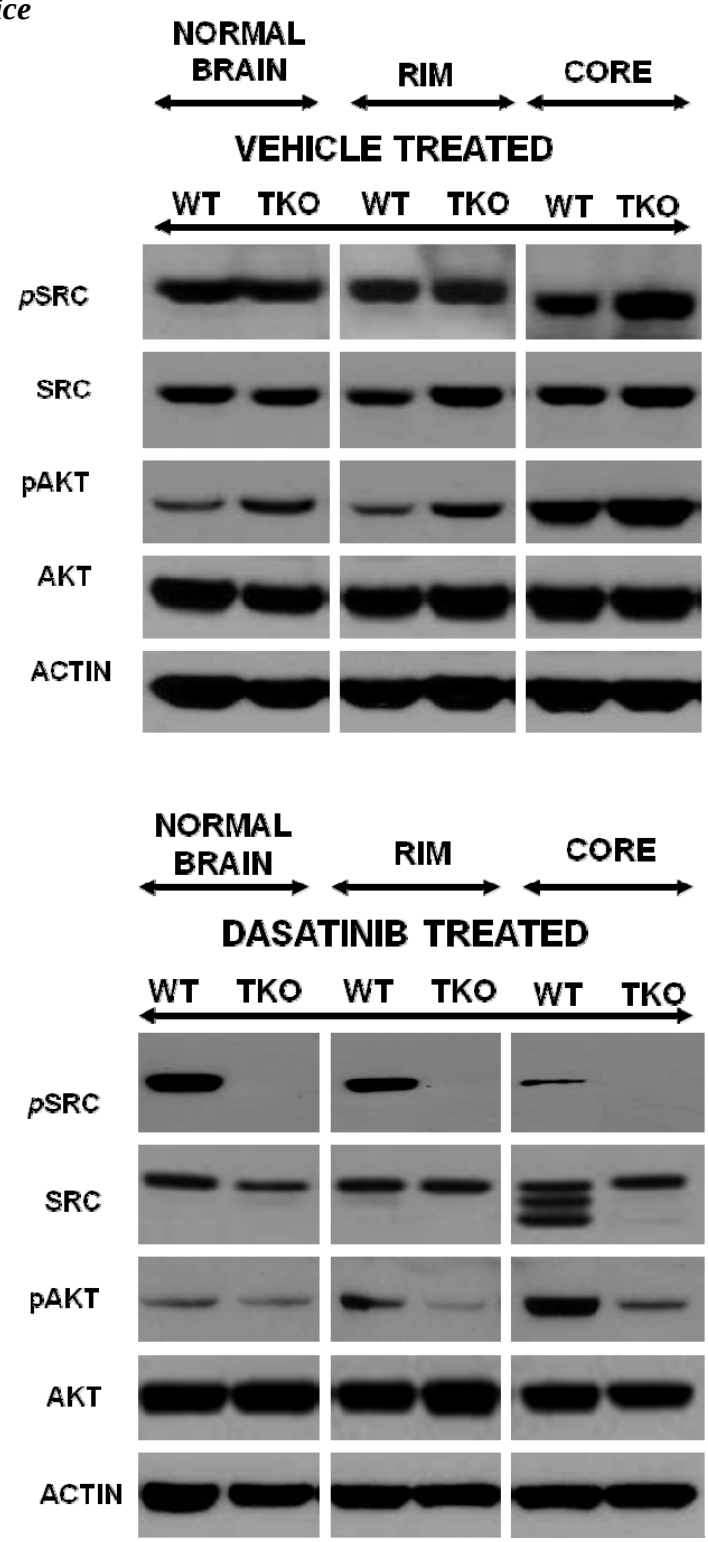

Figure 6.5 Efficacy of dasatinib in the spontaneous mouse model of glioma. After an oral dosing regimen, *Mdr1a/b*$^{-/-}$*Bcrp1*$^{-/-}$ mice treated with dasatinib survived for a significantly longer time compared to the wild-type mice. The median survival in the dasatinib treated wild-type mice was 14 days and increased significantly to 33 days in the *Mdr1a/b*$^{-/-}$*Bcrp1*$^{-/-}$ mice ($p < 0.05$).

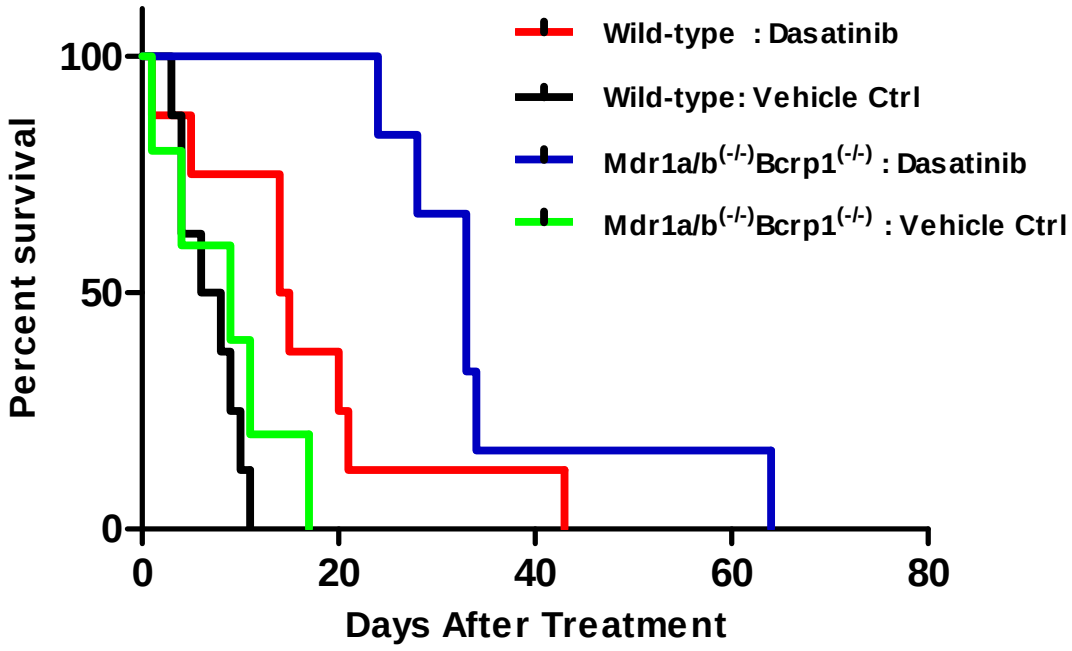

CHAPTER VII

RECAPITULATION

Glioblastoma multiforme is one of the most formidable challenges faced by the neuro-oncology community. Despite decades of research, prognosis is dismal with less than 5 % of glioblastoma patients surviving 5 years post diagnosis. Even radical treatments, such as the now abandoned complete hemispherectomy, do not cure the tumor, which inevitably recurs leading to patient death. The fact that the tumor resides in a tissue protected by the blood-brain barrier (BBB) is one of the reasons why treatment of this disease is particularly challenging. The BBB is a protective barrier that restricts drug penetration into the brain thereby limiting their therapeutic efficacy. P-glycoprotein (P-gp) and breast cancer resistance protein (BCRP) are two important gatekeepers at the BBB that have been shown to restrict transport of many chemotherapeutic drugs to the brain by virtue of their ability to transport drugs back into the brain.Thus, the restriction to drug delivery across the BBB has prevented effective application of potent, peripherally active, drugs against this tumor.

However, the aspect that makes glioblastoma so lethal and virtually incurable is its invasive growth pattern. The lethal glioma cells often evade traditional cancer treatments such as chemotherapy, and quickly invade healthy brain tissue. A historical study showed that, if left untreated, more than 50 % of gliomas infiltrate into the contralateral hemisphere (Matsukado, Y. et al., 1961). The infiltrative nature of the tumor gives rise to satellite lesions in areas away from the main tumor mass, which remain shielded by an intact blood-brain barrier, and eventually give rise to the recurrent tumor. This idea of glioma as a disease of the whole brain lends particular credence to the need to deliver drug across the BBB to encompass not only the central tumor but also its growing edges

away from the boundary of surgical resection. This issue forms the essence of this research project. The objective of this work was to show that active efflux transporters at BBB restrict delivery of potent molecularly-targeted agents to their targets. More importantly, the intention was to demonstrate that the targets in question are in invasive tumor cells that are left behind after surgery and remain shielded behind an intact blood-brain barrier. The ultimate goal of this endeavor is to improve delivery of molecularly-targeted therapy to the tumor and show that this can translate to enhanced efficacy against this lethal disease.

Initial studies were focused on investigating the extent to which molecularly-targeted agents cross the BBB and distribute into the brain. We examined the brain penetration of the EGFR inhibitor gefitinib in FVB mice (***Chapter II***). Gefitinib distribution to the brain was low, with a brain distribution coefficient of less than 10 % in the wild-type mice. When P-gp and BCRP were absent at the BBB in the *Mdr1a/b*$^{-/-}$*Bcrp1*$^{-/-}$ mice, gefitinib was able to cross the BBB to a greater extent and the brain partition coefficient increased by more than 70-fold. This study showed the impact of P-gp and BCRP on the delivery of gefitinib to the brain. An important part of this study was evaluating the integrity of the BBB in the *Mdr1a/b*$^{-/-}$*Bcrp1*$^{-/-}$ mice. Reports of a disproportionate increase in distribution of dual substrates to the brain in these mice had raised questions over the intactness of the BBB in this mouse model. We examined the brain penetration of the vascular markers sucrose and inulin, and found no difference in their brain distribution between the wild-type and *Mdr1a/b*$^{-/-}$*Bcrp1*$^{-/-}$ mice. This confirmed that the dramatic increase in transport

of drugs across the BBB in these mice was not due to a leaky BBB (absence of tight junctions).

We next examined the transport of the multikinase inhibitor sorafenib across the BBB (***Chapter III***). Sorafenib was different than gefitinib and some of the other tyrosine kinase inhibitors in that it seemed to be a better substrate for BCRP, with no evidence of P-gp-mediated transport from the in vitro studies. In vivo, transport of sorafenib across the BBB was poor with a brain partition coefficient of approximately 6 %. The steady-state brain distribution ratio increased 4-fold in the *Bcrp1*$^{-/-}$ mice, as was expected from the in vitro results. Interestingly, steady-state brain-to-plasma ratio was 10-fold greater in the *Mdr1a/b*$^{-/-}$*Bcrp1*$^{-/-}$ mice compared to wild-type. This was unexpected since the in vitro studies showed no evidence of P-gp mediated transport of sorafenib. The increased brain distribution in the combined knockout mice indicated that P-gp was also influential in the efflux of sorafenib at the BBB. We investigated this further by concurrent administration of the P-gp/BCRP inhibitor elacridar along with sorafenib. Brain distribution of sorafenib increased further in the *Bcrp1*$^{-/-}$ and wild-type mice when P-gp was inhibited. This showed that similar to many other tyrosine-kinase inhibitors, both P-gp and BCRP were involved in the efflux of sorafenib at the BBB.

A common finding in the studies with gefitinib and sorafenib was the cooperation of P-gp and BCRP in their efflux at the BBB. The result of this cooperation was a disproportionate increase in brain distribution of the two compounds in the combined P-gp/BCRP knockouts, compared to the single knockout mice. We had previously reported similar findings with dasatinib and there are other published reports of similar results

with other dual substrates. We investigated this cooperation by analyzing the contribution of P-gp and BCRP to the clearance of sorafenib from the brain (***Chapter IV***). The brain efflux index method was used to determine the clearance of sorafenib from brain in the wild-type and genetic knockout mice. The results indicated that BCRP contributed more to the efflux of sorafenib than P-gp. One possibility that could explain the cooperation of P-gp and BCRP at the BBB is their compensatory upregulation in the genetic knockout mice. We examined the expression of P-gp and BCRP in the capillary endothelial cells in the four mouse genotypes and saw no difference in their expression between the wild-type and the P-gp/BCRP knockout mice. These results showed that there are no compensatory changes in expression of P-gp in the BCRP deficient mice, and vice versa. We then explained the P-gp/BCRP cooperation by simple theory based on affinity and capacity dependent carrier-mediated transport, wherein, due to a significantly higher expression at the BBB, P-gp appears to be dominant in the efflux of several dual substrates. We explain how for compounds like sorafenib, which have a better affinity for BCRP and a negligible affinity for P-gp, BCRP, despite its lower expression, is dominant at the BBB.

These studies provided conclusive evidence that delivery of molecularly-targeted agents to the brain can be restricted due to active efflux by P-gp and BCRP. The next study examined an issue central to chemotherapy in glioma: intactness of the BBB in and near the tumor (***Chapter V***). As mentioned earlier, glioma is essentially a disease of the entire brain and tumor cells invade normal brain areas centimeters away from the core. We used an orthotopic xenograft model of glioblastoma and investigated the distribution of

erlotinib to different regions of the brain, *i.e.,* tumor, brain around tumor and normal brain tissue. The results showed that while the BBB is disrupted in the tumor core resulting in high drug concentrations in this region, areas immediately surrounding the tumor had significantly lower concentrations of erlotinib. This indicated that the BBB was sufficiently intact in areas away from the tumor, areas that could represent satellite sites for the invasive tumor cells. When P-gp and BCRP were inhibited using the dual inhibitor elacridar, erlotinib distribution to all three brain regions increased dramatically. This signified that inhibition of drug efflux at the BBB can be a useful strategy to improve drug delivery to the entire brain, especially in areas away from the tumor core, where the BBB is intact and capable of restricting drug distribution.

The final study investigated the ultimate goal of this project and sought to answer the important question; can improving delivery across the BBB result in enhanced efficacy of molecularly-targeted agents against glioma and increase survival? (***Chapter VI***). Using a spontaneous mouse model of glioma we showed that increased delivery of dasatinib to the tumor in the *Mdr1a/b*$^{-/-}$*Bcrp1*$^{-/-}$ mice resulted in enhanced efficacy. Tumor bearing *Mdr1a/b*$^{-/-}$*Bcrp1*$^{-/-}$ mice treated with dasatinib survived significantly longer than the wild-type mice. We also showed that the BBB is heterogeneously disrupted in glioma and this resulted in variable distribution of dasatinib to different regions of the brain. Finally, we showed that dasatinib efficacy in brain regions away from the tumor core, that receive significantly less drug due to the intact BBB, increased dramatically when P-gp and BCRP were absent in the *Mdr1a/b*$^{-/-}$*Bcrp1*$^{-/-}$ mice. This study provided evidence that improving drug delivery to the tumor can result in increased efficacy of molecularly

targeted therapy in glioma. We show that when treating an invasive disease like glioblastoma, it is critical to enhance drug delivery to the entire brain since tumor cells that have invaded normal brain regions are often shielded from chemotherapy by the BBB.

In conclusion, the overall important findings of this work are briefly outlined as follows. 1) We provide in vitro and in vivo evidence that tyrosine kinase inhibitors gefitinib and sorafenib are substrates for the ABC transporters P-gp and BCRP, and as a result their transport across the BBB into the brain is significantly restricted. This finding can have significant implications since adequate delivery of anti-cancer agents to their targets is a prerequisite for efficacy. If therapeutic agents do not reach their intended molecular target, regardless of their potency, they cannot possibly be effective. We show that delivery of these drugs to the brain can be improved by concurrent administration of inhibitors of P-gp and BCRP, such as elacridar. Concurrent therapy with such modulators of drug transport can be utilized as an attractive therapeutic strategy to enhance delivery of CNS therapeutics to the brain. 2) The studies also demonstrate the problems associated with the heterogeneous disruption of the BBB in glioma. The finding that delivery of dasatinib and erlotinib is significantly low in brain regions away from the tumor, and increases when P-gp and BCRP are inhibited, confirms the intactness of BBB in the growing areas of the tumor. The pathophysiological characteristics of glioma result in a disruption of the BBB in the tumor core. However areas immediately adjacent to the tumor remain protected by an intact BBB which continue to limit drug delivery to such regions. These findings are clinically significant because clinical assessment of drug

delivery is often relies on drug concentrations in tumor core (the resected tissue) as a guide for the adequacy of drug delivery. This work shows that this practice can give misleading results. 3) Finally, the work conclusively shows that enhanced drug delivery to the brain can result in improved efficacy against the tumor. The efficacy of dasatinib increased dramatically in tumor bearing mice that were deficient in P-gp and BCRP. Increased survival in these mice indicates that limited drug delivery to the tumor might be a reason behind the failure of potent molecularly-targeted agents in glioma. Overall, this work emphasizes that approaching the treatment of glioma by assuming that the tumor is localized in the contrast-enhancing area (hence resection) will lead to continued failure. The dismal prognosis in glioma may remain unchanged until measures are taken to ensure that promising anti-cancer treatments are delivered effectively to the invasive glioma cells, those hiding behind an intact BBB

Future work in this direction will examine efficacy of a combinatorial treatment regimen in the mouse model of glioma. This combination would include a modulator of drug transport such as elacridar along with one or more molecularly-targeted agents. An important aspect of the use of a transport modulator would be determining if lower systemic doses can achieve therapeutically effective concentrations in the brain. This could serve to reduce the adverse effects that sometimes limit therapy with molecularly-targeted agents. Given the enormous molecular heterogeneity in glioma another strategy that can be evaluated is a combination of different molecularly targeted agents with the aim to shut down multiple signaling processes that feed tumor growth and proliferation.

BIBLIOGRAPHY

CHAPTER IA

1. Altekruse SF, Kosary CL, Krapcho M, et al. (2010) SEER Cancer Statistics Review, 1975-2007, National Cancer Institute. Bethesda, MD, based on November 2009 SEER data submission, posted to the SEER web site, 2010. http://seer.cancer.gov/csr/1975_2007/,

2. CBTRUS. (2010) CBTRUS Statistical Report: Primary Brain and Central Nervous System Tumors Diagnosed in the United States in 2004-2006. Source: Central Brain Tumor Registry of the United States, Hinsdale, IL. website: www.cbtrus.org.

3. Cancer Facts & Figures 2010. Atlanta: American Cancer Society; 2010.

4. Stupp R, Mason WP, van den Bent MJ, et al. (2005) Radiotherapy plus concomitant and adjuvant temozolomide for glioblastoma. *N Engl J Med* **352:** 987-996.

5. Wen PY, Brandes AA. (2009) Treatment of recurrent high-grade gliomas. *Curr Opin Neurol* **22:** 657-664.

6. Pardridge WM. (2005) The blood-brain barrier: bottleneck in brain drug development. *NeuroRx* **2:** 3-14.

7. Berens ME, Giese A. (1999) "...those left behind." Biology and oncology of invasive glioma cells. *Neoplasia* **1:** 208-219.

8. Louis DN, Ohgaki H, Wiestler OD, et al. (2007) The 2007 WHO classification of tumours of the central nervous system. *Acta Neuropathol* **114:** 97-109.

9. Ohgaki H, Kleihues P. (2007) Genetic pathways to primary and secondary glioblastoma. *Am J Pathol* **170:** 1445-1453.

10. Maher EA, Brennan C, Wen PY, et al. (2006) Marked genomic differences characterize primary and secondary glioblastoma subtypes and identify two distinct molecular and clinical secondary glioblastoma entities. *Cancer Res* **66:** 11502-11513.

11. Liang Y, Diehn M, Watson N, et al. (2005) Gene expression profiling reveals molecularly and clinically distinct subtypes of glioblastoma multiforme. *Proc Natl Acad Sci U S A* **102:** 5814-5819.

12. Cancer Genome Atlas Research Network (2008) Comprehensive genomic characterization defines human glioblastoma genes and core pathways. *Nature* **455:** 1061-1068.

13. Wen PY, Kesari S. (2008) Malignant gliomas in adults. *N Engl J Med* **359:** 492-507.

14. Kreisl TN. (2009) Chemotherapy for malignant gliomas. *Semin Radiat Oncol* **19:** 150-154.

15. McGirt MJ, Chaichana KL, Gathinji M, et al. (2009) Independent association of extent of resection with survival in patients with malignant brain astrocytoma. *J Neurosurg* **110:** 156-162.

16. Lacroix M, Abi-Said D, Fourney DR, et al. (2001) A multivariate analysis of 416 patients with glioblastoma multiforme: prognosis, extent of resection, and survival. *J Neurosurg* **95:** 190-198.

17. Niyazi M, Ganswindt U, Schwarz SB, et al. (2010) Irradiation and Bevacizumab in High-Grade Glioma Retreatment Settings. *Int J Radiat Oncol Biol Phys* **Oct 27. [Epub ahead of print]**.

18. Lee CG, Heijn M, di Tomaso E, et al. (2000) Anti-Vascular endothelial growth factor treatment augments tumor radiation response under normoxic or hypoxic conditions. *Cancer Res* **60:** 5565-5570.

19. Libermann TA, Nusbaum HR, Razon N, et al. (1985) Amplification, enhanced expression and possible rearrangement of EGF receptor gene in primary human brain tumours of glial origin. *Nature* **313:** 144-147.

20. Rich JN, Bigner DD. (2004) Development of novel targeted therapies in the treatment of malignant glioma. *Nat Rev Drug Discov* **3:** 430-446.

21. Lund-Johansen M, Bjerkvig R, Humphrey PA, Bigner SH, Bigner DD, Laerum OD. (1990) Effect of epidermal growth factor on glioma cell growth, migration, and invasion in vitro. *Cancer Res* **50:** 6039-6044.

22. Nister M, Claesson-Welsh L, Eriksson A, Heldin CH, Westermark B. (1991) Differential expression of platelet-derived growth factor receptors in human malignant glioma cell lines. *J Biol Chem* **266:** 16755-16763.

23. Guha A, Dashner K, Black PM, Wagner JA, Stiles CD. (1995) Expression of PDGF and PDGF receptors in human astrocytoma operation specimens supports the existence of an autocrine loop. *Int J Cancer* **60:** 168-173.

24. Maher EA, Furnari FB, Bachoo RM, et al. (2001) Malignant glioma: genetics and biology of a grave matter. *Genes Dev* **15:** 1311-1333.

25. Schmidt NO, Westphal M, Hagel C, et al. (1999) Levels of vascular endothelial growth factor, hepatocyte growth factor/scatter factor and basic fibroblast growth factor in human gliomas and their relation to angiogenesis. *Int J Cancer* **84:** 10-18.

26. Plate KH, Breier G, Weich HA, Risau W. (1992) Vascular endothelial growth factor is a potential tumour angiogenesis factor in human gliomas in vivo. *Nature* **359:** 845-848.

27. Mukasa A, Wykosky J, Ligon KL, Chin L, Cavenee WK, Furnari F. (2010) Mutant EGFR is required for maintenance of glioma growth in vivo, and its ablation leads to escape from receptor dependence. *Proc Natl Acad Sci U S A* **107:** 2616-2621.

28. Heimberger AB, Learn CA, Archer GE, et al. (2002) Brain tumors in mice are susceptible to blockade of epidermal growth factor receptor (EGFR) with the oral, specific, EGFR-tyrosine kinase inhibitor ZD1839 (iressa). *Clin Cancer Res* **8:** 3496-3502.

29. Ciardiello F, Caputo R, Bianco R, et al. (2001) Inhibition of growth factor production and angiogenesis in human cancer cells by ZD1839 (Iressa), a selective epidermal growth factor receptor tyrosine kinase inhibitor. *Clin Cancer Res* **7:** 1459-1465.

30. Griffero F, Daga A, Marubbi D, et al. (2009) Different response of human glioma tumor-initiating cells to epidermal growth factor receptor kinase inhibitors. *J Biol Chem* **284:** 7138-7148.

31. Halatsch ME, Gehrke EE, Vougioukas VI, et al. (2004) Inverse correlation of epidermal growth factor receptor messenger RNA induction and suppression of anchorage-independent growth by OSI-774, an epidermal growth factor receptor tyrosine kinase inhibitor, in glioblastoma multiforme cell lines. *J Neurosurg* **100:** 523-533.

32. Preusser M, Gelpi E, Rottenfusser A, et al. (2008) Epithelial Growth Factor Receptor Inhibitors for treatment of recurrent or progressive high grade glioma: an exploratory study. *J Neurooncol* **89:** 211-218.

33. Franceschi E, Cavallo G, Lonardi S, et al. (2007) Gefitinib in patients with progressive high-grade gliomas: a multicentre phase II study by Gruppo Italiano Cooperativo di Neuro-Oncologia (GICNO). *Br J Cancer* **96:** 1047-1051.

34. Rich JN, Reardon DA, Peery T, et al. (2004) Phase II trial of gefitinib in recurrent glioblastoma. *J Clin Oncol* **22:** 133-142.

35. Reardon DA, Desjardins A, Vredenburgh JJ, et al. (2009) Phase 2 trial of erlotinib plus sirolimus in adults with recurrent glioblastoma. *J Neurooncol* **96:** 219-230.

36. Prados MD, Chang SM, Butowski N, et al. (2009) Phase II study of erlotinib plus temozolomide during and after radiation therapy in patients with newly diagnosed glioblastoma multiforme or gliosarcoma. *J Clin Oncol* **27:** 579-584.

37. Raizer JJ, Abrey LE, Lassman AB, et al. (2010) A phase II trial of erlotinib in patients with recurrent malignant gliomas and nonprogressive glioblastoma multiforme postradiation therapy. *Neuro Oncol* **12:** 95-103.

38. Peereboom DM, Shepard DR, Ahluwalia MS, et al. (2009) Phase II trial of erlotinib with temozolomide and radiation in patients with newly diagnosed glioblastoma multiforme. *J Neurooncol* **98:** 93-99.

39. Buchdunger E, Cioffi CL, Law N, et al. (2000) Abl protein-tyrosine kinase inhibitor STI571 inhibits in vitro signal transduction mediated by c-kit and platelet-derived growth factor receptors. *J Pharmacol Exp Ther* **295:** 139-145.

40. Capdeville R, Buchdunger E, Zimmermann J, Matter A. (2002) Glivec (STI571, imatinib), a rationally developed, targeted anticancer drug. *Nat Rev Drug Discov* **1:** 493-502.

41. Ranza E, Mazzini G, Facoetti A, Nano R. (2009) In-vitro effects of the tyrosine kinase inhibitor imatinib on glioblastoma cell proliferation. *J Neurooncol* **96:** 349-357.

42. Geng L, Shinohara ET, Kim D, et al. (2006) STI571 (Gleevec) improves tumor growth delay and survival in irradiated mouse models of glioblastoma. *Int J Radiat Oncol Biol Phys* **64:** 263-271.

43. Kilic T, Alberta JA, Zdunek PR, et al. (2000) Intracranial inhibition of platelet-derived growth factor-mediated glioblastoma cell growth by an orally active kinase inhibitor of the 2-phenylaminopyrimidine class. *Cancer Res* **60:** 5143-5150.

44. Wen PY, Yung WK, Lamborn KR, et al. (2006) Phase I/II study of imatinib mesylate for recurrent malignant gliomas: North American Brain Tumor Consortium Study 99-08. *Clin Cancer Res* **12:** 4899-4907.

45. Raymond E, Brandes AA, Dittrich C, et al. (2008) Phase II study of imatinib in patients with recurrent gliomas of various histologies: a European Organisation for Research and Treatment of Cancer Brain Tumor Group Study. *J Clin Oncol* **26:** 4659-4665.

46. Premkumar DR, Jane EP, Agostino NR, Scialabba JL, Pollack IF. (2010) Dasatinib synergizes with JSI-124 to inhibit growth and migration and induce apoptosis of malignant human glioma cells. *J Carcinog* **9:** 7.

47. Kamoun WS, Ley CD, Farrar CT, et al. (2009) Edema control by cediranib, a vascular endothelial growth factor receptor-targeted kinase inhibitor, prolongs survival despite persistent brain tumor growth in mice. *J Clin Oncol* **27:** 2542-2552.

48. Batchelor TT, Sorensen AG, di Tomaso E, et al. (2007) AZD2171, a pan-VEGF receptor tyrosine kinase inhibitor, normalizes tumor vasculature and alleviates edema in glioblastoma patients. *Cancer Cell* **11:** 83-95.

49. Batchelor TT, Duda DG, di Tomaso E, et al. (2010) Phase II study of cediranib, an oral pan-vascular endothelial growth factor receptor tyrosine kinase inhibitor, in patients with recurrent glioblastoma. *J Clin Oncol* **28:** 2817-2823.

50. Wilhelm SM, Adnane L, Newell P, Villanueva A, Llovet JM, Lynch M. (2008) Preclinical overview of sorafenib, a multikinase inhibitor that targets both Raf and VEGF and PDGF receptor tyrosine kinase signaling. *Mol Cancer Ther* **7:** 3129-3140.

51. O'Farrell AM, Abrams TJ, Yuen HA, et al. (2003) SU11248 is a novel FLT3 tyrosine kinase inhibitor with potent activity in vitro and in vivo. *Blood* **101:** 3597-3605.

52. de Bouard S, Herlin P, Christensen JG, et al. (2007) Antiangiogenic and anti-invasive effects of sunitinib on experimental human glioblastoma. *Neuro Oncol* **9:** 412-423.

53. Siegelin MD, Raskett CM, Gilbert CA, Ross AH, Altieri DC. (2010) Sorafenib exerts anti-glioma activity in vitro and in vivo. *Neurosci Lett* **478:** 165-170.

54. Rich JN, Sathornsumetee S, Keir ST, et al. (2005) ZD6474, a novel tyrosine kinase inhibitor of vascular endothelial growth factor receptor and epidermal growth factor receptor, inhibits tumor growth of multiple nervous system tumors. *Clin Cancer Res* **11:** 8145-8157.

55. Yiin JJ, Hu B, Schornack PA, et al. (2010) ZD6474, a multitargeted inhibitor for receptor tyrosine kinases, suppresses growth of gliomas expressing an epidermal growth factor receptor mutant, EGFRvIII, in the brain. *Mol Cancer Ther* **9:** 929-941.

56. Hu X, Pandolfi PP, Li Y, Koutcher JA, Rosenblum M, Holland EC. (2005) mTOR promotes survival and astrocytic characteristics induced by Pten/AKT signaling in glioblastoma. *Neoplasia* **7:** 356-368.

57. Kreisl TN, Lassman AB, Mischel PS, et al. (2009) A pilot study of everolimus and gefitinib in the treatment of recurrent glioblastoma (GBM). *J Neurooncol* **92:** 99-105.

58. Galanis E, Buckner JC, Maurer MJ, et al. (2005) Phase II trial of temsirolimus (CCI-779) in recurrent glioblastoma multiforme: a North Central Cancer Treatment Group Study. *J Clin Oncol* **23:** 5294-5304.

59. Lee J, Kotliarova S, Kotliarov Y, et al. (2006) Tumor stem cells derived from glioblastomas cultured in bFGF and EGF more closely mirror the phenotype and genotype of primary tumors than do serum-cultured cell lines. *Cancer Cell* **9:** 391-403.

60. Hawkins BT, Davis TP. (2005) The blood-brain barrier/neurovascular unit in health and disease. *Pharmacol Rev* **57:** 173-185.

61. Pardridge WM. (1999) Blood-brain barrier biology and methodology. *J Neurovirol* **5:** 556-569.

62. Pardridge WM. (1998) CNS drug design based on principles of blood-brain barrier transport. *J Neurochem* **70:** 1781-1792.

63. Ajay, Bemis GW, Murcko MA. (1999) Designing libraries with CNS activity. *J Med Chem* **42:** 4942-4951.

64. Vilar S, Chakrabarti M, Costanzi S. (2010) Prediction of passive blood-brain partitioning: straightforward and effective classification models based on in silico derived physicochemical descriptors. *J Mol Graph Model* **28:** 899-903.

65. Mahar Doan KM, Humphreys JE, Webster LO, et al. (2002) Passive permeability and P-glycoprotein-mediated efflux differentiate central nervous system (CNS) and non-CNS marketed drugs. *J Pharmacol Exp Ther* **303:** 1029-1037.

66. Golden PL, Pollack GM. (2003) Blood-brain barrier efflux transport. *J Pharm Sci* **92:** 1739-1753.

67. Kusuhara H, Sugiyama Y. (2005) Active efflux across the blood-brain barrier: role of the solute carrier family. *NeuroRx* **2:** 73-85.

68. Sun H, Dai H, Shaik N, Elmquist WF. (2003) Drug efflux transporters in the CNS. *Adv Drug Deliv Rev* **55:** 83-105.

69. Nicolazzo JA, Katneni K. (2009) Drug transport across the blood-brain barrier and the impact of breast cancer resistance protein (ABCG2). *Curr Top Med Chem* **9:** 130-147.

70. Borst P, Evers R, Kool M, Wijnholds J. (2000) A family of drug transporters: the multidrug resistance-associated proteins. *J Natl Cancer Inst* **92:** 1295-1302.

71. Schinkel AH, Jonker JW. (2003) Mammalian drug efflux transporters of the ATP binding cassette (ABC) family: an overview. *Adv Drug Deliv Rev* **55:** 3-29.

72. Schinkel AH. (1999) P-Glycoprotein, a gatekeeper in the blood-brain barrier. *Adv Drug Deliv Rev* **36:** 179-194.

73. Loscher W, Potschka H. (2005) Role of drug efflux transporters in the brain for drug disposition and treatment of brain diseases. *Prog Neurobiol* **76:** 22-76.

74. Juliano RL, Ling V. (1976) A surface glycoprotein modulating drug permeability in Chinese hamster ovary cell mutants. *Biochim Biophys Acta* **455:** 152-162.

75. Ueda K, Cornwell MM, Gottesman MM, et al. (1986) The mdr1 gene, responsible for multidrug-resistance, codes for P-glycoprotein. *Biochem Biophys Res Commun* **141:** 956-962.

76. Cordon-Cardo C, O'Brien JP, Casals D, et al. (1989) Multidrug-resistance gene (P-glycoprotein) is expressed by endothelial cells at blood-brain barrier sites. *Proc Natl Acad Sci U S A* **86:** 695-698.

77. Thiebaut F, Tsuruo T, Hamada H, Gottesman MM, Pastan I, Willingham MC. (1989) Immunohistochemical localization in normal tissues of different epitopes in the multidrug transport protein P170: evidence for localization in brain capillaries and crossreactivity of one antibody with a muscle protein. *J Histochem Cytochem* **37:** 159-164.

78. Barrand MA, Robertson KJ, von Weikersthal SF. (1995) Comparisons of P-glycoprotein expression in isolated rat brain microvessels and in primary cultures of endothelial cells derived from microvasculature of rat brain, epididymal fat pad and from aorta. *FEBS Lett* **374:** 179-183.

79. Hegmann EJ, Bauer HC, Kerbel RS. (1992) Expression and functional activity of P-glycoprotein in cultured cerebral capillary endothelial cells. *Cancer Res* **52:** 6969-6975.

80. Tsuji A, Terasaki T, Takabatake Y, et al. (1992) P-glycoprotein as the drug efflux pump in primary cultured bovine brain capillary endothelial cells. *Life Sci* **51:** 1427-1437.

81. Beaulieu E, Demeule M, Ghitescu L, Beliveau R. (1997) P-glycoprotein is strongly expressed in the luminal membranes of the endothelium of blood vessels in the brain. *Biochem J* **326 (Pt 2):** 539-544.

82. Schinkel AH, Smit JJ, van Tellingen O, et al. (1994) Disruption of the mouse mdr1a P-glycoprotein gene leads to a deficiency in the blood-brain barrier and to increased sensitivity to drugs. *Cell* **77:** 491-502.

83. Schinkel AH, Mayer U, Wagenaar E, et al. (1997) Normal viability and altered pharmacokinetics in mice lacking mdr1-type (drug-transporting) P-glycoproteins. *Proc Natl Acad Sci U S A* **94:** 4028-4033.

84. Jonker JW, Freeman J, Bolscher E, et al. (2005) Contribution of the ABC transporters Bcrp1 and Mdr1a/1b to the side population phenotype in mammary gland and bone marrow of mice. *Stem Cells* **23:** 1059-1065.

85. Mirski SE, Gerlach JH, Cole SP. (1987) Multidrug resistance in a human small cell lung cancer cell line selected in adriamycin. *Cancer Res* **47:** 2594-2598.

86. Cole SP, Bhardwaj G, Gerlach JH, et al. (1992) Overexpression of a transporter gene in a multidrug-resistant human lung cancer cell line. *Science* **258:** 1650-1654.

87. Haimeur A, Conseil G, Deeley RG, Cole SP. (2004) The MRP-related and BCRP/ABCG2 multidrug resistance proteins: biology, substrate specificity and regulation. *Curr Drug Metab* **5:** 21-53.

88. Huai-Yun H, Secrest DT, Mark KS, et al. (1998) Expression of multidrug resistance-associated protein (MRP) in brain microvessel endothelial cells. *Biochem Biophys Res Commun* **243:** 816-820.

89. Zhang Y, Schuetz JD, Elmquist WF, Miller DW. (2004) Plasma membrane localization of multidrug resistance-associated protein homologs in brain capillary endothelial cells. *J Pharmacol Exp Ther* **311:** 449-455.

90. Nies AT, Jedlitschky G, Konig J, et al. (2004) Expression and immunolocalization of the multidrug resistance proteins, MRP1-MRP6 (ABCC1-ABCC6), in human brain. *Neuroscience* **129:** 349-360.

91. Dombrowski SM, Desai SY, Marroni M, et al. (2001) Overexpression of multiple drug resistance genes in endothelial cells from patients with refractory epilepsy. *Epilepsia* **42:** 1501-1506.

92. Miller DS, Nobmann SN, Gutmann H, Toeroek M, Drewe J, Fricker G. (2000) Xenobiotic transport across isolated brain microvessels studied by confocal microscopy. *Mol Pharmacol* **58:** 1357-1367.

93. Potschka H, Fedrowitz M, Loscher W. (2003) Multidrug resistance protein MRP2 contributes to blood-brain barrier function and restricts antiepileptic drug activity. *J Pharmacol Exp Ther* **306:** 124-131.

94. Potschka H, Loscher W. (2001) Multidrug resistance-associated protein is involved in the regulation of extracellular levels of phenytoin in the brain. *Neuroreport* **12:** 2387-2389.

95. Potschka H, Fedrowitz M, Loscher W. (2001) P-glycoprotein and multidrug resistance-associated protein are involved in the regulation of extracellular levels of the major antiepileptic drug carbamazepine in the brain. *Neuroreport* **12:** 3557-3560.

96. Loscher W, Potschka H. (2002) Role of multidrug transporters in pharmacoresistance to antiepileptic drugs. *J Pharmacol Exp Ther* **301:** 7-14.

97. Sun H, Johnson DR, Finch RA, Sartorelli AC, Miller DW, Elmquist WF. (2001) Transport of fluorescein in MDCKII-MRP1 transfected cells and mrp1-knockout mice. *Biochem Biophys Res Commun* **284:** 863-869.

98. Leggas M, Adachi M, Scheffer GL, et al. (2004) Mrp4 confers resistance to topotecan and protects the brain from chemotherapy. *Mol Cell Biol* **24:** 7612-7621.

99. Doyle LA, Yang W, Abruzzo LV, et al. (1998) A multidrug resistance transporter from human MCF-7 breast cancer cells. *Proc Natl Acad Sci U S A* **95:** 15665-15670.

100. Miyake K, Mickley L, Litman T, et al. (1999) Molecular cloning of cDNAs which are highly overexpressed in mitoxantrone-resistant cells: demonstration of homology to ABC transport genes. *Cancer Res* **59:** 8-13.

101. Allikmets R, Schriml LM, Hutchinson A, Romano-Spica V, Dean M. (1998) A human placenta-specific ATP-binding cassette gene (ABCP) on chromosome 4q22 that is involved in multidrug resistance. *Cancer Res* **58:** 5337-5339.

102. Robey RW, Polgar O, Deeken J, To KW, Bates SE. (2007) ABCG2: determining its relevance in clinical drug resistance. *Cancer Metastasis Rev* **26:** 39-57.

103. Cooray HC, Blackmore CG, Maskell L, Barrand MA. (2002) Localisation of breast cancer resistance protein in microvessel endothelium of human brain. *Neuroreport* **13:** 2059-2063.

104. Hori S, Ohtsuki S, Tachikawa M, et al. (2004) Functional expression of rat ABCG2 on the luminal side of brain capillaries and its enhancement by astrocyte-derived soluble factor(s). *J Neurochem* **90:** 526-536.

105. Cisternino S, Mercier C, Bourasset F, Roux F, Scherrmann JM. (2004) Expression, up-regulation, and transport activity of the multidrug-resistance protein Abcg2 at the mouse blood-brain barrier. *Cancer Res* **64:** 3296-3301.

106. Eisenblatter T, Galla HJ. (2002) A new multidrug resistance protein at the blood-brain barrier. *Biochem Biophys Res Commun* **293:** 1273-1278.

107. Lee YJ, Kusuhara H, Jonker JW, Schinkel AH, Sugiyama Y. (2005) Investigation of efflux transport of dehydroepiandrosterone sulfate and mitoxantrone at the mouse blood-brain barrier: a minor role of breast cancer resistance protein. *J Pharmacol Exp Ther* **312:** 44-52.

108. Zhao R, Raub TJ, Sawada GA, et al. (2009) Breast cancer resistance protein interacts with various compounds in vitro, but plays a minor role in substrate efflux at the blood-brain barrier. *Drug Metab Dispos* **37:** 1251-1258.

109. Enokizono J, Kusuhara H, Ose A, Schinkel AH, Sugiyama Y. (2008) Quantitative investigation of the role of breast cancer resistance protein (Bcrp/Abcg2) in limiting brain and testis penetration of xenobiotic compounds. *Drug Metab Dispos* **36:** 995-1002.

110. Breedveld P, Pluim D, Cipriani G, et al. (2005) The effect of Bcrp1 (Abcg2) on the in vivo pharmacokinetics and brain penetration of imatinib mesylate (Gleevec): implications for the use of breast cancer resistance protein and P-glycoprotein inhibitors to enable the brain penetration of imatinib in patients. *Cancer Res* **65:** 2577-2582.

111. Agarwal S, Sane R, Ohlfest JR, Elmquist WF. (2010) Role of Breast Cancer Resistance Protein (ABCG2/BCRP) in the Distribution of Sorafenib to the Brain. *J Pharmacol Exp Ther* **336:** 223-233.

112. de Vries NA, Zhao J, Kroon E, Buckle T, Beijnen JH, van Tellingen O. (2007) P-glycoprotein and breast cancer resistance protein: two dominant transporters working together in limiting the brain penetration of topotecan. *Clin Cancer Res* **13:** 6440-6449.

113. Polli JW, Olson KL, Chism JP, et al. (2009) An unexpected synergist role of P-glycoprotein and breast cancer resistance protein on the central nervous system penetration of the tyrosine kinase inhibitor lapatinib (N-{3-chloro-4-[(3-fluorobenzyl)oxy]phenyl}-6-[5-({[2-(methylsulfonyl)ethy l]amino}methyl)-2-furyl]-4-quinazolinamine; GW572016). *Drug Metab Dispos* **37:** 439-442.

114. Chen Y, Agarwal S, Shaik NM, Chen C, Yang Z, Elmquist WF. (2009) P-glycoprotein and breast cancer resistance protein influence brain distribution of dasatinib. *J Pharmacol Exp Ther* **330:** 956-963.

115. Lagas JS, van Waterschoot RA, van Tilburg VA, et al. (2009) Brain accumulation of dasatinib is restricted by P-glycoprotein (ABCB1) and breast cancer resistance protein (ABCG2) and can be enhanced by elacridar treatment. *Clin Cancer Res* **15:** 2344-2351.

116. Agarwal S, Sane R, Gallardo JL, Ohlfest JR, Elmquist WF. (2010) Distribution of gefitinib to the brain is limited by P-glycoprotein (ABCB1) and breast cancer resistance protein (ABCG2)-mediated active efflux. *J Pharmacol Exp Ther* **334:** 147-155.

117. Kodaira H, Kusuhara H, Ushiki J, Fuse E, Sugiyama Y. (2010) Kinetic analysis of the cooperation of P-glycoprotein (P-gp/Abcb1) and breast cancer resistance protein (Bcrp/Abcg2) in limiting the brain and testis penetration of erlotinib, flavopiridol, and mitoxantrone. *J Pharmacol Exp Ther* **333:** 788-796.

118. Lagas JS, van Waterschoot RA, Sparidans RW, Wagenaar E, Beijnen JH, Schinkel AH. (2010) Breast cancer resistance protein and P-glycoprotein limit sorafenib brain accumulation. *Mol Cancer Ther* **9:** 319-326.

119. Tanaka Y, Slitt AL, Leazer TM, Maher JM, Klaassen CD. (2005) Tissue distribution and hormonal regulation of the breast cancer resistance protein (Bcrp/Abcg2) in rats and mice. *Biochem Biophys Res Commun* **326:** 181-187.

120. Hofer S, Frei K. (2007) Gefitinib concentrations in human glioblastoma tissue. *J Neurooncol* **82:** 175-176.

121. Jain RK, di Tomaso E, Duda DG, Loeffler JS, Sorensen AG, Batchelor TT. (2007) Angiogenesis in brain tumours. *Nat Rev Neurosci* **8:** 610-622.

122. Gilbertson RJ, Rich JN. (2007) Making a tumour's bed: glioblastoma stem cells and the vascular niche. *Nat Rev Cancer* **7:** 733-736.

123. Silbergeld DL, Chicoine MR. (1997) Isolation and characterization of human malignant glioma cells from histologically normal brain. *J Neurosurg* **86:** 525-531.

124. Fine RL, Chen J, Balmaceda C, et al. (2006) Randomized study of paclitaxel and tamoxifen deposition into human brain tumors: implications for the treatment of metastatic brain tumors. *Clin Cancer Res* **12:** 5770-5776.

125. Pitz MW, Desai A, Grossman SA, Blakeley JO. (2011) Tissue concentration of systemically administered antineoplastic agents in human brain tumors. *J Neurooncol***:** 1-10.

126. Fattori S, Becherini F, Cianfriglia M, Parenti G, Romanini A, Castagna M. (2007) Human brain tumors: multidrug-resistance P-glycoprotein expression in tumor cells and intratumoral capillary endothelial cells. *Virchows Arch* **451:** 81-87.

127. Demeule M, Shedid D, Beaulieu E, et al. (2001) Expression of multidrug-resistance P-glycoprotein (MDR1) in human brain tumors. *Int J Cancer* **93:** 62-66.

128. Nabors MW, Griffin CA, Zehnbauer BA, et al. (1991) Multidrug resistance gene (MDR1) expression in human brain tumors. *J Neurosurg* **75:** 941-946.

129. Spiegl-Kreinecker S, Buchroithner J, Elbling L, et al. (2002) Expression and functional activity of the ABC-transporter proteins P-glycoprotein and multidrug-resistance protein 1 in human brain tumor cells and astrocytes. *J Neurooncol* **57:** 27-36.

130. Decleves X, Fajac A, Lehmann-Che J, et al. (2002) Molecular and functional MDR1-Pgp and MRPs expression in human glioblastoma multiforme cell lines. *Int J Cancer* **98:** 173-180.

131. Ashmore SM, Thomas DG, Darling JL. (1999) Does P-glycoprotein play a role in clinical resistance of malignant astrocytoma? *Anticancer Drugs* **10:** 861-872.

132. Doyle LA, Ross DD. (2003) Multidrug resistance mediated by the breast cancer resistance protein BCRP (ABCG2). *Oncogene* **22:** 7340-7358.

133. Zhou S, Schuetz JD, Bunting KD, et al. (2001) The ABC transporter Bcrp1/ABCG2 is expressed in a wide variety of stem cells and is a molecular determinant of the side-population phenotype. *Nat Med* **7:** 1028-1034.

134. Dean M, Fojo T, Bates S. (2005) Tumour stem cells and drug resistance. *Nat Rev Cancer* **5:** 275-284.

135. Bleau AM, Hambardzumyan D, Ozawa T, et al. (2009) PTEN/PI3K/Akt pathway regulates the side population phenotype and ABCG2 activity in glioma tumor stem-like cells. *Cell Stem Cell* **4:** 226-235.

136. Mohri M, Nitta H, Yamashita J. (2000) Expression of multidrug resistance-associated protein (MRP) in human gliomas. *J Neurooncol* **49:** 105-115.

137. Bronger H, Konig J, Kopplow K, et al. (2005) ABCC drug efflux pumps and organic anion uptake transporters in human gliomas and the blood-tumor barrier. *Cancer Res* **65:** 11419-11428.

138. Calatozzolo C, Gelati M, Ciusani E, et al. (2005) Expression of drug resistance proteins Pgp, MRP1, MRP3, MRP5 and GST-pi in human glioma. *J Neurooncol* **74:** 113-121.

139. Bahr O, Rieger J, Duffner F, Meyermann R, Weller M, Wick W. (2003) P-glycoprotein and multidrug resistance-associated protein mediate specific patterns of

multidrug resistance in malignant glioma cell lines, but not in primary glioma cells. *Brain Pathol* **13:** 482-494.

140. Kuan CT, Wakiya K, Herndon JE, 2nd, et al. (2010) MRP3: a molecular target for human glioblastoma multiforme immunotherapy. *BMC Cancer* **10:** 468.

141. Dai H, Marbach P, Lemaire M, Hayes M, Elmquist WF. (2003) Distribution of STI-571 to the brain is limited by P-glycoprotein-mediated efflux. *J Pharmacol Exp Ther* **304:** 1085-1092.

142. Bihorel S, Camenisch G, Lemaire M, Scherrmann JM. (2007) Influence of breast cancer resistance protein (Abcg2) and p-glycoprotein (Abcb1a) on the transport of imatinib mesylate (Gleevec) across the mouse blood-brain barrier. *J Neurochem* **102:** 1749-1757.

143. Leis JF, Stepan DE, Curtin PT, et al. (2004) Central nervous system failure in patients with chronic myelogenous leukemia lymphoid blast crisis and Philadelphia chromosome positive acute lymphoblastic leukemia treated with imatinib (STI-571). *Leuk Lymphoma* **45:** 695-698.

144. Polli JW, Humphreys JE, Harmon KA, et al. (2008) The role of efflux and uptake transporters in [N-{3-chloro-4-[(3-fluorobenzyl)oxy]phenyl}-6-[5-({[2-(methylsulfonyl)ethy l]amino}methyl)-2-furyl]-4-quinazolinamine (GW572016, lapatinib) disposition and drug interactions. *Drug Metab Dispos* **36:** 695-701.

145. Yang JJ, Milton MN, Yu S, et al. (2010) P-glycoprotein and Breast Cancer Resistance Protein Affect Disposition of Tandutinib, A Tyrosine Kinase Inhibitor. *Drug Metab Lett* **4:** 201-212.

146. de Vries NA, Buckle T, Zhao J, Beijnen JH, Schellens JH, van Tellingen O. (2010) Restricted brain penetration of the tyrosine kinase inhibitor erlotinib due to the drug transporters P-gp and BCRP. *Invest New Drugs***:** 1-7.

147. de Lange EC, Danhof M. (2002) Considerations in the use of cerebrospinal fluid pharmacokinetics to predict brain target concentrations in the clinical setting: implications of the barriers between blood and brain. *Clin Pharmacokinet* **41:** 691-703.

148. Hofer S, Frei K, Rutz HP. (2006) Gefitinib accumulation in glioblastoma tissue. *Cancer Biol Ther* **5:** 483-484.

149. McKillop D, Partridge EA, Kemp JV, et al. (2005) Tumor penetration of gefitinib (Iressa), an epidermal growth factor receptor tyrosine kinase inhibitor. *Mol Cancer Ther* **4:** 641-649.

150. Stewart DJ, Leavens M, Maor M, et al. (1982) Human central nervous system distribution of cis-diamminedichloroplatinum and use as a radiosensitizer in malignant brain tumors. *Cancer Res* **42:** 2474-2479.

151. Stewart DJ, Lu K, Benjamin RS, et al. (1983) Concentration of vinblastine in human intracerebral tumor and other tissues. *J Neurooncol* **1:** 139-144.

152. Stewart DJ, Richard MT, Hugenholtz H, et al. (1984) Penetration of VP-16 (etoposide) into human intracerebral and extracerebral tumors. *J Neurooncol* **2:** 133-139.

153. Blakeley JO, Olson J, Grossman SA, He X, Weingart J, Supko JG. (2009) Effect of blood brain barrier permeability in recurrent high grade gliomas on the intratumoral pharmacokinetics of methotrexate: a microdialysis study. *J Neurooncol* **91:** 51-58.

154. Giese A, Westphal M. (1996) Glioma invasion in the central nervous system. *Neurosurgery* **39:** 235-250; discussion 250-232.

155. Hesselink JR, Press GA. (1988) MR contrast enhancement of intracranial lesions with Gd-DTPA. *Radiol Clin North Am* **26:** 873-887.

156. Lockman PR, Mittapalli RK, Taskar KS, et al. (2010) Heterogeneous blood-tumor barrier permeability determines drug efficacy in experimental brain metastases of breast cancer. *Clin Cancer Res* **16:** 5664-5678.

157. Rosso L, Brock CS, Gallo JM, et al. (2009) A new model for prediction of drug distribution in tumor and normal tissues: pharmacokinetics of temozolomide in glioma patients. *Cancer Res* **69:** 120-127.

158. Molina JR, Hayashi Y, Stephens C, Georgescu MM. (2010) Invasive glioblastoma cells acquire stemness and increased Akt activation. *Neoplasia* **12:** 453-463.

159. Singh SK, Hawkins C, Clarke ID, et al. (2004) Identification of human brain tumour initiating cells. *Nature* **432:** 396-401.

160. Liu G, Yuan X, Zeng Z, et al. (2006) Analysis of gene expression and chemoresistance of CD133+ cancer stem cells in glioblastoma. *Mol Cancer* **5:** 67.

161. Bao S, Wu Q, McLendon RE, et al. (2006) Glioma stem cells promote radioresistance by preferential activation of the DNA damage response. *Nature* **444:** 756-760.

162. Bleau AM, Huse JT, Holland EC. (2009) The ABCG2 resistance network of glioblastoma. *Cell Cycle* **8:** 2936-2944.

163. Nakai E, Park K, Yawata T, et al. (2009) Enhanced MDR1 Expression and Chemoresistance of Cancer Stem Cells Derived from Glioblastoma. *Cancer Invest* **27:** 901-908.

164. Chu L, Huang Q, Zhai DZ, et al. (2007) [Expression and significance of ABCG2 in human malignant glioma]. *Ai Zheng* **26:** 1090-1094.

165. Shervington A, Lu C. (2008) Expression of multidrug resistance genes in normal and cancer stem cells. *Cancer Invest* **26:** 535-542.

166. Westphal M, Hilt DC, Bortey E, et al. (2003) A phase 3 trial of local chemotherapy with biodegradable carmustine (BCNU) wafers (Gliadel wafers) in patients with primary malignant glioma. *Neuro Oncol* **5:** 79-88.

167. Attenello FJ, Mukherjee D, Datoo G, et al. (2008) Use of Gliadel (BCNU) wafer in the surgical treatment of malignant glioma: a 10-year institutional experience. *Ann Surg Oncol* **15:** 2887-2893.

168. Bock HC, Puchner MJ, Lohmann F, et al. (2010) First-line treatment of malignant glioma with carmustine implants followed by concomitant radiochemotherapy: a multicenter experience. *Neurosurg Rev* **33:** 441-449.

169. Bidros DS, Liu JK, Vogelbaum MA. (2009) Future of convection-enhanced delivery in the treatment of brain tumors. *Future Oncol* **6:** 117-125.

170. Kunwar S, Chang S, Westphal M, et al. (2010) Phase III randomized trial of CED of IL13-PE38QQR vs Gliadel wafers for recurrent glioblastoma. *Neuro Oncol* **12:** 871-881.

171. Lidar Z, Mardor Y, Jonas T, et al. (2004) Convection-enhanced delivery of paclitaxel for the treatment of recurrent malignant glioma: a phase I/II clinical study. *J Neurosurg* **100:** 472-479.

172. Kroll RA, Neuwelt EA. (1998) Outwitting the blood-brain barrier for therapeutic purposes: osmotic opening and other means. *Neurosurgery* **42:** 1083-1099; discussion 1099-1100.

173. Nomura T, Inamura T, Black KL. (1994) Intracarotid infusion of bradykinin selectively increases blood-tumor permeability in 9L and C6 brain tumors. *Brain Res* **659:** 62-66.

174. Hall WA, Doolittle ND, Daman M, et al. (2006) Osmotic blood-brain barrier disruption chemotherapy for diffuse pontine gliomas. *J Neurooncol* **77:** 279-284.

175. Boockvar JA, Tsiouris AJ, Hofstetter CP, et al. (2010) Safety and maximum tolerated dose of superselective intraarterial cerebral infusion of bevacizumab after osmotic blood-brain barrier disruption for recurrent malignant glioma. *J Neurosurg* **114:** 624-632.

176. Lhomme C, Joly F, Walker JL, et al. (2008) Phase III study of valspodar (PSC 833) combined with paclitaxel and carboplatin compared with paclitaxel and carboplatin alone in patients with stage IV or suboptimally debulked stage III epithelial ovarian cancer or primary peritoneal cancer. *J Clin Oncol* **26:** 2674-2682.

177. Carlson RW, O'Neill AM, Goldstein LJ, et al. (2006) A pilot phase II trial of valspodar modulation of multidrug resistance to paclitaxel in the treatment of metastatic carcinoma of the breast (E1195): a trial of the Eastern Cooperative Oncology Group. *Cancer Invest* **24:** 677-681.

178. Ruff P, Vorobiof DA, Jordaan JP, et al. (2009) A randomized, placebo-controlled, double-blind phase 2 study of docetaxel compared to docetaxel plus zosuquidar (LY335979) in women with metastatic or locally recurrent breast cancer who have received one prior chemotherapy regimen. *Cancer Chemother Pharmacol* **64:** 763-768.

179. Cripe LD, Uno H, Paietta EM, et al. (2010) Zosuquidar, a novel modulator of P-glycoprotein, does not improve the outcome of older patients with newly diagnosed acute myeloid leukemia: a randomized, placebo-controlled trial of the Eastern Cooperative Oncology Group 3999. *Blood* **116:** 4077-4085.

180. Kruijtzer CM, Beijnen JH, Rosing H, et al. (2002) Increased oral bioavailability of topotecan in combination with the breast cancer resistance protein and P-glycoprotein inhibitor GF120918. *J Clin Oncol* **20:** 2943-2950.

181. Planting AS, Sonneveld P, van der Gaast A, et al. (2005) A phase I and pharmacologic study of the MDR converter GF120918 in combination with doxorubicin in patients with advanced solid tumors. *Cancer Chemother Pharmacol* **55:** 91-99.

182. Sikic BI. (1997) Pharmacologic approaches to reversing multidrug resistance. *Semin Hematol* **34:** 40-47.

183. Reardon DA, Egorin MJ, Quinn JA, et al. (2005) Phase II study of imatinib mesylate plus hydroxyurea in adults with recurrent glioblastoma multiforme. *J Clin Oncol* **23:** 9359-9368.

184. Desjardins A, Quinn JA, Vredenburgh JJ, et al. (2007) Phase II study of imatinib mesylate and hydroxyurea for recurrent grade III malignant gliomas. *J Neurooncol* **83:** 53-60.

185. Lamar RE, Spigel DR, Burris HA, et al. (2009) Phase II trial of radiation therapy/temozolomide followed by temozolomide/sorafenib in the first-line treatment of glioblastoma multiforme (GBM). *ASCO Meeting Abstracts* **27:** 2018.

186. Grisanti S, Pedersini R, Ferrari VD, et al. (2010) Phase II study of sunitinib and irinotecan in patients with recurrent high-grade glioma (HGG). *ASCO Meeting Abstracts* **28:** e12537.

187. Sathornsumetee S, Rich JN, Vredenburgh JJ, et al. (2007) Phase I trial of imatinib mesylate, hydroxyurea and vatalanib for patients with recurrent glioblastoma multiforme (GBM). *2007 ASCO Annual Meeting Proceedings (Post-Meeting Edition)* **Vol 25:** 2027.

CHAPTER 1B

1. Altekruse, S. F., et al. (2010). SEER Cancer Statistics Review, 1975-2007, National Cancer Institute. Bethesda, MD,http://seer.cancer.gov/csr/1975_2007/, based on November 2009 SEER data submission, posted to the SEER web site, 2010.

2. CBTRUS (2010). CBTRUS Statistical Report: Primary Brain and Central Nervous System Tumors Diagnosed in the United States in 2004-2006. Source: Central Brain Tumor Registry of the United States, Hinsdale, IL. website: www.cbtrus.org.

3. Norden, A. D., Wen, P. Y. and Kesari, S. (2005). Brain metastases. *Curr Opin Neurol* **18**(6): 654-61.

4. Palmieri, D., et al. (2007). The biology of metastasis to a sanctuary site. *Clin Cancer Res* **13**(6): 1656-62.

5. Kamar, F. G. and Posner, J. B. (2010). Brain metastases. *Semin Neurol* **30**(3): 217-35.

6. Chamberlain, M. C. (2010). Anticancer therapies and CNS relapse: overcoming blood-brain and blood-cerebrospinal fluid barrier impermeability. *Expert Rev Neurother* **10**(4): 547-61.

7. Hawkins, B. T. and Davis, T. P. (2005). The blood-brain barrier/neurovascular unit in health and disease. *Pharmacol Rev* **57**(2): 173-85.

8. Pardridge, W. M. (1999). Blood-brain barrier biology and methodology. *J Neurovirol* **5**(6): 556-69.

9. Begley, D. J. (2004). ABC transporters and the blood-brain barrier. *Curr Pharm Des* **10**(12): 1295-312.

10. Loscher, W. and Potschka, H. (2005). Blood-brain barrier active efflux transporters: ATP-binding cassette gene family. *NeuroRx* **2**(1): 86-98.

11. Sun, H., et al. (2003). Drug efflux transporters in the CNS. *Adv Drug Deliv Rev* **55**(1): 83-105.

12. Agarwal, S., et al. (2010). Distribution of gefitinib to the brain is limited by P-glycoprotein (ABCB1) and breast cancer resistance protein (ABCG2)-mediated active efflux. *J Pharmacol Exp Ther* **334**(1): 147-55.

13. Agarwal, S., et al. (2011). Role of Breast Cancer Resistance Protein (ABCG2/BCRP) in the Distribution of Sorafenib to the Brain. *J Pharmacol Exp Ther*.

14. Chen, Y., et al. (2009). P-glycoprotein and breast cancer resistance protein influence brain distribution of dasatinib. *J Pharmacol Exp Ther* **330**(3): 956-63.

15. de Vries, N. A., et al. (2007). P-glycoprotein and breast cancer resistance protein: two dominant transporters working together in limiting the brain penetration of topotecan. *Clin Cancer Res* **13**(21): 6440-9.

16. Polli, J. W., et al. (2009). An unexpected synergist role of P-glycoprotein and breast cancer resistance protein on the central nervous system penetration of the tyrosine kinase inhibitor lapatinib (N-{3-chloro-4-[(3-fluorobenzyl)oxy]phenyl}-6-[5-({[2-(methylsulfonyl)ethy l]amino}methyl)-2-furyl]-4-quinazolinamine; GW572016). *Drug Metab Dispos* **37**(2): 439-42.

17. Juliano, R. L. and Ling, V. (1976). A surface glycoprotein modulating drug permeability in Chinese hamster ovary cell mutants. *Biochim Biophys Acta* **455**(1): 152-62.

18. Sharom, F. J. (1997). The P-glycoprotein efflux pump: how does it transport drugs? *J Membr Biol* **160**(3): 161-75.

19. Thiebaut, F., et al. (1989). Immunohistochemical localization in normal tissues of different epitopes in the multidrug transport protein P170: evidence for localization in brain capillaries and crossreactivity of one antibody with a muscle protein. *J Histochem Cytochem* **37**(2): 159-64.

20. Cordon-Cardo, C., et al. (1989). Multidrug-resistance gene (P-glycoprotein) is expressed by endothelial cells at blood-brain barrier sites. *Proc Natl Acad Sci U S A* **86**(2): 695-8.

21. Jette, L. and Beliveau, R. (1993). P-glycoprotein is strongly expressed in brain capillaries. *Adv Exp Med Biol* **331**: 121-5.

22. Jette, L., Tetu, B. and Beliveau, R. (1993). High levels of P-glycoprotein detected in isolated brain capillaries. *Biochim Biophys Acta* **1150**(2): 147-54.

23. Miller, D. S. (2002). Xenobiotic export pumps, endothelin signaling, and tubular nephrotoxicants--a case of molecular hijacking. *J Biochem Mol Toxicol* **16**(3): 121-7.

24. Nobmann, S., Bauer, B. and Fricker, G. (2001). Ivermectin excretion by isolated functionally intact brain endothelial capillaries. *Br J Pharmacol* **132**(3): 722-8.

25. Pekcec, A., et al. (2009). Age-dependent decline of blood-brain barrier P-glycoprotein expression in the canine brain. *Neurobiol Aging*.

26. Samoto, K., et al. (1994). P-glycoprotein expression in brain capillary endothelial cells after focal ischaemia in the rat. *Neurol Res* **16**(3): 217-23.

27. Schlachetzki, F. and Pardridge, W. M. (2003). P-glycoprotein and caveolin-1alpha in endothelium and astrocytes of primate brain. *Neuroreport* **14**(16): 2041-6.

28. Sugawara, I. (1990). Expression and functions of P-glycoprotein (mdr1 gene product) in normal and malignant tissues. *Acta Pathol Jpn* **40**(8): 545-53.

29. Tsai, C. E., et al. (2002). P-glycoprotein expression in mouse brain increases with maturation. *Biol Neonate* **81**(1): 58-64.

30. van der Valk, P., et al. (1990). Distribution of multi-drug resistance-associated P-glycoprotein in normal and neoplastic human tissues. Analysis with 3 monoclonal antibodies recognizing different epitopes of the P-glycoprotein molecule. *Ann Oncol* **1**(1): 56-64.

31. Schinkel, A. H., et al. (1994). Disruption of the mouse mdr1a P-glycoprotein gene leads to a deficiency in the blood-brain barrier and to increased sensitivity to drugs. *Cell* **77**(4): 491-502.

32. Tsuji, A. (1998). P-glycoprotein-mediated efflux transport of anticancer drugs at the blood-brain barrier. *Ther Drug Monit* **20**(5): 588-90.

33. Tsuruo, T., et al. (1981). Overcoming of vincristine resistance in P388 leukemia in vivo and in vitro through enhanced cytotoxicity of vincristine and vinblastine by verapamil. *Cancer Res* **41**(5): 1967-72.

34. Avendano, C. and Menendez, J. C. (2002). Inhibitors of multidrug resistance to antitumor agents (MDR). *Curr Med Chem* **9**(2): 159-93.

35. Pleban, K. and Ecker, G. F. (2005). Inhibitors of p-glycoprotein--lead identification and optimisation. *Mini Rev Med Chem* **5**(2): 153-63.

36. Fellner, S., et al. (2002). Transport of paclitaxel (Taxol) across the blood-brain barrier in vitro and in vivo. *J Clin Invest* **110**(9): 1309-18.

37. Hubensack, M., et al. (2008). Effect of the ABCB1 modulators elacridar and tariquidar on the distribution of paclitaxel in nude mice. *J Cancer Res Clin Oncol* **134**(5): 597-607.

38. Kemper, E. M., et al. (2004). The influence of the P-glycoprotein inhibitor zosuquidar trihydrochloride (LY335979) on the brain penetration of paclitaxel in mice. *Cancer Chemother Pharmacol* **53**(2): 173-8.

39. Kemper, E. M., et al. (2003). Increased penetration of paclitaxel into the brain by inhibition of P-Glycoprotein. *Clin Cancer Res* **9**(7): 2849-55.

40. Kemper, E. M., et al. (2004). Improved penetration of docetaxel into the brain by co-administration of inhibitors of P-glycoprotein. *Eur J Cancer* **40**(8): 1269-74.

41. Joo, K. M., et al. (2008). Oral paclitaxel chemotherapy for brain tumors: ideal combination treatment of paclitaxel and P-glycoprotein inhibitor. *Oncol Rep* **19**(1): 17-23.

42. Hartz, A. M., et al. (2004). Rapid regulation of P-glycoprotein at the blood-brain barrier by endothelin-1. *Mol Pharmacol* **66**(3): 387-94.

43. Hartz, A. M., et al. (2006). Rapid modulation of P-glycoprotein-mediated transport at the blood-brain barrier by tumor necrosis factor-alpha and lipopolysaccharide. *Mol Pharmacol* **69**(2): 462-70.

44. Rigor, R. R., Hawkins, B. T. and Miller, D. S. (2010). Activation of PKC isoform beta(I) at the blood-brain barrier rapidly decreases P-glycoprotein activity and enhances drug delivery to the brain. *J Cereb Blood Flow Metab* **30**(7): 1373-83.

45. Hawkins, B. T., Rigor, R. R. and Miller, D. S. (2010). Rapid loss of blood-brain barrier P-glycoprotein activity through transporter internalization demonstrated using a novel in situ proteolysis protection assay. *J Cereb Blood Flow Metab* **30**(9): 1593-7.

46. Doyle, L. A., et al. (1998). A multidrug resistance transporter from human MCF-7 breast cancer cells. *Proc Natl Acad Sci U S A* **95**(26): 15665-70.

47. Eisenblatter, T. and Galla, H. J. (2002). A new multidrug resistance protein at the blood-brain barrier. *Biochem Biophys Res Commun* **293**(4): 1273-8.

48. Hori, S., et al. (2004). Functional expression of rat ABCG2 on the luminal side of brain capillaries and its enhancement by astrocyte-derived soluble factor(s). *J Neurochem* **90**(3): 526-36.

49. Cooray, H. C., et al. (2002). Localisation of breast cancer resistance protein in microvessel endothelium of human brain. *Neuroreport* **13**(16): 2059-63.

50. Hartz, A. M., et al. (2010). 17-beta-Estradiol: a powerful modulator of blood-brain barrier BCRP activity. *J Cereb Blood Flow Metab* **30**(10): 1742-55.

51. Lee, G., et al. (2007). Expression of the ATP-binding cassette membrane transporter, ABCG2, in human and rodent brain microvessel endothelial and glial cell culture systems. *Pharm Res* **24**(7): 1262-74.

52. Warren, M. S., et al. (2009). Comparative gene expression profiles of ABC transporters in brain microvessel endothelial cells and brain in five species including human. *Pharmacol Res* **59**(6): 404-13.

53. Islam, M. O., et al. (2005). Functional expression of ABCG2 transporter in human neural stem/progenitor cells. *Neurosci Res* **52**(1): 75-82.

54. Zhou, S., et al. (2001). The ABC transporter Bcrp1/ABCG2 is expressed in a wide variety of stem cells and is a molecular determinant of the side-population phenotype. *Nat Med* **7**(9): 1028-34.

55. Krishnamurthy, P., et al. (2004). The stem cell marker Bcrp/ABCG2 enhances hypoxic cell survival through interactions with heme. *J Biol Chem* **279**(23): 24218-25.

56. Sakata, S., et al. (2010). ATP-binding cassette transporters in primary central nervous system lymphoma: decreased expression of MDR1 P-glycoprotein and breast cancer resistance protein in tumor capillary endothelial cells. *Oncol Rep* **25**(2): 333-9.

57. Bleau, A. M., et al. (2009). PTEN/PI3K/Akt pathway regulates the side population phenotype and ABCG2 activity in glioma tumor stem-like cells. *Cell Stem Cell* **4**(3): 226-35.

58. Bleau, A. M., Huse, J. T. and Holland, E. C. (2009). The ABCG2 resistance network of glioblastoma. *Cell Cycle* **8**(18): 2936-44.

59. Ginguene, C., et al. (2010). P-glycoprotein (ABCB1) and breast cancer resistance protein (ABCG2) localize in the microvessels forming the blood-tumor barrier in ependymomas. *Brain Pathol* **20**(5): 926-35.

60. Allen, J. D., et al. (1999). The mouse Bcrp1/Mxr/Abcp gene: amplification and overexpression in cell lines selected for resistance to topotecan, mitoxantrone, or doxorubicin. *Cancer Res* **59**(17): 4237-41.

61. Sarkadi, B., et al. (2004). ABCG2 -- a transporter for all seasons. *FEBS Lett* **567**(1): 116-20.

62. Mi, Y. J., et al. (2010). Apatinib (YN968D1) reverses multidrug resistance by inhibiting the efflux function of multiple ATP-binding cassette transporters. *Cancer Res* **70**(20): 7981-91.

63. Perry, J., et al. (2010). A synergistic interaction between lapatinib and chemotherapy agents in a panel of cell lines is due to the inhibition of the efflux pump BCRP. *Mol Cancer Ther* **9**(12): 3322-9.

64. Shukla, S., Sauna, Z. E. and Ambudkar, S. V. (2008). Evidence for the interaction of imatinib at the transport-substrate site(s) of the multidrug-resistance-linked ABC drug transporters ABCB1 (P-glycoprotein) and ABCG2. *Leukemia* **22**(2): 445-7.

65. Yang, J. J., et al. (2010). P-glycoprotein and breast cancer resistance protein affect disposition of tandutinib, a tyrosine kinase inhibitor. *Drug Metab Lett* **4**(4): 201-12.

66. Han, B. and Zhang, J. T. (2004). Multidrug resistance in cancer chemotherapy and xenobiotic protection mediated by the half ATP-binding cassette transporter ABCG2. *Curr Med Chem Anticancer Agents* **4**(1): 31-42.

67. Schellens, J. H., et al. (2000). Transport of topoisomerase I inhibitors by the breast cancer resistance protein. Potential clinical implications. *Ann N Y Acad Sci* **922**: 188-94.

68. Rabindran, S. K., et al. (2000). Fumitremorgin C reverses multidrug resistance in cells transfected with the breast cancer resistance protein. *Cancer Res* **60**(1): 47-50.

69. Allen, J. D., et al. (2002). Potent and specific inhibition of the breast cancer resistance protein multidrug transporter in vitro and in mouse intestine by a novel analogue of fumitremorgin C. *Mol Cancer Ther* **1**(6): 417-25.

70. Bihorel, S., et al. (2007). Influence of breast cancer resistance protein (Abcg2) and p-glycoprotein (Abcb1a) on the transport of imatinib mesylate (Gleevec) across the mouse blood-brain barrier. *J Neurochem* **102**(6): 1749-57.

71. Breedveld, P., et al. (2005). The effect of Bcrp1 (Abcg2) on the in vivo pharmacokinetics and brain penetration of imatinib mesylate (Gleevec): implications for the use of breast cancer resistance protein and P-glycoprotein inhibitors to enable the brain penetration of imatinib in patients. *Cancer Res* **65**(7): 2577-82.

72. Breedveld, P., Beijnen, J. H. and Schellens, J. H. (2006). Use of P-glycoprotein and BCRP inhibitors to improve oral bioavailability and CNS penetration of anticancer drugs. *Trends Pharmacol Sci* **27**(1): 17-24.

73. Imai, Y., et al. (2002). Estrone and 17beta-estradiol reverse breast cancer resistance protein-mediated multidrug resistance. *Jpn J Cancer Res* **93**(3): 231-5.

74. Ee, P. L., et al. (2004). Identification of a novel estrogen response element in the breast cancer resistance protein (ABCG2) gene. *Cancer Res* **64**(4): 1247-51.

75. Mogi, M., et al. (2003). Akt signaling regulates side population cell phenotype via Bcrp1 translocation. *J Biol Chem* **278**(40): 39068-75.

76. Takada, T., et al. (2005). Regulation of the cell surface expression of human BCRP/ABCG2 by the phosphorylation state of Akt in polarized cells. *Drug Metab Dispos* **33**(7): 905-9.

77. Hartz, A. M., et al. (2010). Estrogen receptor beta signaling through phosphatase and tensin homolog/phosphoinositide 3-kinase/Akt/glycogen synthase kinase 3 down-regulates blood-brain barrier breast cancer resistance protein. *J Pharmacol Exp Ther* **334**(2): 467-76.

78. Lee, Y. J., et al. (2005). Investigation of efflux transport of dehydroepiandrosterone sulfate and mitoxantrone at the mouse blood-brain barrier: a minor role of breast cancer resistance protein. *J Pharmacol Exp Ther* **312**(1): 44-52.

79. Pan, G., Giri, N. and Elmquist, W. F. (2007). Abcg2/Bcrp1 mediates the polarized transport of antiretroviral nucleosides abacavir and zidovudine. *Drug Metab Dispos* **35**(7): 1165-73.

80. Giri, N., et al. (2008). Investigation of the role of breast cancer resistance protein (Bcrp/Abcg2) on pharmacokinetics and central nervous system penetration of abacavir and zidovudine in the mouse. *Drug Metab Dispos* **36**(8): 1476-84.

81. Zhao, R., et al. (2009). Breast cancer resistance protein interacts with various compounds in vitro, but plays a minor role in substrate efflux at the blood-brain barrier. *Drug Metab Dispos* **37**(6): 1251-8.

82. Cisternino, S., et al. (2004). Expression, up-regulation, and transport activity of the multidrug-resistance protein Abcg2 at the mouse blood-brain barrier. *Cancer Res* **64**(9): 3296-301.

83. Enokizono, J., et al. (2008). Quantitative investigation of the role of breast cancer resistance protein (Bcrp/Abcg2) in limiting brain and testis penetration of xenobiotic compounds. *Drug Metab Dispos* **36**(6): 995-1002.

84. Jonker, J. W., et al. (2005). Contribution of the ABC transporters Bcrp1 and Mdr1a/1b to the side population phenotype in mammary gland and bone marrow of mice. *Stem Cells* **23**(8): 1059-65.

85. de Vries, N. A., et al. (2010). Restricted brain penetration of the tyrosine kinase inhibitor erlotinib due to the drug transporters P-gp and BCRP. *Invest New Drugs*.

86. Kodaira, H., et al. (2010). Kinetic analysis of the cooperation of P-glycoprotein (P-gp/Abcb1) and breast cancer resistance protein (Bcrp/Abcg2) in limiting the brain and testis penetration of erlotinib, flavopiridol, and mitoxantrone. *J Pharmacol Exp Ther* **333**(3): 788-96.

87. Kawamura, K., et al. (2010). Evaluation of Limiting Brain Penetration Related to P-glycoprotein and Breast Cancer Resistance Protein Using [¹¹C]GF120918 by PET in Mice. *Molecular Imaging and Biology* **13**(1): 152-160.

88. Kamiie, J., et al. (2008). Quantitative atlas of membrane transporter proteins: development and application of a highly sensitive simultaneous LC/MS/MS method combined with novel in-silico peptide selection criteria. *Pharm Res* **25**(6): 1469-83.

89. Hyafil, F., et al. (1993). In vitro and in vivo reversal of multidrug resistance by GF120918, an acridonecarboxamide derivative. *Cancer Res* **53**(19): 4595-602.

90. Cutler, L., et al. (2006). Development of a P-glycoprotein knockout model in rodents to define species differences in its functional effect at the blood-brain barrier. *J Pharm Sci* **95**(9): 1944-53.

91. Jin, L., et al. (2010). Impact of p-glycoprotein inhibition and lipopolysaccharide administration on blood-brain barrier transport of colistin in mice. *Antimicrob Agents Chemother* **55**(2): 502-7.

92. Oostendorp, R. L., et al. (2009). The effect of P-gp (Mdr1a/1b), BCRP (Bcrp1) and P-gp/BCRP inhibitors on the in vivo absorption, distribution, metabolism and excretion of imatinib. *Invest New Drugs* **27**(1): 31-40.

93. Polli, J. W., et al. (1999). Role of P-glycoprotein on the CNS disposition of amprenavir (141W94), an HIV protease inhibitor. *Pharm Res* **16**(8): 1206-12.

94. Shi, Z., et al. (2007). Erlotinib (Tarceva, OSI-774) antagonizes ATP-binding cassette subfamily B member 1 and ATP-binding cassette subfamily G member 2-mediated drug resistance. *Cancer Res* **67**(22): 11012-20.

95. Leggas, M., et al. (2006). Gefitinib modulates the function of multiple ATP-binding cassette transporters in vivo. *Cancer Res* **66**(9): 4802-7.

96. Dai, C. L., et al. (2008). Lapatinib (Tykerb, GW572016) reverses multidrug resistance in cancer cells by inhibiting the activity of ATP-binding cassette subfamily B member 1 and G member 2. *Cancer Res* **68**(19): 7905-14.

97. Dai, C. L., et al. (2009). Sensitization of ABCB1 overexpressing cells to chemotherapeutic agents by FG020326 via binding to ABCB1 and inhibiting its function. *Biochem Pharmacol* **78**(4): 355-64.

98. Zhuang, Y., et al. (2006). Topotecan central nervous system penetration is altered by a tyrosine kinase inhibitor. *Cancer Res* **66**(23): 11305-13.

99. Carcaboso, A. M., et al. (2010). Tyrosine kinase inhibitor gefitinib enhances topotecan penetration of gliomas. *Cancer Res* **70**(11): 4499-508.

100. Furman, W. L., et al. (2009). Tyrosine kinase inhibitor enhances the bioavailability of oral irinotecan in pediatric patients with refractory solid tumors. *J Clin Oncol* **27**(27): 4599-604.

101. Nakanishi, T., et al. (2006). Complex interaction of BCRP/ABCG2 and imatinib in BCR-ABL-expressing cells: BCRP-mediated resistance to imatinib is attenuated by imatinib-induced reduction of BCRP expression. *Blood* **108**(2): 678-84.

CHAPTER II

1. Wen PY, Kesari S. (2008) Malignant gliomas in adults. *N Engl J Med* **359:** 492-507.

2. CBTRUS. (2008) CBTRUS 2008 statistical report: Primary Brain Tumors in the United States, 2000-2004, Central Brain Tumor Registry of the United States.

3. Davis FG, Kupelian V, Freels S, McCarthy B, Surawicz T. (2001) Prevalence estimates for primary brain tumors in the United States by behavior and major histology groups. *Neuro Oncol* **3:** 152-158.

4. Brandes AA, Franceschi E, Tosoni A, Hegi ME, Stupp R. (2008) Epidermal growth factor receptor inhibitors in neuro-oncology: hopes and disappointments. *Clin Cancer Res* **14:** 957-960.

5. Omuro AM, Faivre S, Raymond E. (2007) Lessons learned in the development of targeted therapy for malignant gliomas. *Mol Cancer Ther* **6:** 1909-1919.

6. Arteaga CL, Johnson DH. (2001) Tyrosine kinase inhibitors-ZD1839 (Iressa). *Curr Opin Oncol* **13:** 491-498.

7. Ciardiello F, Tortora G. (2001) A novel approach in the treatment of cancer: targeting the epidermal growth factor receptor. *Clin Cancer Res* **7:** 2958-2970.

8. Culy CR, Faulds D. (2002) Gefitinib. *Drugs* **62:** 2237-2248; discussion 2249-2250.

9. Giaccone G, Herbst RS, Manegold C, et al. (2004) Gefitinib in combination with gemcitabine and cisplatin in advanced non-small-cell lung cancer: a phase III trial--INTACT 1. *J Clin Oncol* **22:** 777-784.

10. Herbst RS, Giaccone G, Schiller JH, et al. (2004) Gefitinib in combination with paclitaxel and carboplatin in advanced non-small-cell lung cancer: a phase III trial--INTACT 2. *J Clin Oncol* **22:** 785-794.

11. Franceschi E, Cavallo G, Lonardi S, et al. (2007) Gefitinib in patients with progressive high-grade gliomas: a multicentre phase II study by Gruppo Italiano Cooperativo di Neuro-Oncologia (GICNO). *Br J Cancer* **96:** 1047-1051.

12. Rich JN, Reardon DA, Peery T, et al. (2004) Phase II trial of gefitinib in recurrent glioblastoma. *J Clin Oncol* **22:** 133-142.

13. Mellinghoff IK, Cloughesy TF, Mischel PS. (2007) PTEN-mediated resistance to epidermal growth factor receptor kinase inhibitors. *Clin Cancer Res* **13:** 378-381.

14. Mellinghoff IK, Wang MY, Vivanco I, et al. (2005) Molecular determinants of the response of glioblastomas to EGFR kinase inhibitors. *N Engl J Med* **353:** 2012-2024.

15. Sarkaria JN, Yang L, Grogan PT, et al. (2007) Identification of molecular characteristics correlated with glioblastoma sensitivity to EGFR kinase inhibition through use of an intracranial xenograft test panel. *Mol Cancer Ther* **6:** 1167-1174.

16. Stommel JM, Kimmelman AC, Ying H, et al. (2007) Coactivation of receptor tyrosine kinases affects the response of tumor cells to targeted therapies. *Science* **318:** 287-290.

17. Kuratsu J, Itoyama Y, Uemura S, Ushio Y. (1989) [Regrowth patterns of glioma--cases of glioma regrew away from the original tumor]. *Gan No Rinsho* **35:** 1255-1260.

18. Silbergeld DL, Chicoine MR. (1997) Isolation and characterization of human malignant glioma cells from histologically normal brain. *J Neurosurg* **86:** 525-531.

19. Gottesman MM, Fojo T, Bates SE. (2002) Multidrug resistance in cancer: role of ATP-dependent transporters. *Nat Rev Cancer* **2:** 48-58.

20. Loscher W, Potschka H. (2005) Role of drug efflux transporters in the brain for drug disposition and treatment of brain diseases. *Prog Neurobiol* **76:** 22-76.

21. Fletcher JI, Haber M, Henderson MJ, Norris MD. (2010) ABC transporters in cancer: more than just drug efflux pumps. *Nat Rev Cancer* **10:** 147-156.

22. Elkind NB, Szentpetery Z, Apati A, et al. (2005) Multidrug transporter ABCG2 prevents tumor cell death induced by the epidermal growth factor receptor inhibitor Iressa (ZD1839, Gefitinib). *Cancer Res* **65:** 1770-1777.

23. Leggas M, Panetta JC, Zhuang Y, et al. (2006) Gefitinib modulates the function of multiple ATP-binding cassette transporters in vivo. *Cancer Res* **66:** 4802-4807.

24. Dantzig AH, Shepard RL, Law KL, et al. (1999) Selectivity of the multidrug resistance modulator, LY335979, for P-glycoprotein and effect on cytochrome P-450 activities. *J Pharmacol Exp Ther* **290:** 854-862.

25. Allen JD, van Loevezijn A, Lakhai JM, et al. (2002) Potent and specific inhibition of the breast cancer resistance protein multidrug transporter in vitro and in mouse intestine by a novel analogue of fumitremorgin C. *Molecular Cancer Therapeutics* **1:** 417-425.

26. Wang S, Guo P, Wang X, Zhou Q, Gallo JM. (2008) Preclinical pharmacokinetic/pharmacodynamic models of gefitinib and the design of equivalent dosing regimens in EGFR wild-type and mutant tumor models. *Mol Cancer Ther* **7:** 407-417.

27. Mukasa A, Wykosky J, Ligon KL, Chin L, Cavenee WK, Furnari F. (2010) Mutant EGFR is required for maintenance of glioma growth in vivo, and its ablation leads to escape from receptor dependence. *Proc Natl Acad Sci U S A* **107:** 2616-2621.

28. Lieberman FS CT, Fine H, Kuhn J, Lamborn L, Malkin M, Robbins HI, Yung WA, Wen P and Prados M (2004) NABTC phase I–II study of ZD-1839 for recurrent malignant gliomas and unresectable meningiomas. *Journal of Clinical Oncology, 2004 ASCO Annual Meeting Proceedings (Post-Meeting Edition)* **22:** abs 1510.

29. Dai H, Marbach P, Lemaire M, Hayes M, Elmquist WF. (2003) Distribution of STI-571 to the brain is limited by P-glycoprotein-mediated efflux. *J Pharmacol Exp Ther* **304:** 1085-1092.

30. Chen Y, Agarwal S, Shaik NM, Chen C, Yang Z, Elmquist WF. (2009) P-glycoprotein and Breast Cancer Resistance Protein Influence Brain Distribution of Dasatinib. *J Pharmacol Exp Ther*.

31. Lagas JS, van Waterschoot RA, van Tilburg VA, et al. (2009) Brain accumulation of dasatinib is restricted by P-glycoprotein (ABCB1) and breast cancer resistance protein (ABCG2) and can be enhanced by elacridar treatment. *Clin Cancer Res* **15:** 2344-2351.

32. Polli JW, Olson KL, Chism JP, et al. (2009) An unexpected synergist role of P-glycoprotein and breast cancer resistance protein on the central nervous system penetration of the tyrosine kinase inhibitor lapatinib (N-{3-chloro-4-[(3-fluorobenzyl)oxy]phenyl}-6-[5-({[2-(methylsulfonyl)ethy l]amino}methyl)-2-furyl]-4-quinazolinamine; GW572016). *Drug Metab Dispos* **37:** 439-442.

33. Kamath AV, Wang J, Lee FY, Marathe PH. (2008) Preclinical pharmacokinetics and in vitro metabolism of dasatinib (BMS-354825): a potent oral multi-targeted kinase inhibitor against SRC and BCR-ABL. *Cancer Chemother Pharmacol* **61:** 365-376.

34. Lagas JS, van Waterschoot RA, Sparidans RW, Wagenaar E, Beijnen JH, Schinkel AH. (2010) Breast cancer resistance protein and P-glycoprotein limit sorafenib brain accumulation. *Mol Cancer Ther* **9:** 319-326.

35. Oostendorp RL, Buckle T, Beijnen JH, van Tellingen O, Schellens JH. (2009) The effect of P-gp (Mdr1a/1b), BCRP (Bcrp1) and P-gp/BCRP inhibitors on the in vivo absorption, distribution, metabolism and excretion of imatinib. *Invest New Drugs* **27:** 31-40.

36. Lee G, Babakhanian K, Ramaswamy M, Prat A, Wosik K, Bendayan R. (2007) Expression of the ATP-binding cassette membrane transporter, ABCG2, in human and rodent brain microvessel endothelial and glial cell culture systems. *Pharm Res* **24:** 1262-1274.

37. Hofer S, Frei K. (2007) Gefitinib concentrations in human glioblastoma tissue. *J Neurooncol* **82:** 175-176.

38. McKillop D, Partridge EA, Kemp JV, et al. (2005) Tumor penetration of gefitinib (Iressa), an epidermal growth factor receptor tyrosine kinase inhibitor. *Mol Cancer Ther* **4:** 641-649.

39. Blakeley JO, Olson J, Grossman SA, He X, Weingart J, Supko JG. (2009) Effect of blood brain barrier permeability in recurrent high grade gliomas on the intratumoral pharmacokinetics of methotrexate: a microdialysis study. *J Neurooncol* **91:** 51-58.

40. Fine RL, Chen J, Balmaceda C, et al. (2006) Randomized study of paclitaxel and tamoxifen deposition into human brain tumors: implications for the treatment of metastatic brain tumors. *Clin Cancer Res* **12:** 5770-5776.

CHAPTER III

1. Begley DJ. (2004) ABC transporters and the blood-brain barrier. *Curr Pharm Des* **10:** 1295-1312.

2. Loscher W, Potschka H. (2005) Blood-brain barrier active efflux transporters: ATP-binding cassette gene family. *NeuroRx* **2:** 86-98.

3. Sun H, Dai H, Shaik N, Elmquist WF. (2003) Drug efflux transporters in the CNS. *Adv Drug Deliv Rev* **55:** 83-105.

4. Litman T, Brangi M, Hudson E, et al. (2000) The multidrug-resistant phenotype associated with overexpression of the new ABC half-transporter, MXR (ABCG2). *J Cell Sci* **113 (Pt 11):** 2011-2021.

5. Agarwal S, Sane R, Gallardo JL, Ohlfest JR, Elmquist WF. (2010) Distribution of gefitinib to the brain is limited by P-glycoprotein (ABCB1) and breast cancer resistance protein (ABCG2)-mediated active efflux. *J Pharmacol Exp Ther* **334:** 147-155.

6. Chen Y, Agarwal S, Shaik NM, Chen C, Yang Z, Elmquist WF. (2009) P-glycoprotein and breast cancer resistance protein influence brain distribution of dasatinib. *J Pharmacol Exp Ther* **330:** 956-963.

7. de Vries NA, Zhao J, Kroon E, Buckle T, Beijnen JH, van Tellingen O. (2007) P-glycoprotein and breast cancer resistance protein: two dominant transporters working together in limiting the brain penetration of topotecan. *Clin Cancer Res* **13:** 6440-6449.

8. Polli JW, Humphreys JE, Harmon KA, et al. (2008) The role of efflux and uptake transporters in [N-{3-chloro-4-[(3-fluorobenzyl)oxy]phenyl}-6-[5-({[2-(methylsulfonyl)ethy l]amino}methyl)-2-furyl]-4-quinazolinamine (GW572016, lapatinib) disposition and drug interactions. *Drug Metab Dispos* **36:** 695-701.

9. Zhao R, Raub TJ, Sawada GA, et al. (2009) Breast cancer resistance protein interacts with various compounds in vitro, but plays a minor role in substrate efflux at the blood-brain barrier. *Drug Metab Dispos* **37:** 1251-1258.

10. Lee YJ, Kusuhara H, Jonker JW, Schinkel AH, Sugiyama Y. (2005) Investigation of efflux transport of dehydroepiandrosterone sulfate and mitoxantrone at the mouse

blood-brain barrier: a minor role of breast cancer resistance protein. *J Pharmacol Exp Ther* **312:** 44-52.

11. Zwick E, Bange J, Ullrich A. (2001) Receptor tyrosine kinase signalling as a target for cancer intervention strategies. *Endocr Relat Cancer* **8:** 161-173.

12. Polli JW, Olson KL, Chism JP, et al. (2009) An unexpected synergist role of P-glycoprotein and breast cancer resistance protein on the central nervous system penetration of the tyrosine kinase inhibitor lapatinib (N-{3-chloro-4-[(3-fluorobenzyl)oxy]phenyl}-6-[5-({[2-(methylsulfonyl)ethy l]amino}methyl)-2-furyl]-4-quinazolinamine; GW572016). *Drug Metab Dispos* **37:** 439-442.

13. Shi Z, Peng XX, Kim IW, et al. (2007) Erlotinib (Tarceva, OSI-774) antagonizes ATP-binding cassette subfamily B member 1 and ATP-binding cassette subfamily G member 2-mediated drug resistance. *Cancer Res* **67:** 11012-11020.

14. Shukla S, Robey RW, Bates SE, Ambudkar SV. (2009) Sunitinib (Sutent, SU11248), a small-molecule receptor tyrosine kinase inhibitor, blocks function of the ATP-binding cassette (ABC) transporters P-glycoprotein (ABCB1) and ABCG2. *Drug Metab Dispos* **37:** 359-365.

15. Hu S, Chen Z, Franke R, et al. (2009) Interaction of the multikinase inhibitors sorafenib and sunitinib with solute carriers and ATP-binding cassette transporters. *Clin Cancer Res* **15:** 6062-6069.

16. Dai H, Marbach P, Lemaire M, Hayes M, Elmquist WF. (2003) Distribution of STI-571 to the brain is limited by P-glycoprotein-mediated efflux. *J Pharmacol Exp Ther* **304:** 1085-1092.

17. Wilhelm S, Carter C, Lynch M, et al. (2006) Discovery and development of sorafenib: a multikinase inhibitor for treating cancer. *Nat Rev Drug Discov* **5:** 835-844.

18. Bellmunt J, Eisen T, Fishman M, Quinn D. (2006) Experience with sorafenib and adverse event management. *Crit Rev Oncol Hematol*.

19. Wilhelm SM, Adnane L, Newell P, Villanueva A, Llovet JM, Lynch M. (2008) Preclinical overview of sorafenib, a multikinase inhibitor that targets both Raf and VEGF and PDGF receptor tyrosine kinase signaling. *Mol Cancer Ther* **7:** 3129-3140.

20. Yang F, Brown C, Buettner R, et al. (2010) Sorafenib induces growth arrest and apoptosis of human glioblastoma cells through the dephosphorylation of signal transducers and activators of transcription 3. *Mol Cancer Ther* **9:** 953-962.

21. Siegelin MD, Raskett CM, Gilbert CA, Ross AH, Altieri DC. (2010) Sorafenib exerts anti-glioma activity in vitro and in vivo. *Neurosci Lett* **478:** 165-170.

22. Scott BJ, Quant EC, McNamara MB, Ryg PA, Batchelor TT, Wen PY. (2010) Bevacizumab salvage therapy following progression in high-grade glioma patients treated with VEGF receptor tyrosine kinase inhibitors. *Neuro Oncol* **12:** 603-607.

23. Nabors LB, Rosenfeld M, Chamberlain M, et al. (2007) A phase I trial of sorafenib (BAY 43-9006) for patients with recurrent or progressive malignant glioma (NABTT 0401). *J Clin Oncol (Meeting Abstracts)* **25:** 2058.

24. Wen PY, Cloughesy T, Kuhn J, et al. (2009) Phase I/II study of sorafenib and temsirolimus for patients with recurrent glioblastoma (GBM) (NABTC 05-02). *J Clin Oncol (Meeting Abstracts)* **27:** 2006-.

25. Kuratsu J, Itoyama Y, Uemura S, Ushio Y. (1989) [Regrowth patterns of glioma--cases of glioma regrew away from the original tumor]. *Gan No Rinsho* **35:** 1255-1260.

26. Silbergeld DL, Chicoine MR. (1997) Isolation and characterization of human malignant glioma cells from histologically normal brain. *J Neurosurg* **86:** 525-531.

27. Blakeley JO, Olson J, Grossman SA, He X, Weingart J, Supko JG. (2009) Effect of blood brain barrier permeability in recurrent high grade gliomas on the intratumoral pharmacokinetics of methotrexate: a microdialysis study. *J Neurooncol* **91:** 51-58.

28. Lagas JS, van Waterschoot RA, Sparidans RW, Wagenaar E, Beijnen JH, Schinkel AH. (2010) Breast cancer resistance protein and P-glycoprotein limit sorafenib brain accumulation. *Mol Cancer Ther* **9:** 319-326.

29. Gnoth MJ, Sandmann S, Engel K, Radtke M. (2010) In vitro to in vivo comparison of the substrate characteristics of Sorafenib tosylate towards P-glycoprotein. *Drug Metab Dispos* **38:** 1341-1346.

30. Dantzig AH, Shepard RL, Law KL, et al. (1999) Selectivity of the multidrug resistance modulator, LY335979, for P-glycoprotein and effect on cytochrome P-450 activities. *J Pharmacol Exp Ther* **290:** 854-862.

31. Allen JD, van Loevezijn A, Lakhai JM, et al. (2002) Potent and specific inhibition of the breast cancer resistance protein multidrug transporter in vitro and in mouse intestine by a novel analogue of fumitremorgin C. *Mol Cancer Ther* **1:** 417-425.

32. Bailer AJ. (1988) Testing for the equality of area under the curves when using destructive measurement techniques. *J Pharmacokinet Biopharm* **16:** 303-309.

33. Nedelman JR, Jia X. (1998) An extension of Satterthwaite's approximation applied to pharmacokinetics. *J Biopharm Stat* **8:** 317-328.

34. Wen PY, Kesari S. (2008) Malignant gliomas in adults. *N Engl J Med* **359:** 492-507.

35. Duran I, HottÃ© SJ, Hirte H, et al. (2007) Phase I Targeted Combination Trial of Sorafenib and Erlotinib in Patients with Advanced Solid Tumors. *Clinical Cancer Research* **13:** 4849-4857.

36. Richly H, Henning BF, Kupsch P, et al. (2006) Results of a Phase I trial of sorafenib (BAY 43-9006) in combination with doxorubicin in patients with refractory solid tumors. *Annals of Oncology* **17:** 866-873.

37. Giri N, Agarwal S, Shaik N, Pan G, Chen Y, Elmquist WF. (2009) Substrate-dependent breast cancer resistance protein (Bcrp1/Abcg2)-mediated interactions: consideration of multiple binding sites in in vitro assay design. *Drug Metab Dispos* **37:** 560-570.

38. Lagas JS, van Waterschoot RA, van Tilburg VA, et al. (2009) Brain accumulation of dasatinib is restricted by P-glycoprotein (ABCB1) and breast cancer resistance protein (ABCG2) and can be enhanced by elacridar treatment. *Clin Cancer Res* **15:** 2344-2351.

39. Kodaira H, Kusuhara H, Ushiki J, Fuse E, Sugiyama Y. (2010) Kinetic analysis of the cooperation of P-glycoprotein (P-gp/Abcb1) and breast cancer resistance protein (Bcrp/Abcg2) in limiting the brain and testis penetration of erlotinib, flavopiridol, and mitoxantrone. *J Pharmacol Exp Ther* **333:** 788-796.

40. Breedveld P, Pluim D, Cipriani G, et al. (2005) The Effect of Bcrp1 (Abcg2) on the In vivo Pharmacokinetics and Brain Penetration of Imatinib Mesylate (Gleevec): Implications for the Use of Breast Cancer Resistance Protein and P-Glycoprotein Inhibitors to Enable the Brain Penetration of Imatinib in Patients. *Cancer Research* **65:** 2577-2582.

41. Warren MS, Zerangue N, Woodford K, et al. (2009) Comparative gene expression profiles of ABC transporters in brain microvessel endothelial cells and brain in five species including human. *Pharmacol Res* **59:** 404-413.

42. Kamiie J, Ohtsuki S, Iwase R, et al. (2008) Quantitative atlas of membrane transporter proteins: development and application of a highly sensitive simultaneous LC/MS/MS method combined with novel in-silico peptide selection criteria. *Pharm Res* **25:** 1469-1483.

43. Enokizono J, Kusuhara H, Ose A, Schinkel AH, Sugiyama Y. (2008) Quantitative investigation of the role of breast cancer resistance protein (Bcrp/Abcg2) in limiting brain and testis penetration of xenobiotic compounds. *Drug Metab Dispos* **36:** 995-1002.

CHAPTER IV

1. Neuwelt, E., et al. (2008). Strategies to advance translational research into brain barriers. *Lancet Neurol* **7**(1): 84-96.

2. Neuwelt, E. A., et al. (2011). Engaging neuroscience to advance translational research in brain barrier biology. *Nat Rev Neurosci* **12**(3): 169-82.

3. Schinkel, A. H. and Jonker, J. W. (2003). Mammalian drug efflux transporters of the ATP binding cassette (ABC) family: an overview. *Adv Drug Deliv Rev* **55**(1): 3-29.

4. Loscher, W. and Potschka, H. (2005). Blood-brain barrier active efflux transporters: ATP-binding cassette gene family. *NeuroRx* **2**(1): 86-98.

5. Cordon-Cardo, C., et al. (1989). Multidrug-resistance gene (P-glycoprotein) is expressed by endothelial cells at blood-brain barrier sites. *Proc Natl Acad Sci U S A* **86**(2): 695-8.

6. Deeken, J. F. and Loscher, W. (2007). The blood-brain barrier and cancer: transporters, treatment, and Trojan horses. *Clin Cancer Res* **13**(6): 1663-74.

7. Cooray, H. C., et al. (2002). Localisation of breast cancer resistance protein in microvessel endothelium of human brain. *Neuroreport* **13**(16): 2059-63.

8. Agarwal, S., et al. (2011). The role of the breast cancer resistance protein (ABCG2) in the distribution of sorafenib to the brain. *J Pharmacol Exp Ther* **336**(1): 223-33.

9. Breedveld, P., et al. (2005). The Effect of Bcrp1 (Abcg2) on the In vivo Pharmacokinetics and Brain Penetration of Imatinib Mesylate (Gleevec): Implications for the Use of Breast Cancer Resistance Protein and P-Glycoprotein Inhibitors to Enable the Brain Penetration of Imatinib in Patients. *Cancer Research* **65**(7): 2577-2582.

10. Enokizono, J., et al. (2008). Quantitative investigation of the role of breast cancer resistance protein (Bcrp/Abcg2) in limiting brain and testis penetration of xenobiotic compounds. *Drug Metab Dispos* **36**(6): 995-1002.

11. de Vries, N. A., et al. (2007). P-glycoprotein and breast cancer resistance protein: two dominant transporters working together in limiting the brain penetration of topotecan. *Clin Cancer Res* **13**(21): 6440-9.

12. Polli, J. W., et al. (2009). An unexpected synergist role of P-glycoprotein and breast cancer resistance protein on the central nervous system penetration of the tyrosine kinase inhibitor lapatinib (N-{3-chloro-4-[(3-fluorobenzyl)oxy]phenyl}-6-[5-({[2-(methylsulfonyl)ethy l]amino}methyl)-2-furyl]-4-quinazolinamine; GW572016). *Drug Metab Dispos* **37**(2): 439-42.

13. Chen, Y., et al. (2009). P-glycoprotein and breast cancer resistance protein influence brain distribution of dasatinib. *J Pharmacol Exp Ther* **330**(3): 956-63.

14. Agarwal, S., et al. (2010). Distribution of gefitinib to the brain is limited by P-glycoprotein (ABCB1) and breast cancer resistance protein (ABCG2)-mediated active efflux. *J Pharmacol Exp Ther* **334**(1): 147-55.

15. de Vries, N. A., et al. (2010). Restricted brain penetration of the tyrosine kinase inhibitor erlotinib due to the drug transporters P-gp and BCRP. *Invest New Drugs*.

16. Kodaira, H., et al. (2010). Kinetic analysis of the cooperation of P-glycoprotein (P-gp/Abcb1) and breast cancer resistance protein (Bcrp/Abcg2) in limiting the brain and testis penetration of erlotinib, flavopiridol, and mitoxantrone. *J Pharmacol Exp Ther* **333**(3): 788-96.

17. Yang, J. J., et al. (2010). P-glycoprotein and breast cancer resistance protein affect disposition of tandutinib, a tyrosine kinase inhibitor. *Drug Metab Lett* **4**(4): 201-12.

18. Kakee, A., Terasaki, T. and Sugiyama, Y. (1996). Brain efflux index as a novel method of analyzing efflux transport at the blood-brain barrier. *J Pharmacol Exp Ther* **277**(3): 1550-9.

19. Friden, M., et al. (2009). Development of a high-throughput brain slice method for studying drug distribution in the central nervous system. *Drug Metab Dispos* **37**(6): 1226-33.

20. Hartz, A. M., et al. (2010). 17-beta-Estradiol: a powerful modulator of blood-brain barrier BCRP activity. *J Cereb Blood Flow Metab* **30**(10): 1742-55.

21. Cisternino, S., et al. (2004). Expression, up-regulation, and transport activity of the multidrug-resistance protein Abcg2 at the mouse blood-brain barrier. *Cancer Res* **64**(9): 3296-301.

22. Tanaka, Y., et al. (2005). Tissue distribution and hormonal regulation of the breast cancer resistance protein (Bcrp/Abcg2) in rats and mice. *Biochem Biophys Res Commun*

326(1): 181-7.

23. Lee, Y. J., et al. (2005). Investigation of efflux transport of dehydroepiandrosterone sulfate and mitoxantrone at the mouse blood-brain barrier: a minor role of breast cancer resistance protein. *J Pharmacol Exp Ther* **312**(1): 44-52.

24. Pan, G., Giri, N. and Elmquist, W. F. (2007). Abcg2/Bcrp1 mediates the polarized transport of antiretroviral nucleosides abacavir and zidovudine. *Drug Metab Dispos* **35**(7): 1165-73.

25. Giri, N., et al. (2008). Investigation of the role of breast cancer resistance protein (Bcrp/Abcg2) on pharmacokinetics and central nervous system penetration of abacavir and zidovudine in the mouse. *Drug Metab Dispos* **36**(8): 1476-84.

26. Zhao, R., et al. (2009). Breast cancer resistance protein interacts with various compounds in vitro, but plays a minor role in substrate efflux at the blood-brain barrier. *Drug Metab Dispos* **37**(6): 1251-8.

27. Kamiie, J., et al. (2008). Quantitative atlas of membrane transporter proteins: development and application of a highly sensitive simultaneous LC/MS/MS method combined with novel in-silico peptide selection criteria. *Pharm Res* **25**(6): 1469-83.

28. Agarwal, S., et al. (2010). Role of Breast Cancer Resistance Protein (ABCG2/BCRP) in the Distribution of Sorafenib to the Brain. *J Pharmacol Exp Ther*.

29. Uchida, Y., et al. (2011). Quantitative targeted absolute proteomics of human blood-brain barrier transporters and receptors. *J Neurochem* **117**(2): 333-45.

CHAPTER V

1. Berens, M. E. and Giese, A. (1999). "...those left behind." Biology and oncology of invasive glioma cells. *Neoplasia* **1**(3): 208-19.

2. Grossman, S. A., et al. (2010). Survival of patients with newly diagnosed glioblastoma treated with radiation and temozolomide in research studies in the United States. *Clin Cancer Res* **16**(8): 2443-9.

3. Bell, E., Jr. and Karnosh, L. J. (1949). Cerebral hemispherectomy; report of a case 10 years after operation. *J Neurosurg* **6**(4): 285-93.

4. Scherer, H.-J. (1938). Structural development in gliomas. *Am. J Cancer* **34**: 334-351.

5. Matsukado, Y., Maccarty, C. S. and Kernohan, J. W. (1961). The growth of glioblastoma multiforme (astrocytomas, grades 3 and 4) in neurosurgical practice. *J Neurosurg* **18**: 636-44.

6. Wen, P. Y. and Brandes, A. A. (2009). Treatment of recurrent high-grade gliomas. *Curr Opin Neurol* **22**(6): 657-64.

7. Wen, P. Y. and Kesari, S. (2008). Malignant gliomas in adults. *N Engl J Med* **359**(5): 492-507.

8. Huang, T. T., et al. (2009). Targeted therapy for malignant glioma patients: lessons learned and the road ahead. *Neurotherapeutics* **6**(3): 500-12.

9. Pardridge, W. M. (2005). The blood-brain barrier: bottleneck in brain drug development. *NeuroRx* **2**(1): 3-14.

10. Schinkel, A. H. and Jonker, J. W. (2003). Mammalian drug efflux transporters of the ATP binding cassette (ABC) family: an overview. *Adv Drug Deliv Rev* **55**(1): 3-29.

11. Hofer, S. and Frei, K. (2007). Gefitinib concentrations in human glioblastoma tissue. *J Neurooncol* **82**(2): 175-6.

12. Pitz, M. W., et al. (2011). Tissue concentration of systemically administered antineoplastic agents in human brain tumors. *J Neurooncol*.

13. Fine, R. L., et al. (2006). Randomized study of paclitaxel and tamoxifen deposition into human brain tumors: implications for the treatment of metastatic brain tumors. *Clin Cancer Res* **12**(19): 5770-6.

14. Rosso, L., et al. (2009). A new model for prediction of drug distribution in tumor and normal tissues: pharmacokinetics of temozolomide in glioma patients. *Cancer Res* **69**(1): 120-7.

15. Marchetti, S., et al. (2008). Effect of the ATP-binding cassette drug transporters ABCB1, ABCG2, and ABCC2 on erlotinib hydrochloride (Tarceva) disposition in in vitro and in vivo pharmacokinetic studies employing Bcrp1-/-/Mdr1a/1b-/- (triple-knockout) and wild-type mice. *Mol Cancer Ther* **7**(8): 2280-7.

16. Stupp, R., et al. (2005). Radiotherapy plus concomitant and adjuvant temozolomide for glioblastoma. *N Engl J Med* **352**(10): 987-96.

17. Blakeley, J. O., et al. (2009). Effect of blood brain barrier permeability in recurrent high grade gliomas on the intratumoral pharmacokinetics of methotrexate: a microdialysis study. *J Neurooncol* **91**(1): 51-8.

18. de Vries, N. A., et al. (2010). Restricted brain penetration of the tyrosine kinase inhibitor erlotinib due to the drug transporters P-gp and BCRP. *Invest New Drugs*: 1-7.

19. Elmeliegy, M. A., et al. Role of ATP-binding cassette and solute carrier transporters in erlotinib CNS penetration and intracellular accumulation. *Clin Cancer Res* **17**(1): 89-99.

20. Kodaira, H., et al. (2010). Kinetic analysis of the cooperation of P-glycoprotein (P-gp/Abcb1) and breast cancer resistance protein (Bcrp/Abcg2) in limiting the brain and testis penetration of erlotinib, flavopiridol, and mitoxantrone. *J Pharmacol Exp Ther* **333**(3): 788-96.

21. Agarwal, S., et al. (2010). Distribution of gefitinib to the brain is limited by P-glycoprotein (ABCB1) and breast cancer resistance protein (ABCG2)-mediated active efflux. *J Pharmacol Exp Ther* **334**(1): 147-55.

22. Agarwal, S., et al. (2011). Role of Breast Cancer Resistance Protein (ABCG2/BCRP) in the Distribution of Sorafenib to the Brain. *J Pharmacol Exp Ther* **336**(1): 223-33.

23. Chen, Y., et al. (2009). P-glycoprotein and breast cancer resistance protein

influence brain distribution of dasatinib. *J Pharmacol Exp Ther* **330**(3): 956-63.

24. Dai, H., et al. (2003). Distribution of STI-571 to the brain is limited by P-glycoprotein-mediated efflux. *J Pharmacol Exp Ther* **304**(3): 1085-92.

25. Lagas, J. S., et al. (2009). Brain accumulation of dasatinib is restricted by P-glycoprotein (ABCB1) and breast cancer resistance protein (ABCG2) and can be enhanced by elacridar treatment. *Clin Cancer Res* **15**(7): 2344-51.

26. Polli, J. W., et al. (2009). An unexpected synergist role of P-glycoprotein and breast cancer resistance protein on the central nervous system penetration of the tyrosine kinase inhibitor lapatinib (N-{3-chloro-4-[(3-fluorobenzyl)oxy]phenyl}-6-[5-({[2-(methylsulfonyl)ethy l]amino}methyl)-2-furyl]-4-quinazolinamine; GW572016). *Drug Metab Dispos* **37**(2): 439-42.

27. Hyafil, F., et al. (1993). In vitro and in vivo reversal of multidrug resistance by GF120918, an acridonecarboxamide derivative. *Cancer Res* **53**(19): 4595-602.

28. Breedveld, P., et al. (2005). The effect of Bcrp1 (Abcg2) on the in vivo pharmacokinetics and brain penetration of imatinib mesylate (Gleevec): implications for the use of breast cancer resistance protein and P-glycoprotein inhibitors to enable the brain penetration of imatinib in patients. *Cancer Res* **65**(7): 2577-82.

29. Peereboom, D. M., et al. (2009). Phase II trial of erlotinib with temozolomide and radiation in patients with newly diagnosed glioblastoma multiforme. *J Neurooncol* **98**(1): 93-9.

30. Prados, M. D., et al. (2009). Phase II study of erlotinib plus temozolomide during and after radiation therapy in patients with newly diagnosed glioblastoma multiforme or gliosarcoma. *J Clin Oncol* **27**(4): 579-84.

31. Raizer, J. J., et al. (2010). A phase II trial of erlotinib in patients with recurrent malignant gliomas and nonprogressive glioblastoma multiforme postradiation therapy. *Neuro Oncol* **12**(1): 95-103.

32. Reardon, D. A., et al. (2009). Phase 2 trial of erlotinib plus sirolimus in adults with recurrent glioblastoma. *J Neurooncol* **96**(2): 219-30.

CHAPTER VI

1. Davis, F. G., et al. (2001). Prevalence estimates for primary brain tumors in the United States by behavior and major histology groups. *Neuro Oncol* **3**(3): 152-8.

2. Wen, P. Y. and Kesari, S. (2008). Malignant gliomas in adults. *N Engl J Med* **359**(5): 492-507.

3. Grossman, S. A., et al. (2010). Survival of patients with newly diagnosed glioblastoma treated with radiation and temozolomide in research studies in the United States. *Clin Cancer Res* **16**(8): 2443-9.

4. Wen, P. Y. and Brandes, A. A. (2009). Treatment of recurrent high-grade gliomas. *Curr Opin Neurol* **22**(6): 657-64.

5. McGirt, M. J., et al. (2009). Independent association of extent of resection with survival in patients with malignant brain astrocytoma. *J Neurosurg* **110**(1): 156-62.

6. Stupp, R., et al. (2005). Radiotherapy plus concomitant and adjuvant temozolomide for glioblastoma. *N Engl J Med* **352**(10): 987-96.

7. Collins, V. P. (2007). Mechanisms of disease: genetic predictors of response to treatment in brain tumors. *Nat Clin Pract Oncol* **4**(6): 362-74.

8. De Witt Hamer, P. C. (2010). Small molecule kinase inhibitors in glioblastoma: a systematic review of clinical studies. *Neuro Oncol* **12**(3): 304-16.

9. Deeken, J. F. and Loscher, W. (2007). The blood-brain barrier and cancer: transporters, treatment, and Trojan horses. *Clin Cancer Res* **13**(6): 1663-74.

10. Pardridge, W. M. (2005). The blood-brain barrier: bottleneck in brain drug development. *NeuroRx* **2**(1): 3-14.

11. Schinkel, A. H. and Jonker, J. W. (2003). Mammalian drug efflux transporters of the ATP binding cassette (ABC) family: an overview. *Adv Drug Deliv Rev* **55**(1): 3-29.

12. Agarwal, S., et al. (2010). Distribution of gefitinib to the brain is limited by P-glycoprotein (ABCB1) and breast cancer resistance protein (ABCG2)-mediated active efflux. *J Pharmacol Exp Ther* **334**(1): 147-55.

13. Agarwal, S., et al. (2010). Role of Breast Cancer Resistance Protein (ABCG2/BCRP) in the Distribution of Sorafenib to the Brain. *J Pharmacol Exp Ther* **336**(1): 223-33.

14. Chen, Y., et al. (2009). P-glycoprotein and breast cancer resistance protein influence brain distribution of dasatinib. *J Pharmacol Exp Ther* **330**(3): 956-63.

15. Dai, H., et al. (2003). Distribution of STI-571 to the brain is limited by P-glycoprotein-mediated efflux. *J Pharmacol Exp Ther* **304**(3): 1085-92.

16. de Vries, N. A., et al. (2010). Restricted brain penetration of the tyrosine kinase inhibitor erlotinib due to the drug transporters P-gp and BCRP. *Invest New Drugs*: 1-7.

17. de Vries, N. A., et al. (2007). P-glycoprotein and breast cancer resistance protein: two dominant transporters working together in limiting the brain penetration of topotecan. *Clin Cancer Res* **13**(21): 6440-9.

18. Polli, J. W., et al. (2009). An unexpected synergist role of P-glycoprotein and breast cancer resistance protein on the central nervous system penetration of the tyrosine kinase inhibitor lapatinib (N-{3-chloro-4-[(3-fluorobenzyl)oxy]phenyl}-6-[5-({[2-(methylsulfonyl)ethy l]amino}methyl)-2-furyl]-4-quinazolinamine; GW572016). *Drug Metab Dispos* **37**(2): 439-42.

19. Tang, S. C., et al. (2011). Brain accumulation of sunitinib is restricted by P-glycoprotein (ABCB1) and breast cancer resistance protein (ABCG2) and can be enhanced by oral elacridar and sunitinib coadministration. *Int J Cancer*.

20. Ahluwalia, M. S., et al. (2010). Targeting SRC in glioblastoma tumors and brain metastases: rationale and preclinical studies. *Cancer Lett* **298**(2): 139-49.

21. Lombardo, L. J., et al. (2004). Discovery of N-(2-chloro-6-methyl- phenyl)-2-(6-(4-(2-hydroxyethyl)- piperazin-1-yl)-2-methylpyrimidin-4- ylamino)thiazole-5-carboxamide (BMS-354825), a dual Src/Abl kinase inhibitor with potent antitumor activity in preclinical assays. *J Med Chem* **47**(27): 6658-61.

22. Premkumar, D. R., et al. (2010). Dasatinib synergizes with JSI-124 to inhibit growth and migration and induce apoptosis of malignant human glioma cells. *J Carcinog* **9**.

23. Hofer, S. and Frei, K. (2007). Gefitinib concentrations in human glioblastoma tissue. *J Neurooncol* **82**(2): 175-6.

24. Hofer, S., Frei, K. and Rutz, H. P. (2006). Gefitinib accumulation in glioblastoma tissue. *Cancer Biol Ther* **5**(5): 483-4.

25. Berens, M. E. and Giese, A. (1999). "...those left behind." Biology and oncology of invasive glioma cells. *Neoplasia* **1**(3): 208-19.

26. Wiesner, S. M., et al. (2009). De novo induction of genetically engineered brain tumors in mice using plasmid DNA. *Cancer Res* **69**(2): 431-9.

27. Pitz, M. W., et al. (2011). Tissue concentration of systemically administered antineoplastic agents in human brain tumors. *J Neurooncol*.

28. Fine, R. L., et al. (2006). Randomized study of paclitaxel and tamoxifen deposition into human brain tumors: implications for the treatment of metastatic brain tumors. *Clin Cancer Res* **12**(19): 5770-6.

29. Rosso, L., et al. (2009). A new model for prediction of drug distribution in tumor and normal tissues: pharmacokinetics of temozolomide in glioma patients. *Cancer Res* **69**(1): 120-7.

30. Lockman, P. R., et al. (2010). Heterogeneous blood-tumor barrier permeability determines drug efficacy in experimental brain metastases of breast cancer. *Clin Cancer Res* **16**(23): 5664-78.

31. Lagas, J. S., et al. (2009). Brain accumulation of dasatinib is restricted by P-glycoprotein (ABCB1) and breast cancer resistance protein (ABCG2) and can be enhanced by elacridar treatment. *Clin Cancer Res* **15**(7): 2344-51.

32. Blakeley, J. O., et al. (2009). Effect of blood brain barrier permeability in recurrent high grade gliomas on the intratumoral pharmacokinetics of methotrexate: a microdialysis study. *J Neurooncol* **91**(1): 51-8.

33. Shi, Z., et al. (2007). Erlotinib (Tarceva, OSI-774) antagonizes ATP-binding cassette subfamily B member 1 and ATP-binding cassette subfamily G member 2-mediated drug resistance. *Cancer Res* **67**(22): 11012-20.

34. Leggas, M., et al. (2006). Gefitinib modulates the function of multiple ATP-binding cassette transporters in vivo. *Cancer Res* **66**(9): 4802-7.

35. Dai, C. L., et al. (2008). Lapatinib (Tykerb, GW572016) reverses multidrug resistance in cancer cells by inhibiting the activity of ATP-binding cassette subfamily B

member 1 and G member 2. *Cancer Res* **68**(19): 7905-14.

36. Dai, C. L., et al. (2009). Sensitization of ABCB1 overexpressing cells to chemotherapeutic agents by FG020326 via binding to ABCB1 and inhibiting its function. *Biochem Pharmacol* **78**(4): 355-64.

37. Zhuang, Y., et al. (2006). Topotecan central nervous system penetration is altered by a tyrosine kinase inhibitor. *Cancer Res* **66**(23): 11305-13.

38. Carcaboso, A. M., et al. (2010). Tyrosine kinase inhibitor gefitinib enhances topotecan penetration of gliomas. *Cancer Res* **70**(11): 4499-508.

APPENDICES

APPENDIX I

Analytical Methods for Quantification of Tyrosine Kinase Inhibitors

1.1 LC-MS/MS Conditions

Compounds	Mobile Phase		MS Polarity	Mass Transition	Retention Time (min)
	Acetonitrile	Formate Buffer			
Gefitinib	32 %	68 % (pH = 4)	positive	446.9 →128.1	5.7
Erlotinib	45 %	55 %	positive	395.1 → 278.9	5.1
Sorafenib	68 %	32 %	positive	465.0 → 251.9	5.9
Dasatinib	32 %	68 % (pH = 4)	positive	488 → 409	4.9
AG1478	68 % / 45%	32 % / 55 %	positive	316.6 → 300.9	3.6

1.2 Composition of formate buffer:

20 mM ammonium formate in distilled water, containing 1 % formic acid. Unadjusted pH of the buffer was approximately 3.4. pH was adjusted to 4 using ammonium hydroxide for gefitinib and dasatinib.

1.3 Stock solutions, calibration standards, and quality control samples

Stock solutions a concentration of 1 mg/ml were prepared by dissolving 10 mg compound in 10 mL of methanol and stored in glass vials. The stock solution was diluted to prepare eight calibration standards at the following concentrations: 2.5, 5, 10, 25, 50, 100, 250 and 500 ng/mL. Quality control (QC) samples were prepared independently at

three different concentrations including: the low QC, 7.5 ng/mL, the medium QC, 75 ng/mL and the high QC; 750 ng/mL. All solutions were stored at -80 °C.

1.4 Sample preparation and Liquid-Liquid Extraction

Sample preparation steps were similar for all compounds. Prior to analysis, frozen samples were thawed at ambient temperature. A 50µL aliquot of plasma or a 100 µL aliquot of brain homogenate in polypropylene tubes was used for analysis of samples. A volume of 100µL of the internal standard solution was added to the samples followed by alkalinization of samples by addition of an equal volume of pH 11 buffer (1 mM sodium hydroxide, 0.5 mM sodium bicarbonate). Samples were then extracted by addition of 1 ml of ice-cold ethyl acetate and shaking vigorously on a mechanical shaker for 10 minutes. Sample tubes were then centrifuged at 7500 r.p.m. for 15 minutes at 4°C. A volume of 800µL of the top organic layer was transferred to fresh polypropylene tubes and dried under nitrogen. Samples were reconstituted in 100µL mobile phase and transferred to glass auto sampler vials, and a volume of 10µL sample was injected in the HPLC system using a temperature controlled autosampling device maintained at 10°C.

1.5 Calibration Curves

Calibration curves were computed using the ratio of the peak area of analyte and internal standard by using a least-squares linear regression analysis and $1/Y$ or $1/Y^2$ weighting. The parameters of each calibration curve were used to compute back-calculated concentrations and to obtain values for the QC samples and unknown samples by interpolation.

APPENDIX II

Validation of LC-MS/MS Method for Analysis of Gefitinib in Plasma

2.1 Method Validation

Method validation runs for tissue plasma calibrator standards and QCs were performed on three consecutive days and included a calibration curve and QC samples, at three different concentrations, in triplicate. The accuracy and precision of the assay was assessed by the mean relative percentage deviation (DEV) from the nominal concentrations and the within- and between-run precision, respectively. The accuracy for each tested concentration was calculated as:

$$DEV = 100 \times \left\{ \frac{([Gefitinib_{mean}] - [Gefitinib_{nominal}])}{[Gefitinib_{nominal}]} \right\}$$

Estimates of the between-run precision were obtained by one-way analysis of variance (ANOVA) using the run day as the classification variable. The between-groups mean square (MS_{bet}), the within-groups mean square (MS_{wit}), and the grand mean (GM) of the observed concentrations across runs were calculated using the Sigma Stat Software. The between run precision (BRP), expressed as a percentage relative standard deviation, was defined as:

$$BRP = 100 \times \left\{ \frac{\sqrt{((MS_{between} - MS_{within})/n)}}{Grand\ Mean} \right\}$$

where *n* represents the number of replicate observations within each run. For each concentration, the estimate of the within-run precision (WRP) was calculated as:

$$WRP = 100 \times \left\{ \frac{\sqrt{(MS_{within}/n)}}{Grand\ Mean} \right\}$$

2.2 Results

	Nominal Concentration (ng/mL)		
	7.5	75	750
Accuracy (%)	102	103	105.7
Concentration (ng/mL) *	7.6 ± 0.8	77.2 ± 5.6	793.0 ± 73.1
Precision (%)			
Within run (WRP)	10.73	5.96	8.3
Between run (BRP)	NS	4.82	4.66
Variability Expected (%)			
Within assay	10.7	6	8.3
Total	10.1	7.7	9.5
Number of samples	9	9	9

* Values are Mean ± SD, **NS** – No significant variation between run